



<https://theses.gla.ac.uk/>

Theses Digitisation:

<https://www.gla.ac.uk/myglasgow/research/enlighten/theses/digitisation/>

This is a digitised version of the original print thesis.

Copyright and moral rights for this work are retained by the author

A copy can be downloaded for personal non-commercial research or study,
without prior permission or charge

This work cannot be reproduced or quoted extensively from without first
obtaining permission in writing from the author

The content must not be changed in any way or sold commercially in any
format or medium without the formal permission of the author

When referring to this work, full bibliographic details including the author,
title, awarding institution and date of the thesis must be given

Enlighten: Theses

<https://theses.gla.ac.uk/>
research-enlighten@glasgow.ac.uk

ASPECTS OF CYTOTOXIC DRUG PENETRATION

Submission for the degree of M.D.

by

David James Kerr



MSc, MBChB, MRCP

Department of Medical Oncology
1 Horselethill Road
University of Glasgow
Glasgow
G12 9LX

ProQuest Number: 10948172

All rights reserved

INFORMATION TO ALL USERS

The quality of this reproduction is dependent upon the quality of the copy submitted.

In the unlikely event that the author did not send a complete manuscript and there are missing pages, these will be noted. Also, if material had to be removed, a note will indicate the deletion.



ProQuest 10948172

Published by ProQuest LLC (2018). Copyright of the Dissertation is held by the Author.

All rights reserved.

This work is protected against unauthorized copying under Title 17, United States Code
Microform Edition © ProQuest LLC.

ProQuest LLC.
789 East Eisenhower Parkway
P.O. Box 1346
Ann Arbor, MI 48106 – 1346

INDEX

CHAPTER TITLES	i
ACKNOWLEDGEMENTS	iii
LIST OF TABLES	iv
LIST OF FIGURES	vi

CONTENTS		PAGE /
CHAPTER 1	Review of cytotoxic drug penetration and statement of the aims of the thesis.	1
CHAPTER 2	Cellular uptake and disposition of adriamycin and 4'-deoxydoxorubicin and its relationship to cytotoxicity in human non small cell lung cancer monolayers.	22
CHAPTER 3	Penetration and relative cytotoxicity of adriamycin and 4'-deoxydoxorubicin in human lung tumour spheroids.	42
CHAPTER 4	Intratumoural distribution and pharmacokinetics of adriamycin and 4'-deoxydoxorubicin in rats bearing a methyl cholanthrene induced sarcoma.	66
CHAPTER 5	Cellular accumulation and spheroid penetration of lipophilic anthracycline analogues	86
CHAPTER 6	The effect of the non-ionic surfactant, Brij 30 on cellular uptake and cytotoxicity of adriamycin in monolayer and spheroid culture systems.	117
CHAPTER 7	The pharmacokinetics and disposition of adriamycin following its administration, in solution or encapsulated in niosomal vesicles, to tumour bearing nude mice.	137

CONTENTS (cont)	PAGE /
CHAPTER 8 Antitumour activity of niosome encapsulated adriamycin in monolayer, spheroid and xenograft.	156
CHAPTER 9 Cellular uptake and cytotoxicity of daunomycin and a complex of daunomycin - low density lipoprotein in monolayer and spheroid.	168
CHAPTER 10 The association of gap junctional communication with cytotoxic drug resistance and intercellular drug transfer.	185
CHAPTER 11 A concentration-effect model for spheroid diffusion.	202
CHAPTER 12 Clinical Relevance and Future Aims.	211
REFERENCES 	228
LIST OF PUBLICATIONS 	238

This study was carried out in the Department of Medical Oncology, University of Glasgow. I am most grateful to Professor S B Kaye for his support and guidance and for allowing me the full use of the facilities in his laboratory.

Various members of staff from the department have also contributed practical advice, including Dr R I Freshney and Dr J Cummings. Mr G J Morrison assisted with HPLC analysis of adriamycin tissue concentrations, and I am indebted to him.

The spheroid studies were performed in the Radiobiology Laboratories in Belvidere Hospital, and Dr T Wheldon offered the use of his laboratory and gave advice freely. Gratitude is due also to Mr T Downey, who performed electron microscopy, Miss S Hynds who synthesised low density lipoprotein-daunomycin complexes and Professor A T Florence, Department of Pharmacy, Strathclyde University who synthesised adriamycin containing niosomes.

I am grateful to the Cancer Research Campaign for financial support during the tenure of this research fellowship.

AUTHOR'S STATEMENT

The work described in this thesis was performed personally by the author unless otherwise stated as above, or in the text.

LIST OF TABLES

<u>TABLES</u>	<u>PAGE</u>
3.1 Growth delay of L-DAN spheroids exposed to different concentrations of adriamycin or 4'-deoxy for a fixed time (one hour)	54
3.1 Growth delay of L-DAN spheroids exposed to a fixed concentration of adriamycin (10 ug/ml) for different lengths of time.	55
4.1 Peak drug concentration, AUC and metabolites in rat serum following intravenous administration of adriamycin and 4'-deoxy.	78
4.2 Peak drug concentration, AUC and metabolites in rat heart following intravenous administration of adriamycin and 4'-deoxy.	79
4.3 Peak drug concentration, AUC and metabolites in the MC40A tumour following intravenous administration of adriamycin and 4'-deoxy.	80
4.4 The percentage increase in tumour volume with time following intravenous treatment with adriamycin, 4'-deoxydoxorubicin or normal saline.	81
5.1 Intracellular drug levels following monolayer exposure to equivalent of 5 ug/ml for one hour.	96
5.2 Intracellular adriamycin levels following co-incubation with a variety of different drugs.	97
5.3 Composite growth curve analysis for spheroids treated with 4'-deoxydoxorubicin.	98-100
5.4 Composite growth curve analysis for spheroids treated with daunomycin	101-103
5.5 Composite growth curve analysis for spheroids treated with adriamycin	104-106
5.6 Composite growth curve analysis for spheroids treated with 4-demethoxydaunomycin	107-108
5.7 Composite growth curve analysis for spheroids treated with 4'-deoxy, 4'-iodo doxorubicin.	109-111

LIST OF TABLES

<u>TABLES</u>	<u>PAGE</u>
5.8 The relative potency of anthracycline compounds in vitro, assessed by monolayer clonogenic cell survival and spheroid growth delay	112
6.1 Adriamycin ID90 in monolayers.	129
6.2 Spheroid growth delay in reponse to adriamycin.	129
7.1 Comparative total tissue and plasma contents of adriamycin following administration of free or niosome encapsulated drug.	148
8.1 Spheroid growth delay in reponse to treatment with free and niosome bound adriamycin.	163
8.2 The percentage increase in tumour volume with time, following treatment with free adriamycin, niosome encapsulated adriamycin or normal saline.	164
9.1 Intracellular levels of daunomycin and daunomycin following treatment of L-DAN monolayers with identical concentrations of daunomycin with LDL-daunomycin	180
9.2 Spheroid growth delay following treatment with daunomycin of LDL-dauno at differing concentrations for 1 hour.	181
10.1 Non small cell lung cancer lines used in the gap junction study.	196
10.2 The cytotoxicity data for each cell line	197
10.3 The order of ranking gap junction formation is from high to low, whereas cell sensitivity data is ranked from most resistant to most sensitive.	198
11.1 The actual and predicted xenograft clonogenic surviving fraction according to the concentration-effect model.	216
11.2 The fractional clonogenic cell kill per annulus for different drug diffusion gradients shown in figure 11.2	217
11.3 The effect of varying the composition of the cell cycle compartments, and hence drug sensitivity, of concentric spheroid annuli.	218

<u>Figures</u>	<u>PAGE</u>
1.1 Drug equilibria between the vascular compartment and site of action.	19
1.2 Schematic patterns of vascularisation. A capillary surrounded by viable cells is indicated in a. Regions with different capillary architectures are shown in b, c and d.	20
1.3 Examples of negative effects (left) and positive effects (right) on the patient, due to insufficient vascularisation of the tumour.	20
1.4 Clonogenic cell survival vs cumulative adriamycin exposure for monolayer, spheroid and xenograft of the MGH-UI line.	21
2.1 Intracellular levels of adriamycin following exposure to a range of external drug concentrations for up to 3 hours. Each point represents the mean of 4 experiments and the vertical bar denotes 1 standard deviation.	33
2.2 Intracellular levels of 4'-deoxy following exposure to a range of external drug concentrations for up to 2 hours. Each point represents the mean of 4 experiments and the vertical bar denotes 1 standard deviation.	34
2.3 The relationship between intracellular and extra-cellular drug concentrations for adriamycin (●) and 4'-deoxy (○). Each point is the mean of 4 experiments and the vertical bar denotes 1 standard deviation.	35
2.4 Clonogenic survival for LDAN monolayers exposed to adriamycin (●) or 4'-deoxy (○). Each point represents the mean of 4 experiments and the vertical bar denotes 1 standard deviation.	36
2.5 The relationship between intracellular drug concentration and cell survival. Each point is the mean of 4 experiments.	37
2.6 The relationship between clonogenic cell survival and the duration of exposure at constant drug concentration, 5 µg/ml. (Adriamycin, ●; 4'-deoxy ○). The curves were computer fitted to data from 2 experiments.	38

LIST OF FIGURES (cont)

FIGURE	PAGE
2.7 Intracellular levels of 4'-deoxydoxorubicinol after exposure to a range of concentrations of 4'-deoxy. Each point is the mean of 4 experiments and the vertical bar denotes 1 standard deviation.	39
2.8 Fluorescent electron micrograph showing adriamycin bound to cell nuclei in monolayer (magnification x 100).	40
2.9 Fluorescent electron micrograph showing 4'-deoxy distributed within the cytoplasm in a granular fashion, with some binding to the nucleus and nuclear membrane (magnification x 100).	40
2.10 Electron micrograph of LDAN cell A) Normal Cell B) Cell treated with 4'-deoxy. Note nuclear disruption and chromatolysis and cytoplasmic lysosomal vesicles (arrowed) (magnification x 2950).	41
3.1 Diagrammatic representation of experimental spheroid protocol.	56
3.2 a The relationship between intracellular adriamycin levels and extracellular pH. Each point is the mean of 5 experiments and the vertical bar denotes 1 standard deviation.	57
3.2 b The effect of pH on the ionisation of a weak acid. The acid is 50% ionised at a pH = pKa. At higher pH values it became increasingly more ionised. A mirror image could be constructed for a weak base.	57
3.3 Clonogenic survival of monolayer cells in the plateau (Δ, \circ) or exponential (Δ, \circ) phase of growth, after exposure to adriamycin (\circ, \bullet) or 4'-deoxy (Δ, \blacktriangle). Each point is the mean of 4 experiments and the vertical bars represent 1 standard deviation.	58
3.4 Spheroid growth delay after exposure to various concentrations of adriamycin. Control $\circ-\circ$; 1 $\mu\text{g/ml}$ $\circ-\circ$; 3 $\mu\text{g/ml}$ $\bullet-\bullet$; 5 $\mu\text{g/ml}$ $\times-\times$; 10 $\mu\text{g/ml}$ $\ast-\ast$; 15 $\mu\text{g/ml}$ $\ast\cdots\ast$.	59
3.5 Dependence of regrowth delay on drug concentration, with fixed duration of exposure. Adriamycin, 4'-deoxy.	60

LIST OF FIGURES

<u>FIGURES</u>	<u>PAGE</u>
3.6 Clonogenic cell survival of monolayers (Δ , \circ) and disaggregated spheroids (\blacktriangle , \bullet) following exposure to adriamycin (\circ , \bullet) or 4'-deoxy (Δ , \blacktriangle). The curves are computer fitted to the mean of 2 experiments	61
3.7 The relationship between clonogenic cell survival and the duration of adriamycin exposure at fixed concentration (10 $\mu\text{g/ml}$).	62
3.8 The dependence of spheroid growth delay on the duration of exposure to adriamycin at fixed concentration (10 $\mu\text{g/ml}$).	63
3.9 Section through an L-DAN spheroid stained with haematoxylin and eosin (magnification x 100).	64
3.10 External surface of an L-DAN spheroid exposed to adriamycin. The outer 3 - 4 cell layers are most highly labelled with drug and there is a clear diffusion gradient within the spheroid (magnification x 100)	64
3.11 External surface of an L-DAN spheroid exposed to 4'-deoxy. The drug has diffused further into the spheroid and the external cells are more highly labelled compared to adriamycin (magnification x 100)	65
4.1 Haematoxylin and eosin stained section of the MC40 tumour. Note the vascular annulus on the periphery of the tumour (magnification x 100)	82
4.2 Fluorescent photomicrograph of rat cardiac muscle following infusion of adriamycin (magnification x 100)	82
4.3 Fluorescent photomicrograph of rat liver following infusion of adriamycin (magnification x 100).	83
4.4 Fluorescent photomicrograph of rat skeletal muscle following infusion of adriamycin (magnification x 100)	83
4.5 Fluorescent photomicrograph of adriamycin treated MC40A tumour. The drug is localised predominantly on the periphery of the tumour, with relatively poor diffusion into the centre of the tumour (magnification x 25)	84

LIST OF FIGURES

<u>FIGURES</u>	<u>PAGE</u>
4.6 Fluorescent photomicrograph of 4'-deoxy treated MC40A tumour. The drug has diffused further into the central, avascular region of the tumour compared to adriamycin (magnification x 25)	84
4.7 Electron micrograph of adriamycin treated rat heart showing mitochondrial swelling and disruption (magnification x 5900)	
4.8 Electron micrograph of adriamycin treated rat heart showing a high power view of mitochondrial vesiculation (magnification x 4300)	85
5.1 a The movement of a solute (S) into a pore created by lateral diffusion of lipids in the outer leaflet of the cell membrane is shown. When a space appears in the inner membrane leaflet, the solute is free to diffuse into the cytoplasm.	113
5.1 b Membrane pores can be created by re-organisation of the polar lipid heads or by a transmembrane protein which allows diffusion of drug molecules of specific size, shape and charge	113
5.2 The structure of adriamycin and its metabolites.	114
5.3 Clonogenic cell survival vs log drug concentration	115
5.4 Fluorescent photomicrograph of L-DAN spheroid exposed to 4'-deoxy, 4'-iododoxorubicin 2 µg/ml for 1 hour (magnification x 100)	116
6.1 The time course of cellular accumulation of adriamycin (fixed drug concentration of 5 µg/ml)	130
6.2 Clonogenic cell survival curves	131
6.3 Clonogenic cell survival in monolayers and disaggregated spheroids following treatment with adriamycin + Brij 30.	132
6.4 Electron micrograph of L-DAN cells exposed in monolayer to Brij 30, 1 µl/ml. There is evidence of complete cytolysis (magnification x 4900)	133

LIST OF FIGURES (cont)

FIGURE	PAGE
6.5 Electron micrograph of L-DAN cells exposed in monolayer to Brij 30, 0.1 μ l/ml. There is evidence of external/internal membrane disruption and clumping of nuclear chromatin (magnification x 2950)	133
6.6 Electron micrograph of L-DAN cells exposed in monolayer to Brij 30, 0.01 μ l/ml. There is evidence of minor alterations in intracellular membrane structure (magnification x 4900)	134
6.7 Low power electron micrograph of L-DAN spheroids showing compact cellular packing (magnification x 1300)	134
6.8 High power electron micrograph of L-DAN spheroids showing close membrane apposition and a desmosomal junction (magnification x 9800)	135
6.9 Stylised dose-response curves of clonogenic cell survival vs log adriamycin concentration.	136
7.1 Phase contrast photomicrograph of a multilamellar niosome containing adriamycin (magnification x 100)	149
7.2 Plasma concentration-time profile following treatment with free adriamycin and niosome encapsulated adriamycin.	150
7.3 Hepatic concentration-time profile following treatment with free adriamycin or niosome bound adriamycin	151
7.4 a Hepatic metabolite levels after treatment with niosomal adriamycin	152
7.4 b Hepatic metabolite levels after treatment with free adriamycin	152
7.5 Renal concentration-time profile following treatment with free adriamycin or niosome encapsulated adriamycin.	153
7.6 Cardiac concentration time profile following treatment with free adriamycin or niosome bound adriamycin	154

LIST OF FIGURES

<u>FIGURES</u>	<u>PAGE</u>
7.7 Tumour concentration-time profile following treatment with free adriamycin and niosome encapsulated adriamycin	155
8.1 Correlation of tumour volume (caliper measurements) with weight of excised tumour for treated and untreated wil xenografts.	165
8.2 Clonogenic survival of L-DAN monolayers following treatment with free adriamycin or niosome encapsulated adriamycin.	166
8.3 The relationship between tumour mass and time following treatment with free adriamycin, niosome bound adriamycin or 0.9% saline as control.	167
9.1 Intracellular uptake and metabolism of daunomycin after exposure to free drug of LDL - associated drug.	182
9.2 Clonogenic cell survival for monolayers and disaggregated spheroids following exposure to daunomycin of LDL-daunomycin	183
9.3 Relationship between LDL binding and degradation to external concentration in L-DAN cells grown in monolayer culture.	184
10.1 The McNutt-Weinstein Model	199
10.2 Autoradiographs showing the distribution of ³ H-uridine in cells.	200
10.3 Correlation between gap junction formation and cytotoxic drug resistance.	201
11.1 Dose-response curves for clonogenic cell kill vs log drug concentration in MGH-UI monolayers and spheroids	219
11.2 Diagrammatic representation of spheroid annuli	220
11.3 Arbitrary drug exposure gradients from the spheroid surface to its centre.	220

Review of cytotoxic drug penetration and statement of the aims of the thesis.

Introduction

The aim of cancer chemotherapy is to eradicate clinically manifest or microscopic metastases. There is increasing recognition of the fact that poor drug penetration into solid tumours may be an important aspect of cytotoxic drug resistance (Sutherland et al, 1979). Diminished access of chemotherapeutic agents to clonogenic cells in tumour nodules may be related to altered vasculature or drug penetration barriers. Penetration, therefore, will be determined by the concentration of free drug in the tumour vascular compartment and subsequent transport barriers interposed between the cytotoxic agent and its site of pharmacological action.

The introduction of the multicellular tumour spheroid system has proved a useful in vitro model for studying dynamic aspects of drug penetration. The use of this model circumvents the problems of drug disposition in vivo, but general pharmacokinetic principles can still be applied to analyses of the data obtained. The purpose of this introductory chapter is to describe:-

1. The mode of passage of a drug from its site of administration to its site of pharmacological action.
2. The application of pharmacokinetic principles to drug penetration.
3. The role of multicellular spheroids as in vitro models for drug penetration studies.

PASSAGE OF DRUG FROM ITS SITE OF ADMINISTRATION TO ITS SITE OF
PHARMACOLOGICAL ACTION

Once a water soluble drug enters the circulation from its site of administration, it becomes rapidly and widely disseminated throughout the body, via the blood stream. There will usually be a dynamic equilibrium between drug at binding sites, including sites of biological action and drug in intracellular or interstitial fluid. Further equilibria exist between drug in these compartments and free drug in plasma water, implying an indirect relationship between measured plasma drug levels and drug concentration at receptor sites (fig 1.1).

1.1 Plasma protein binding

Depending on the physico-chemical properties of the cytotoxic agent, it will partition to a varying extent, between blood cells, plasma protein and plasma water. Plasma protein binding has a number of consequences. It will determine the relative amount of free drug available for tumour interaction, provide a "store" or buffer stabilising sudden alterations in drug availability and is a possible site of drug interaction regarding drug displacement phenomena.

There are a number of modes of egress for a cytotoxic drug from the circulation. If sufficiently lipid soluble, it can diffuse through the capillary endothelial lining into the extracellular fluid, whereas small polar compounds can diffuse out through water filled pores between capillary endothelial junctions. Specific active transport mechanisms exist for a few molecules, e.g. hormones, amino acids, and it is possible that cytotoxic drugs could compete for these systems.

Malignant tumours appear to derive their vascular supply from newly formed vessels and by incorporation of existing vessels from host tissues (Papadimitriou and Woods, 1974). The anatomy of the tumour microangiarchitecture is altered, with thin walled arterioles deficient in medial smooth muscle and adrenergic innervation (Mattson and Peterson, 1981). No formal studies of drug diffusibility across tumour capillary endothelium have been undertaken but it would appear anatomically, if not functionally, that they might present a less well defined drug barrier. There is some evidence to suggest that tumour cells can participate in and be contiguous with the host derived endothelial lining. This implies that cytotoxic agents could exert their effect locally on the tumour cells incorporated into the endothelial lining of the vessels and alter drug permeability or induce local vascular collapse.

In a series of classical experiments Goldacre and Sylven (1962) demonstrated that the blood borne dye, lissamine green, did not diffuse into central regions of solid murine tumours grown

subcutaneously. Nevertheless, it was possible to regrow these tumours from tissue fragments transplanted from the dye-free regions. The authors considered that, in the animal tumour model studied, there were areas of the tumour vasculature which were not contiguous with the host circulation, yet were supportive of tumour growth. If the tumour microvasculature is compartmentalised in this way, it will lead to marked intratumoural differences in drug exposure depending on the ability of the drug in question to diffuse or be transported from the peripheral tumour vascular ring, in direct continuity with the systemic circulation, into the central region of solid tumours. (figures 1.2 and 1.3)

1.3 Diffusion through interstitial fluid

/5

Within interstitial fluid, drug can partition between interstitial water and protein (consisting of structural proteins such as collagen and extravascular plasma proteins). It is possible that drug-cell surface interactions could occur with formation of ionic, Van der Waals or dipole-dipole bonds. The degree to which interstitial water will permeate throughout the tumour will depend on the compact "packing" of tumour cells and the tightness of intercellular junctions. This varies for different tumour types from simple membrane apposition to tight desmosomal junctions (Weinstein et al, 1979).

Cell junctions in tumour cells can be grouped into two major categories. The first category includes junctions at which surface membranes of neighbouring cells come into direct contact (eg occludens junction, "gap" or nexus junctions, and probably septate desmosomes). These junctions can be further subclassified according to differences in the components within the interior of the junctional membranes. The second general category includes junctions where the surface membranes of adjacent cells are separated by a 15 - 35 nm interspace (eg adherens junctions). This interspace typically contains electron-dense proteinaceous material. Junctions in this category can be subclassified on the basis of the morphology of cytoplasmic and extracellular material associated with the membrane at the junction.

The primary function of these junctions is complex, and depends to a large part on their tissue of origin. They control cell to cell adhesion, transepithelial permeability, modulate ionic coupling between cells by providing channels across cell membranes and metabolically couple cells when nutrients or intermediate metabolites of low molecular weight are exchanged by diffusion through gap junctions.

1.4 Transcellular drug transport

There are several potential mechanisms whereby a drug molecule might pass through cellular membranes to reach the cytoplasm. These include diffusion through water filled membrane pores if the molecule is small and sufficiently polar to dissolve in water; diffusion of lipophilic drugs through the lipid domain of the cell membrane; carrier mediated transport systems which may be either passive (governed by drug concentration gradients) or active (coupled to energy expenditure). There is some evidence to suggest that adriamycin enters cells by diffusion of the electroneutral molecule through the lipid domain of the cell membrane (Dalmark, 1981; Dalmark and Storm, 1981; Dalmark, 1982). The degree of passive diffusion is determined by - the concentration gradient across the membrane; membrane thickness; total surface area of membrane exposed to drug; duration of drug-cell contact; membrane permeability. As previously mentioned, the physico-chemical properties of the drug are also important, particularly charge and lipid solubility.

There is microheterogeneity of intratumoural pH, related to areas of necrosis and hypoxia (Vaupel et al, 1981; Acker et al, 1982). Basic drugs such as adriamycin (pKa 7.6-8.2), will tend to ionise at acidic pH and thus limit their ability to cross lipid membranes (fig 1.1). The oil-water partition co-efficient remains a useful marker of lipid solubility and will determine the ease with which the drug can traverse the lipid portion of the cell membrane. Adriamycin has the particular property of self-association to form dimeric structures through a π electron interaction of the tetracyclic anthraquinone rings (Dalmark, 1981). Because of this phenomenon, the kinetics of cell uptake of adriamycin appear to

fulfil the criteria for a carrier mediated, saturable system. However careful analysis of experimental data derived from Dalmark (1981) favours the explanation that adriamycin is transported by diffusion of the monomer through the cell membrane.

Once in the cytoplasm, the drug may have to cross further intracellular membranes before reaching its site of pharmacological action. In common with other compartments through which the drug has diffused, there is a potential for reversible or irreversible binding to intracytoplasmic macromolecules, e.g. protein, RNA, cytoplasmic membrane systems (fig 1.1).

Cell-cell transfer of active drug molecules may be accomplished by different means. Drug could be transported by specific transport or efflux systems, or by simple diffusion through the lipid domain of the membrane. The compactness of tumour cells and the number and type of intercellular connections would determine whether drug passes directly from cell to cell or is first transported into an intercellular space. Intercellular channels have been demonstrated by electron microscopy after staining with uranyl acetate (Weinstein et al, 1979), and this could represent a relatively rapid method of drug penetration to the centre of solid nodules (a "snakes and ladders" analogy would be appropriate).

Gap junctions are semipermeable intercellular connections which allow transfer of relatively small molecules (up to a molecular weight of around 1000) e.g. cyclic nucleotides (Lowenstein, 1981). In addition the junctions have specific shape and charge characteristics. It would seem possible that some cytotoxic drugs, particularly the antimetabolites, could use gap junctions as a rapid mode of intercellular transport.

THE APPLICATION OF GENERAL PHARMACOKINETIC PRINCIPLES OF ANALYSIS
OF DRUG PENETRATION

1.6

Advances in analytical techniques have allowed precise measurement of a wide range of cytotoxic drugs. Gel filtration, ultrafiltration and plasma dialysis allow determination of free drug, but usually whole plasma measurements are quoted. This, of course, gives only indirect evidence of the amount of drug at its site of action. It is possible, in certain cases to measure simultaneous plasma and intratumoural drug concentrations and to relate these by pharmacokinetic models.

Measurement of tumoural drug levels is a means of assessing drug penetration in a quantitative way, however if the cytotoxic agent is compartmentalised within the tumour, drug content expressed per total tumour weight would give an "average" value which would fail to take account of intratumoural disposition. One further drawback which limits the amount of information derived from measuring drug within solid tumours is the lack of a pharmacodynamic model which relates the tumoural pharmacokinetics to response. This field has recently been well reviewed by Powis (1985) but there are few clinical studies in which attempts are made to relate a drugs pharmacokinetic parameters to response.

A concentration - effect model has been designed and tested for adriamycin in nude mice bearing tumour xenografts (Chapter 11).

1.7 Volume of drug distribution

The volume of distribution (V_d) of a drug may be defined as a proportionality constant which relates the plasma concentration to the total amount of drug present in the body. This parameter has no direct physiological meaning but there are "ideal substances" which distribute into discrete compartments with physiological values. If a drug has extensive intracellular binding sites, then it will have a large V_d . The calcium channel blocker verapamil has been shown to enhance the cytotoxicity of adriamycin in vitro, probably by inhibiting active anthracycline efflux (Kaye and Merry, 1985). We have recently demonstrated that co-administration of verapamil and adriamycin to patients with limited stage small cell lung cancer results in a significant pharmacokinetic interaction. There is an apparent increase in the peripheral compartmental V_d of adriamycin associated with administration of verapamil. Verapamil is a vasodilator and increases tumour blood flow by 50% in rats bearing a hind limb sarcoma (Kaelin et al, 1982). Alterations in intracellular binding or vasodilation with increased peripheral tissue adriamycin delivery could explain the altered V_d in this study.

We have already defined the factors which control passive diffusion of drug molecules. All mathematical expressions describing diffusion have terms including the concentration gradient, and duration of drug exposure. With regard to penetration by passive diffusion, it would seem most appropriate to relate this to the integral of concentration x time from zero to infinity (i.e. area under the curve of the plasma concentration time curve). This expression would relate total tumour drug exposure, and would therefore seem to be a better measure of drug penetration, possibly, than peak plasma drug levels.

However, this may not hold for all drugs. Intracellular levels of adriamycin and daunomycin in leukaemic cells have been measured after rapid (10 minutes) or prolonged (24 hours) drug infusion (Peterson and Paul, 1983). Despite similarity in the plasma AUC's for rapid and prolonged infusions, the intracellular peak levels and AUC's were some 2-3 times higher after prolonged infusion. It would appear that for certain drugs, the temporal component assumes greater importance than the term denoting the concentration gradient, in determining the degree of intracellular drug uptake by passive diffusion.

There has been some interest in the study of tumour blood flow and its potential manipulation using a variety of vasoactive drugs. Reports have been made of increased, normal or decreased sensitivity to vasoactive drugs on the tumour microvascular bed (Mattson and Peterson, 1981). The hypothesis underlying this work is that increasing tumour blood flow relative to normal tissue flow should provide enhanced delivery of chemotherapeutic drugs and perhaps increase tumour oxygenation. Organ clearance of a drug can be determined by a subtractive technique, if drug concentration measurements can be made in arterial and draining venous blood:

$$U = \frac{Q \cdot C_A - C_V}{C_A} = Q \cdot E$$

(U = organ clearance, Q = blood flow, C_A = arterial drug concentration, C_V = venous drug concentration, E = extraction ratio).

If the extraction ratio is low, the tumour drug clearance will be relatively unaffected by alterations in blood flow. However, if the extraction ratio is high, then clearance will be proportional to blood flow. There are little data concerning tumour drug extraction ratios, but if they are low, then manoeuvres to increase tumour blood flow would have relatively little therapeutic benefit.

1.10 THE MULTICELLULAR SPHEROID AS AN IN VITRO MODEL FOR STUDIES

ON DRUG PENETRATION

The multicellular spheroid model was developed as a 3-dimensional system of intermediate complexity between monolayer and solid tumours grown in vivo, which would simulate the growth properties, cellular kinetics and microenvironment of a micro-metastasis prior to vascularisation. It is therefore possible to study drug penetration and distribution within solid tumours free from the constraints associated with host animal drug distribution and anomalies of tumour vasculature.

A number of techniques have been devised to study the penetration of drugs into spheroids. Conventional autoradiographic methods have been used successfully to demonstrate binding of methotrexate to dihydrofolate reductase in human osteosarcoma spheroids. Using this technique, West et al (1980) demonstrated that methotrexate has limited ability to penetrate avascular tumour spheroids. They compared the degree of penetration of methotrexate to the growth fraction of the tumour, as measured by the tritiated thymidine labelling index, and found that the growth fraction was much greater than the fraction of cells reached by methotrexate.

Nederman et al (1981) have developed a "dry" method, which does not disturb the distribution of water soluble substances, based on freeze-drying and vapour fixation of spheroids prior to preparation for autoradiography. They examined the penetration properties of a number of low molecular weight substances such as ^3H -D-Leucine ^3H -thymidine and the cytotoxic drugs ^3H -5-fluorouracil and ^3H -vinblastine. 5-fluorouracil distributes rapidly and evenly through human glioma spheroids whereas vinblastine is localised to the outer 3 - 4 cell layers.

Wibe (1982) has described the effects of vincristine on NHIK 3025 spheroids, derived from a cell line originating from a human cervical carcinoma in situ. Following a series of sequential trypsinisation procedures and plating of cells from concentric spheroid layers, he showed that cells from the interior of the spheroid were relatively resistant to vincristine and that this could be explained in part by failure of vincristine penetration. A similar experimental approach was employed by Wilson et al (1981), in determining the cytotoxic activity of 4'(9-acridinyl amino) methanesulphon-m-anisidide (m-AMSA) in multicellular spheroids grown from Chinese hamster V79-171 cells. The resistance of spheroid cells to m-AMSA was a result of the slowly cycling state of the cells and drug transport limitations.

The original observation made on resistance to adriamycin in EMT-6 mammary tumour cell spheroids was made by Sutherland (1979). These workers determined the distribution of the natural fluorescence of adriamycin equivalents by direct fluorescent microscopy. A concentration gradient of fluorescence was observed from the outside to the centre of spheroids even after exposure to high drug concentrations ($10 \mu\text{g/ml}$) for prolonged times (2 hours). Cells from enzymatically dissociated spheroids took up more drug than intact spheroids further indicating the existence of a significant diffusion barrier. By using a selective disaggregation technique after intact spheroids had been exposed to the drug it was possible to show directly that the inner spheroid cells were more resistant. The resistance was not due to differences in the cell cycle state of these inner cells therefore they concluded that in addition to drug penetration barriers, other factors related to the metabolic state of the cells and the microenvironment were implicated.

Similar studies have been performed which make use of the fluorescent properties of adriamycin. Durand (1981) used microfluorometric flow cytometry to determine the intracellular adriamycin content of disaggregated V79 spheroids. These studies confirmed the existence of a marked diffusion gradient for the drug. Intracellular fluorescence correlated well with cell survival from the various populations recovered from different spheroid layers. Durand (1982) has recently demonstrated that fluorescence activated cell sorting using the bisbenzamide stain, Hoechst 33342, can be used to separate cells as a function of depth within multicellular spheroids. The basis for the separation procedure is that the fluorescent DNA stain, as a result of its high avidity for cellular DNA, exhibits a marked diffusion/consumption gradient when it has to pass through several cell layers. Using a dual laser FACS 440, it proved possible to estimate intracellular levels of adriamycin and the DNA stain simultaneously, thus allowing correlation of cellular adriamycin content with "spheroid depth". The result of these elegant experiments are in agreement with the earlier work.

Erlichman and Vidgen (1984) examined the cytotoxic activity of adriamycin in the MGH-UI human bladder carcinoma line, grown as monolayer culture, as spheroids and xenografts in immune deprived mice. These studies suggested that adriamycin penetrates poorly into solid tissues, that in vitro clonogenic survival following adriamycin exposure of a cell suspension may predict falsely for drug sensitivity to chemotherapy and that the spheroid model more closely parallels the in vivo effects that does monolayer culture. This study was unusual in that dual cytotoxic end points for the

effect of adriamycin on the solid tumour grown subcutaneously were compared, namely growth delay and clonogenicity of the disaggregated tumour. These workers, and others, have shown that prolonged growth delay in response to adriamycin treatment is not necessarily associated with significant clonogenic cell kill. Growth delay is complex and depends on cell cycle time and the rate of cell loss, in addition to clonogenic cell kill. This study is therefore most useful as it allows comparison of monolayer, spheroid and xenograft survival directly, by means of clonogenicity. In an attempt to reveal that the spheroid model more closely parallels the in vivo effects than monolayer for adriamycin, the data presented by these authors has been ordered by introducing a term for "drug exposure". It is impossible to compare clonogenic survival in vitro and in vivo as the modes of drug exposure differ so widely. However, using a pharmacokinetic model developed to describe the pharmacokinetics of adriamycin in nude mice bearing human lung tumour xenografts (see Chapter 11) it is possible to derive a term for tumour drug exposure in vivo (by working out the cumulative area under the curve for adriamycin to which the tumour is likely to be exposed). It is also possible to convert the drug exposures in vitro to a cumulative AUC, and the result of their data, expressed in this way are summarised in fig 1.4. The clonogenic survival curve for spheroids, for an identical cumulative AUC is considerably closer to that seen for solid tumour than monolayer. Nevertheless, the clonogenic survival in spheroids is less than that for solid tumour indicating the intermediate complexity of the spheroid as a model for in vitro prediction of drug sensitivity.

Several factors may be partly responsible for the dramatic increase in drug resistance of cells exposed in spheroids compared to exponentially growing cells in monolayer; differing drug metabolism in spheroid cells related to hypoxia; gradients in diffusion of nutrients to the spheroid core; protection of spheroid cells by intercellular communication; drug resistance of central hypoxic cells; differing cell kinetic parameters, with a predominance of slowly cycling and non-cycling cells in the centre of the spheroid; reduced drug availability due to penetration barriers. It would seem unlikely that any single factor could explain spheroid cell resistance, rather a combination of factors which will vary for different drugs.

AIMS OF THESIS

The aims of this thesis are summarised as follows:-

- a) Investigation of the cellular pharmacokinetics of adriamycin accumulation in human lung tumour monolayers and its relationship to cytotoxicity.
- b) Comparison of the rate, degree of uptake and cellular localisation of lipophilic derivatives of adriamycin in monolayer systems
- c) Comparison of adriamycin and lipophilic anthracycline derivatives in multicellular spheroids with regard to differential penetration and cytotoxicity.
- d) Identification of putative adriamycin penetration enhancing agents, such as membrane permeabilisers, in monolayer and their further study in spheroid culture systems.

- e) Investigation of the distribution and penetration of adriamycin in solid tumour systems
- f) Comparison of the pharmacokinetics and cytotoxicity of adriamycin and adriamycin encapsulated in slow release surfactant vesicles (niosomes) in nude mice bearing human lung tumour xenografts.

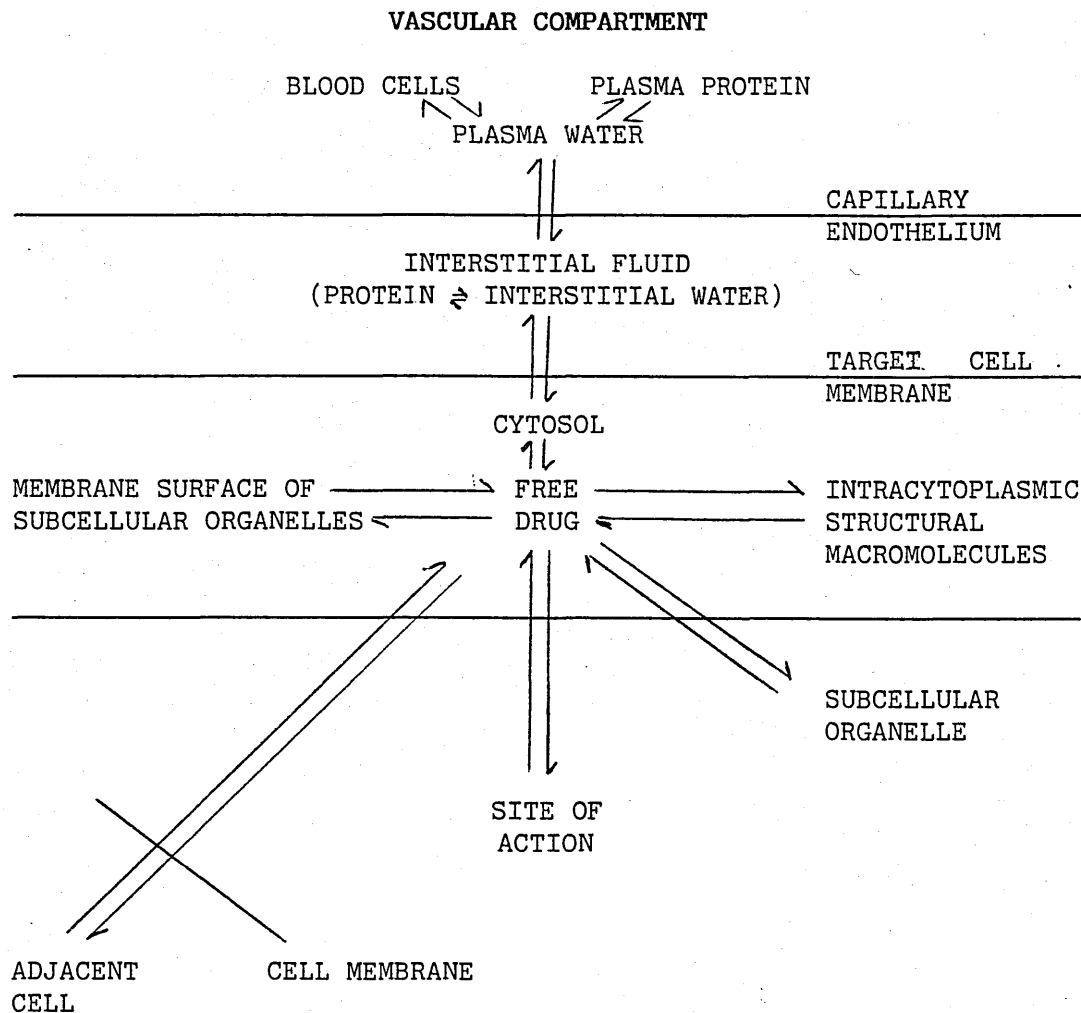


Figure 1.1 Drug equilibria between the vascular compartment and site of action.

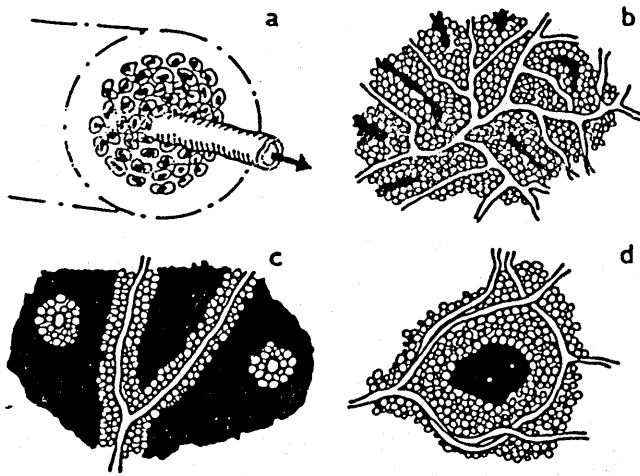


Figure 1.2 Schematic patterns of vascularisation. A capillary surrounded by viable cells is indicated in a. Regions with different capillary architectures are shown in b, c and d.

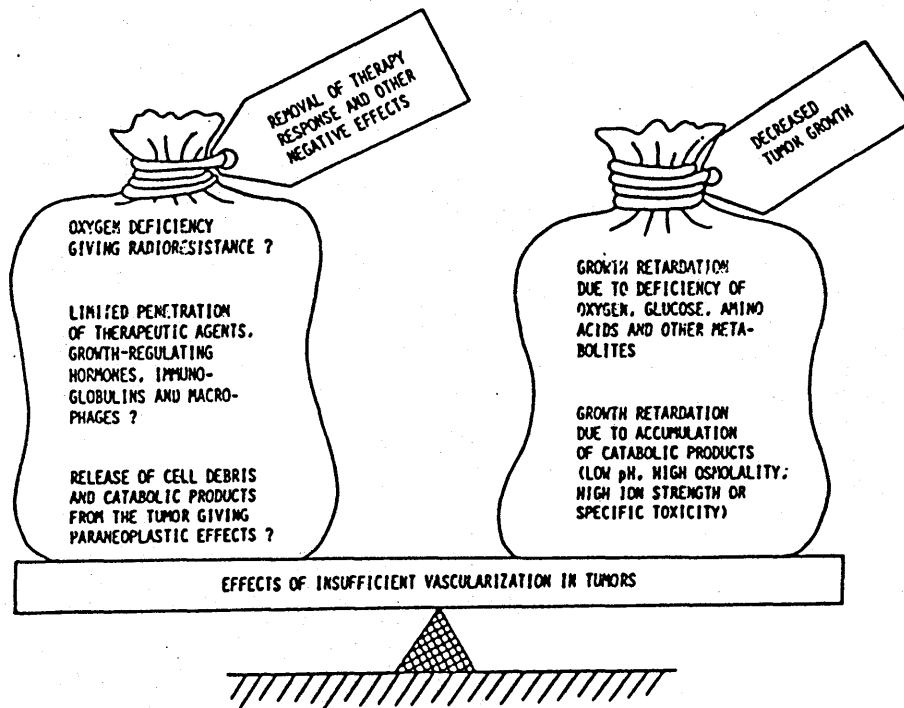
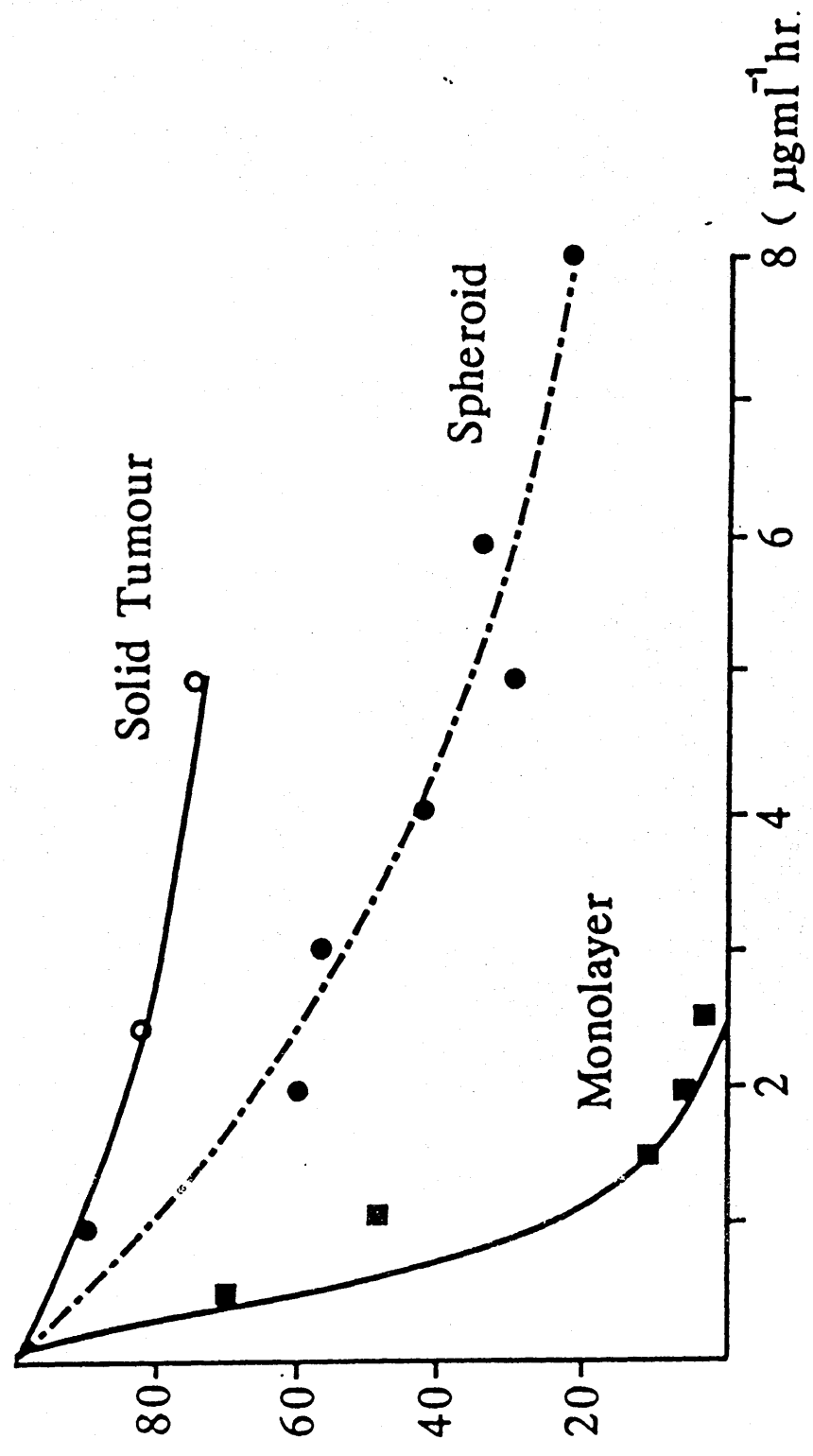


Figure 1.3 Examples of negative effects (left) and positive effects (right) on the patient, due to insufficient vascularisation of the tumour.

**% Clonogenic cell survival
(MGH-UI Human Bladder Carcinoma Line)**



**Drug Concentration
(Cumulative AUC for Cxt curve)**

Figure 1.4 Clonogenic cell survival vs cumulative adriamycin exposure for monolayer, spheroid and xenograft of the MGH-UI cell line.

Cellular uptake and disposition of adriamycin and 4'-deoxydoxorubicin and its relationship to cytotoxicity in human non small cell lung cancer monolayers.

2.1. INTRODUCTION

4'Deoxydoxorubicin (4'-deoxy) is a new adriamycin analogue synthesised by removal of the hydroxyl group on the 4' position of the daunosamine sugar (Fig 5.2). The compound is less cardiotoxic than the parent drug and in a series of experimental tumours in the mouse, it showed antitumoral activity similar to and potency generally superior to that of adriamycin (Arcamone, 1977; Arlandini et al, 1977; Di Marco et al, 1977). Although the derivatised drug differs only in substitution of a single hydroxyl group, this confers notably different physico-chemical properties on the compound. 4'-deoxy is considerably more lipophilic than adriamycin and would therefore be expected to cross the lipid domain of the tumour cell membrane with greater facility. In this chapter, we report the relationship between intracellular levels of the two drugs and the corresponding cytotoxicity to human non-small cell lung tumour cells in the exponential phase of monolayer growth.

Cell culture: The L-DAN cell line was derived from our own patient with squamous cell lung cancer. The cells were maintained as a monolayer in exponential growth on Ham's F-10/DMEM medium (50:50) with 8mM sodium bicarbonate supplemented with foetal calf serum. All experiments were carried out in the exponential phase of growth and the cloning efficiency of these cells ranged between 20-25%.

Conditions of drug exposure and determination of cell survival :

L-DAN monolayers were exposed to a range of drug concentrations for differing times. The drugs were kindly supplied by Farmitalia Carlo Erba, and were administered to the cells in culture medium after dissolution in normal saline. After drug exposure, the cells were washed twice with ice cold phosphate buffered saline in order to remove loosely bound or surface absorbed drug. The cells were then harvested with 0.25% trypsin in PBS, centrifuged, washed once in ice cold medium and counted (Coulter Counter Ltd, Poole, England). The cells were then resuspended in distilled water and the resulting cell lysate was frozen and stored at -20°C until drug extraction and analysis was performed.

During the clonogenic assay for cell survival, the monolayers were either exposed to the cytotoxic agents for one hour over a wide concentration range (0.1 $\mu\text{g}/\text{ml}$ to 10 $\mu\text{g}/\text{ml}$) in growth medium or were exposed at a constant concentration of 5 $\mu\text{g}/\text{ml}$ for differing times (15-60 min). After drug exposure the cells were trypsinised, centrifuged and washed with ice cold medium. The cells were then diluted in medium and plated at 200 cells/ml into 5cm diameter petri dishes. The plates were incubated for 12 days

in a humid 2% CO₂ atmosphere. The colonies were then fixed and stained with a solution of methylene blue (0.1%) in 70% ethanol and colonies of >40 cells were counted. Following the usual convention the cloning efficiency of the treated cells was expressed as a percentage of control survival.

Drug measurement: Intracellular levels of drug were measured by extraction from the cell lysate with a mixture of chloroform and isopropanol and subsequent analysis by high pressure liquid chromatography (HPLC) utilising a fluorescent detector. This method has been described in our laboratory (Cummings et al, 1984) and allows detection of both parent drug and metabolites. All solvents were of HPLC grade and the limit of detection of the assay was 1 ng. Results were expressed as ng/10⁵ cells.

Determination of oil-water partition coefficient: Lipid solubility was determined by measuring the partition of the drug between butanol and Tris-HCl buffer and expressing the result as the solvent/aqueous concentration ratio (Brodie, 1964).

Intracellular localisation of the drug: The cells were exposed in monolayer to the drugs at a concentration of 5µg/ml in medium for up to six hours. When the incubation had been completed the drug containing medium was removed and the cells washed with ice cold medium. A coverslip was mounted in uvinert and the cells examined under a Polyvar fluorescent microscope ($\lambda_{excitation} = 486 \text{ nm}$; $\lambda_{emission} = 550 \text{ nm}$) using oil immersion (x400 magnification). In a separate experiment the cells were fixed with formol saline and

stained by Altmann's technique in order to demonstrate the cytoplasmic distribution of mitochondria. In addition, after exposure to both drugs (10 $\mu\text{g/ml}$) for 2 hours, the cells were prepared routinely for electron microscopy. (sec 4.2)

Statistical analysis: Drug uptake curves were fitted using a non-linear regressive technique on an in house programme based on the Marquhardt algorithm (Bevington, 1978).

The effect of intracellular drug concentration and duration of exposure on uptake by cells: The time course of uptake of adriamycin and 4'-deoxy (figs 2.1 and 2.2) showed that the intra-cellular drug concentration was dependent on the drug concentration in the medium and the duration of drug-cell contact. Clearly 4'-deoxy (oil-water partition coefficient, 16.2) was taken up more rapidly and to a greater extent than the less lipophilic parent compound adriamycin (oil-water partition coefficient, 6.3). Using computer fitted data it was possible to calculate the initial rate of drug uptake.

The respective maximal rates of drug influx were V_{max} , Adriamycin = $0.156 \text{ ng}/10^5 \text{ cell}/\text{min}$ and V_{max} , 4'-deoxy = $30 \text{ ng}/10^5 \text{ cell}/\text{min}$. Fig 2.3 shows the relationship between intracellular and extracellular drug levels after exposure of one hour (the duration of cell-drug contact during the clonogenic assay).

Correlation between external and internal concentrations and cell survival: Based on extracellular drug concentrations, there is no significant difference in cell survival comparing adriamycin and 4'-deoxy (Fig 2.4). The ID_{90} for adriamycin ($2.1 \mu\text{g}/\text{ml}$) and 4'-deoxy ($2.2 \mu\text{g}/\text{ml}$) are virtually identical, on the basis of medium concentration. However, if intracellular levels of drugs are plotted against cell survival (Fig 2.5), adriamycin achieves greater cell kill at relatively lower internal drug concentrations (LD_{90} adriamycin = $3.5 \text{ ng}/10^5 \text{ cells}$; intracellular LD_{90} 4'-deoxy = $72 \text{ ng}/10^5 \text{ cells}$).

Relationship between cell survival and the duration of drug

exposure: The greater the duration of drug exposure at constant concentration, the greater the degree of cell kill (Fig 2.6). The relationship between cell survival and time was biexponential for 4'-deoxy, with relatively greater cell kill after short drug exposures than adriamycin.

Intracellular drug metabolism: There was no evidence of drug metabolism occurring in the medium. 4'-deoxy was metabolised within the cells to its alcohol, 4'-deoxydoxorubicinol (Fig 2.7). The enzyme responsible for this (Bachur, 1979) is a ubiquitous cytoplasmic enzyme, NADPH-dependent aldo-keto reductase. The rate of alcohol formation was relatively constant over a wide range of external drug concentrations which may imply that the enzyme was not saturated despite the relatively high intracellular drug concentrations achieved. We were unable to detect adriamycinol in the adriamycin treated cells. It is possible that the alcohol is being formed but is below the limit of detection in our HPLC assay as the intracellular levels of the parent drug is low.

Intracellular localisation of drug: The monolayers were examined sequentially for 6 hours after exposure to both drugs at fixed concentration (5 μ g/ml). Intracellular adriamycin was confined to the nucleus as far as could be determined by light microscopy (fig 2.8). 4'-deoxy was localised solely within the nucleus with incubations for 10 minutes but granular cytoplasmic fluorescence had appeared by 20 minutes and thereafter increased in degree until it predominated (fig 2.9). We considered the possibility that 4'-deoxy was binding to mitochondria within the cytoplasm,

however, Altman's mitochondrial stain demonstrated a different size and distribution of granules from these "stained" by 4'-deoxy. Ultrastructural studies (Fig 2.10) showed marked nuclear disruption and chromatolysis after treatment with both drugs. However, large lysosomal vesicles were seen in the cells treated with 4'-deoxy.

2.4 DISCUSSION

We have demonstrated that deletion of a hydroxyl group on the daunosamine moiety profoundly alters the physico-chemical properties of adriamycin, particularly lipid solubility. The increased lipophilicity of 4'-deoxy as manifested by the elevated oil-water partition coefficient, is probably the main factor contributing to the increased rate and cellular uptake seen with this drug in our monolayer systems. Cassaza (1979) has reviewed the relationship between cell uptake in vitro and the partition coefficient of anthracycline analogues, and for groups of homogeneous derivatives it would seem that lipid solubility is an important determinant of cell uptake. Di Marco et al (1977) have compared cell uptake of the two drugs over a limited concentration-time range in a suspension of L1210 cells. They expressed intracellular drug levels as the ratio of moles drug bound/mole DNA and found a 14-times greater accumulation of 4'-deoxy in that cell system.

Biological membranes are lipid in nature and the ease with which a drug molecule will cross a membrane will depend, in part, on its ability to dissolve in the lipid domain of the cell membrane. Skovsgaard (1978) demonstrated that membrane transport is rate limiting for adriamycin uptake in Ehrlich ascites tumour cells and he proposed a carrier mediated drug transport mechanism. However, more recently, Dalmark (Dalmark, 1981; Dalmark and Storm, 1981; Dalmark, 1982) has presented transport data from human erythrocytes and Ehrlich ascites tumour cells, from which it appears that adriamycin transport takes place by free diffusion of the electroneutral molecule through the lipid domain of the cell membrane. Adriamycin can self-associate through hydrophobic interaction in aqueous solution and form dimers to which the cell

is relatively impermeant. This situation would mimic a carrier mediated transport process although transport of the permeant takes place by simple Fickian diffusion. This may be the explanation for the earlier finding of Skovsgaard. Our results would tend to support Dalmark's hypothesis in that the more lipid soluble drug is accumulated to a greater degree.

On the basis of extracellular drug concentrations, cell kill was virtually identical for both adriamycin and 4'-deoxy. However, the correlation between intracellular drug concentrations and cytotoxicity differed for adriamycin and 4'-deoxy. For a given intracellular concentration, adriamycin is more cytotoxic than 4'-deoxy. The log cell survival plot (Fig 2.5) for adriamycin is linear over the intracellular concentration range whereas the curve for 4'-deoxy is biphasic with a relative plateau after 1% cell survival

The relationship between cell survival and the duration of drug exposure is mono-exponential for adriamycin and biexponential for 4'-deoxy. There is relatively greater cell kill during short drug exposure for 4'-deoxy, which is probably related to the rapid rate of cell uptake. It is interesting to note that the curves for cell survival vs. intracellular drug concentration, and cell survival vs. duration of drug exposure are both biphasic. It is possible that the initial rapid phase of drug uptake is the major determinant of cytotoxicity.

These results are similar to those reported by Bhuyan et al (1981) who studied intracellular uptake of another lipophilic anthracycline, 7-con-0-methylnogarol (7-OMEN) in chinese hamster ovary, B16 and L1210 cells in culture. 7-OMEN was taken up more

rapidly in Bl6 cells than adriamycin and had a biphasic cell survival curve. The biphasic curve may implicate a resistant subpopulation or, perhaps more likely as Bhuyan commented, may be a characteristic of a drug which showed predominant accumulation in the cytoplasm.

The time course of drug distribution within the cell is conspicuously different, as demonstrated by fluorescent microscopy. Adriamycin was located mainly within the nucleus whereas 4'-deoxy was distributed both in the nucleus and in a granular fashion within the cytoplasm. Initially we considered the possibility that 4'-deoxy was binding to mitochondrial structures but conventional histochemical localisation of mitochondria using Altmann's stain showed an entirely different distribution. Facchinetti et al (1978) studied the time course of intracellular distribution of adriamycin and N-trifluoroacetyladiamycin-14-valerate (NTAV) in mouse peritoneal macrophages. They found that adriamycin cytofluorescence, at higher extracellular concentrations than used in our experiments, was seen initially in the nucleus and later appeared in a granular distribution within the cytoplasm. The lipophilic derivative NTAV localised within the cytoplasm in a granular fashion with a similar distribution to 4'-deoxy. Ultrastructural studies showed that NTAV was bound within intracytoplasmic vesicles of an amorphous nature. Electron microscopy following cellular exposure to 4'-deoxy revealed large lysosomal vesicles, which could have been the fluorescent granular structures seen on light microscopy in this present study.

It would only require approximately 2-5% of total intracellular 4'-deoxy to bind to the nucleus to give levels approximate to total intracellular adriamycin (for a given concentration/time exposure). Fluorescent microscopy is a rather insensitive method of quantitating the amount of drug present within specific cell structures but it is possible that nuclear binding of 4'-deoxy is occurring to a significant extent although fluorescent light microscopy reveals a predominantly cytoplasmic distribution. Egorin et al (1980) have shown that DNA can quench the fluorescence of some anthracyclines more than that of others, which may be a further contributing factor.

These results indicate that the relationship between cytotoxicity and intracellular drug levels is complex when comparing a lipophilic derivative with its parent compound. The importance of anthracyclenic cytofluorescence distribution is unknown. Egorin et al (1980) have examined the intracellular localisation of a number of different anthracyclines and have shown that there is no correlation between the intracellular distribution of drug after exposure to intact cells and accumulation by isolated nuclei. It is possible that differential nuclear-cytoplasmic localisation may not be related to different modes of drug action at cellular level but may represent intracytoplasmic storage for lipophilic drugs. As a result of these findings in monolayer, these drugs were then compared in a multicellular spheroid model.

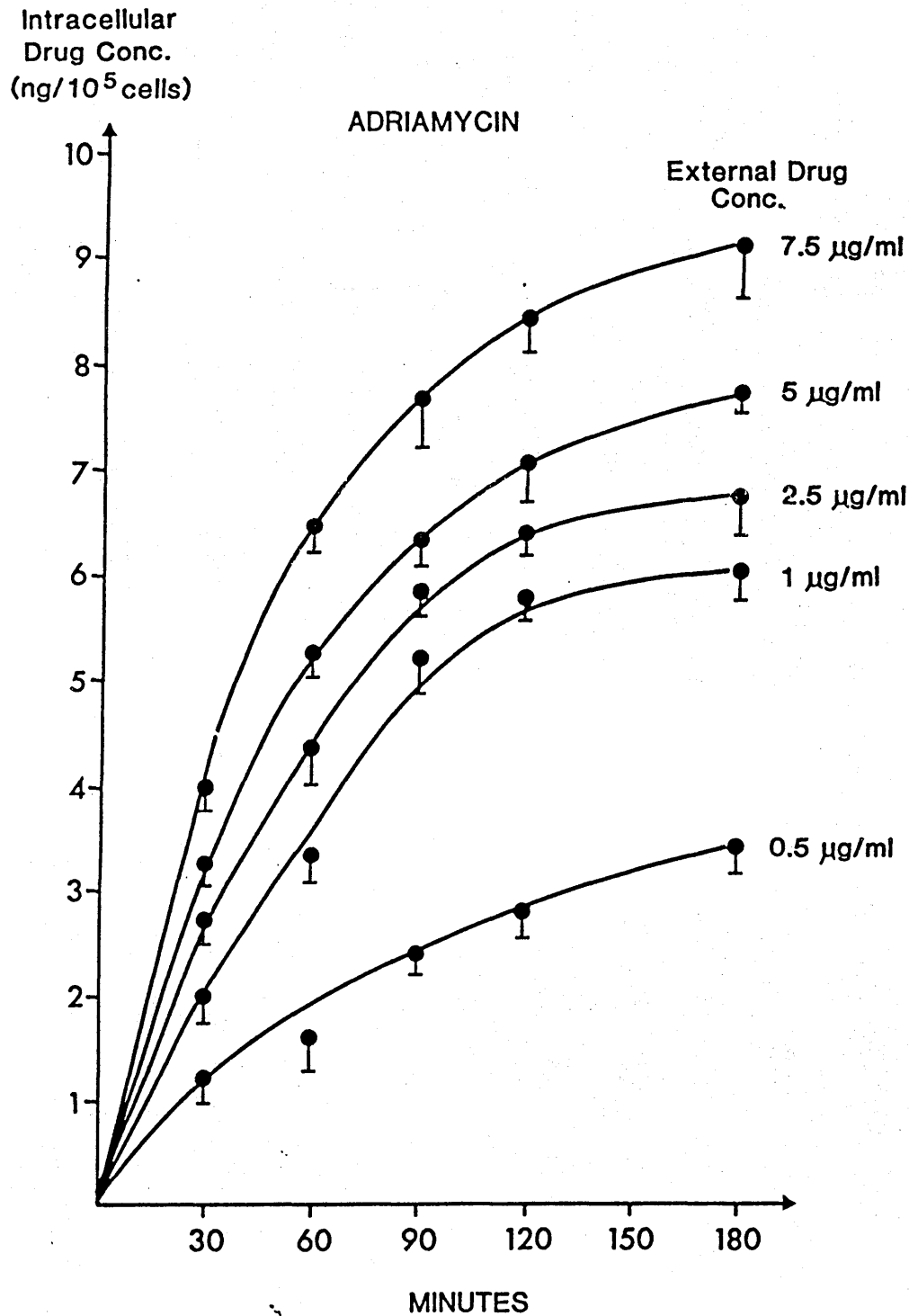


Figure 2.1 Intracellular levels of adriamycin following exposure to a range of external drug concentrations for up to 3 hours. Each point represents the mean of 4 experiments and the vertical bar denotes 1 stand deviation.

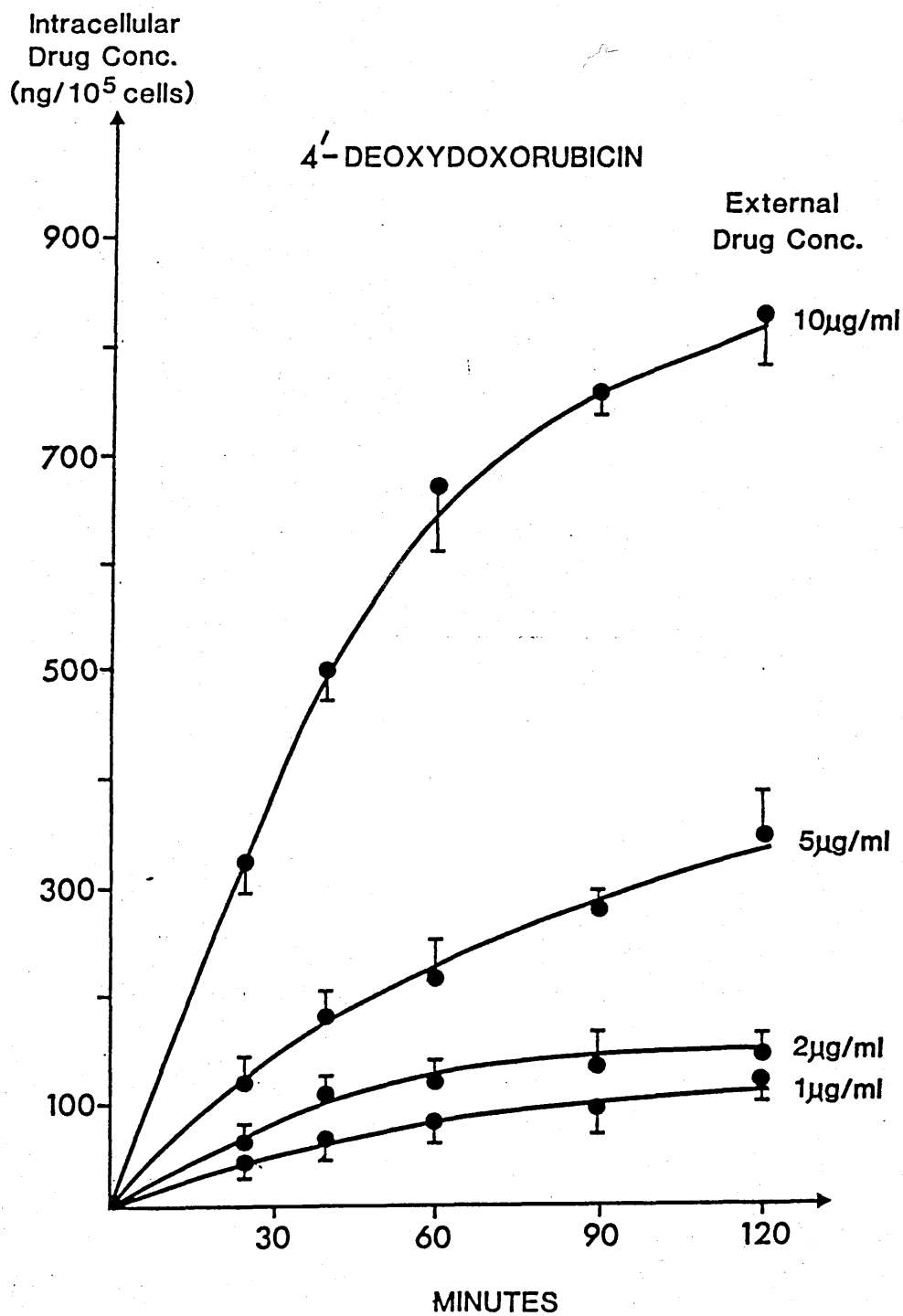


Figure 2.2 Intracellular levels of 4'-deoxy following exposure to a range of external drug concentrations for up to 2 hours. Each point represents the mean of 4 experiments and the vertical bar denotes 1 standard deviation.

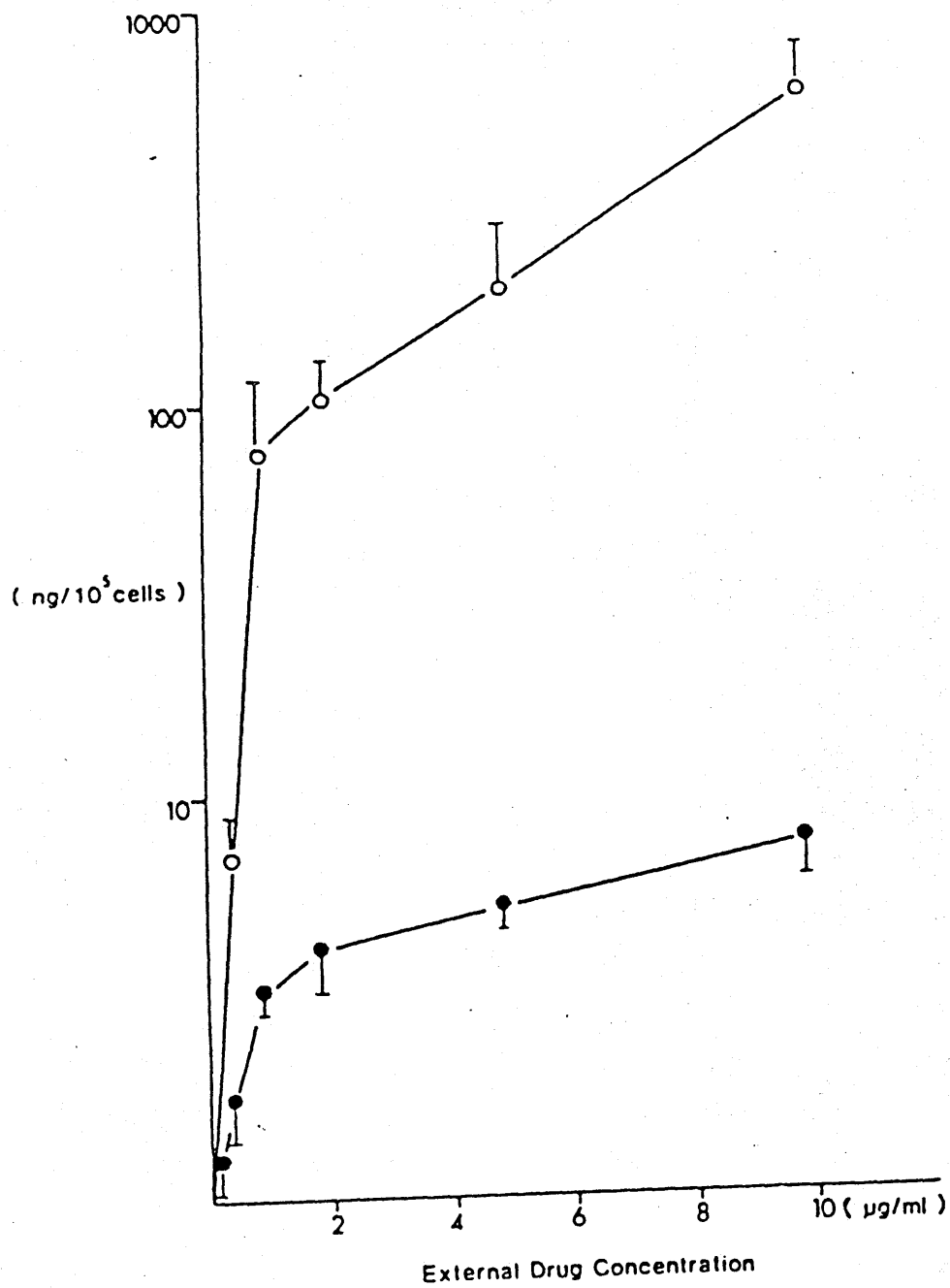


Figure 2.3 The relationship between intracellular and extracellular drug concentrations for adriamycin (●) and 4'-deoxy (○). Each point is the mean of 4 experiments and the vertical bar denotes 1 standard deviation.

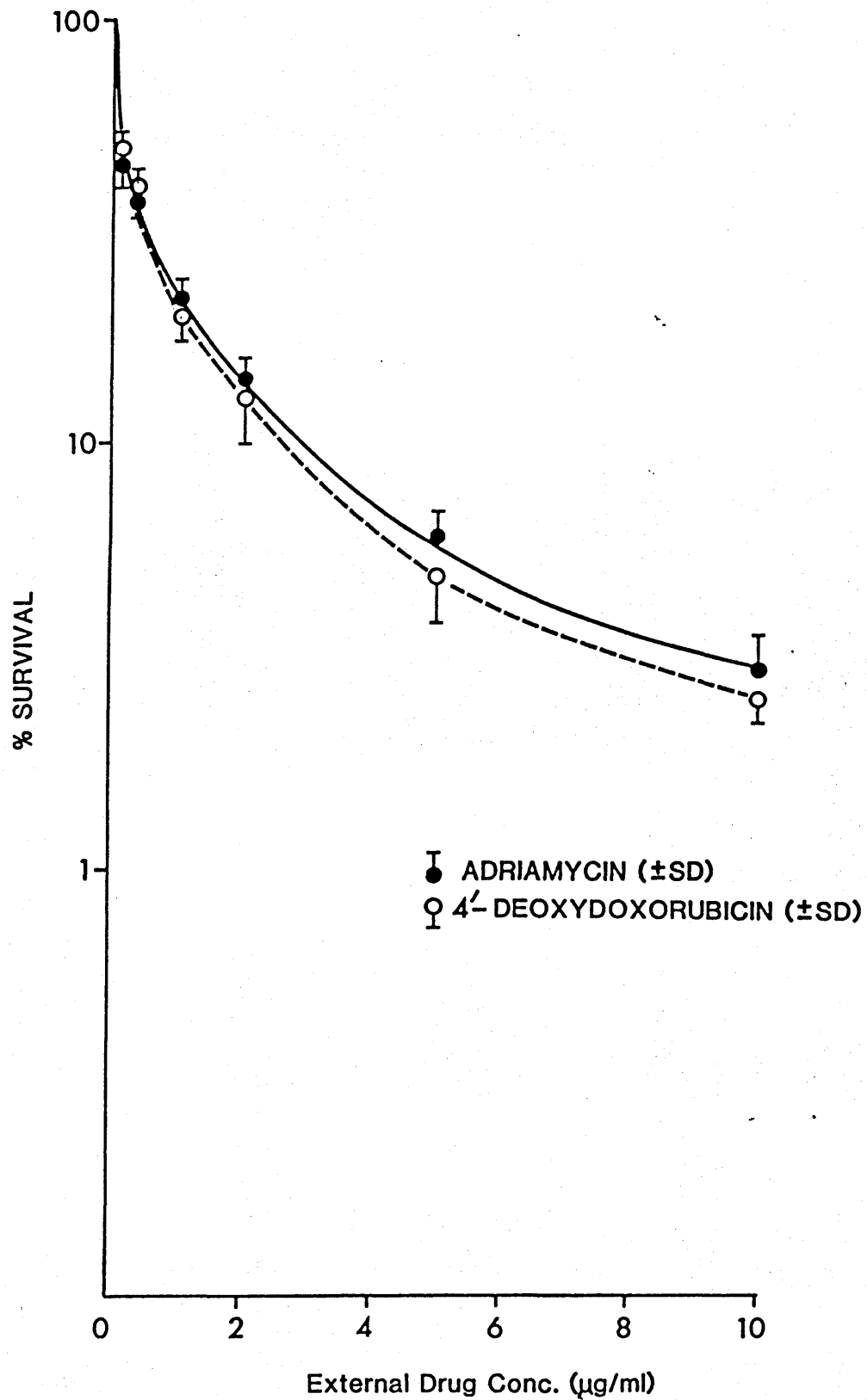


Figure 2.4 Clonogenic survival for LDAN monolayers exposed to adriamycin (●) or 4'-deoxy (○). Each point represents the mean of 4 experiments and the vertical bar denotes 1 standard deviation.

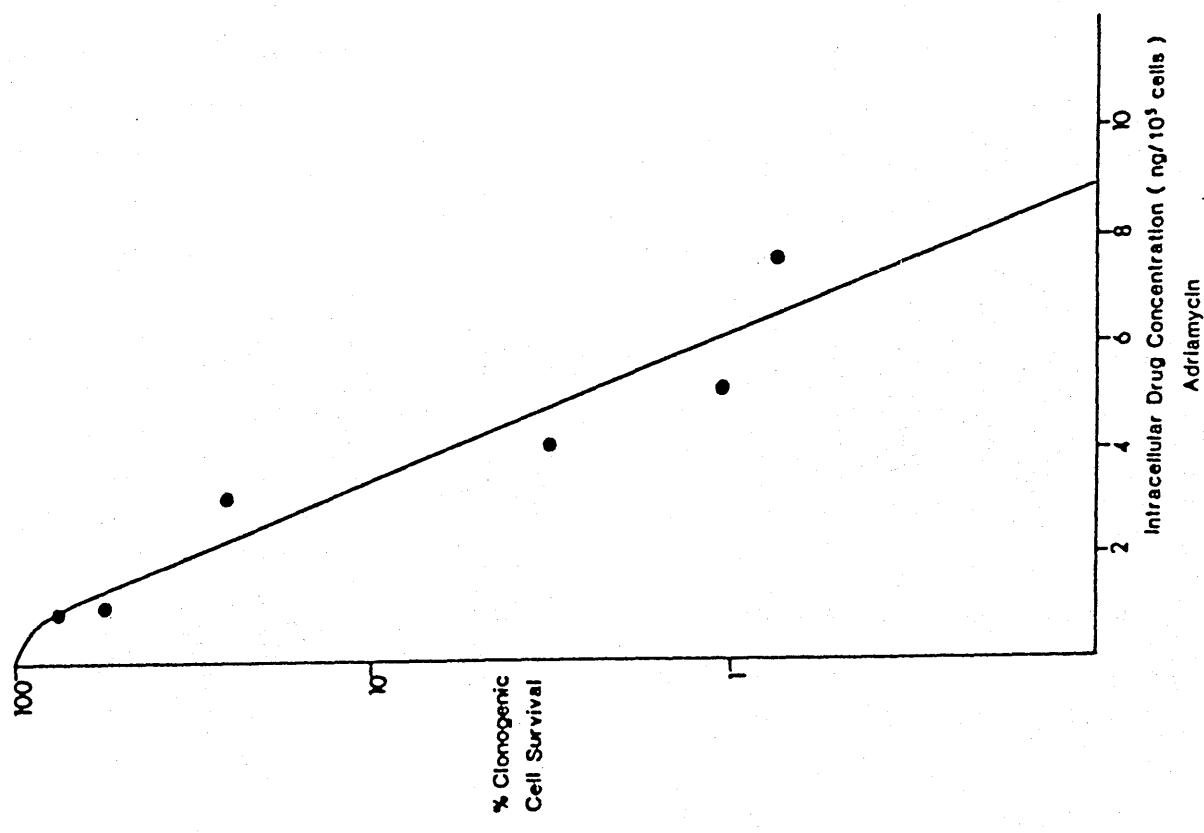
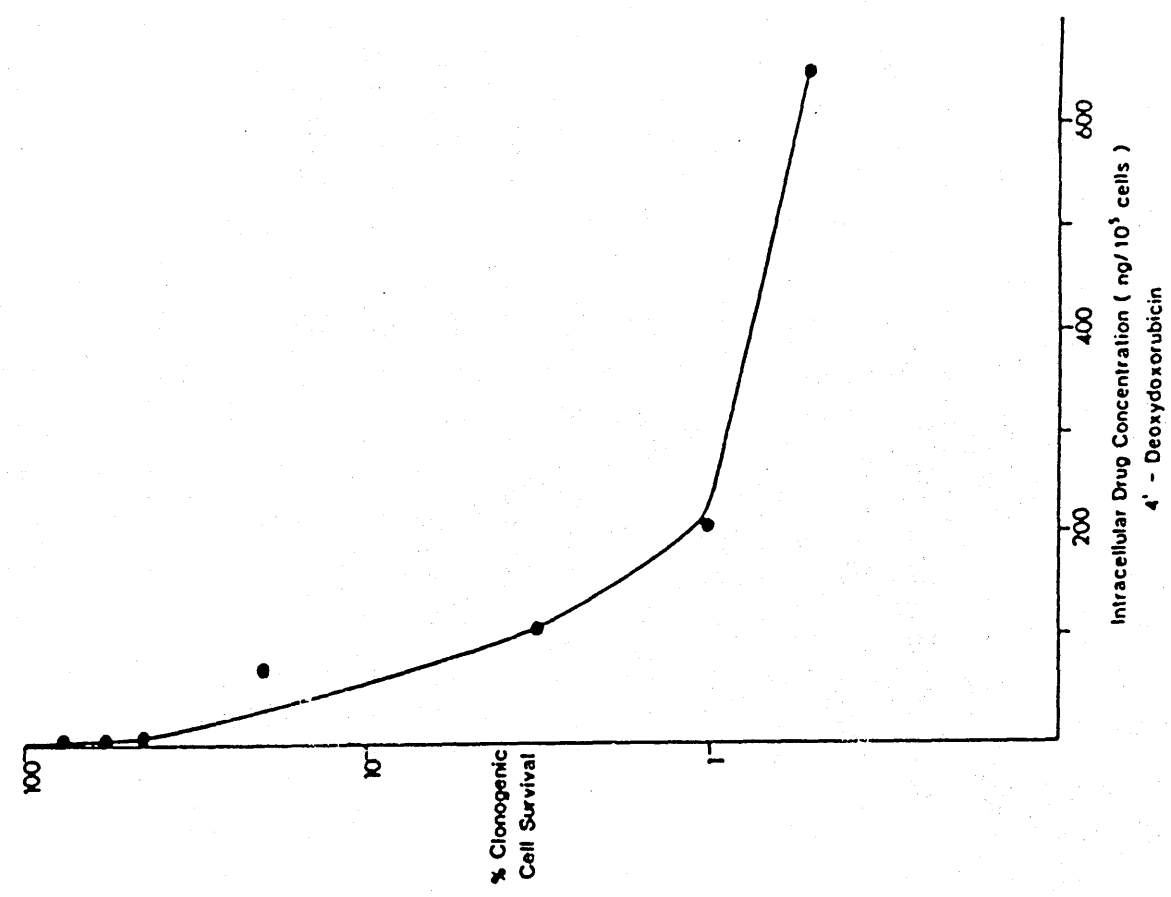


Figure 2.5 The relationship between intracellular drug concentrations and cell survival. Each point is the mean of 4 experiments.

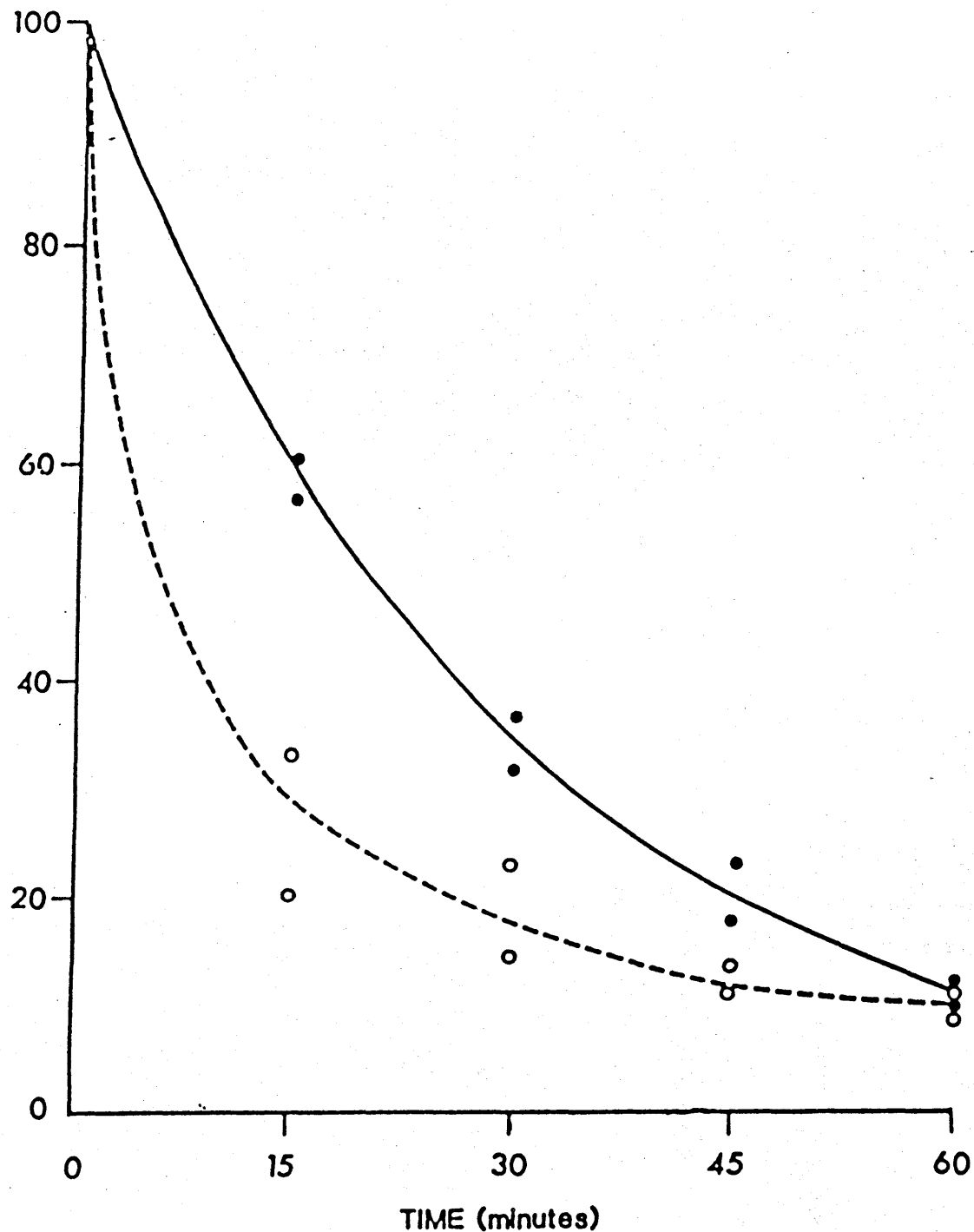
% CLONOGENIC
CELL SURVIVAL

Figure 2.6 The relationship between clonogenic cell survival and the duration of exposure at constant drug concentration, 5 ug/ml. (Adriamycin, ● ; 4'-deoxy ○). The curves were computer fitted to data from 2 experiments.

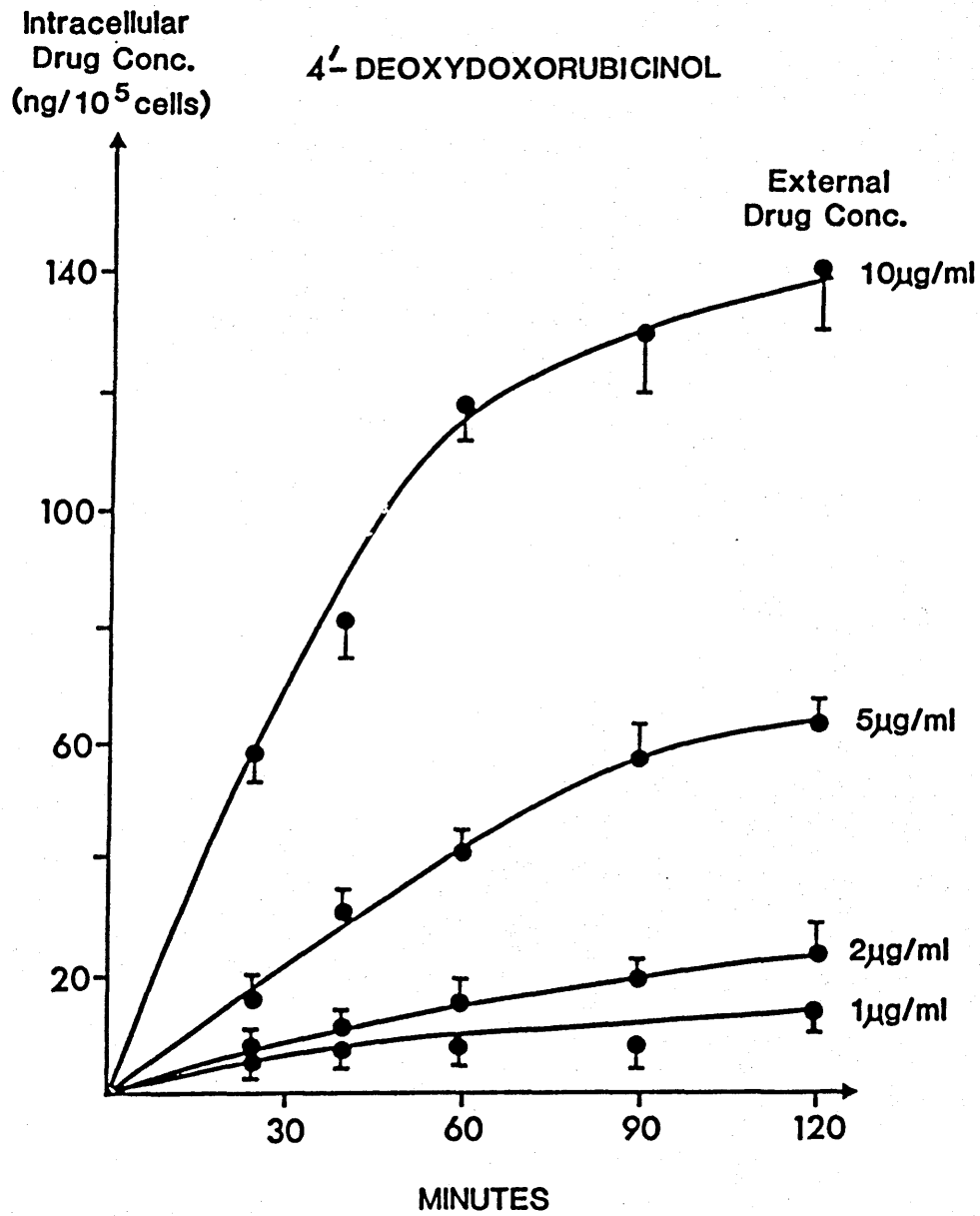


Figure 2.7 Intracellular levels of 4'-deoxydoxorubicinol after exposure to a range of concentrations of 4'-deoxy. Each point is the mean of 4 experiments and the vertical bar denotes 1 standard deviation.

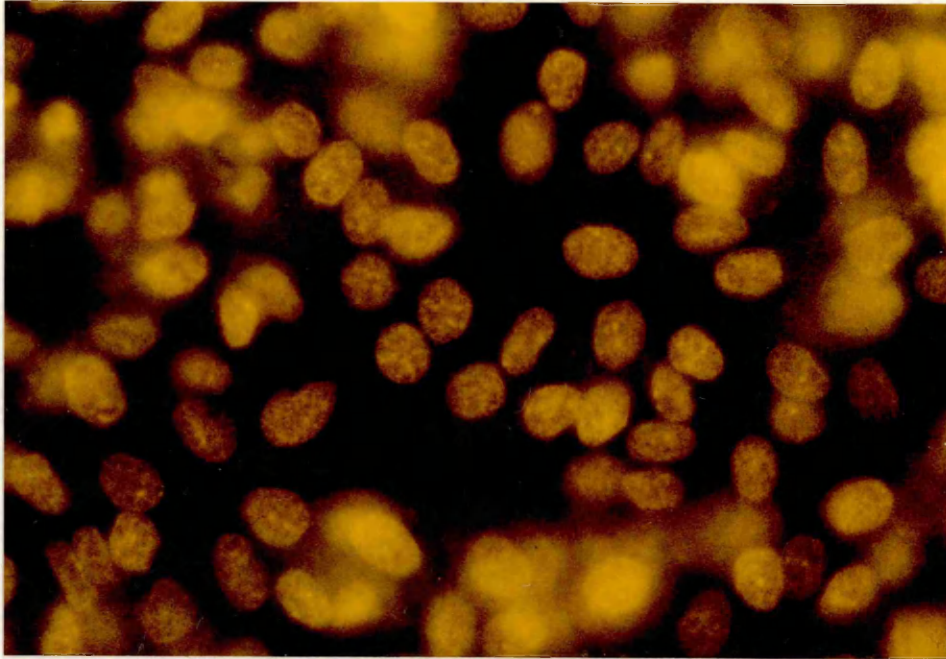


Figure 2.8 Fluorescent photomicrograph of L-DAN monolayers treated with adriamycin ($2 \mu\text{g}/\text{ml}$ for 2 hours). Nuclear staining is evident (magnification $\times 150$).

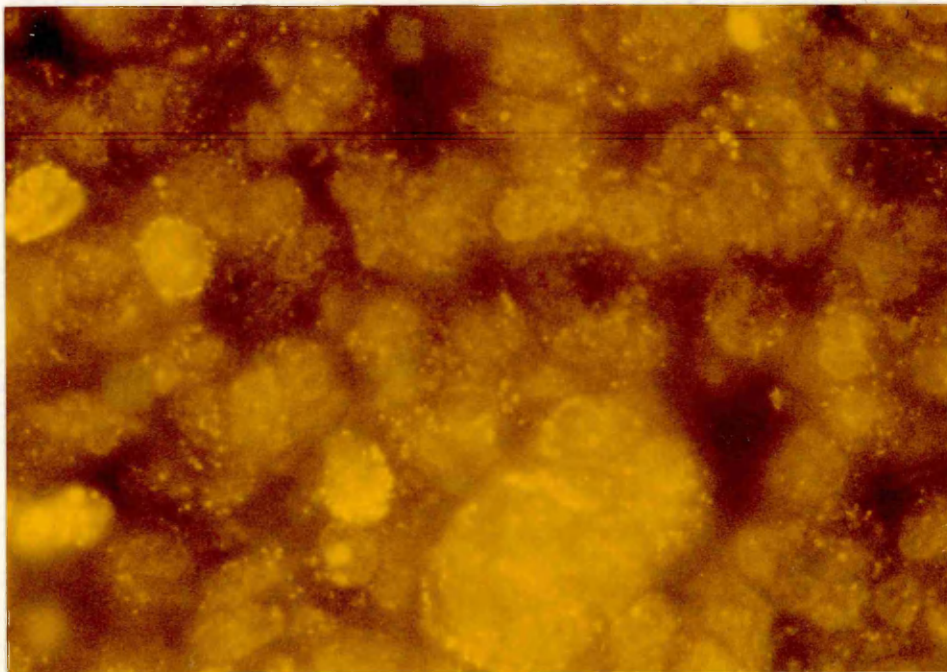


Figure 2.9 Fluorescent photomicrograph of L-DAN monolayers treated with 4'-deoxy ($2 \mu\text{g}/\text{ml}$ for 2 hours). There is granular, cytoplasmic fluorescence in addition to nuclear and nuclear envelope staining (magnification $\times 150$).

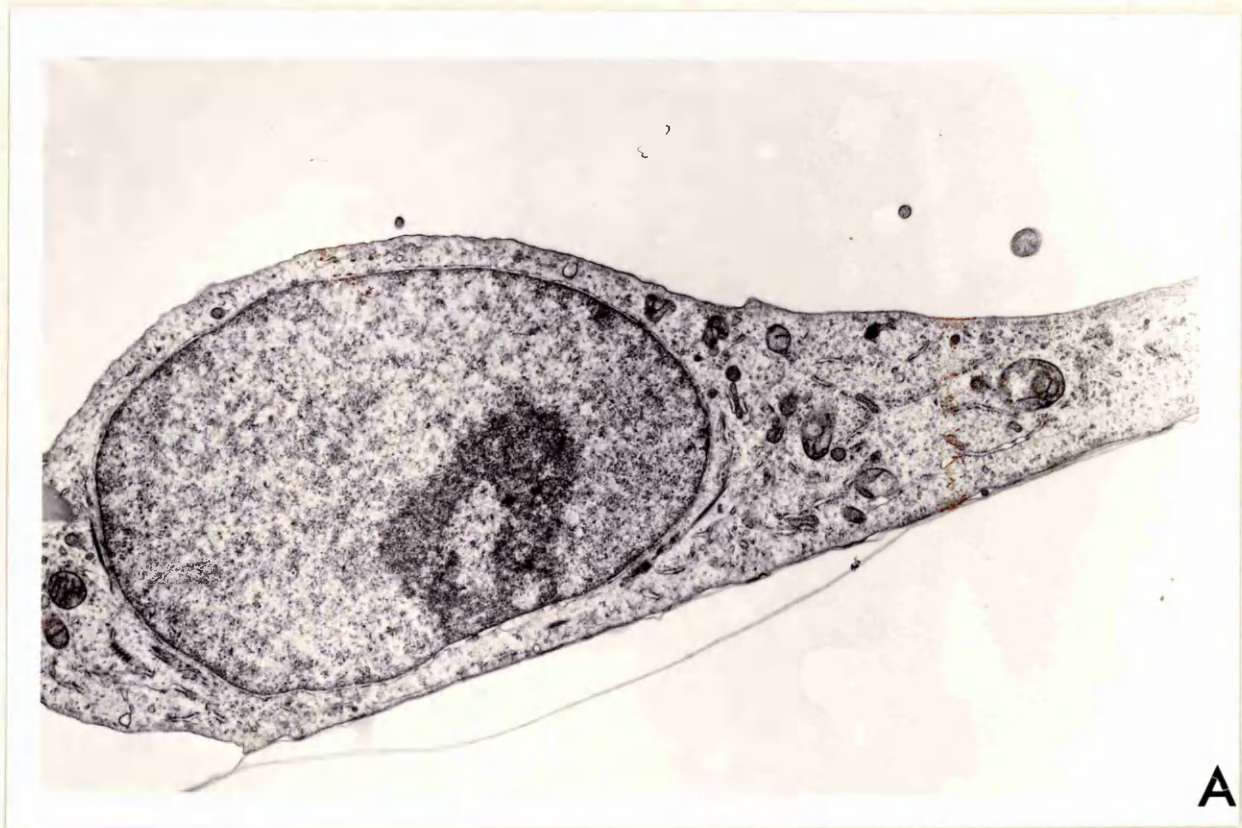
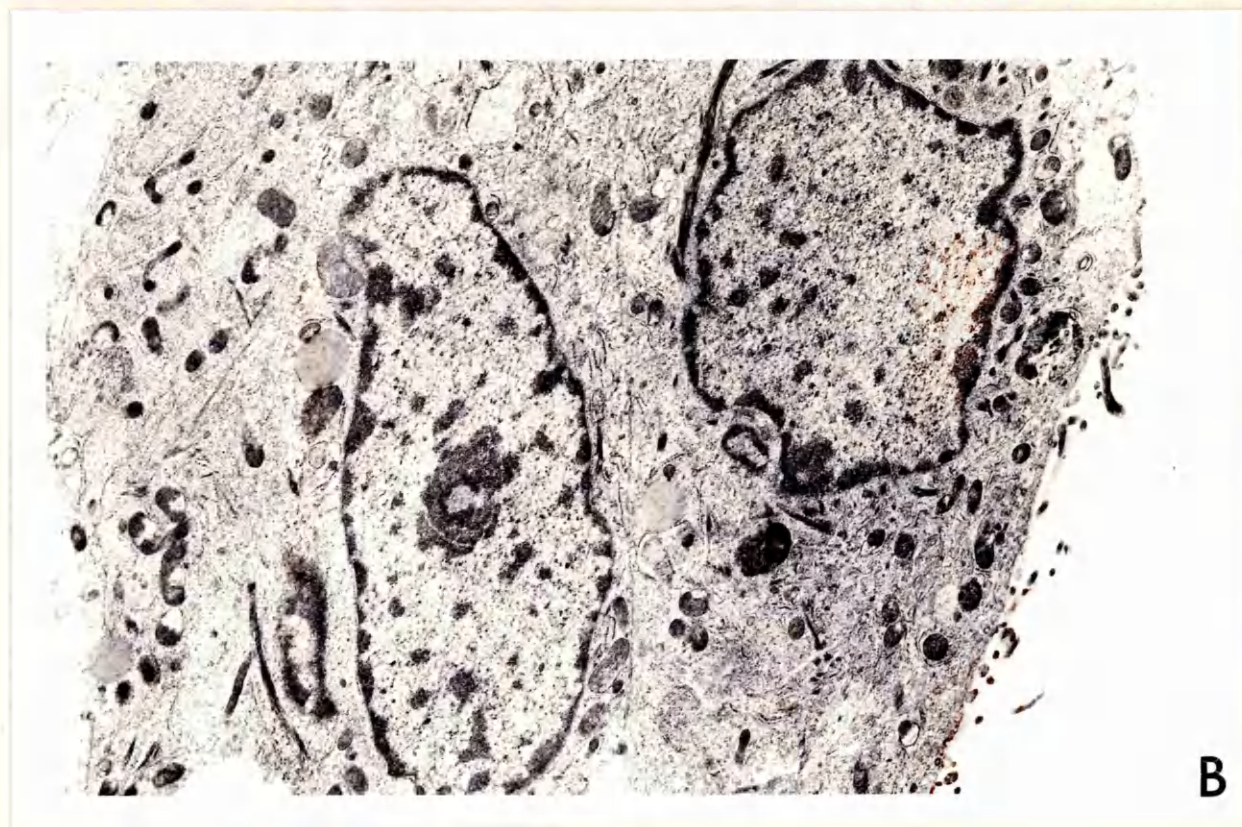
**A****B**

Figure 2.10 Electron micrograph of L-DAN cell. A) Normal Cell
B) Cell treated with 4-β'-deoxy. Note nuclear disruption and chromatolysis and cytoplasmic lysosomal vesicles (arrowed) (magnification x 2950)

CHAPTER 3

Penetration and relative cytotoxicity of adriamycin and 4'-deoxydoxorubicin in human lung tumour spheroids.

3.1 INTRODUCTION

The multicellular spheroid model was developed as a system of intermediate complexity between solid tumours and monolayers in which 3-dimensional growth of cells creates microenvironments that simulate micrometastatic foci (Sutherland et al, 1981). Resistance of intact spheroid cells to drug treatment has been reported for a number of cytotoxic agents and the existence of drug penetration barriers has been postulated (Nederman et al, 1981)

Fluorescent microscopic (Sutherland et al, 1979) and flow cytometric (Durand, 1981) studies have shown that adriamycin is localised within the outer cell layers of V79 Chinese Hamster spheroids and that the inner spheroid core cells are relatively resistant to the cytotoxic effects of the drug. We have shown that 4'-deoxydoxorubicin (4'-deoxy), a lipophilic derivative of adriamycin is taken up more rapidly and to a greater extent than the parent drug by human lung tumour cells grown as monolayers, although its cytotoxic activity in this system is similar to that of adriamycin. In this study we have assessed differential penetration of the two drugs in human lung tumour spheroids by Fluorescent microscopy and have compared their cytotoxic effects in spheroid and monolayer.

Cell Culture: The L-DAN cell line was derived from our own patient with squamous lung cancer. The cells were maintained as a monolayer in exponential growth in Ham's F10/DMEM (50:50) with 8mM NaHCO₃ supplemented with foetal calf serum. The monolayers were disaggregated enzymatically with 0.25% trypsin in PBS and the resultant cell suspension used to provide cells for initiation of tumour spheroids, using the "agar underlay" static method (Yuhás et al, 1977).

During growth delay experiments, spheroid size was monitored by twice weekly measurement of cross-sectional areas of individual spheroids using a "Micromeasurements" image analysis system coupled via a television camera to an inverted optical microscope (Twentyman, 1982). These area measurements were subsequently converted to volumes, assuming spherical geometry.

Conditions of drug exposure and determination of cell survival:

L-DAN monolayers and spheroids were exposed to both drugs over a range of concentrations (0.1 - 20 µg/ml) for 1 hour, or at a fixed drug concentration of 10 µg/ml for varying periods of time (15 minutes - 2 hours). The monolayers were treated in both the exponential and plateau phase of growth. Exponentially growing cells were harvested on day 3, plateau phase cells on day 7. The drugs were kindly supplied by Farmitalia Carlo Erba and were administered to the cells in culture medium after dissolution in normal saline.

After treatment, the monolayer cells were harvested with 0.25% trypsin in PBS, centrifuged and washed with ice cold medium.

The cells were then diluted in medium and seeded at 200 cells/ml in 5 cm petri dishes. The plates were incubated for 12 days in a humid 2% CO₂ atmosphere. The colonies were then fixed and stained with methylene blue and colonies of >40 cells were counted. Following the usual convention the cloning efficiency of the untreated cells was normalised to 100% and the cloning efficiency of the treated cells was expressed as a percentage of control survival.

Spheroids from two flasks were pooled and a number of glass universal tubes were prepared, each containing two to three hundred spheroids with a mean diameter of approximately 350µm. The spheroids were treated with similar drug concentrations and durations of exposure as used in monolayer at 37 °C with intermittent agitation. At the end of this period the spheroids were allowed to sediment, the drug containing medium was removed and they were washed with fresh, ice cold medium. The spheroids were then resuspended in medium and subdivided for assays of response. (figure 3.1)

Approximately half of the spheroids were incubated with 0.125% trypsin in PBS for 15 minutes at 37 °C, after which the trypsin was removed and replaced with fresh medium. The spheroids were then mechanically disaggregated to a single cell suspension by repeated pipetting. The clonogenic assay was repeated as previously described.

A pasteur pipette was used to transfer spheroids from the other group to agar coated wells on a plastic tissue culture multidish with 1 spheroid per well. Twenty four spheroids were taken from each treatment group, and area measurements were made

twice weekly as described. It was possible therefore to measure treatment induced growth delay, which was defined as the time taken for median spheroid volumes to increase by a factor of ten above initial size.

Determination of intracellular drug levels: The pH of adriamycin containing culture medium (5 µg/ml) was adjusted to give a range from pH 5.5 - 8.5 (pH meter; Inio Electronics Ltd). The monolayers were exposed for 30 minutes to the drug containing culture medium, and incubated at 37 °C. The cells were then washed twice with ice cold PBS and harvested by a brief exposure to trypsin and counted by a Coulter Counter. Adriamycin was extracted from the resulting cell suspension by vortexing with organic solvents (Chloroform and isopropanol) and measured by an HPLC technique with fluorescence detection, previously described by our laboratory (Cumming et al, 1984). Extracted drug was expressed as ng/10⁵ cells.

Fluorescent microscopy: Intact spheroids approximately 500 µm in diameter were exposed to adriamycin and 4'-deoxy for varying times (30 mins to 4 hours) with a medium concentration of 5 µg/ml. The spheroids were then washed to remove loosely bound drug, placed in gelatin capsules filled with OCT embedding gel (Lurker Labs Ltd) and frozen in liquid nitrogen. Thin sections (6 µm) were subsequently cut using a cryotome, mounted in uvinert and examined under a Polyvar fluorescent microscope (λ excitation = 486; λ emission = 550 nm).

Effect of pH on adriamycin uptake in monolayer: Intracellular adriamycin levels have been plotted against extracellular pH (Fig 3.2 a + b). The curve was fitted by non-linear least squares and is sigmoidal in shape. There is a 7.5-fold difference in intracellular drug levels from pH 5.5 to pH 8.5. Fifty per cent of total drug uptake occurred at approximately pH 7.5.

Cell survival in spheroids and monolayers: Each experiment was repeated at least 4 times, but for the sake of clarity the results of 2 experiments are shown in each figure. All the curves were computer fitted to the data shown.

Based on extracellular drug concentrations, there is no significant difference in clonogenic cell survival after treatment of monolayers in the exponential or plateau phase of growth with the two drugs (Fig 3.3). On the basis of external drug concentration, plateau phase cells are considerably more resistant to both drugs than exponentially growing cells. The respective exponential ID_{90} 's for adriamycin and 4'-deoxy are 2.4 μ g/ml and 2.2 μ g/ml and the plateau phase ID_{50} 's are 3.2 μ g/ml and 3.5 μ g/ml. Typical spheroid growth delay data after treatment with a range of adriamycin concentrations are shown in Fig 3.4. The control curve follows Gompertzian kinetics and the treated spheroids regrow at a rate parallel to control. It is apparent that 4'-deoxy induces relatively larger delays in growth for equivalent drug concentrations (Table 3.1, Fig 3.5). Clonogenic cell survival after disaggregation of treated spheroids was significantly higher

for a given dose than for monolayer, and differed for the two drugs (Fig 3.6). Adoption of spheroid configuration confers a degree of resistance to drug treatment, relative to monolayer, which is partially overcome by 4'-deoxy.

The longer the duration of exposure of the monolayers to adriamycin, the greater the clonogenic cell kill. There is an apparent log linear relationship between the duration of adriamycin exposure in monolayer and clonogenic cell kill at fixed drug concentrations (Fig 3.7). Clonogenic cell survival after disaggregation of intact spheroids decreased with increasing duration of exposure but was higher than for monolayer and the spheroid cell survival curve is biexponential.

Spheroid growth delay, as a function of drug exposure time, is summarised in Table 3.2. It is apparent that a plateau phase is achieved with no further significant increases in growth delay with drug exposures of greater than 90 minutes (Fig 3.8)

Fluorescent microscopy: It was possible to evaluate the degree of penetration qualitatively using fluorescence microscopy. Sections stained with haematoxylin and eosin showed that there are approximately 10-12 cell layers from the outer layer to the centre in spheroids approximately 300-400 μ m in diameter, with a necrotic centre (Fig 3.9). After drug exposure, (5 μ g/ml for 2 hours) adriamycin was seen in the nuclei of the outer 3-4 cells, (Fig 3.10) whereas 4'-deoxy had penetrated further to a depth of 6-7 cell layers (Fig 3.11). Prolongation of drug exposure times did not appear to significantly enhance further drug penetration.

3.4 DISCUSSION

We have shown that the 3-dimensional structure of the spheroid confers a degree of resistance to the anthracyclines adriamycin and 4'-deoxydoxorubicin, relative to the monolayer. A number of factors have been considered relevant to cytotoxic drug resistance in spheroids, including - intrinsic cellular drug resistance; failure of drug penetration; alteration in cell cycle kinetics; microenvironmental changes within the spheroid which could affect the physicochemical properties of the drug; protection of spheroid cells by intercellular communication; drug resistance of central hypoxic cells (Wibe, 1980). One would expect that the phenomenon of drug resistance in cells grown as spheroids is likely to be a combination of these factors. We have compared identical cells in monolayer and spheroid, therefore the difference in spheroid sensitivity is unlikely to be due to intrinsic drug resistance.

The cell cycle distribution is not identical when comparing cells grown as spheroids and monolayer. Actively cycling cells tend to predominate on the exterior layers of the spheroid, whereas plateau phase cells tend to make up the majority of internal cells. Chambers et al (1984) have shown that there is a complex relationship between intracellular adriamycin levels and the proliferative state of EMT6 cells. For a given intracellular concentration of drug, plateau phase cells were found to be relatively more resistant than exponentially growing cells. We have shown that human lung tumour plateau phase cells are significantly more resistant to adriamycin and 4'-deoxy but to a similar degree (Fig 3.3).

It is possible that the degree of resistance conferred by adoption of spheroid configuration could be explained, at least in part, by the unfavourable proliferative state of spheroid cells. Nevertheless, despite both drugs having identical effects on monolayer cells in both phases of growth, 4'-deoxy is significantly more toxic to multicellular spheroids. Kwok and Twentyman have compared the response to adriamycin of EMT6 cells, treated as intact or diasaggregated spheroids. In that study, the cell cycle distribution of the two cell populations was identical, and yet it was apparent that the sensitivity of disaggregated spheroid cells was greater than that of intact spheroids.

The duration of drug exposure is an important determinant of survival. There is a linear relationship between the two for monolayer, at least over the times used in these experiments. However, the clonogenic cell survival curve was biphasic, for disaggregated spheroid cells, with a lesser degree of cell kill. This plateau effect is also seen when spheroid growth delay is plotted against time (Fig 3.8) with no further apparent increase in growth delay with drug exposures of greater than 90 minutes. Fluorescent microscopy shows that even after prolonged exposure to adriamycin (up to 4 hours) the drug does not reach the centre of the spheroid. This may explain the disparity in shape between the monolayer and disaggregated spheroid cell survival curves.

Adriamycin is a basic drug (pK 8) and the amino group of the daunosamine sugar moiety is likely to be protonated at acidic pH (the amount of ionised drug can be derived from the Henderson-Hasselbach equation) (Fig 3.2b)

We have shown the dependence of cellular drug uptake on external pH, in monolayer (Fig 3.2a). Using microelectrodes, Acker et al (1982) have demonstrated significant gradients in oxygen, pH and glucose from the external to internal spheroid cell layers. There is some histological evidence on central necrosis in spheroids of approximately 400 μm in diameter, which would be likely to be associated with a relatively acidic pH. This pH gradient may therefore influence adriamycin ionisation and hence be a contributory factor to the failure of the drug to penetrate to the centre of the spheroid core. This is consistent with the concept that adriamycin enters the cell by diffusion of the electroneutral molecule through the lipid domain of the cell membrane.

Both adriamycin and 4'-deoxy cause significant growth delays (Table 3.1) without a very marked degree of clonogenic cell kill (Fig 3.6). For example, 4'-deoxy induces spheroid growth delay of approximately 25 days following exposure to 10 $\mu\text{g}/\text{ml}$ for 1 hour, whereas an identical drug exposure yields only 60% clonogenic cell kill.

Figure 3.4 shows a series of growth and regrowth curves for L-DAN spheroids following treatment with adriamycin. Untreated spheroids grow exponentially, with a doubling time of approximately 3 days until a diameter of about 700-800 μm was reached, after which growth slowed in a Gompertzian retardation phase. Treated spheroids exhibited either a static phase, or a regression phase (depending on dose) which was followed by a recovery of the growth curve to a pattern similar to that for untreated spheroids. The exponential portions of these regrowth curves were, to a reasonable approximation parallel to each other and to the corresponding

portion of the control growth curve. Clonogenic survival curves may, in principle, be deduced from such data by back-extrapolation of regrowth curves to zero dose.

Such deductions have previously been attempted as a means of obtaining 'in situ' survival curves for experimental tumour irradiated in vivo but, in that situation, the analysis is complicated by the existence of the tumour bed effect, the limited proliferation potential of 'doomed cells' and the difficulty of obtaining accurate measurements of the regrowing tumour over an adequate range of sizes (Wheldon, 1980). For spheroids, the problem is simpler in that the tumour bed effect is necessarily absent in vitro, observations over a wide range of sizes are feasible and (at least for the present spheroid line) doomed cell proliferation evidently does not substantially influence regrowth. The effect of mitotic delay would be negligible at these doses. It seems reasonable to interpret these spheroid response data as being consistent with the instantaneous reduction by cytotoxic drug treatment of clonogenic cell number in each spheroid from $N_0^{(-)}$ (immediately before treatment) to $N_0^{(+)}$ immediately after the treatment (with the surviving cells immediately resuming exponential growth). The quantity $N_0^{(+)}$ will be proportional to the Y-intercept (at zero dose) of the extrapolated exponential portion of the regrowth curve i.e. it is proportional to the volume from which the spheroids 'apparently' regrew. The clonogenic surviving fraction following treatment (S) is then simply the ratio $N_0^{(+)}$ to $N_0^{(-)}$. By repetition of this estimation procedure at each dose level for which regrowth curves are available a dose-dependent survival curve may be estimated for the cells of the spheroid.

The surviving fraction was calculated, but the clonogenic cell survival predicted by the growth delay data was considerably lower than that found by actually cloning disaggregated spheroids. At the highest drug concentrations used, the difference between the predicted and actual clonogenic survival differed by 100 fold.

There are a number of other factors which can contribute to growth delay apart from clonogenic cell kill. Steel (1977) has proposed the following formula for changes in tumour cell-cycle kinetics.

$$\frac{T_d}{T_c} = \frac{\log 2}{(1 - \theta) \log (GF + 1)}$$

T_c = length of tumour cell cycle, GF = growth fraction

θ = rate of cell loss T_d = tumour volume doubling time.

It is possible that the anthracyclic compounds cause prolonged growth delays in a number of ways; incurring a cell-cycle delay; reduction in the growth fraction of the tumour; an increased rate of cell loss. Growth delay is therefore a complex end point in assessing the relative potency of cytotoxic drugs but is presumably valid if members of the same generic class of compounds are compared.

4'-deoxy induced a longer growth delay and greater clonogenic cell kill than adriamycin. There is no difference in the cell cycle specificity of the two drugs, but we have demonstrated that the lipophilic analogue partitions into the spheroid more rapidly, and to a greater degree. It is tempting to speculate that

adriamycin penetration is a relatively important aspect of spheroid drug resistance in our model system, and that we have partially overcome this by using a lipophilic analogue. The 3-dimensional spheroid model may be an important additional method by which new lipophilic analogues of existing cytotoxic drugs should be assessed preclinically, as part of the selection procedure for further development.

CONCENTRATION ($\mu\text{g/ml}$)	MEDIAN GROWTH DELAY (days) *	95% CONFIDENCE LIMITS **
---------------------------------------	---------------------------------	-----------------------------

ADRIAMYCIN

0	8.1	6.3-8.9
1	11.5	10.0-14.2
5	13.1	12.0-14.9
10	17.3	15.4-18.3
12.5	16.4	15.3-17.9
20	17.4	14.5-19.2

4'-DEOXY

0 (control)	6.4	5.0-6.8
1	15.9	13.0-18.5
5	19.4	15.4-20.5
10	24.9	NA***
15	29.5	NA

* The growth delay was taken to be time to reach x 10 original volume.

** Approximate 95% confidence limits on median spheroid volumes were calculated by the method of Nair (cited by Colquhoun, 1971). Growth curves were constructed for each experimental group using upper and lower limits on median volume. Growth delay values were obtained from each of these curves and are referred to as 95% confidence limits on median spheroid growth delay.

*** NA - not assessable (upper bound required extrapolation beyond available data).

TABLE 3.1 - Growth delay of L-DAN spheroids exposed to different concentrations of adriamycin or 4'-deoxy for a fixed time (one hour).

ADRIAMYCIN EXPOSURE TIME (min)	MEDIAN GROWTH* DELAY (days)	95% CONFIDENCE LIMITS** (days)
0	8.5	7.0-10.2
15	10.6	9.0-12.0
30	13.0	11.3-14.5
60	20.4	19.0-26.5
90	27.5	22.2-30.2
120	27.5	19.5-30.0

* The growth delay was taken to be time to reach x 5 original spheroid volume.

** Approximate 95% confidence limits on medium spheroid volumes were calculated by the method of Nair (cited by Colquhoun, 1971). Growth curves were constructed for each experimental group using upper and lower limits on median volume. Growth delay values were obtained from each of these curves and are referred to as 95% confidence limits on median spheroid growth delay.

TABLE 3.2 - Growth delay of L-DAN spheroids exposed to a fixed concentration of adriamycin (10 μ g/ml) for different lengths of time.

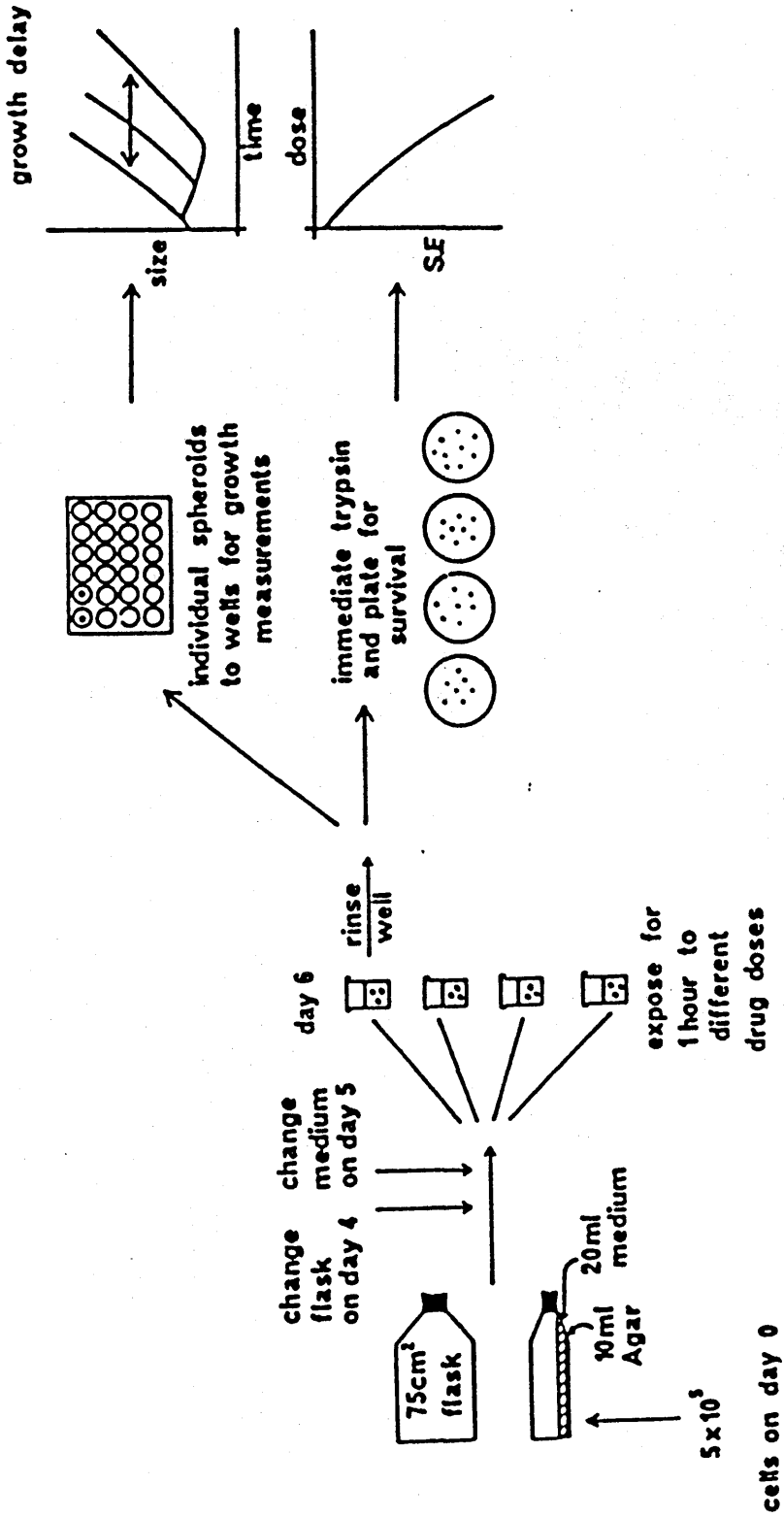


Figure 3.1 Diagrammatic representation of experimental spheroid protocol.

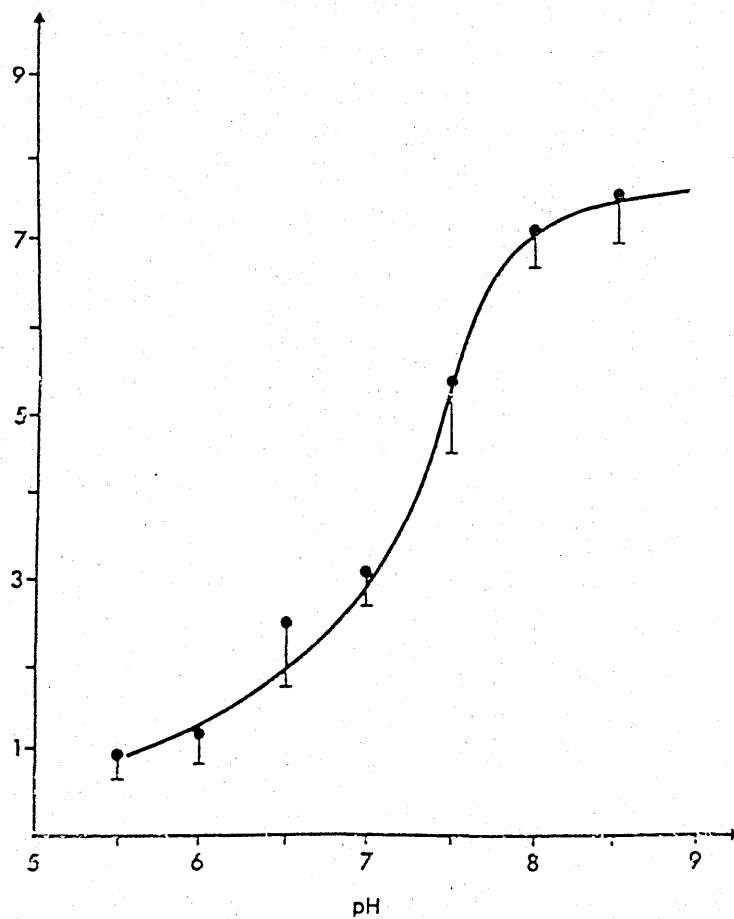


Figure 32a The relationship between intracellular adriamycin levels and extracellular pH. Each point is the mean of 5 experiments and the vertical bars denote 1 standard deviation.

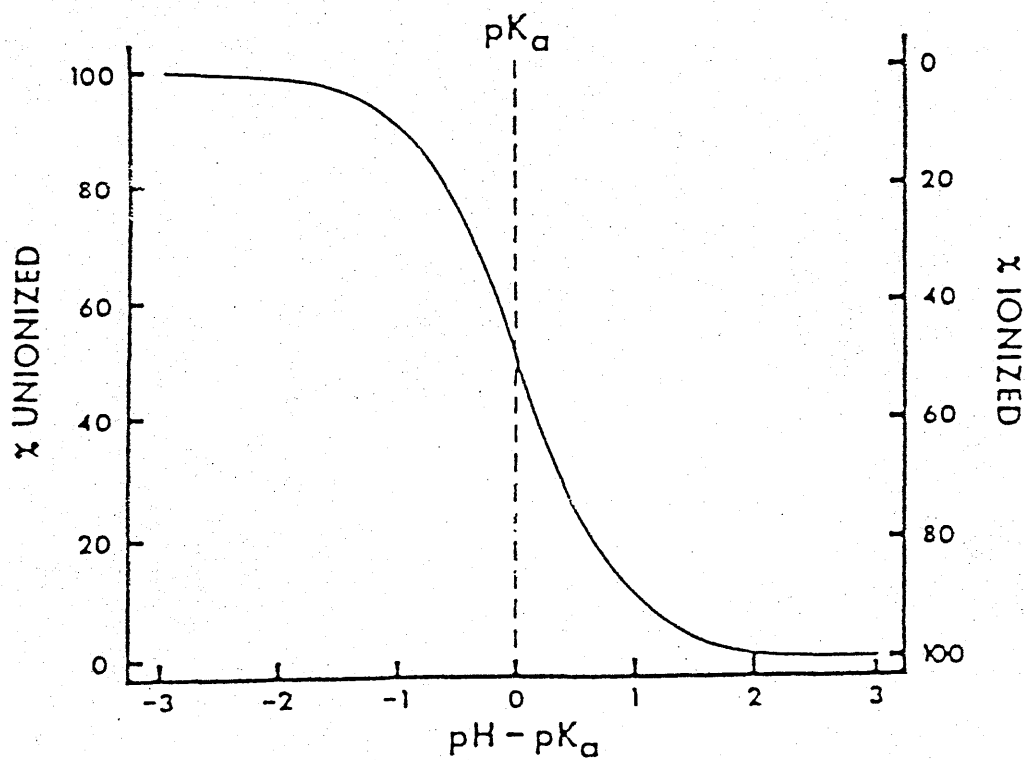


Figure 32b The effect of pH on the ionisation of a weak acid. The acid is 50% ionised at a pH = pka. At higher pH values it becomes increasingly more ionised. A mirror image could be constructed for a weak base.

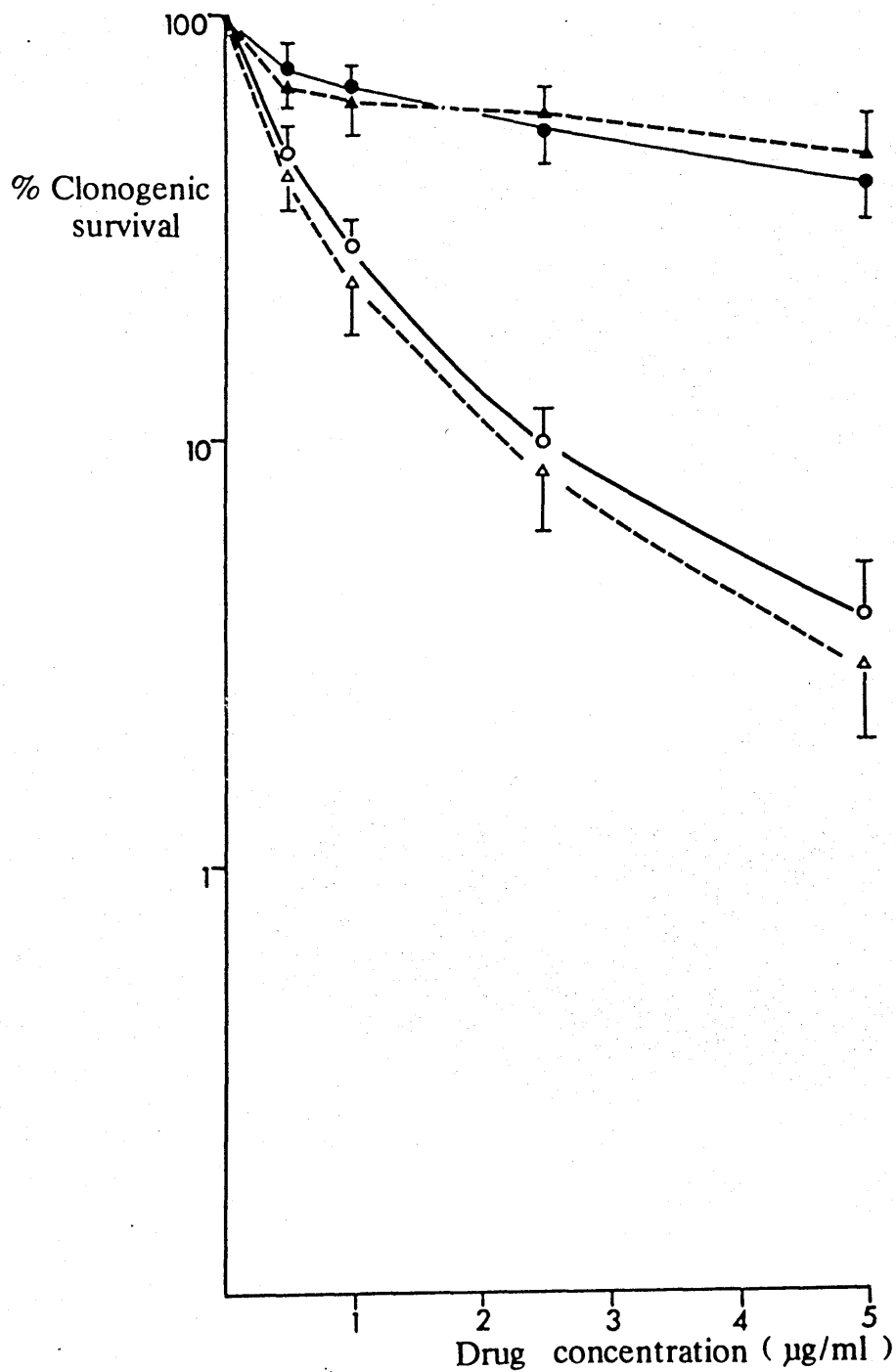


Figure 3.3 Clonogenic survival of monolayer cells in the plateau (▲, ●) or exponential (△, ○) phase of growth, after exposure to adriamycin (○, ●) or 4'-deoxy (△, ▲). Each point is the mean of 4 experiments and the vertical bars represent 1 standard deviation.

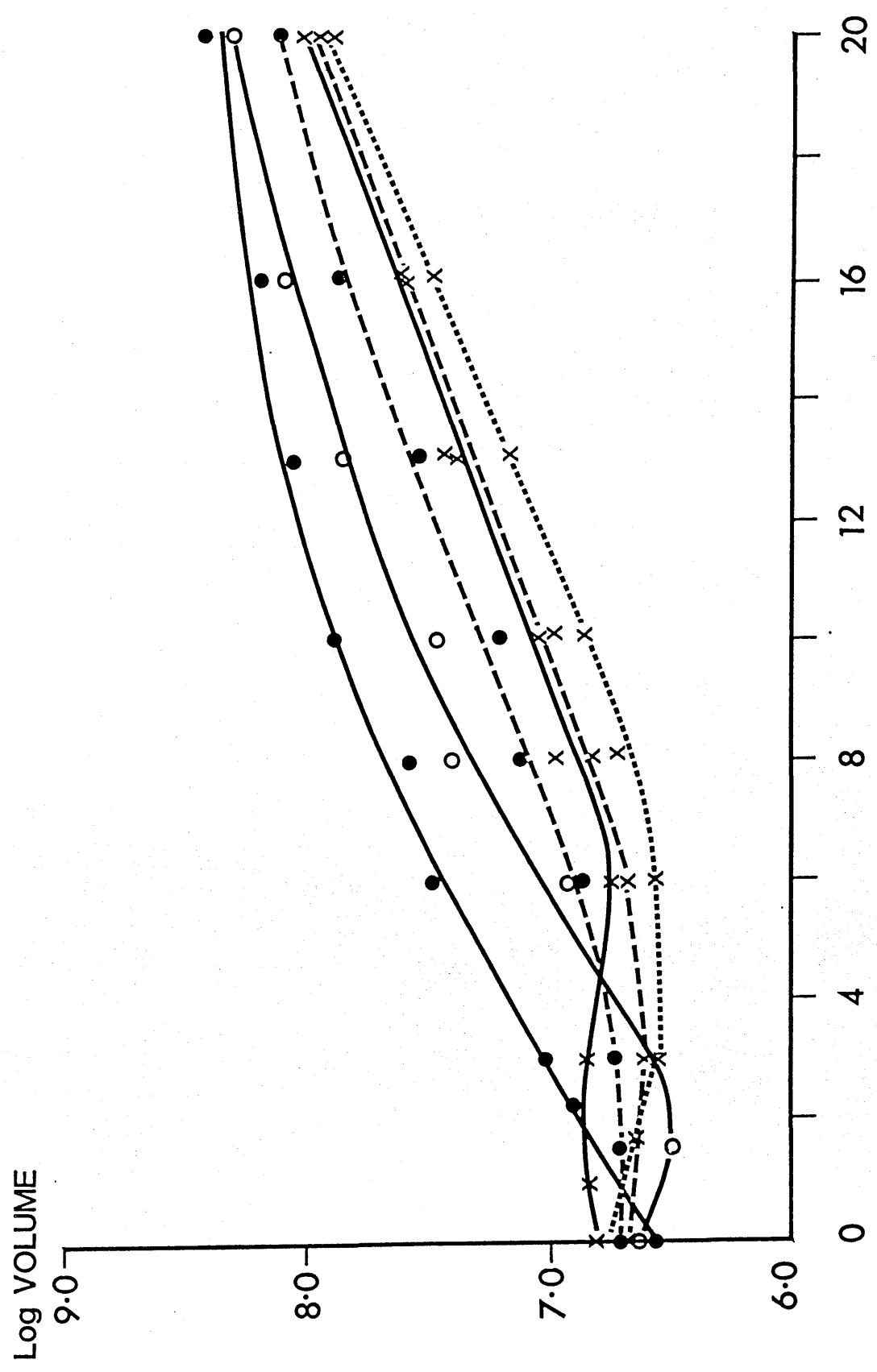


Figure 3.4 Spheroid growth delay after exposure to various concentrations of adriamycin. Control ●—● ; 1 µg/ml ○—○ ; 3 µg/ml ●—● ; 5 µg/ml ×—× ; 10 µg/ml ×—× ; 15 µg/ml ×—×.

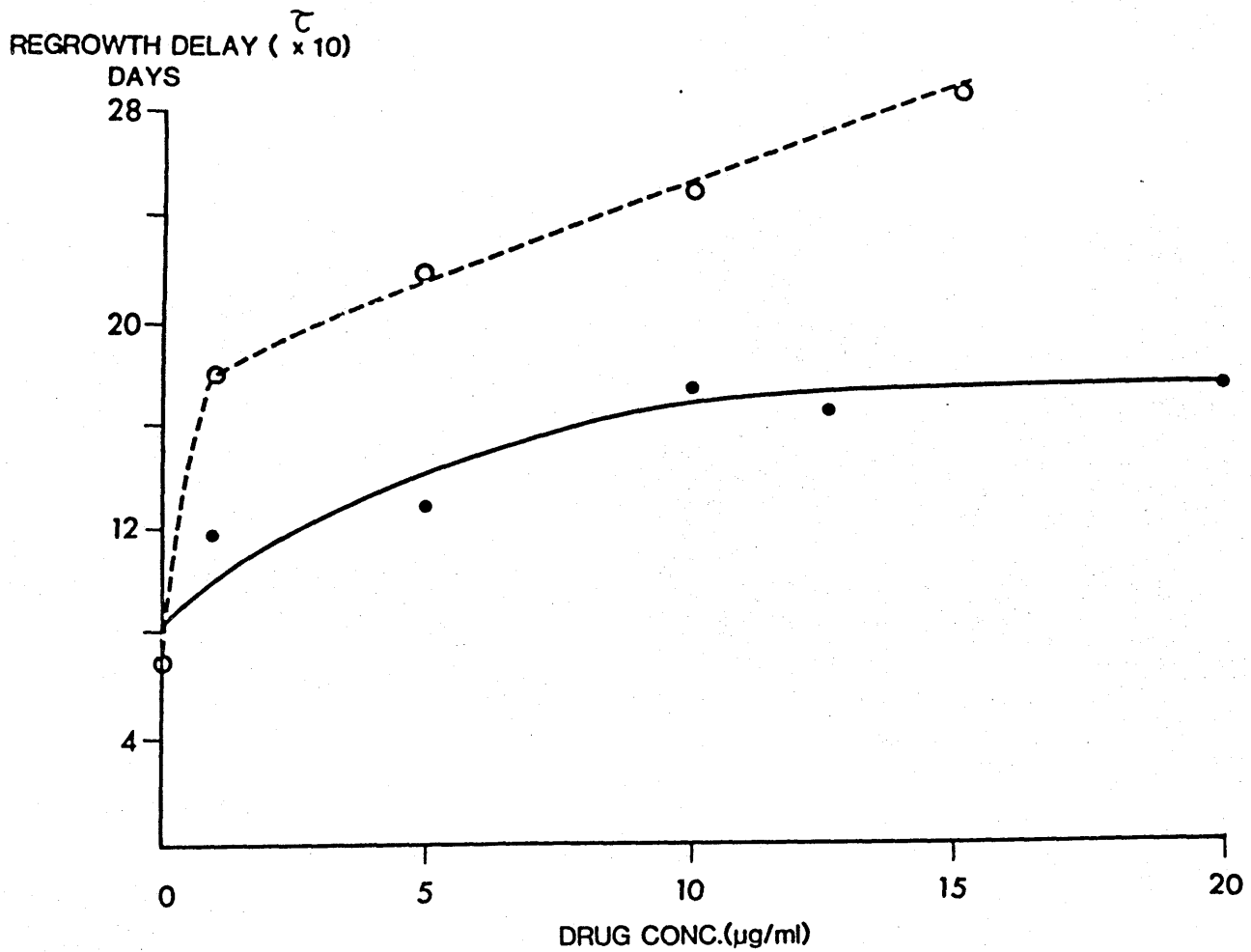


Figure 3.5 Dependence of regrowth delay on drug concentration, with fixed duration of exposure

Adriamycin ●—●
4'-deoxy ○--○

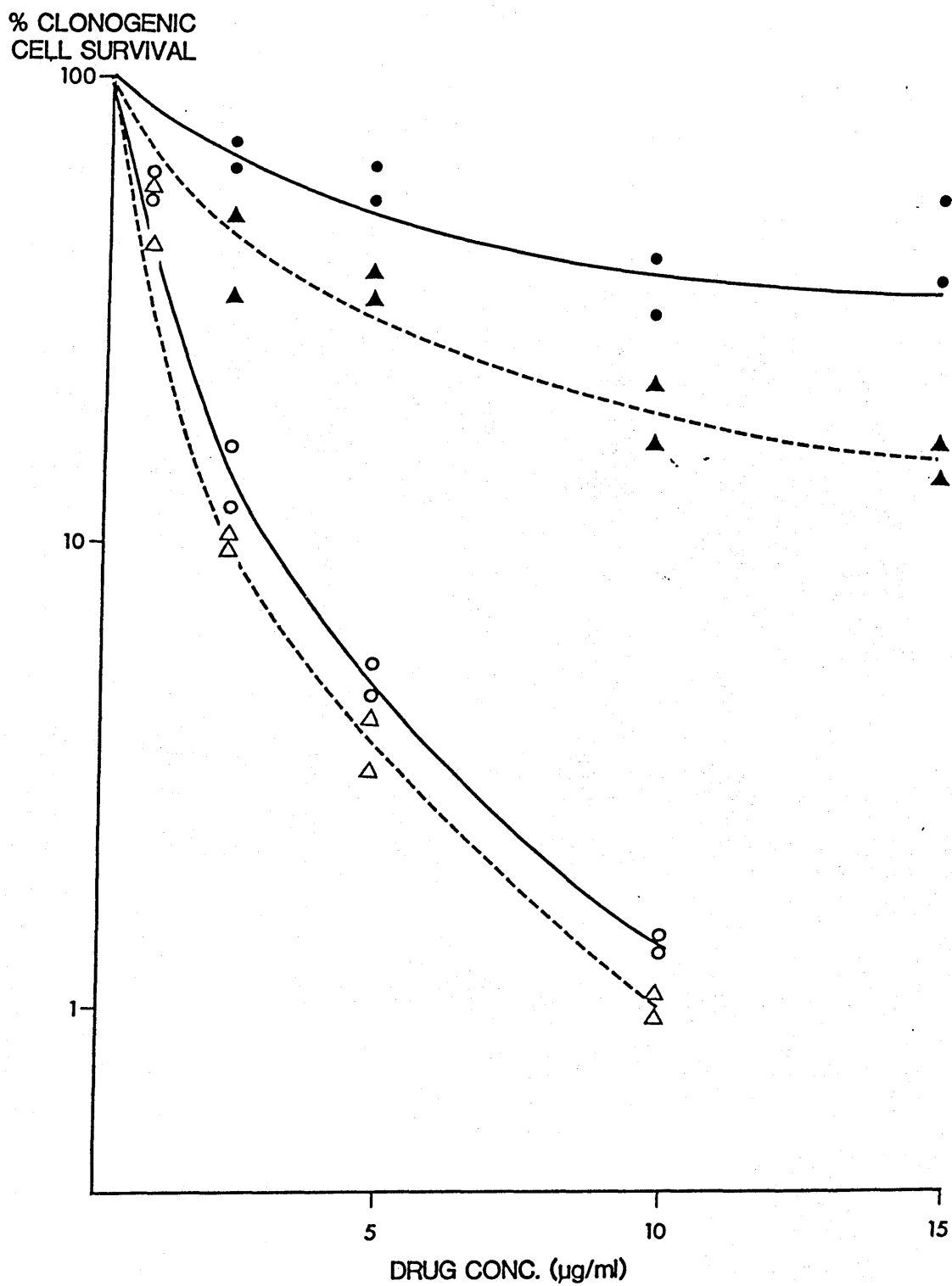


Figure 3.6 Clonogenic cell survival of monolayers (Δ , \circ) and disaggregated spheroids (\blacktriangle , \bullet) following exposure to adriamycin (\circ , \bullet) or 4'-deoxy (Δ , \blacktriangle). The curves are computer fitted to the mean of 2 experiments.

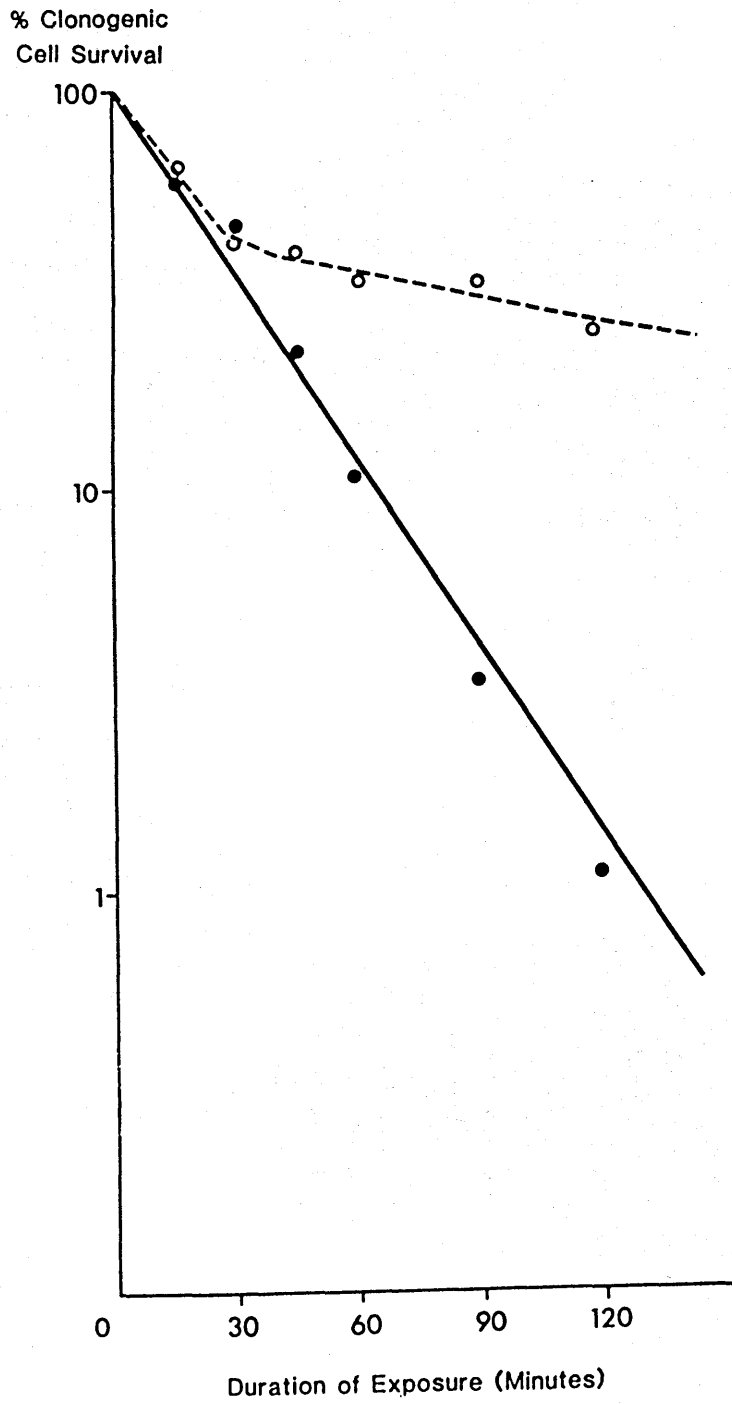


Figure 3.7 The relationship between clonogenic cell survival and the duration of adriamycin exposure at fixed concentration (10 $\mu\text{g/ml}$)

Monolayer ●————●
Disaggregated spheroid ○-----○

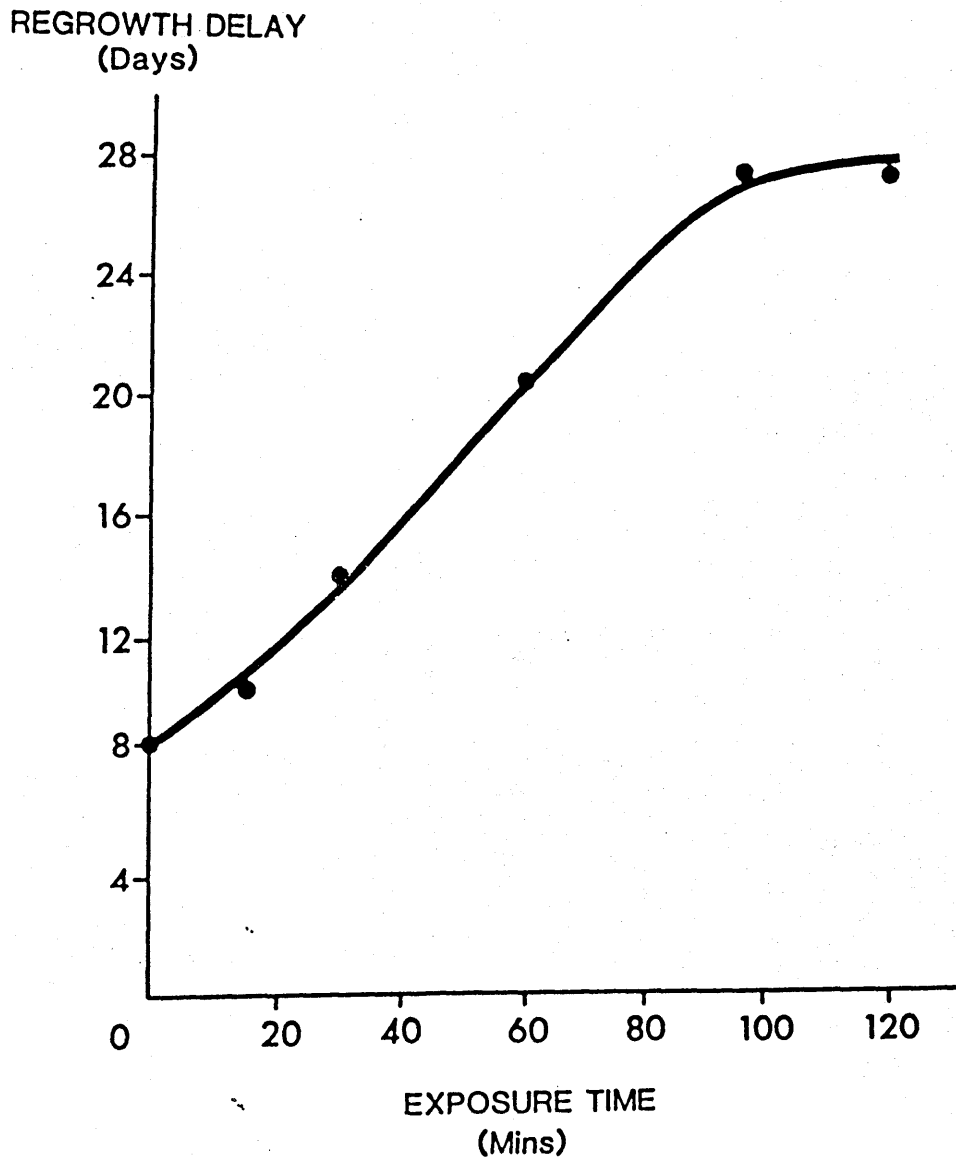


Figure 3.8 The dependence of spheroid growth delay on the duration of exposure to adriamycin at fixed concentration (10 ug/ml).

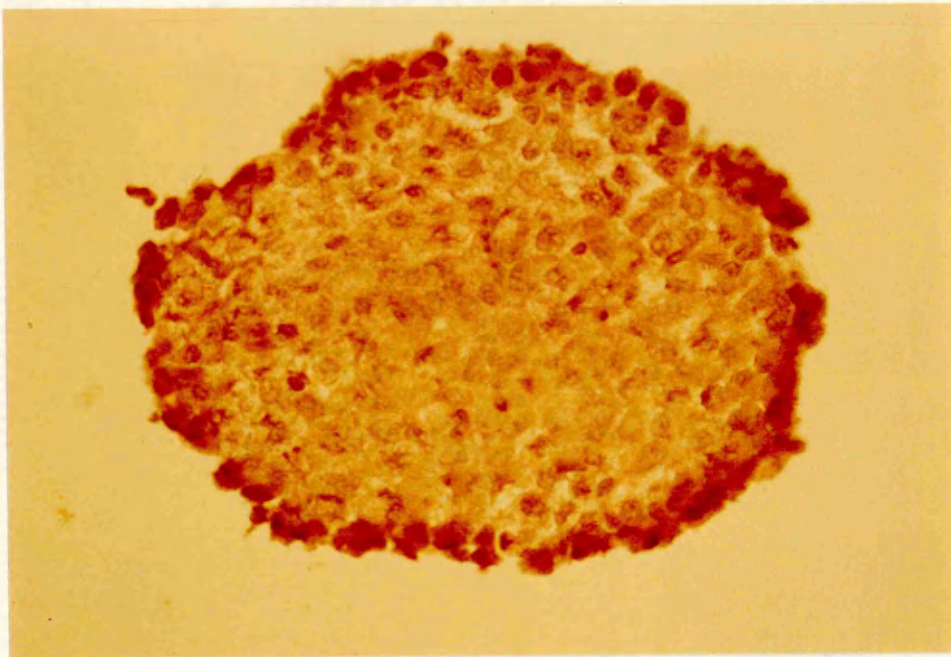


Figure 3.9. Section through an L-DAN spheroid stained with haematoxylin and eosin (magnification x 100)

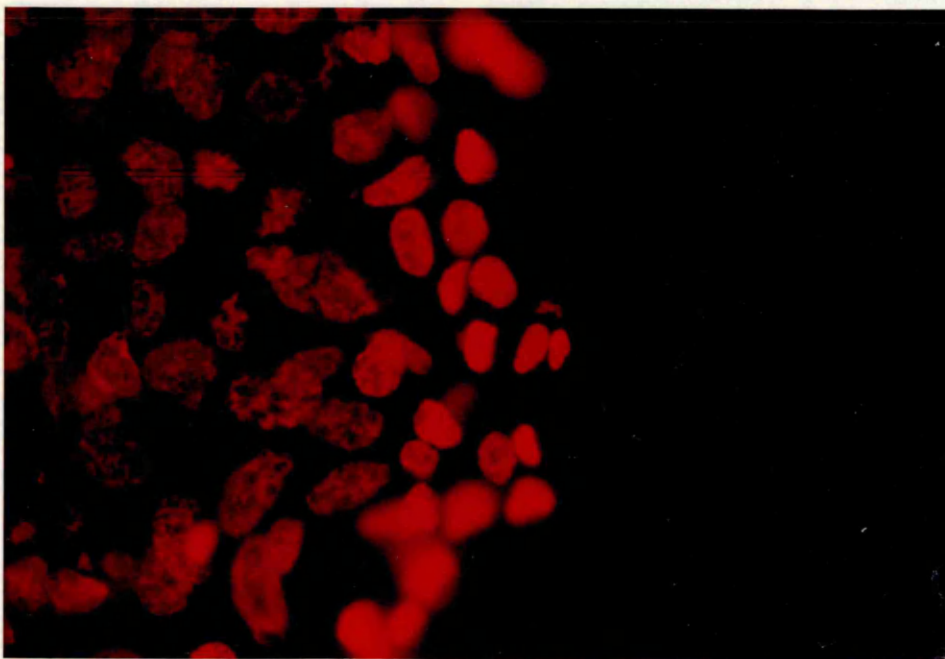


Figure 3.10. External surface of an L-DAN spheroid exposed to adriamycin. The outer 3 - 4 cell layers are most highly labelled with drug and there is a clear diffusion gradient within the spheroid (magnification x 100).

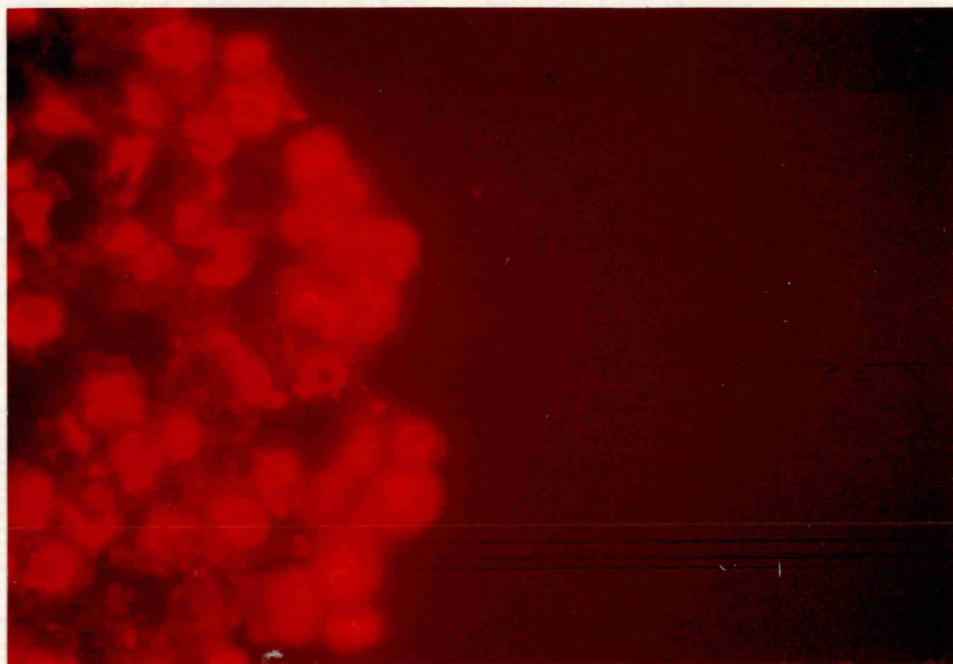


Figure 3.11 External surface of an L-DAN spheroid exposed to 4'-deoxy. The drug has diffused further into the spheroid and the external cells are more highly labelled compared to adriamycin (magnification x 100)

Intratumoural distribution and pharmacokinetics of adriamycin and 4'-deoxydoxorubicin in rats bearing a methyl cholanthrene induced sarcoma.

4.1 INTRODUCTION

Thus far, the comparative subcellular localisation and spheroid diffusion gradients of adriamycin and 4'-deoxy have been described. One would predict, from the work of Goldacre and Sylven, that the distribution of these cytotoxic drugs would not be homogenous within solid tumours, given the apparent penetration barriers facing anthracyclines in tumour spheroids a few hundred microns in diameter.

Ozols et al (1981) examined the penetration of adriamycin into murine ovarian cancer cells grown intraperitoneally in C3HeB/FeJ mice. Adriamycin-specific intranuclear fluorescence was detected in the ascites cells soon after an intraperitoneal dose, but was undetectable at any time following an equitoxic intravenous dose. Interestingly, adriamycin given intraperitoneally penetrated only into the outermost 4 to 6 cell layers of the solid intra-abdominal tumour nodules whereas after the intravenous route adriamycin-specific fluorescence was observed in a patchy distribution throughout the tumour. The authors concluded that intraperitoneal administration of adriamycin has both pharmacokinetic and tissue penetration advantages over the standard intravenous route for ovarian tumour confined to the abdominal cavity.

Durand has recently introduced a method for separating tumour cells as a function of their distance from the blood supply. The

basis for this separation procedure is that the fluorescent bisbenzamide stain, Hoechst 33342, as a result of its high avidity for cellular DNA, exhibits a marked diffusion/consumption gradient when it has to pass through several cell layers. This results in a situation where the cells closest to the drug "resevoir" i.e. media in the case of multicell spheroids or blood supply in the case of solid tumours in vivo, become more intensely stained. Preliminary results from that laboratory following treatment of Lewis lung carcinoma bearing mice with adriamycin or external beam radiotherapy indicate that tumour cell survival can be related to the intensity of dye staining (the most intensely labelled cells, which are therefore closest to the blood supply, are most sensitive to X-rays or adriamycin).

In this chapter, the intratumoural distribution, pharmacokinetics and antitumour activity of adriamycin and 4'-deoxy has been examined in tumour bearing (MC40A) rats utilising fluorescence microscopy. In addition the relative cardiac toxicity of the two compounds has been assessed by electron microscopy.

Drug administration For the drug distribution studies, adriamycin (40 mg/Kg) and 4'-deoxy (20 mg/kg) were administered in equitoxic doses by continuous intravenous infusion over a period of 2 hours (Vickers Automatic Pump, Vickers Engineering, England). Both drugs were reconstituted in normal saline immediately prior to use. The rats were anaesthetised using a nose cone connected to a Flutec 3 anaesthetic machine which delivered 2% Halothane in nitrous oxide for the duration of the infusion. A fine polyethylene cannula was inserted into the left carotid artery and was heparinised and connected by a Luer lock to the Vickers pump.

MC40A Tumour This tumour is a methyl cholanthrene induced fibrosarcoma. The tumour was passaged surgically in approximately 100 mg fragments, and implanted, under light ether anaesthesia, in the recipient Wistar rat's (inbred community) flank. When the tumours were approximately 1.5 cm in diameter, tumour growth delay experiments were instituted. Three groups of 10 animals were treated with 10 mg/Kg intravenously of adriamycin or 4'-deoxy and normal saline as control. Tumour volumes were measured by bidimensional estimation of tumour diameter using special calipers. These estimates of tumour volume were made 3 times weekly for 14 days.

Tissue preparation for fluorescent studies At the end of the drug infusion, the rats were sacrificed by exsanguination. Heart, liver, one kidney, a portion of skeletal muscle from the gastrocnemius and the tumour were excised, washed in ice cold saline and blotted

dry. The tissues were then immersed in liquid nitrogen and stored frozen at -70°C . $6\ \mu\text{m}$ sections were then cut on a cryostat and mounted in uvinert.

The slides were examined for adriamycin specific fluorescence using a Polyvar fluorescent microscope (λ excitation = 468 nm; λ emission = 550 nm).

Tissue preparation for drug levels - Tumour bearing Wistar rats were treated 7 days after tumour transplantation. Adriamycin or 4'-deoxy was administered by intravenous bolus at identical doses of 10 mg/kg. Following drug administration two animals from each group were sacrificed by cervical dislocation (0, 15 minutes, 30 minutes, 1 hour, 2 hours, 4 hours, 8 hours, 12 hours and 24 hours). A blood sample was collected from the inferior vena cava, and the heart and tumour excised and washed free of blood with normal saline. The blood sample was centrifuged at 2000 rpm for 5 minutes and the plasma separated and stored at -70°C with the tissue samples until analysed.

Drug assay Prior to extraction, plasma and tissues were allowed to thaw at room temperature. One to two grams of heart and tumour were suspended in 3 vol of buffered normal saline - and finely minced with an Ultra Turnes electrically driven rotating cutting blade for 30 seconds. A homogenate was produced with five up and down strokes with a Potter Elvehjem homogeniser. Light microscopy confirmed that the cells were disrupted by this procedure. Daunorubicin was added to 1 ml of homogenate as an internal

standard. One ml of tissue homogenate was treated with 33% (W/V) silver nitrate (0.2 ml per homogenate) for 10 min at 4°C in the vortex evaporator with vigorous shaking (the vigorous shaking was important for good recovery). Immediately 5 volumes of chloroform/propan-2-ol (2:1) was added to the homogenate mixture and the parent drugs and their metabolites were extracted by vortexing for a further 30 minutes. Three phases were separated by centrifugation at 1000 rpm for 15 minutes. The upper aqueous phase was discarded by aspiration, the lower organic phase was decanted over the middle tissue pellet into a clean test tube and evaporated to dryness in the vortex evaporator at 40°C and 25 mm Hg of vacuum. The dry extracts were reconstituted in a small volume of methanol and were then ready for HPLC separation as previously described (sec 2.2).

Pharmacokinetic analyses The area under the curve ($AUC_{0-\infty}$) for plasma and tissue drug content was calculated by the trapezoidal rule. Pharmacokinetic parameters were estimated by non linear least squares fitting using an in-house programme based on the Marquardt algorithm (Bevington, 1978). Statistical comparisons were made using paired Student's t-test with Bonferroni correction where applicable.

Electron Microscopic assessment of cardiac toxicity Wistar rats were treated by intravenous administration of 15 mg/Kg adriamycin or 4'-deoxy. This dose of drug has been previously associated with the development of a subacute cardiomyopathy in rats 1 - 4 days following treatment with adriamycin. Two days after treatment the rats were sacrificed, their hearts dissected and the ventricular apices fixed in freshly prepared 1.5% glutaraldehyde and post-fixed in 1% osmium tetroxide. They were then dehydrated in graded ethanols and embedded in Epon-Araldite.

Thin sections, cut at 250-500 A° with a Reichert OmU-2 ultramicrotome, were mounted on Formvar-coated 200-mesh copper grids. These sections were stained with lead citrate and uranyl acetate and examined with a Jeoko 100B electron microscope. In addition the hearts of 3 untreated rats were similarly prepared for electron microscopic study and served as histologic controls.

Fluorescence localisation studies Under the conditions described, adriamycin fluoresces orange. Initial examination of formalin-fixed tumour sections stained with haematoxylin and eosin revealed an anaplastic carcinoma, with no central necrosis and a peripheral, annular complex of small arterioles and capillaries (Fig 4.1). Fluorescent studies with the fluorescein conjugated antibody directed against endothelial factor VIII showed a similar distribution of blood vessels, mainly on the peripheral rim of the tumour, although centrally penetrating arterioles and capillaries were demonstrated in the tumour core.

Drug specific fluorescence was detected only within cell nuclei of the various organs examined. Both adriamycin and 4'-deoxy appeared to be homogeneously distributed in heart muscle, liver, kidney and skeletal muscle with relatively intense intranuclear fluorescence (fig 4.2 - 4.4). The situation was markedly different in the tumour with a faint ring of drug specific fluorescence seen on the periphery of the tumour, and a marked diffusion gradient declining from the periphery to the centre of the tumour (fig 4.5). The staining associated with 4'-deoxy was relatively more intense (implying a greater amount of drug bound) and had penetrated further from the vascular annulus (fig 4.6)

Drug pharmacokinetics The relevant kinetic parameters are summarised in tables 4.1 - 4.3. Peak drug levels in tumour and heart for 4'-deoxy are significantly higher ($P < 0.05$) despite a lower peak serum concentration compared to adriamycin. Total drug exposure, as

assessed by the area under the concentration time curve, for tumour, heart and plasma was greater following treatment with 4'-deoxy. The pattern of intracardiac metabolism of the two drugs was different. There was significant (75%) metabolism of adriamycin to the 7-deoxyaglycones of the parent drug and adriamycinol. This contrasts with the cardiac fate of 4'-deoxy, where over 90% of the parent drug was present unchanged.

Electron Microscopic assessment of cardiac toxicity

Ultrastructural alterations in rat myocardium in response to anthracycline treatment have already been described (Mettler et al, 1977). Mitochondrial swelling, vacuolation and dense body formation were seen following administration of adriamycin and 4'-deoxy which conforms to the histopathological changes previously reported (fig 4.7 and 4.8). Using the scoring systems introduced by Bertazzoli et al (1979), the extent of cardiac damage was quantified and found to be similar for the two drugs (approximately, grade 0.5)

Antitumour efficacy of adriamycin and 4'-deoxy The tumour volumes following treatment with equimolar doses of adriamycin and 4'-deoxy are summarised in table 4.4. Adriamycin does not significantly alter the tumour growth kinetics of the MC-40A fibrosarcoma relative to control. In stark contrast, there is no further growth of the tumours following treatment with 4'-deoxy. All of the controls survived, whereas one in the adriamycin group and 3 in the 4'-deoxy group had died by the time of final tumour assessment.

The lipophilic analogue, 4'-deoxy, has a different disposition in tumour bearing rats than adriamycin. Despite a lower peak concentration in plasma, 4'-deoxy achieves significantly higher peak levels in tumour and heart. Total drug exposure, estimated by the area under the plasma or tissue concentration time curve, is higher for plasma, heart and tumour.

In addition to these pharmacokinetic parameters which imply increased drug penetration, 4'-deoxy appears to diffuse further into the tumour substance from the external vascular ring. It is possible that 4'-deoxy is more diffusible by virtue of its higher oil-water partition coefficient and can leave the vascular compartment with relatively greater ease.

By virtue of these properties, if there is a relationship between clonogenic cell kill and intracellular drug levels, then 4'-deoxy would be expected to be more potent than adriamycin at equitoxic doses.

It is apparent from the tumour growth delay experiments that 4'-deoxy is significantly ($p < 0.01$) more active than adriamycin in equimolar doses in this tumour model. However, there were more drug associated deaths (30%) in the 4'-deoxy treated groups than in adriamycin treated (10%) by the experiment's end point. The ideal doses to compare cytotoxic drugs in vivo are equitoxic as this gives a logical basis for deriving relative therapeutic ratios. The equitoxic dose is usually dependent upon the relative degree of myelosuppression caused rather than on chronic toxicity such as cardiomyopathy. Cassaza (1975) has reported that 4'-deoxy is more active in a number of murine tumours in vivo, at equitoxic doses, than adriamycin.

This has potential therapeutic implications in man. There is a growing awareness that adjuvant chemotherapy following debulking of the primary tumour by surgery or sterilisation by radiation can have survival benefits. This situation has been best documented by Bonadonna et al (1976) following adjuvant chemotherapy with cyclophosphamide, methotrexate and 5-Fluorouracil for breast cancer patients treated by mastectomy. If the multicellular spheroid is a representative model for a micrometastasis prior to vascularisation, precisely the stage of disease that adjuvant chemotherapy is aimed at, then it is apparent that significant drug penetration barriers and associated cytotoxic drug resistance will be present at this early period in the metastasis' natural history. In view of our findings on the penetration properties of 4'-deoxy in vitro and in vivo, then a case might well be made for adjuvant trials of chemotherapy inclusive of lipophilic cytotoxic analogues.

Adriamycin-induced cardiomyopathy is a severe total dose-limiting side effect in patients treated with this powerful anti-neoplastic agent. Several inconclusive studies have been performed on animals and man to clarify the mechanism of toxicity and to find putative protective substances for this untoward side effect (Unverferth et al, 1982). New anthracycline analogues are tested extensively in animal model systems predictive of cardiotoxicity in the hope that chemical modification of the drug's structure will produce an active congener which is less cardiotoxic. On the basis of electron microscopic examination of rat ventricular apices it appears that adriamycin and 4'-deoxy are equally cardiotoxic when administered in equimolar doses.

There is thought to be an association between peak intracardiac drug levels and the development of cardiomyopathy, yet peak levels of 4'-deoxy are considerably higher than those of adriamycin. The pattern of intracardiac drug metabolism also differs; there is extensive conversion of adriamycin to its 7-deoxyaglycone, whereas 4'-deoxy is largely unchanged. Although one would expect 4'-deoxy to be more cardiotoxic on the basis of cardiac pharmacokinetics, this may be offset by differential metabolism of adriamycin to its 7-deoxyaglycone. A hypothesis has been advanced that a portion of the cardiac toxic effects are mediated by free radical production within myocytes from the anthracycline (Bachur, 1979). The 7-deoxyaglycones are considered metabolic "markers" of intracellular free radical production and it would appear that adriamycin is being metabolised within rat cardiac cells via a pathway that would ensure damaging free radical production. There is no evidence of free radical production at the concentrations seen within cardiac cells for 4'-deoxy, which may produce its cardiotoxic effect by a different mechanism (Unverferth et al, 1982).

One would have predicted from the preceding in vitro experiments that 4'-deoxy would have different penetration and pharmacokinetic characteristics on the basis of its physico-chemical properties. Although intratumoural levels of 4'-deoxy were higher than the corresponding values for adriamycin, peak intracardiac levels were increased also. According to the pharmacokinetic hypothesis, 4'-deoxy would have been expected to cause a greater degree of cardiotoxicity. Possibly by virtue of a different pathway of cardiac drug metabolism, adriamycin and 4'-deoxy are similarly toxic to heart myocytes.

When extrapolating from an in vitro situation, such as the multicellular spheroid model, it is important to recognise the importance of the therapeutic ratio (effective dose/toxic dose) in vivo. If a novel analogue of a pre-existing cytotoxic agent were introduced which was considerably more potent than the parent compound in vitro, this need not translate into a clinically, exploitable improvement in the therapeutic ratio, if the drug's toxicity is similarly enhanced.

With regard to cardiomyopathy, one would predict that 4'-deoxy would have a greater therapeutic ratio in rats bearing the MC40A sarcoma.

Compound	Adriamycin		4'-deoxy		Terminal half life (hr)
	Peak conc. ($\mu\text{g/ml}$)	AUC ($\mu\text{g/ml hr}$)	Peak conc. ($\mu\text{g/ml}$)	AUC ($\mu\text{g/ml hr}$)	
Parent drug	3.4 ± 0.4	0.67	1.1 ± 0.2	0.76	21 ± 3
Alcohol	0.07 ± 0.01	0.23	ND	ND	ND
7-deoxyaglycone of parent drug	ND	ND	ND	ND	ND
7-deoxyaglycone of alcohol	0.6 ± 0.05	0.13	0.13 ± 0.03	0.32	9.6 ± 0.9

TABLE 4.1 Peak drug concentration, AUC and metabolites in rat serum following intravenous administration of adriamycin and 4'-deoxy (\pm standard deviation).

Compound	Adriamycin		4'-deoxy	
	Peak Concentration (µg/ml)	AUC (µg/g hr)	Peak Concentration (µg/g)	AUC (µg/g hr)
Parent drug	2.3 ± 0.8	47	10.3 ± 1.2	68
Alcohol	ND	ND	ND	ND
7-deoxyglycone				
of parent drug	0.78 ± 0.2	24	0.27 ± 0.1	3.8
7-deoxyglycone				
of alcohol	0.68 ± 0.15	35	0.08 ± 0.02	0.8

TABLE 4.2 Peak drug concentration, AUC and metabolites in rate heart following intravenous administration of adriamycin and 4'-deoxy (± standard deviation)

Compound	Adriamycin Peak Concentration ($\mu\text{g/g}$)	AUC ($\mu\text{g/g hr}$)	4'-deoxy Peak Concentration ($\mu\text{g/g}$)	AUC ($\mu\text{g/g hr}$)
Parent drug	2.4 ± 0.25	59.8	4.45 ± 0.55	150
Alcohol	ND	ND	ND	ND
7-deoxyglycone of parent drug	0.009 ± 0.001	0.069	0.003 ± 0.001	0.128
7-deoxyglycone of alcohol	0.001 ± 0.001	0.021	0.002 ± 0.001	0.048

TABLE 4.3 Peak drug concentration, AUC and metabolites in the MC40A tumour following intravenous administration of adriamycin and 4'-deoxy (\pm standard deviation)

Day	Control	Adriamycin	4'-deoxydoxorubicin
0	100	100	100
2	120 \pm 4	123 \pm 6	112 \pm 6
4	156 \pm 10	148 \pm 14	109 \pm 3
6	192 \pm 11	180 \pm 12	121 \pm 14
8	210 \pm 9	198 \pm 18	108 \pm 16
10	262 \pm 22	232 \pm 17	107 \pm 14

Table 4.4 The percentage increase in tumour volume (taking mean pretreatment volumes as 100%) with time following intravenous treatment with adriamycin (10 mg/kg), 4'-deoxydoxorubicin (10 mg/kg) or normal saline (control). There was no statistical difference in tumour growth rates between control and adriamycin treated animals, whereas 4'-deoxy virtually abolished tumour growth ($p < 0.01$, compared to control at all time points after day 2).

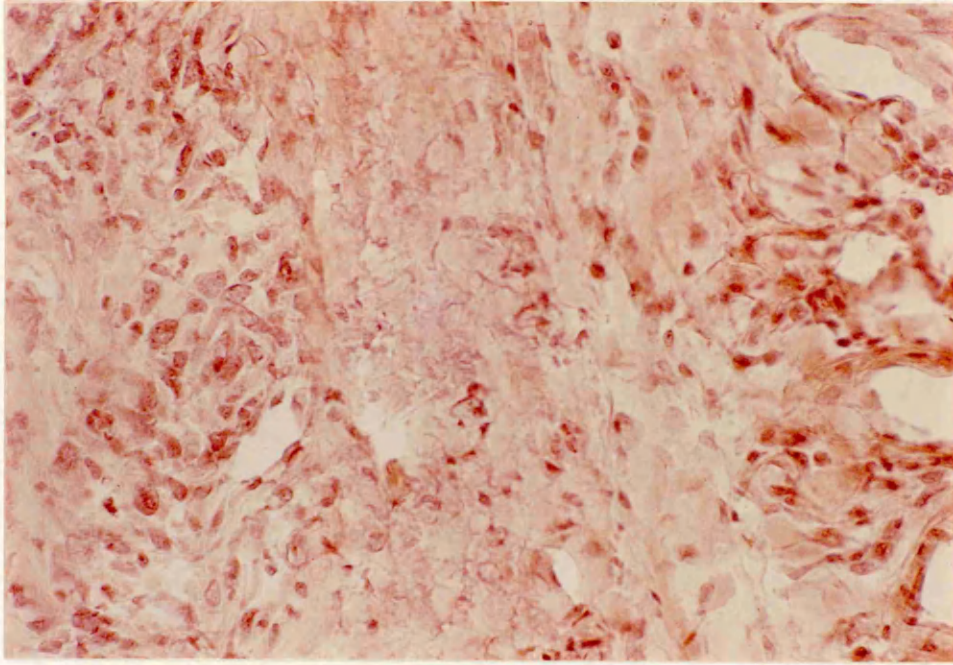


Figure 4.1 Haematoxylin and eosin stained section of the MC40 tumour. Note the vascular annulus on the periphery of the tumour (magnification x 100)



Figure 4.2 Fluorescent photomicrograph of rat cardiac muscle following infusion of adriamycin (magnification x 100)



Figure 4.3 Fluorescent photomicrograph of rat liver following infusion of adriamycin (magnification x 100)



Figure 4.4 Fluorescent photomicrograph of rat skeletal muscle following infusion of adriamycin (magnification x 100)

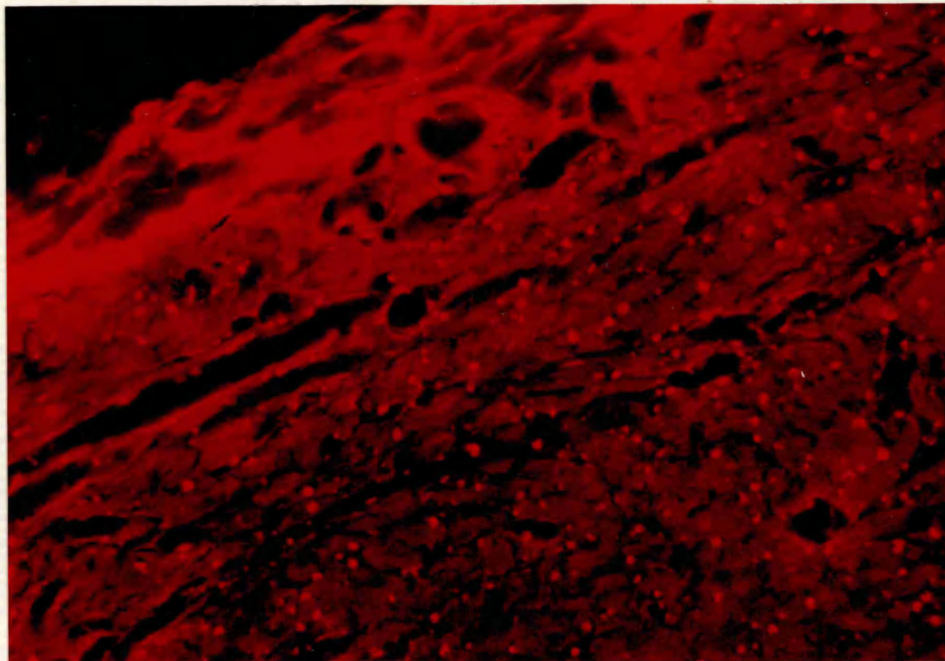


Figure 4.5 Fluorescent photomicrograph of adriamycin treated MC40A tumour. The drug is localised predominantly on the periphery of the tumour, with relatively poor diffusion into the centre of the tumour (magnification x 25).

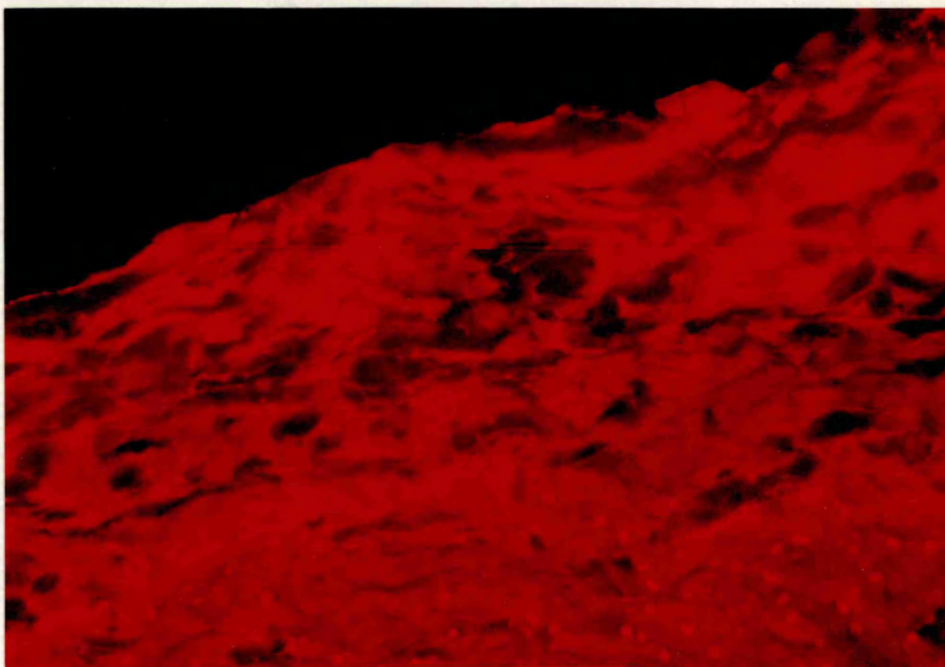


Figure 4.6 Fluorescent photomicrograph of 4'-deoxy treated MC40A tumour. The drug has diffused further into the central, avascular region of the tumour compared to adriamycin (magnification x 25)

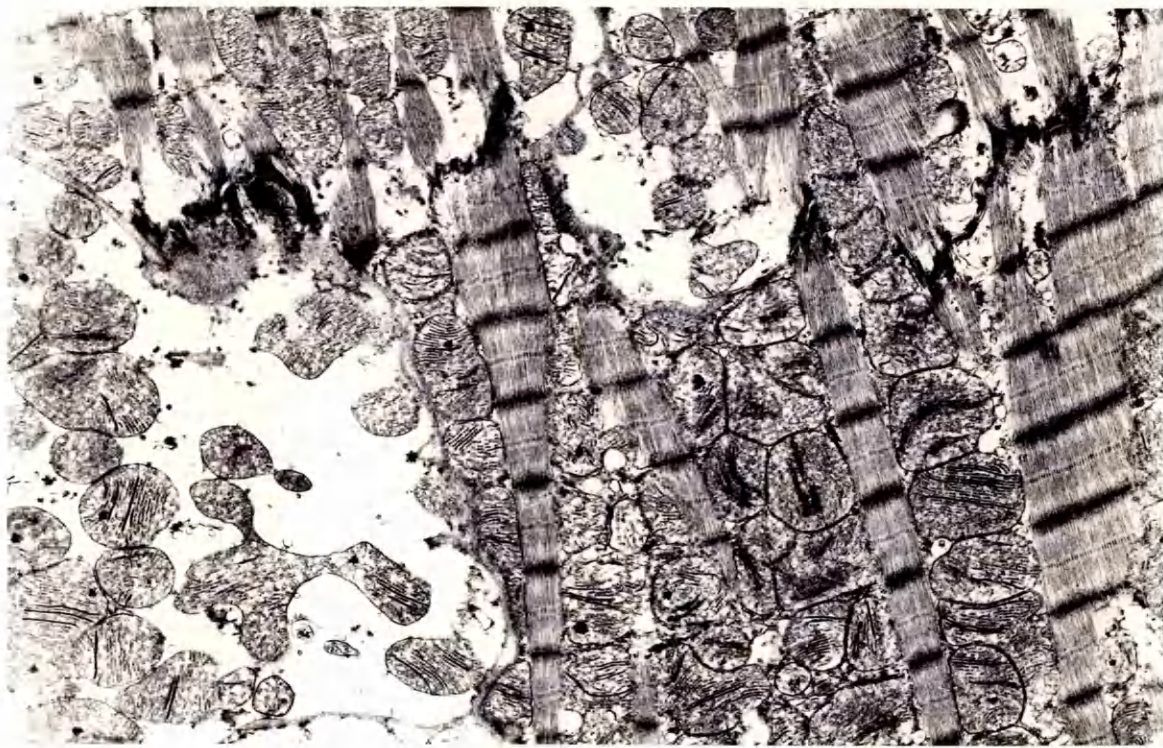


Figure 4.7 Electron micrograph of adriamycin treated rat heart showing mitochondrial swelling and disruption (magnification x 5900)

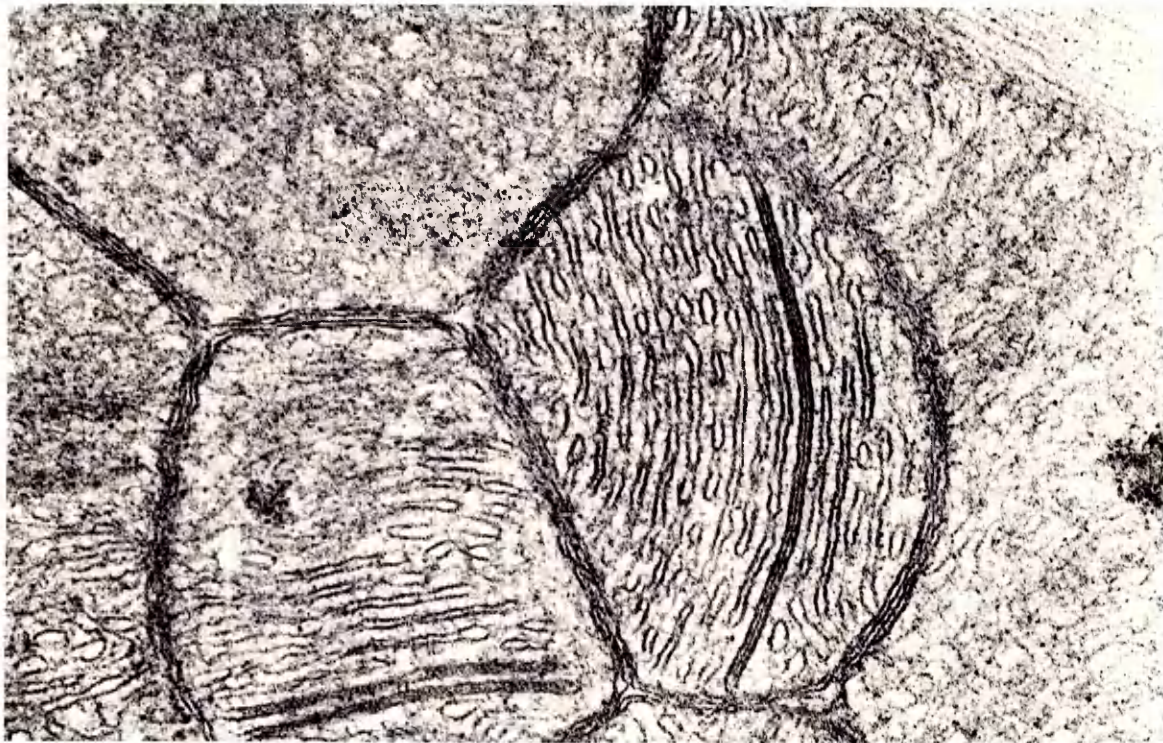


Figure 4.8 Electron micrograph of adriamycin treated rat heart showing a high power view of mitochondrial vesiculation (magnification x 43000)

Cellular accumulation and spheroid penetration of lipophilic anthracycline analogues

5.1. INTRODUCTION

If, as hypothesised, adriamycin diffuses through the lipid domain of the cell membrane, then its rate of diffusion will obey Fick's first law in which the flux per unit area of a molecule through the membrane (J) depends on the diffusion coefficient of the molecule (D) and its concentration gradient across the membrane dc/dx :

$$J = D \, dc/dx$$

D is a complex term and depends on the physico-chemical properties of the drug molecule and the biological membrane. The drug membrane permeability barrier might be overcome by altering the properties of the drug or by increasing membrane fluidity.

There are three properties of a drug molecule that are central to the issue of its transmembrane movement; its lipid solubility, the extent to which it is ionised and its molecular size. Together, these factors determine whether a molecule will move from one biological compartment to another separated by a membranous structure, and provide some basis for predicting the rate and extent of such transmembrane inter compartment movement (Brodie, 1964).

The lattice model of membrane diffusion (fig 5.1) adequately accounts for rates of transport of many non-electrolytes. In this model diffusion, occurs by the movement of the permeant molecule into a "vacancy" in the lattice structure of the membrane (fig 5.1). The principle energetic barrier to diffusion in this case is the activation energy required to move the substrate from the aqueous phase into the apolar environment of the phospholipid bilayer. There is a correlation between membrane permeability and the hydrophobicity of the permeant molecule. The postulated "vacancies" in the lattice are envisaged as temporary discontinuities created by lateral movement of the phospholipid molecules. High rates of diffusion, and therefore increased membrane fluidity, can occur by pretreating the membrane with surface active or "chaotropic" agents. (Wilson, 1978).

In this chapter, the cellular uptake and cytotoxicity of a series of lipophilic anthracycline analogues is described. A number of cytotoxic agents and drugs (eg anti-emetics) have membrane surface active properties, yet the pharmacodynamics of anticancer drug interaction at the level of the cell membrane has not been generally considered. In this section, the effect of a number of common anticancer drugs and agents which might be coadministered in combination with adriamycin, on adriamycin transport is examined.

5.2 Materials and Methods

Monolayer and Spheroid culture - the cell culture conditions used for monolayer and spheroids have been described (sec 3.2)

Determination of monolayer clonogenic survival and spheroid growth delay.

The details of the clonogenic assay and means of assessing spheroid growth delay have been previously annotated (sec 3.2). The anthracyclines used in this study were kindly supplied by Farmitalia Carol Erba Ltd., and were dissolved in normal saline prior to use. The chemical structures are shown in figure 5.2. Tumour cells (both monolayer and spheroid) were treated over a wide concentration range specific to the individual drug being studied; adriamycin (0.1 - 10 $\mu\text{g/ml}$); daunomycin, (0.1 - 10 $\mu\text{g/ml}$); 4-demethoxydaunorubicin (0.05 - 5 $\mu\text{g/ml}$); 4'-deoxy-4'-iododoxorubicin (0.0005 - 1 $\mu\text{g/ml}$); 4'-deoxydoxorubicin (0.1 - 10 $\mu\text{g/ml}$).

Determination of intracellular anthracycline levels

Monolayers of L-DAN cells were exposed to a fixed drug concentration for one hour. The drug concentration differed for each analogue used, and the final intracellular drug concentration was scaled up, as if the cells had been exposed to an external concentration of 5 $\mu\text{g/ml}$. The cells were then harvested, counted and intracellular anthracycline concentrations were measured as previously described (sec 2.2). Additional experiments were performed wherein adriamycin (5 $\mu\text{g/ml}$) was conincubated with putative "penetration enhancers" for one hour. The concentration of the drug used was calculated from its known pharmacokinetics to correspond to maximum achievable plasma levels at clinically employed doses;

metoclopramide (2 $\mu\text{g}/\text{ml}$); prochlorperazine (10 $\mu\text{g}/\text{ml}$); chlorpromazine (50 $\mu\text{g}/\text{ml}$); hydrocortisone ($2 \times 10^{-6}\text{M}$); dexamethasone (10^{-6}M).

An identical series of experiments was performed with cytotoxic agents commonly used in combination therapy with adriamycin; bleomycin (10 $\mu\text{g}/\text{ml}$); VP-16 (50 $\mu\text{g}/\text{ml}$); cis platinum (10 $\mu\text{g}/\text{ml}$); vincristine ($5 \times 10^{-8}\text{M}$); 5-fluorouracil (200 $\mu\text{g}/\text{ml}$); methotrexate (10^{-5}M); flavone acetic acid (LM975), (200 $\mu\text{g}/\text{ml}$). Each experiment was repeated five times and statistical analysis was by Students t-test with Bonferonni's correction, where applicable. Correlation analyses were done using Spearman's rank correlation test.

Fluorescent microscopic assessment of intraspheroid drug penetration

Spheroids of 400 μm in diameter were incubated at a fixed drug concentration for one hour. Thereafter the spheroids were prepared for fluorescent microscopy as previously described (sec 3.2)

Intracellular anthracycline levels

The intracellular concentrations achieved for the different anthracycline analogues are summarised in table 5.1 with the butanol/Tris-buffer partition coefficients of the individual compounds. There was a degree of intracellular metabolism of daunomycin (50%) and 4-demethoxydaunomycin (15%) to their respective alcohols, but in the interest of clarity, only total intracellular drug (i.e. parent drug + alcohol) levels are presented. There would appear to be a linear relationship between hydrophobicity, as estimated by the oil/water partition coefficient, and intracellular drug concentration ($r = 0.99$, $P < 0.01$)

The only drug which significantly affected adriamycin uptake in the coincubation experiments was flavone acetic acid (Table 5.2). This inhibited the cellular accumulation of adriamycin such that total intracellular adriamycin levels were $< 10\%$ of control.

Relative cytotoxicity of the anthracycline analogues

The composite spheroid growth curve analysis for each of the anthracyclines used are shown in tables 5.3 - 5.7.

The clonogenic ID_{90} for monolayers, and the drug concentration which produced a doubling in growth delay relative to control is summarised for individual analogues in table 5.8 (the monolayer cell survival curves are shown in figure 5.3).

There is no correlation between monolayer potency and the oil/water partition coefficients, but this relationship is confounded mainly by 4'-deoxydoxorubicin.

There is a linear correlation ($r = 0.99$, $p < 0.01$) between \log [concentration which doubles growth delay relative to control] and \log [oil/water partition coefficient] and \log [intracellular drug level].

Spheroid drug diffusion gradients; fluorescent microscopy

Under the experimental conditions used, it was possible to differentiate the pattern of spheroid penetration for adriamycin from those of the hydrophobic analogues. It was not, however, possible to distinguish the diffusion patterns of the analogues from each other. By one hour, the drugs had diffused to a depth of 6 - 8 cell layers from the external spheroid surface (Fig 5.4). All visible drug was bound to the nucleus and there was no evidence of cytoplasmic fluorescence. Due to the relative insensitivity of fluorescence microscopy and the variable quenching caused by nuclear binding of different anthracyclines (Crooke and Dunvernoy, 1980; Egorin et al, 1980) it was not possible to make a quantitative analysis of relative diffusion for the lipophilic derivatives.

The more hydrophobic the molecule the greater the degree of cellular drug uptake. This is consistent with the hypothesis that the anthracyclines diffuse through the lipid domain of the cell membrane (Dalmark and Storm), 1981). According to Fick's law, the more lipophilic anthracycline congeners have higher diffusion coefficients (D) than the parent compound. There is a correlation between membrane permeability and hydrophobicity which can be explained by the lattice theory of transmembrane diffusion. The more lipophilic the molecule, the less activation energy is required to move the substrate from the aqueous phase into the relatively apolar environment of the membrane. Therefore the bioenergetics of transmembrane diffusion favours the more hydrophobic derivatives. As mentioned previously, the oil/water partition coefficient is not the only determinant of transcellular drug movement. The anthracyclines have an ionisable amino group on the daunosamine sugar with a pK_a of 7.5 - 8. The degree of ionisation of the drug molecule is important, as a charged drug moiety will not cross the membrane. The dependence of adriamycin uptake on external pH has already been demonstrated (sec 3.3). The sigmoid curve of intracellular drug vs pH (fig 3.2a) conforms to the calculated curve of degree of drug ionisation vs pH (fig 3.2b).

The third variable which orders transmembrane inter-compartmental drug transfer is molecular size. Prabhakar et al (1986) have correlated in vitro antitumour activity (inhibition of growth of human lymphoblastic leukaemia cells) of several adriamycin analogues with the van der Waals volume of the substituents. Activity was also found to be well correlated with first-order valence molecular connectivity index. On the basis of their findings, the authors concluded that cytotoxic activity would be

affected by the steric influence and to some extent by the electronic configuration of the substituent groups appended to the tetracyclic ring backbone.

There does not appear to be a direct relationship between lipophilicity and cytotoxic efficacy in monolayer. Although a log linear relationship between intracellular adriamycin concentration and clonogenic cell kill exists, (sec 2.2) this is not the case for 4'-deoxy. This presumably accounts for the disparity between the oil/water partition coefficient and the degree of clonogenic cell kill, at least for 4'-deoxy. The mode of action of the anthracyclines is thought to depend on the ability of these drugs to intercalate into DNA and thus prevent DNA synthesis (Dano et al, 1972; Rozenzweig et al, 1975 Arlandini et al, 1977; Bachur, 1979; Cassaza, 1979; Cassaza, 1980; Schwartz, 1983; Terasaki, 1984). However, there is no association between the DNA binding constants of individual analogues and cytotoxic end points in vitro (Israel and Potti, 1982) Given the disparity between cytotoxic efficacy and relative affinity for DNA intercalation, this implies either that the anthracyclines have different modes of cytotoxic action, or that some other stage in the interaction between drug and intact cell is rate limiting. Alberts and Dorr (1982) have reviewed the many proposed mechanisms of action of adriamycin, including intracellular free radical production, anti-mitochondrial effects and surface active membrane properties, yet concluded that inhibition of DNA synthesis still seems the most likely means of the drug exerting its cytotoxic effects. This also seems to be the case for the other anthracycline compounds used in this study (Cassaza, 1980).

The rate limiting step with regard to cellular accumulation of drug molecules is transmembrane transport. In this respect, the cell membrane can be likened to a sheet of synthetic rubber such is its ability to retard drug diffusion. As demonstrated, there is a relationship between hydrophobicity and intracellular drug levels, but not between hydrophobicity and clonogenic cell survival. By syllogistic reasoning this implies that there is not a direct relationship between intracellular drug levels and clonogenic cell survival (correlation $r = 0.23$, $p > 0.4$). It is apparent that of the relatively limited series of derivatives tested, 4'-deoxy would appear to behave differently from the other analogues and confounds the correlations between intracellular drug concentration and hydrophobicity with monolayer clonogenic survival. One major reported difference between 4'-deoxy and the other congeners is its inability to form free radicals in vitro, and it is possible that this difference obfuscates a structure-activity relationship in monolayer culture.

There does appear to be a correlation between the log of the concentration of drug which doubles spheroid growth delay and log oil/water partition coefficient and ($r = 0.99$, $P < 0.01$) and log intracellular drug levels in monolayer ($r = 0.99$, $P < 0.01$). It was impossible, however, to correlate spheroid diffusion depth with either of these parameters due to the insensitivity of the fluorescent microscopic technique used. Presumably, the greater the ease with which the drug molecules cross the cell membrane, the greater will be the degree of intercompartmental membrane transport within the spheroid. The more drug which is taken up into the external spheroid ring, the greater the concentration gradient which

which will drive diffusion of the drug into the substance of the spheroid.

There was no enhancement of adriamycin uptake by any of the drugs listed in Table 5.2. It is of note that flavone acetic acid, an experimental therapeutic agent which is currently undergoing phase I clinical assessment, significantly decreased adriamycin uptake. The mechanism of this is unknown, however the class of flavonoid aglycones are thought to inhibit membrane transport of a variety of compounds and this may explain its inhibition of adriamycin uptake.

There have been reports of chlorpromazine, lignocaine and octanol (Dalmark and Storm, 1981) increasing the permeability of tumour cell membranes to adriamycin, but at concentrations far in excess of these pharmacologically achievable. It is unlikely therefore, that there is any significant pharmacodynamic interaction between adriamycin and the drugs listed in Table 5.2, in common clinical practice.

Compound	Intracellular Concentration (ng/10 ⁵ cells)	Oil/Water Partition Coefficient
Adriamycin	14 ± 2	6.3
Daunomycin	154 ± 27	17.8
4'-deoxydoxorubicin	170 ± 15	15.0
4-demethoxydaunomycin	400 ± 67	32.3
4'-iodo,4'-deoxydoxorubicin	1961 ± 156	126

Table 5.1 Intracellular drug levels (± standard deviation) following monolayer exposure to equivalent of 5 µg/ml for one hour. Oil/water partitioning was carried out with butanol/tris-buffer.

Compound	Intracellular Adriamycin Concentration (ng/10 ⁵ cells)
Adriamycin alone	14 ± 2
Adriamycin + VP16	16 ± 2.5
Adriamycin + 5-fluorouracil	18 ± 4
Adriamycin + bleomycin	13 ± 3.2
Adriamycin + cisplatin	17 ± 5.2
Adriamycin + methotrexate	11 ± 6.2
Adriamycin + flavone acetic acid	0.9 ± 0.25 (p < 0.01)
Adriamycin + metoclopramide	15 ± 3.2
Adriamycin + prochlorperazine	14 ± 4.1
Adriamycin + hydrocortisone	13 ± 1.9
Adriamycin + chlorpromazine	18 ± 3.4
Adriamycin + dexamethasone	18 ± 3.6

TABLE 5.2 Intracellular Adriamycin levels (± standard deviation) following co-incubation with a variety of different drugs.

COMPOSITE GROWTH CURVE ANALYSIS

Drug Concentration ($\mu\text{g/ml}$)	Day	No. of Spheroids	Median Diameter (μm)	95% Confidence Limits	Log Volume	95% Confidence Limits
Control	0	19	234.0	217.0 269.4	6.827	6.729 7.010
	5	19	432.6	387.6 444.2	7.746	7.714 7.815
	7	18	474.0	462.5 499.6	7.746	7.714 7.815
	12	13	630.3	579.8 673.3	8.118	8.009 8.204
1	0	23	201.9	195.4 225.7	6.634	6.592 6.779
	5	23	287.7	247.2 309.0	7.096	6.898 7.189
	7	23	298.5	278.7 315.1	7.144	7.054 7.215
	12	23	307.0	276.4 321.1	7.180	7.044 7.239
	14	23	321.1	294.2 360.4	7.239	7.125 7.389
	18	23	363.9	334.7 445.7	7.402	7.293 7.666
	20	23	428.2	360.4 466.6	7.614	7.389 7.726
	25	22	507.0	365.6 563.1	7.834	7.408 7.971
	27	19	502.1	386.0 584.1	7.821	7.479 8.019

Table 5.3 Composite growth curve analysis for spheroids treated with 4'-deoxydoxorubicin.

COMPOSITE GROWTH CURVE ANALYSIS (cont)

Drug Concentration ($\mu\text{g/ml}$)	Day	No. of Spheroids	Median Diameter (μm)	95% Confidence Limits	Log Volume	95% Confidence Limits
5	0	21	247.2	222.8 259.8	6.898	6.773 6.963
	5	21	276.4	264.6 298.5	7.044	6.987 7.144
	7	21	298.5	278.7 311.1	7.144	7.054 7.198
	12	21	281.0	274.1 304.9	7.065	7.033 7.171
	14	21	315.1	285.5 322.8	7.215	7.086 7.286
	18	21	330.9	309.0 360.4	7.278	7.189 7.389
	20	21	342.3	315.1 370.8	7.322	7.215 7.426
	10	0	18	264.6	222.8 281.0	6.986
	5	18	254.6	231.2 264.6	6.936	6.811 6.987
	7	18	271.7	234.0 289.9	7.021	6.827 7.106
	12	18	257.3	239.4 292.1	6.950	6.856 7.115
	14	18	280.8	247.2 304.9	7.064	6.898 7.171
	18	18	302.7	283.2 384.3	7.162	7.075 7.473
	20	18	318.1	283.2 417.7	7.227	7.075 7.581
	25	17	375.9	323.1 519.5	7.444	7.247 7.866
	27	13	392.5	353.2 588.5	7.501	7.363 8.028

Table 5.3 Composite growth curve analysis for spheroids treated with 4'-deoxydoxorubicin.

COMPOSITE GROWTH CURVE ANALYSIS (cont)

Drug Concentration ($\mu\text{g/ml}$)	Day	No. of Spheroids	Median Diameter (μm)	95% Confidence Limits	Log Volume	95% Confidence Limits
15	0	18	276.4	225.7 289.9	7.043	6.779 7.106
	5	18	254.8	242.0 264.6	6.938	6.870 6.987
	7	18	252.2	247.2 294.2	6.975	6.898 7.125
	12	18	237.8	211.1 254.8	6.847	6.692 6.938
	14	18	248.3	217.0 274.1	6.903	6.729 7.033
	18	18	268.2	228.5 281.0	7.004	6.796 7.065
	20	17	276.4	267.0 296.4	7.044	6.999 7.135
	25	15	296.4	285.5 342.3	7.135	7.086 7.322
	27	6	328.7	309.0 524.4	7.268	7.189 7.878
	20	0	13	211.1	195.4 247.2	6.692
5		12	276.4	22.8 276.4	7.044	6.763 7.044
7		13	220.0	217.0 222.8	6.746	6.729 6.763
12		13	220.0	217.0 242.0	6.746	6.729 6.870
14		10	169.2	159.6 208.1	6.404	6.328 6.674
18		8	171.1	155.5 208.1	6.418	6.294 6.674

Table 5.3 Composite growth curve analysis for spheroids treated with 4'-deoxydoxorubicin.

COMPOSITE GROWTH CURVE ANALYSIS

Drug Concentration ($\mu\text{g/ml}$)	Day	No. of Spheroids	Median Diameter (μm)	95% Confidence Limits	Log Volume	95% Confidence Limits	
Control	0	23	242.0	195.4 271.7	6.871	6.592 7.022	
	2	23	311.1	254.8 342.3	7.198	6.938 7.322	
	7	23	520.8	463.9 549.3	7.869	7.718 7.938	
	9	23	584.1	530.5 604.5	8.019	7.893 8.063	
	14	23	717.2	684.5 748.5	8.286	8.225 8.342	
	16	21	767.8	728.7 822.2	8.375	8.307 8.464	
	21	3	845.9	845.9 845.9	8.501	8.501 8.501	
	0.5	0	15	254.8	231.2 281.0	6.938	6.811 7.065
		2	15	304.9	276.4 325.1	7.171	7.044 7.255
		7	15	389.2	347.8 402.1	7.490	7.343 7.532
9		15	431.2	386.0 455.6	7.623	7.479 7.695	
14		15	558.5	522.0 607.7	7.960	7.872 8.070	
16		15	585.2	543.5 636.3	8.021	7.925 8.130	
21		15	730.4	647.2 770.3	8.310	8.152 8.379	
23		11	789.1	575.4 866.0	8.410	7.999 8.532	

Table 5.4 Composite growth curve analysis for spheroids treated with daunomycin

COMPOSITE GROWTH CURVE ANALYSIS (cont)

Drug Concentration ($\mu\text{g/ml}$)	Day	No. of Spheroids	Median Diameter (μm)	95% Confidence Limits	Log Volume	95% Confidence Limits	
1	0	21	267.0	252.3 287.7	6.999	6.925 7.096	
	2	21	298.5	283.2 313.1	7.144	7.075 7.206	
	7	21	323.1	311.1 338.5	7.247	7.198 7.308	
	9	21	374.2	362.1 395.7	7.438	7.396 7.511	
	14	21	513.4	486.6 565.3	7.850	7.781 7.976	
	16	21	585.2	518.3 629.3	8.021	7.863 8.116	
	21	21	667.6	622.1 689.1	8.192	8.101 8.234	
	23	21	711.9	658.9 733.0	8.276	8.175 8.314	
	2.5	0	19	281.0	262.2 309.0	7.065	6.975 7.189
		2	19	311.1	285.5 338.5	7.198	7.086 7.308
7		19	327.0	304.9 367.4	7.263	7.171 7.414	
9		19	384.3	356.8 416.1	7.473	7.376 7.577	
14		19	508.4	457.0 622.1	7.838	7.699 8.101	
16		19	537.6	480.1 645.3	7.910	7.763 8.148	
21		19	674.2	600.3 755.3	8.205	8.054 8.353	
23		19	741.6	642.3 806.6	8.330	8.142 8.439	
28		13	710.1	637.3 848.9	8.273	8.132 8.506	

Table 5.4 Composite growth curve analysis for spheroids treated with daunomycin.

COMPOSITE GROWTH CURVE ANALYSIS (cont)

Drug Concentration ($\mu\text{g/ml}$)	Day	No. of Spheroids	Median Diameter (μm)	95% Confidence Limits	Log Volume	95% Confidence Limits
5	0	18	251.0	234.0 276.4	6.918	6.827 7.044
	2	18	263.4	257.3 300.7	6.981	6.950 7.153
	7	18	283.2	257.3 321.1	7.075	6.950 7.239
	9	18	296.4	285.5 340.4	7.135	7.086 7.315
	14	18	384.3	351.4 416.1	7.473	7.357 7.577
	16	18	434.7	382.7 498.3	7.633	7.467 7.811
	21	17	575.4	530.5 608.7	7.999	7.893 8.072
	23	17	619.1	572.0 633.3	8.094	7.991 8.124
	28	13	664.7	606.6 681.7	8.187	8.068 8.220

Table 5.4 Composite growth curve analysis for spheroid treated with daunomycin.

COMPOSITE GROWTH CURVE ANALYSIS

Drug Concentration ($\mu\text{g/ml}$)	Day	No. of Spheroids	Median Diameter (μm)	95% Confidence Limits	Log Volume	95% Confidence Limits
Control	3	19	271.7	228.5 311.1	7.022	6.796 7.198
	6	19	387.6	370.8 434.1	7.484	7.426 7.632
	8	19	441.4	387.6 532.9	7.653	7.484 7.899
0	10	19	529.3	441.4 545.8	7.890	7.653 7.930
	13	19	601.3	480.1 619.1	8.056	7.763 8.094
	16	19	665.6	609.7 705.6	8.189	8.074 8.265
	20	14	754.5	706.5 827.6	8.352	8.266 8.473
1	3	23	198.7	142.7 254.8	6.613	6.183 6.938
	6	23	247.2	201.9 315.1	6.898	6.634 7.215
	8	23	360.4	269.4 382.7	7.389	7.010 7.467
	10	23	382.7	313.1 442.8	7.467	7.206 7.658
	13	22	511.5	369.1 561.9	7.846	7.420 7.968
	16	22	628.2	518.3 683.6	8.113	7.863 8.223
	20	20	744.1	622.1 831.5	8.334	8.101 8.479

Table 5.5 Composite growth curve analysis for spheroids treated with adriamycin.

COMPOSITE GROWTH CURVE ANALYSIS (cont)

Drug Concentration ($\mu\text{g/ml}$)	Day	No. of Spheroids	Median Diameter (μm)	95% Confidence Limits	Log Volume	95% Confidence Limits
5	3	21	217.0	188.8 244.6	6.729	6.547 6.885
	6	21	242.0	225.7 276.4	6.870	6.779 7.044
	8	21	294.2	262.2 342.3	7.125	6.975 7.322
	10	21	315.1	294.2 397.3	7.215	7.125 7.516
	13	21	408.4	379.3 474.4	7.552	7.456 7.745
	16	21	524.4	461.1 620.1	7.878	7.710 8.096
10	3	19	195.4	163.5 234.0	6.592	6.360 6.827
	6	19	214.1	198.7 264.6	6.711	6.613 6.987
	8	19	259.8	222.8 278.7	6.963	6.763 7.054
	10	19	264.6	236.7 302.8	6.987	6.842 7.162
	13	19	365.6	302.8 375.9	7.408	7.162 7.444
	16	19	455.6	394.1 468.0	7.695	7.506 7.730
	20	17	529.3	512.1 596.0	7.890	7.847 8.045

Table 5.5 Composite growth curve analysis for spheroids treated with adriamycin.

COMPOSITE GROWTH CURVE ANALYSIS (cont)

Drug Concentration ($\mu\text{g/ml}$)	Day	No. of Spheroids	Median Diameter (μm)	95% Confidence Limits	Log Volume	95% Confidence Limits
12.5	3	16	238.0	195.4 267.0	6.849	6.592 6.999
	6	16	217.0	188.8 259.8	6.728	6.547 6.963
	8	16	234.0	217.0 262.2	6.826	6.729 6.975
	10	16	275.2	252.3 307.0	7.038	6.925 7.180
	13	16	365.5	311.1 387.6	7.408	7.198 7.484
	16	16	440.6	390.9 481.4	7.651	7.495 7.766
	20	16	550.1	490.6 606.6	7.940	7.791 8.068
	20	19	201.9	159.6 236.7	6.634	6.328 6.842
20	6	19	192.2	171.1 247.2	6.570	6.419 6.898
	8	19	214.1	178.4 262.2	6.711	6.473 6.975
	10	19	231.2	195.4 313.1	6.811	6.592 7.206
	13	19	296.4	259.8 392.5	7.135	6.963 7.501
	16	19	386.0	355.0 498.3	7.479	7.370 7.811
	20	19	566.4	449.9 622.1	7.978	7.678 8.101

Table 5.5 Composite growth curve analysis for spheroids treated with adriamycin.

COMPOSITE GROWTH CURVE ANALYSIS

Drug Concentration ($\mu\text{g/ml}$)	Day	No. of Spheroids	Median Diameter (μm)	95% Confidence Limits	Log Volume	95% Confidence Limits
Control	0	20	183.7	178.4 - 192.2	6.511	6.473 - 6.570
	2	20	276.2	244.6 - 313.1	7.041	6.885 - 7.206
	7	20	449.2	394.1 - 462.5	7.676	7.506 - 7.714
	9	20	494.4	449.9 - 526.8	7.801	7.678 - 7.884
	14	20	584.1	572.0 - 596.0	8.019	7.991 - 8.045
	16	16	627.7	608.7 - 668.5	8.112	8.072 - 8.194
0.1	0	17	225.7	208.1 - 262.2	6.779	6.674 - 6.975
	2	17	244.6	217.0 - 262.2	6.885	6.729 - 6.975
	7	17	252.3	234.0 - 285.5	6.925	6.827 - 7.086
	9	17	281.0	274.1 - 296.4	7.065	7.033 - 7.135
	14	17	347.8	317.2 - 398.9	7.343	7.223 - 7.522
	16	17	403.7	370.8 - 438.5	7.537	7.426 - 7.645
	21	16	459.0	429.7 - 566.4	7.704	7.618 - 7.978
	23	10	495.0	469.3 - 594.9	7.803	7.733 - 8.042

Table 5.6 Composite growth curve analysis for spheroids treated with 4-demethoxydaunomycin.

COMPOSITE GROWTH CURVE ANALYSIS (cont)

Drug Concentration ($\mu\text{g/ml}$)	Day	No. of Spheroids	Median Diameter (μm)	95% Confidence Limits	Log Volume	95% Confidence Limits	
0.5	0	16	197.1	174.8 - 234.0	6.603	6.447 - 6.827	
	2	16	197.1	188.8 - 231.2	6.603	6.547 - 6.811	
	7	16	197.1	181.9 - 228.5	6.603	6.499 - 6.796	
	9	16	214.1	198.7 - 234.0	6.711	6.613 - 6.827	
	14	16	236.6	211.1 - 281.0	6.840	6.692 - 7.065	
	16	16	288.8	257.3 - 332.8	7.101	6.950 - 7.286	
	21	14	328.8	309.0 - 403.7	7.269	7.189 - 7.537	
	23	12	365.6	340.4 - 481.4	7.408	7.315 - 7.766	
	1	0	17	192.2	174.8 - 211.1	6.570	6.447 - 6.692
		2	17	188.8	174.8 - 198.7	6.547	6.447 - 6.613
		7	17	192.2	174.8 - 211.1	6.570	6.447 - 6.692
		9	17	211.1	188.8 - 234.0	6.692	6.547 - 6.827
14		17	236.7	220.0 - 264.6	6.842	6.746 - 6.987	
16		15	289.9	259.8 - 317.2	7.106	6.963 - 7.223	
21		12	312.0	292.1 - 342.3	7.201	7.115 - 7.322	
23		8	363.8	332.8 - 663.7	7.401	7.286 - 8.185	

Table 5.6 Composite growth curve analysis for spheroids treated with 4-demethoxydaunomycin

COMPOSITE GROWTH CURVE ANALYSIS

Drug Concentration ($\mu\text{g/ml}$)	Day	No. of Spheroids	Median Diameter (μm)	95% Confidence Limits	Log Volume	95% Confidence Limits
Control	0	20	200.3	178.4 211.1	6.624	6.473 6.692
	3	20	293.2	271.7 315.1	7.120	7.022 7.215
	6	20	443.5	437.0 468.0	7.660	7.641 7.730
	9	20	555.1	542.3 613.9	7.952	7.922 8.083
	13	20	670.9	659.9 706.5	8.199	8.177 8.266
	17	20	795.5	791.5 810.6	8.421	8.414 8.445
	0.005	0	19	195.4	174.8 211.1	6.592
	3	19	220.0	188.8 228.5	6.746	6.547 6.796
	6	19	236.7	214.1 264.6	6.842	6.711 6.987
	9	19	281.0	242.0 317.2	7.065	6.871 7.223
	13	19	437.0	356.8 468.0	7.641	7.376 7.730
	17	19	586.3	476.1 633.3	8.023	7.752 8.124
	20	19	714.5	619.1 728.7	8.281	8.094 8.307
	24	9	979.2	827.6 1099.8	8.692	8.473 8.843

Table 5.7 Composite growth Curve analysis for spheroids treated with 4'-deoxy, 4'-iodo doxorubicin.

COMPOSITE GROWTH CURVE ANALYSIS (cont)

Drug Concentration ($\mu\text{g/ml}$)	Day	No. of Spheroids	Median Diameter (μm)	95% Confidence Limits	Log Volume	95% Confidence Limits	
0.01	0	19	195.4	174.8 214.1	6.592	6.447 6.711	
	3	19	198.7	171.1 211.1	6.613	6.419 6.692	
	6	19	211.1	192.2 220.0	6.692	6.570 6.746	
	9	19	222.8	208.1 247.2	6.763	6.674 6.898	
	13	19	269.4	228.5 321.1	7.010	6.796 7.239	
	17	19	325.1	287.7 435.6	7.255	7.096 7.636	
	20	18	429.7	338.5 540.0	7.618	7.308 7.916	
	24	14	581.9	468.0 655.0	8.013	7.730 8.168	
	0.05	0	20	208.1	171.1 220.0	6.674	6.419 6.746
		3	20	190.5	181.9 208.1	6.559	6.499 6.674
6		20	178.4	171.1 195.4	6.473	6.419 6.592	
9		20	178.4	171.1 195.4	6.473	6.419 6.592	
13		19	220.0	185.4 252.3	6.746	6.523 6.925	
17		16	247.2	192.2 285.5	6.898	6.570 7.086	
20		10	303.7	222.8 321.1	7.166	6.763 7.239	
24		10	323.0	222.8 358.6	7.246	6.763 7.383	

Table 5.7 Composite growth curve analysis for spheroids treated with 4'-deoxy, 4'-iodo doxorubicin

COMPOSITE GROWTH CURVE ANALYSIS (cont)

Drug Concentration ($\mu\text{g/ml}$)	Day	No. of Spheroids	Median Diameter (μm)	95% Confidence Limits	Log Volume	95% Confidence Limits
0.1	0	20	190.5	174.8 198.7	6.559	6.447 6.613
	3	20	173.0	155.5 192.2	6.433	6.294 6.570
	6	20	174.8	163.5 188.8	6.447	6.360 6.547
	9	20	163.5	159.6 171.1	6.360	6.328 6.419
	13	20	171.1	159.6 185.4	6.419	6.328 6.523
	17	15	178.1	159.6 185.4	6.473	6.328 6.523
	20	12	208.1	208.1 211.1	6.674	6.674 6.692
	24	12	215.6	208.1 249.8	6.720	6.674 6.912

Table 5.7 Composite growth curve analysis for spheroids treated with 4'-deoxy, 4'-iodo doxorubicin.

Compound	Monolayer Clonogenic ID ₉₀ (ug/ml)	Spheroid Growth Delay (ug/ml)
Adriamycin	2.2	10
Daunorubicin	1	0.6
4'-deoxydoxorubicin	2.1	0.68
4-demethoxydaunorubicin	0.1	0.05
4'-deoxy, 4'-iododoxorubicin	0.007	0.004

TABLE 5.8 The relative potency of anthracycline compounds in vitro, assessed by monolayer clonogenic cell survival and spheroid growth delay. The drug concentration producing a doubling in spheroid growth delay relative to control is quoted.

(a) Lattice theory

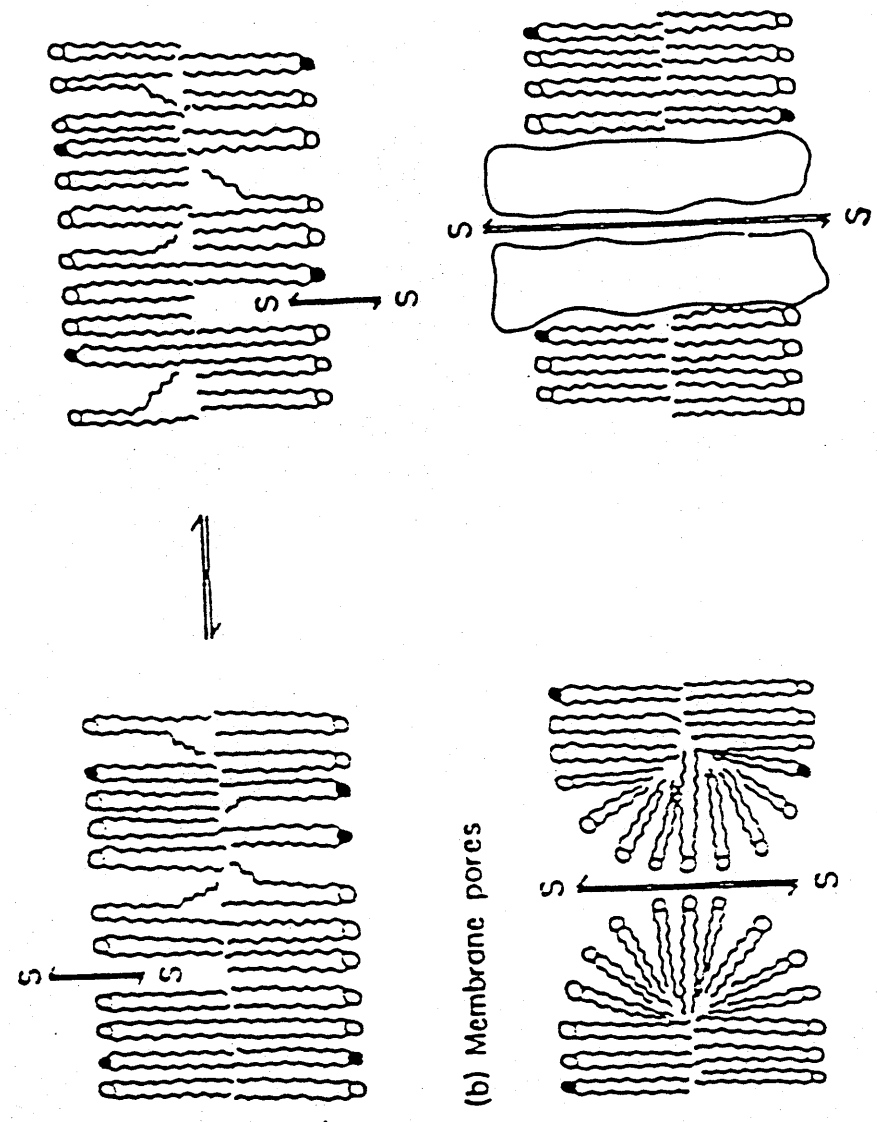
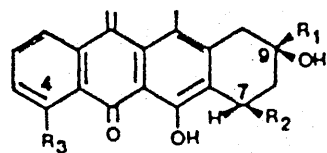


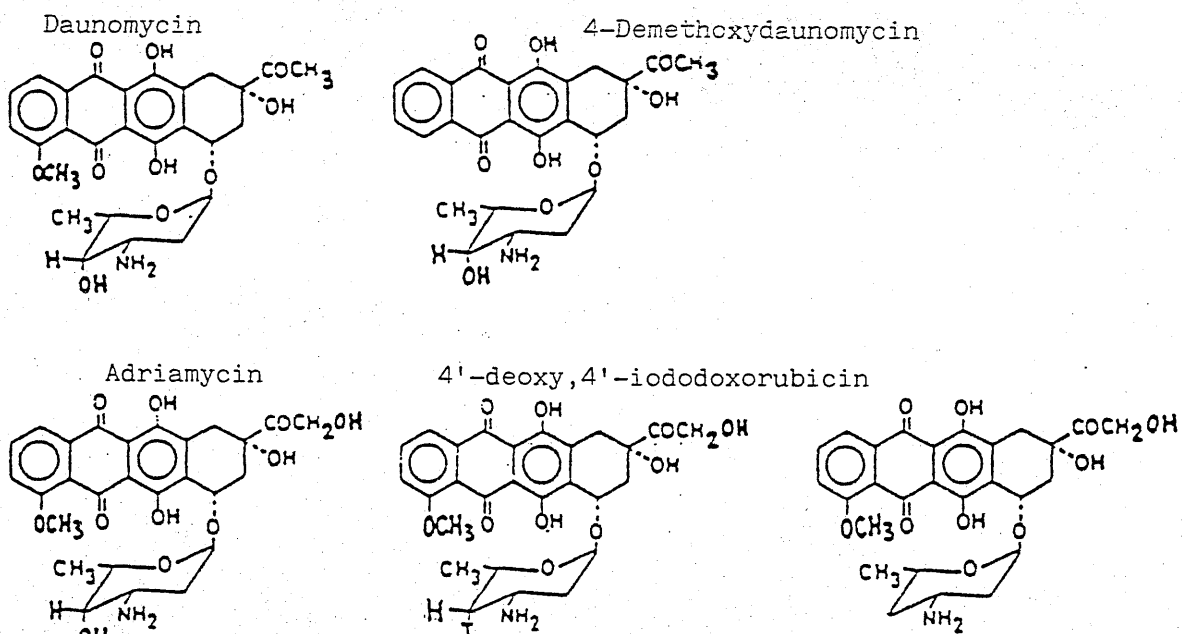
Figure 5.1 (a) The movement of a solute (S) into a pore created by lateral diffusion of lipids in the outer leaflet of the cell membrane is shown. When a space appears in the inner membrane leaflet, the solute is free to diffuse into the cytoplasm. (b) Membrane pores can be created by reorganisation of the polar lipid heads or by a transmembrane protein which allows diffusion of drug molecules of specific size, shape and charge.



COMPOUND	R ₁	R ₂	R ₃
1 ADR	$\begin{array}{c} \text{O} \\ \parallel \\ -\text{C}-\text{CH}_2\text{OH} \\ 13 \end{array}$		$\begin{array}{c} \\ \text{OCH}_3 \end{array}$
2 AOL	$\begin{array}{c} \text{OH} \\ \\ -\text{C}-\text{CH}_2\text{OH} \\ \\ \text{H} \end{array}$		$\begin{array}{c} \\ \text{OCH}_3 \end{array}$
3 ADR-ONE	$\begin{array}{c} \text{O} \\ \parallel \\ -\text{C}-\text{CH}_2\text{OH} \end{array}$	$\begin{array}{c} \\ \text{OH} \end{array}$	$\begin{array}{c} \\ \text{OCH}_3 \end{array}$
4 AOL-ONE	$\begin{array}{c} \text{OH} \\ \\ -\text{C}-\text{CH}_2\text{OH} \\ \\ \text{H} \end{array}$	$\begin{array}{c} \\ \text{OH} \end{array}$	$\begin{array}{c} \\ \text{OCH}_3 \end{array}$
5 ADR-DONE	$\begin{array}{c} \text{O} \\ \parallel \\ -\text{C}-\text{CH}_2\text{OH} \end{array}$	$\begin{array}{c} \\ \text{H} \end{array}$	$\begin{array}{c} \\ \text{OCH}_3 \end{array}$
6 AOL-DONE	$\begin{array}{c} \text{OH} \\ \\ -\text{C}-\text{CH}_2\text{OH} \\ \\ \text{H} \end{array}$	$\begin{array}{c} \\ \text{H} \end{array}$	$\begin{array}{c} \\ \text{OCH}_3 \end{array}$

Figure 5.2 The structure of adriamycin and its metabolites.

1. Adriamycin
2. Adriamycinol
3. 7-deoxyglycone of adriamycin
4. 7-deoxyglycone of adriamycinol
5. 7-deoxyglycone of adriamycin
6. 7-deoxyglycone of adriamycinol



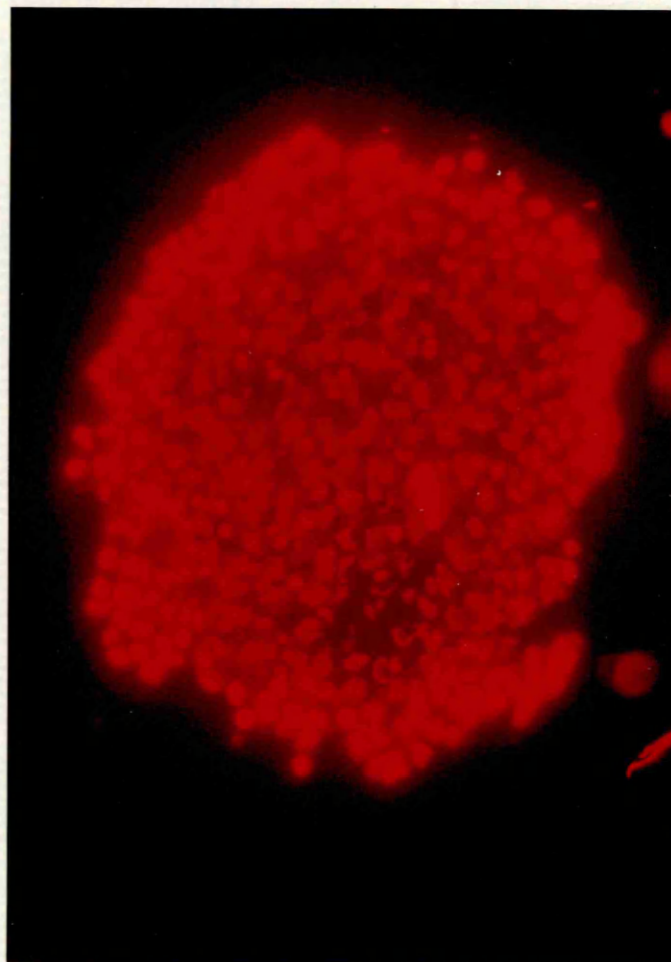


Figure 5.4 Fluorescent photomicrograph of an L-DAN spheroid exposed to 4'-deoxy, 4'-iododoxorubicin 2 ug/ml for 1 hour (magnification x 100)

The effect of the non-ionic surfactant, Brij 30 on cellular uptake and cytotoxicity of adriamycin in monolayer and spheroid culture systems.

6.1 INTRODUCTION

Studies in several mammalian cell culture systems have shown that experimentally developed resistance to adriamycin is associated with reduced membrane permeability to the drug (Riehm and Biedler, 1971; Dano et al, 1972; Kaye and Merry, 1985). Levin's calculations (Levin et al, 1980) showed that the slow diffusion of drug into tumour could limit the effectiveness of chemotherapy, and have encouraged the search for penetration enhancers (Azmin et al, 1985). Many non-ionic surfactants particularly of the poly(oxyethylene) alkyl and aryl ether class interact with biological membranes increasing their permeability and allowing increased trans-membrane solute transport (Florence et al, 1984). While the mechanisms are not fully understood, interaction of the surfactant molecules with the membrane occurs following adsorption and the disruption of membrane integrity and function is at the centre of many of their observed biological effects (Florence, 1981).

Not all surfactants are capable of inducing increased membrane fluidity and drug transport. However the nonionic detergent polysorbate 80 has been reported to increase the absorption of methotrexate (Azmin et al, 1985) and to potentiate the anti-neoplastic effect of adriamycin in vivo and in vitro (Riehm and Biedler, 1972; Seeber et al, 1978; Cassazza et al, 1978). These effects were attributed to an increase in cellular drug uptake in the presence of the detergent, presumably mediated by altered membrane fluidity (Seeber et al, 1978).

In this chapter we have assessed the effect of an alkyl ether polyoxyethylated surfactant, one of a series of surfactants studied to determine the relationship between structure and influence on membrane permeability (Watters et al, 1982) on the cellular accumulation and cytotoxicity of adriamycin in monolayer and spheroid culture systems. A lauryl ether, Brij 30, was chosen because of the finding that this alkyl chain length was optimum in enhancing permeability in other test systems.

Monolayer culture: The L-DAN cell line was derived from our own patient with squamous lung cancer. The cells were maintained as a monolayer in exponential growth in Ham's F10/DMEM (50:50) with 8mM NaHCO_3 supplemented with foetal calf serum. Chronic mouse myeloid leukaemia (M1R1 cell line) and mouse granulocyte cells were maintained in RPMI 1640 medium supplemented with 10 -15% foetal calf serum.

Conditions of drug exposure and determination of cell survival: The monolayers were exposed to adriamycin (Farmitalia Carlo Erba), Brij 30 (Atlas Chemical Industries, England) and a combination of the two over a range of concentrations for one hour. The clonogenic dose response curve for Brij 30 was determined over a concentration range of 0.003-0.3 μ l/ml. During combined treatment, the concentration of Brij 30 was fixed and the concentration of adriamycin varied from 0.1-10 μ g/ml.

After treatment, L-DAN monolayers were harvested with 0.25% trypsin in PBS, centrifuged and washed with ice cold medium. The cells were then diluted in medium and seeded at 200 cell/ml in 5 cm petri dishes. The plates were incubated for 12 days in a humid 2% CO_2 atmosphere. The colonies were then fixed and stained with crystal violet and colonies of ≥ 40 cells were counted. Clonogenic cell survival for the mouse granulocytes and M1R1 cells was determined from an agar capillary method (Maurer and Henry, 1976). Following the usual convention, the cloning efficiency of the untreated cells was normalised to 100% and the cloning efficiency of the treated cells was expressed as a percentage of control survival.

Spheroid culture: L-DAN monolayers were disaggregated enzymatically with 0.25% trypsin in PBS and the resultant cell suspension used to provide cells for initiation of tumour spheroids, using the "agar underlay" static method (Yuh as et al, 1977).

Cytotoxic drug efficacy was assessed by measuring spheroid growth delay and disaggregated spheroid clonogenic survival. Spheroids from two flasks were pooled and a number of glass universal tubes were prepared each containing 200-300 spheroids with a mean diameter of approximately 350 μ m. The spheroids were treated with similar drug concentrations as used in monolayer for one hour at 37°C with intermittent agitation. At the end of this period the spheroids were allowed to sediment, the drug containing medium was removed and they were washed with fresh, ice cold medium. The spheroids were then resuspended in medium and subdivided for assays of response.

For clonogenic assay approximately half of the spheroids were incubated with 0.125% trypsin in PBS for 15 minutes at 37°C, after which the trypsin was removed and replaced with fresh medium. The spheroids were then mechanically disaggregated to a single cell suspension by repeated pipetting. The clonogenic assay was performed as previously described.

For spheroid growth delay measurement spheroids from the other group were transferred to agar coated wells in a plastic tissue culture multidish with one spheroid per well. Twenty-four spheroids were taken from each treatment group and measurements of cross-sectional area of individual spheroids were made twice weekly using a Micromeritics image analysis system coupled via a television

camera to an inverted optical microscope. The area measurements were subsequently converted to volumes, assuming spherical geometry. Sequential estimates of median spheroid volume were made and growth delay could be calculated from the time taken for median spheroid volume to increase by a factor of ten above initial size (Twentyman, 1980).

Determination of intracellular drug levels: L-DAN monolayers were exposed to adriamycin (5 μ g/ml) and Brij 30 (0.01 μ g/ml) for varying times (0.5-2 hours). The cells were then washed twice with ice cold PBS, harvested by brief trypsinisation, counted (Coulter Counter Ltd, England) and resuspended in distilled water. Adriamycin was then extracted and measured by reversed phase high pressure liquid chromatography with fluorescence detection, as previously described (Cummings et al, 1984). Adriamycin levels were expressed as ng/10⁵ cells. Drug uptake curves were fitted by the method of least squares.

Fluorescent and electron microscopy: Intact spheroids approximately 500 μ m in diameter were exposed to adriamycin (5 μ g/ml) + Brij 30 (0.01 μ g/ml) for varying times. The spheroids were then washed to remove loosely bound drug, placed in gelatin capsules filled with OCT embedding gel (Lurker Labs Ltd) and frozen in liquid nitrogen. Thin cryotome sections (6 μ m) were mounted in uvinert and examined under a Polyvar fluorescent microscope (λ excitation = 468 nm; λ emission = 550 nm).

The effect of Brij 30 on the morphology and ultrastructure of L-DAN cells was assessed by electron microscopy. Monolayers of intact cells were exposed to Brij 30 (0.01 - 1 μ l/ml) for one hour and the cells subsequently processed for routine electron microscopy (sec 4.2). Untreated L-DAN spheroids were prepared for electron microscopy in order to demonstrate the compactness of cellular stacking and intercellular junctional apposition.

Intracellular drug levels: the relationship between intracellular adriamycin levels and time, for a fixed external drug concentration, is curvilinear. The intracellular adriamycin levels are significantly higher for the L-DAN cell line, at all time points following combined treatment with the surfactant (fig 6.1).

Monolayer survival: clonogenic cell survival after treatment with adriamycin + Brij 30 is summarised in Fig 6.2 for the L-DAN cell line, MlRl cell line and mouse granulocytes. The adriamycin concentration found to inhibit 90% clonogenic cell survival (ID_{90}) for each cell line is summarised in table 6.1.

L-DAN: Brij 30 alone, at the concentration used in these experiments (0.01ul/ml), reduced clonogenic survival by approximately 10% so this was subtracted from the figure attributed to combined treatment. Clearly, combined treatment significantly enhances the cytotoxicity of adriamycin.

MlRl/Mouse granulocytes: the concentration of Brij 30 (0.07ul/ml) used in these experiments was not cytotoxic. There is no difference in the response of myeloid leukaemic cells or granulocytes to adriamycin over the concentration range used. The combination of adriamycin and Brij 30 is significantly more toxic to both cell lines than adriamycin alone, however the tumour cells are more adversely affected than the granulocytes. It would appear that Brij 30 selectively enhances the activity of adriamycin in the tumour cell line at lower drug concentrations (0.1-0.6ug/ml) by approximately 20% (figure 6.2).

L-DAN spheroid survival: growth delay over a range of adriamycin concentrations was determined in the presence and absence of Brij 30 (Table 6.2). Co-treatment with the surfactant induces significantly longer growth delays at each adriamycin concentration.

Disaggregated spheroid clonogenic cell survival is higher than for monolayer at identical adriamycin concentrations implying that adoption of the spheroid configuration confers a degree of resistance to adriamycin (Fig 6.3). Treatment with Brij 30 significantly improves ($P < 0.05$ at drug concentrations $0.2 \mu\text{g/ml}$) the clonogenic cell kill of adriamycin, but it is still less than that found in monolayer (Fig 6.3).

Fluorescence and electron microscopy: it was possible to determine qualitatively the degree of adriamycin penetration into the spheroids. The spheroids are approximately 16-20 cell layers in diameter, and adriamycin had diffused into the outer 3-4 layers after incubation for one hour. Brij 30 increased the penetration depth to approximately 6-7 cell layers.

Electron microscopy revealed that Brij 30 alone caused significant ultrastructural alterations to L-DAN cells which were concentration dependent. These ranged from complete cytolysis ($1 \mu\text{l/ml}$) to minimal structural membrane changes in the plasma membrane and intracytoplasmic organelles at $0.01 \mu\text{l/ml}$ (figs 6.4 - 6.6).

Low power electron micrographs of L-DAN spheroids show that the cells are packed in a compact fashion with little intercellular space (fig 6.7). High power views show a variety of intercellular junctions including gap junctions and "tight" desmosomal or maculae adherentes junctions (fig 6.8)

In this present study we have shown that combined treatment with Brij 30 enhances the cellular uptake of adriamycin and significantly improves its cytotoxicity in monolayer (human lung and mouse myeloma) and spheroid culture systems. This effect is probably mediated by facilitated cellular uptake of adriamycin, which we found to be 2 - 3 fold higher in L-DAN monolayers in the presence of surfactant.

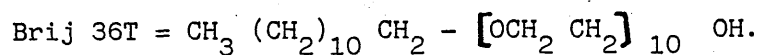
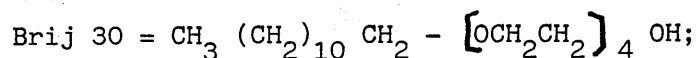
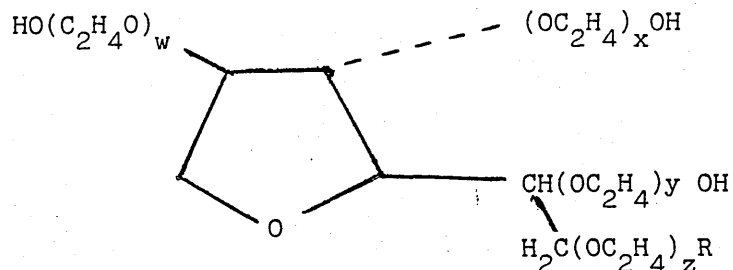
If the clonogenic survival vs concentration curves were redrawn as sigmoid pharmacological dose response curves (fig 6.9), it is apparent that the effect of Brij 30 is to shift the curves to the left, which is compatible with its proposed mode of action in increasing membrane permeability to adriamycin.

It is interesting to note that despite virtually identical sensitivity to adriamycin alone, the combination of adriamycin and Brij 30 is differentially cytotoxic to the leukaemia cells; as can be seen in fig 6.9 this effect occurs at clinically relevant concentrations of adriamycin (Benjamin et al, 1977).

The electron microscopic data suggest that the surfactant is altering membrane structure in some way, although the technique is too insensitive to give detailed information on the degree of membrane disruption. Spheroid fluorescent microscopy indicated that Brij 30 tends to increase the depth to which adriamycin can penetrate. We have not examined the penetration properties of the surfactant itself, however it presumably diffuses into the spheroid to a depth of at least 6 - 7 cell layers where it could increase intercellular diffusion of adriamycin.

Sum of W, XY, Z is 20;

R is $(C_{17}H_{33}) COO$



Surfactants are amphipathic molecules and their relative hydrophobicity is described by a hydrophile-liphophile balance (HLB) number; the higher the HLM number, the more hydrophilic the molecule. Tween 80 (HLB = 14.9) and Brij 36T (HLB = 15.2) are evidently more hydrophilic than Brij 30 (HLB = 9.7). The optimum HLB for surfactant-mediated increases in permeability depends on the nature of the membrane as well as the surfactant series and drug under study (Florence et al, 1984). The lower the HLB the greater the affinity of the surfactant activity is limited by aqueous insolubility. Steric factors also intrude. The areas/molecule of Brij 30 and 36T are 0.38 nm^2 and 1.09 nm^2 respectively. The latter was most active on the isolated rabbit gastric mucosa (Walters et al, 1982) and on adsorption through rat nasal mucosa (Hirai et al, 1981).

The lattice model for drug diffusion across the cell membrane has been previously described (sec 5.1). Cell treatment with chaotropic agents such as amphipathic surfactants would be expected to increase membrane fluidity and lateral diffusion of phospholipids. This increases the statistical probability of transient gaps in the membrane appearing to allow greater drug diffusion into the cell.

It is possible that this increased cellular permeability accounts for the apparent synergy of Brij 30 with adriamycin in the cell lines studied. There is a small but significant enhancement of the activity of adriamycin + Brij 30 against tumour cells relative to normal granulocytes. This could reflect a differential membrane response to the surfactant by normal and neoplastic cells and may impart a degree of selectivity to combination treatment with surfactant and cytotoxic.

In summary, we have demonstrated that the non-ionic polyoxyethylated surfactant Brij 30 enhances cellular accumulation of adriamycin and its antineoplastic activity in vitro.

Cell Line	Adriamycin ID ₉₀ (ug/ml)	
	+	-
	Brij 30	Brij 30
L-DAN	0.6	2.4 a
MIRI	0.4	1.9 a, b
Mouse granulocytes	0.8	1.5 a, b

TABLE 6.1 Adriamycin ID₉₀ (± Brij 30) in monolayers. The ID₉₀ values were derived by non linear least squares fit of the clonogenic survival data. a: Significant difference (p < 0.05) by Student's t-test, comparing ID₉₀'s ± Brij 30, b: significant difference (p < 0.05) by Student's t-test, comparing ID₉₀'s for MIRI and mouse granulocytes (+ Brij 30)

Adriamycin Concentration (ug/ml)	Growth delay (days)	
	+	-
	Brij 30	Brij 30
Control	9 (7.2 - 10)	8.1 (6.3 - 8.9)
2	16.8 (13.1 - 17.6)	11.5 (10 - 14.2)
5	19 (18 - 21.5)	13 (12 - 14.9)
10	35 (28.6 - 37.2)	17.3 (15.4 - 18.3)
15	37 (27.3 - 40.1)	18.2 (16.1 - 19.4)

TABLE 6.2 Spheroid growth delay in response to adriamycin (± Brij 30). The values in brackets encompass the 95% confidence

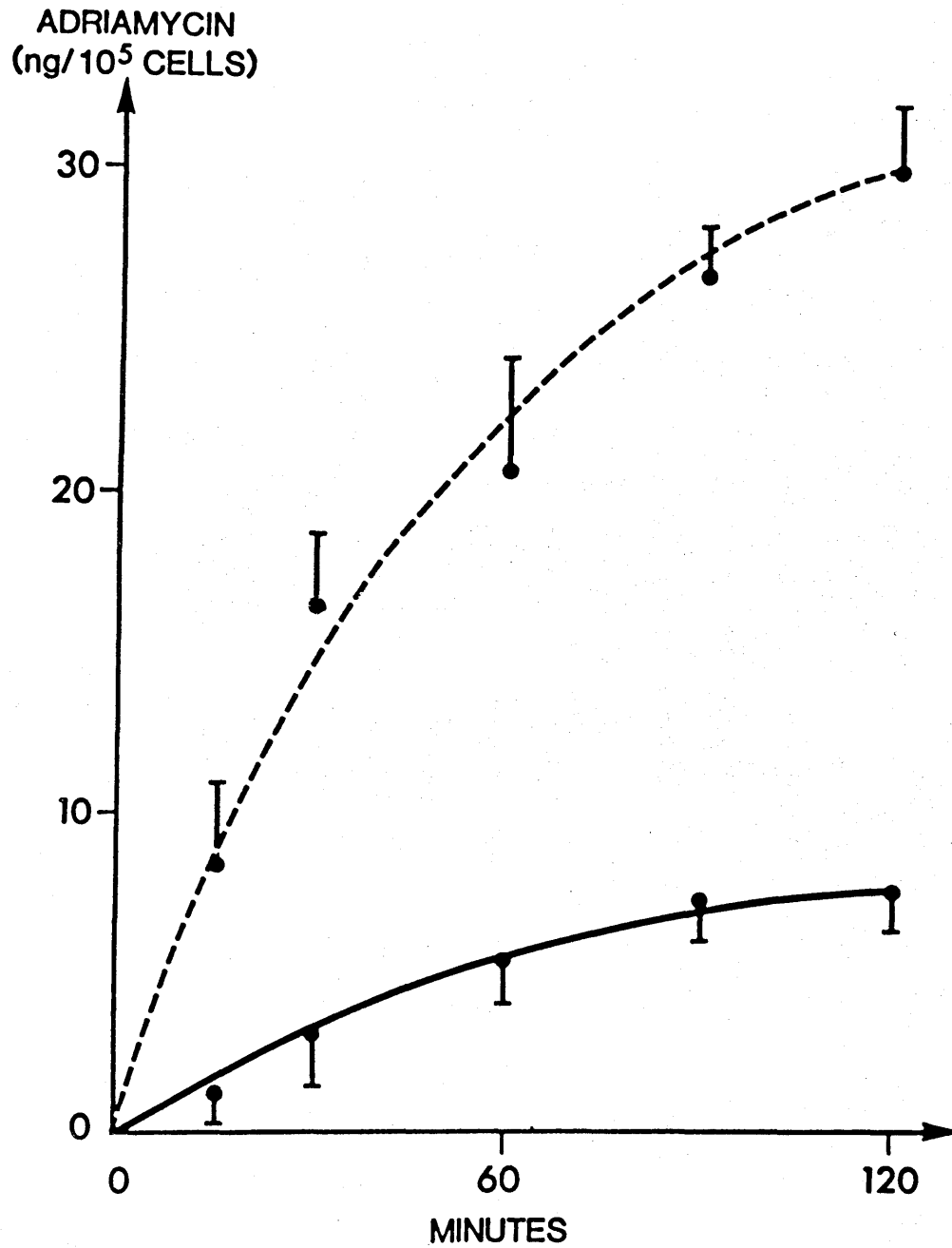


Figure 6.1 The time course of cellular accumulation of adriamycin (fixed drug concentration of 5 ug/ml)

Adriamycin alone —————
 Adriamycin + Brij 30 (0.01 ul/ml) - - - - -

Each point represents the mean of 5 experiments and the vertical bars represent 1 standard deviation

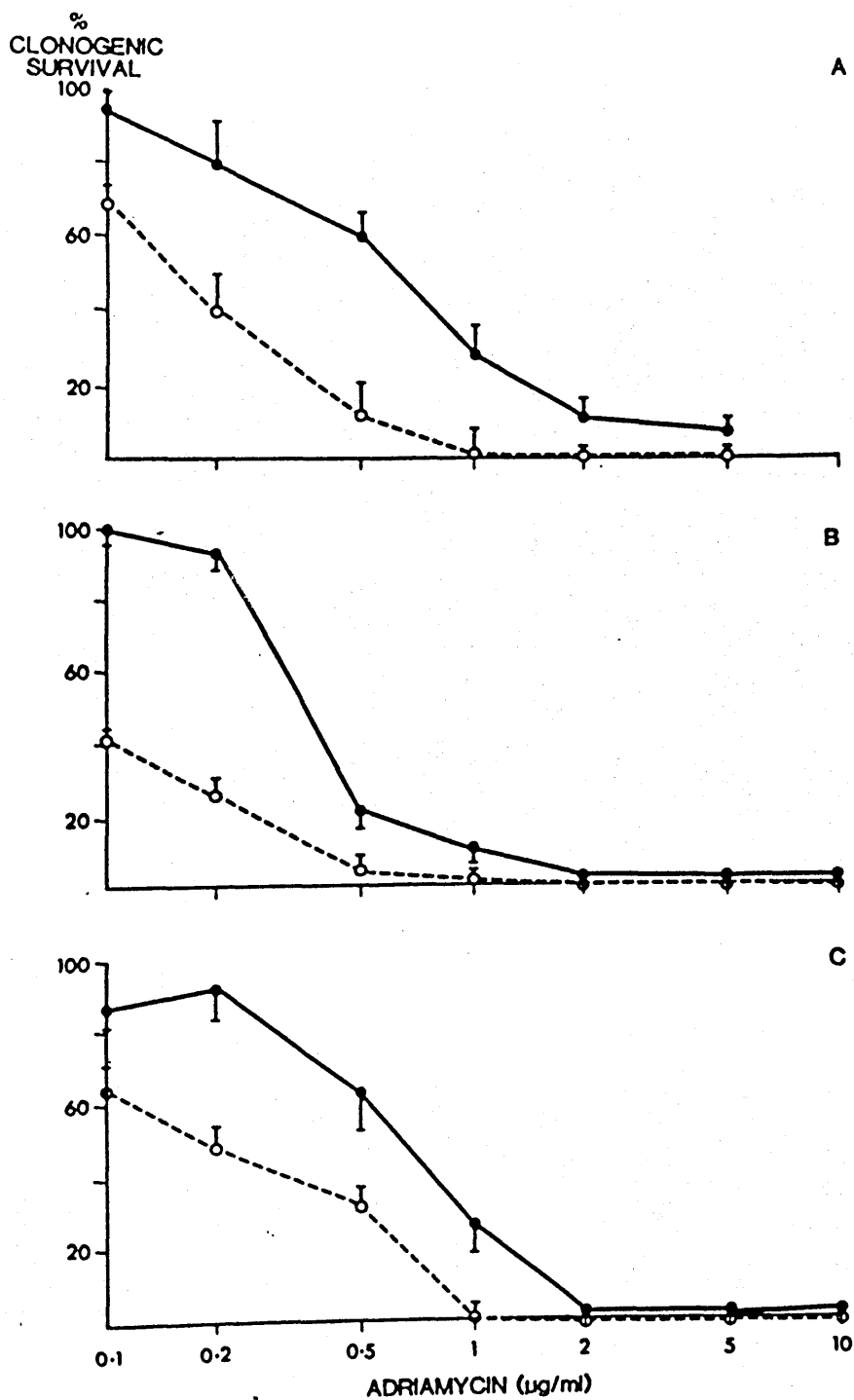


Figure 6.2 Clonogenic cell survival curves for

- A LDAN cell line
- B MRI cell line
- C Normal granulocytes

Adriamycin alone ●——●
 Adriamycin + Brij 30 ○——○

Each point is the mean of 5 experiments and the vertical bass represents 1 standard deviation

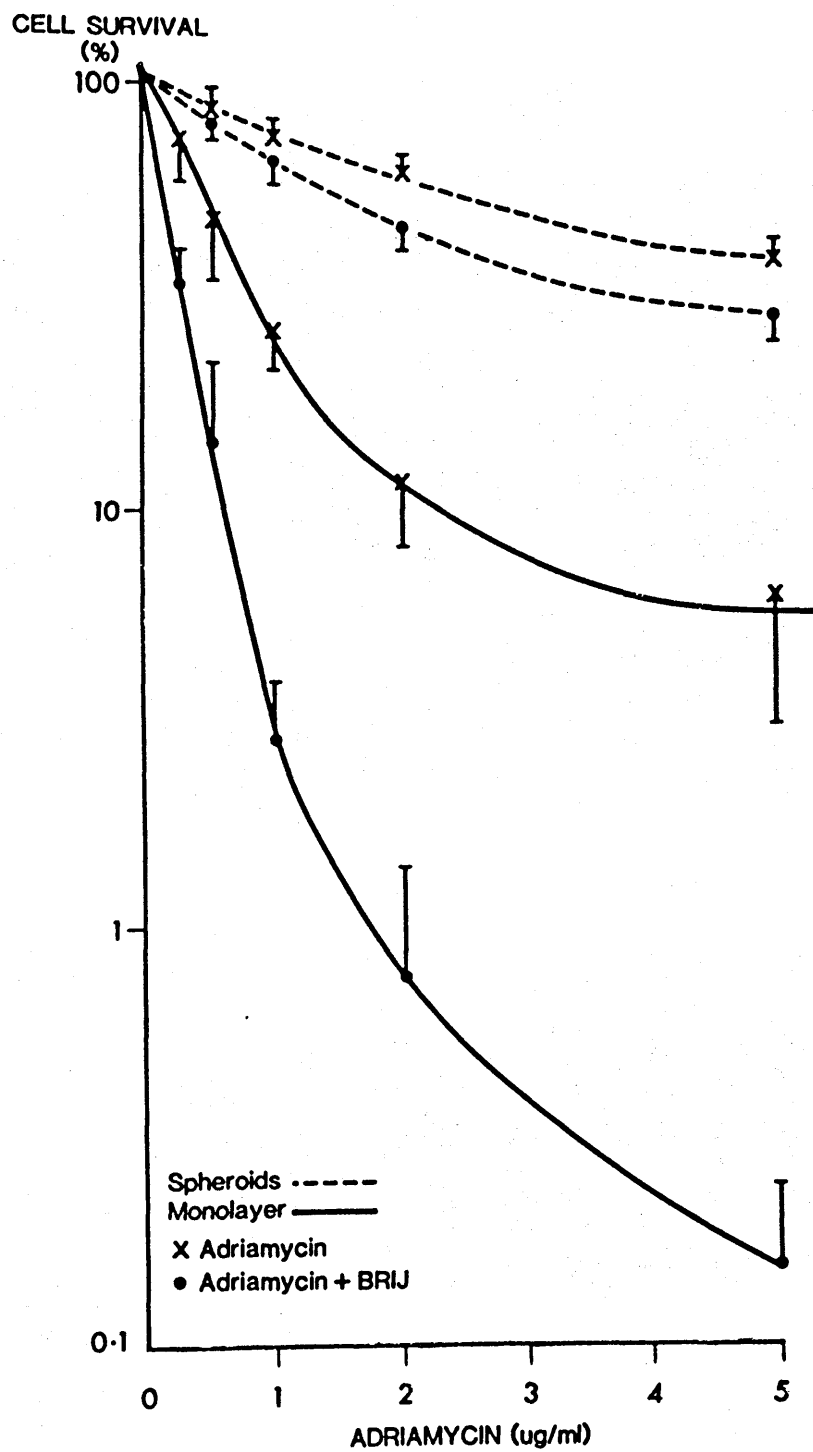


Figure 6.3 Clonogenic cell survival in monolayers and disaggregated spheroids following treatment with adriamycin \pm Brij 30



Figure 6.4 Electron micrograph of L-DAN cells exposed in monolayer to Brij 30, 1 $\mu\text{l}/\text{ml}$. There is evidence of complete cytolysis (magnification x 4900)

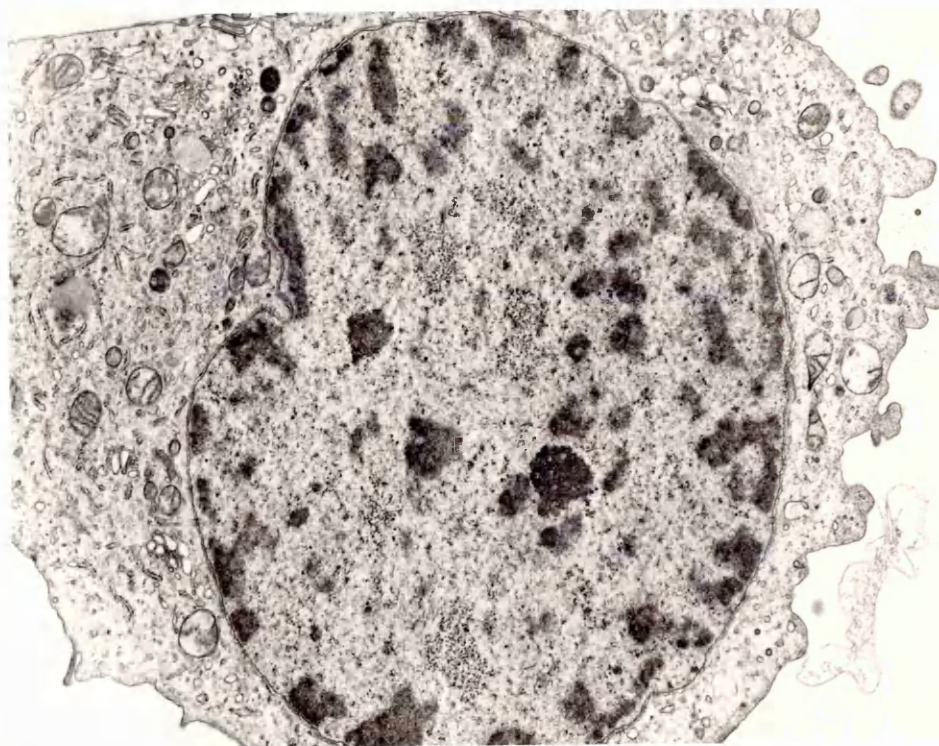


Figure 6.5 Electron micrograph of L-DAN cells exposed in monolayer to Brij 30, 0.1 $\mu\text{l}/\text{ml}$. There is evidence of external/internal membrane disruption and clumping of nuclear chromatin (magnification x 2950).

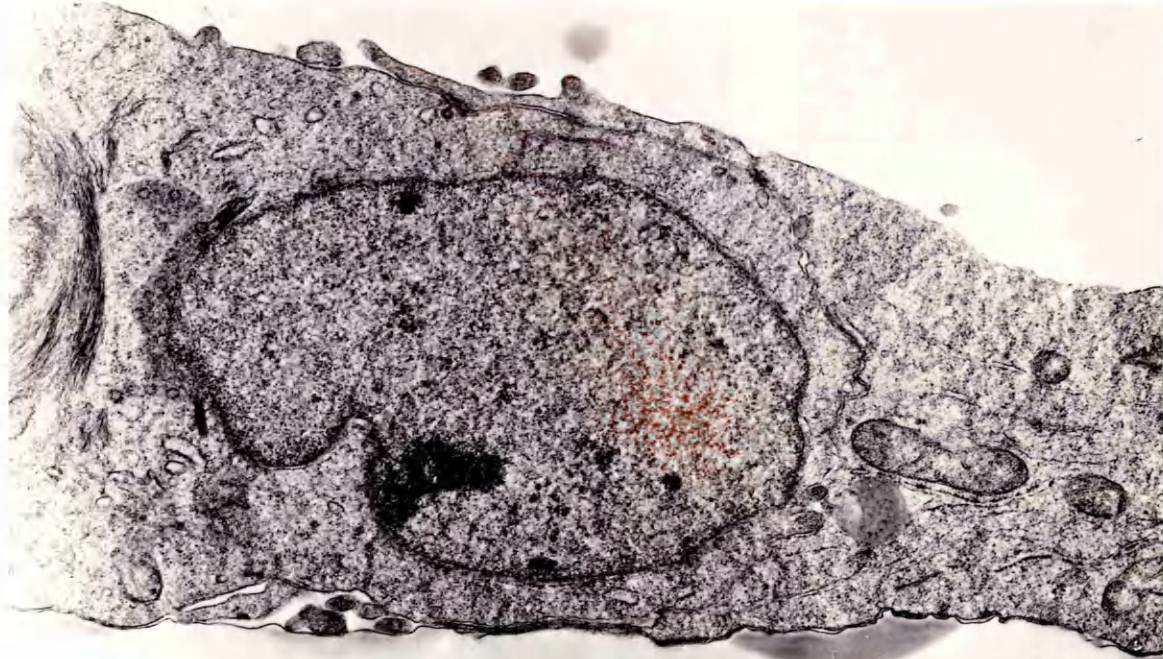


Figure 6.6 Electron micrograph of L-DAN cells exposed in monolayer to Brij 30, 0.01 ul/ml. There is evidence of minor alterations in intracellular membrane structure (magnification x 4900)

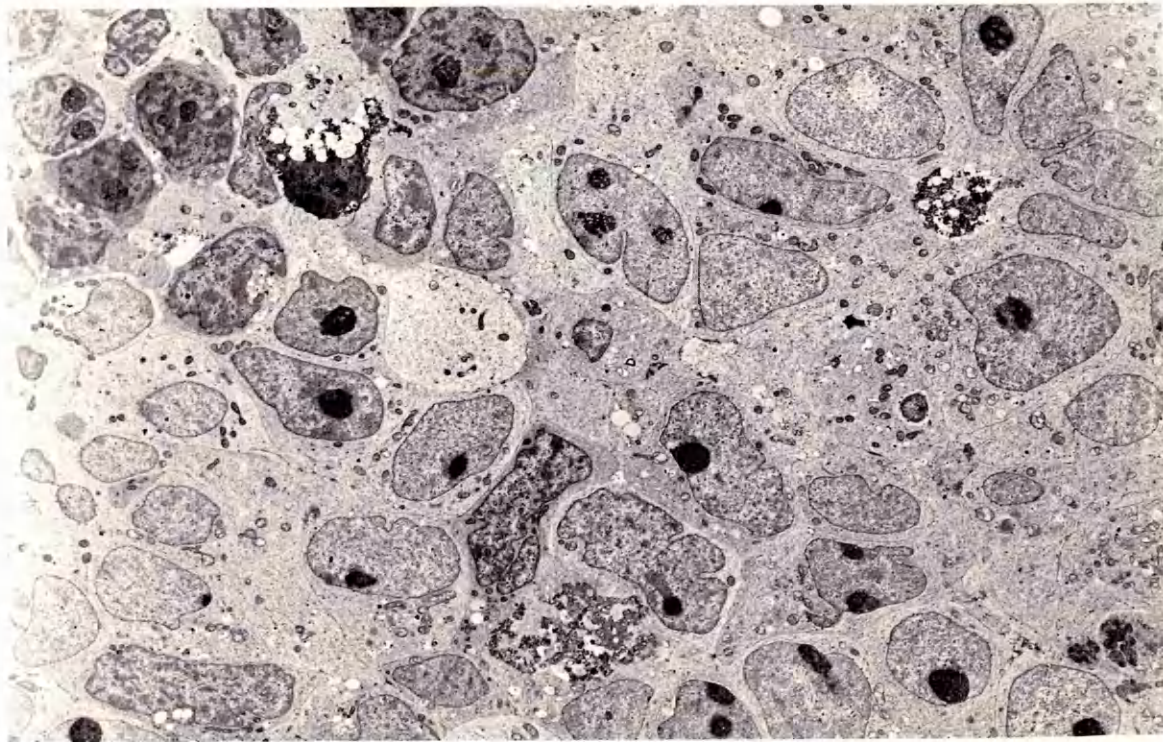


Figure 6.7 Low power electron micrograph of L-DAN spheroids showing compact cellular packing (magnification x 1300)

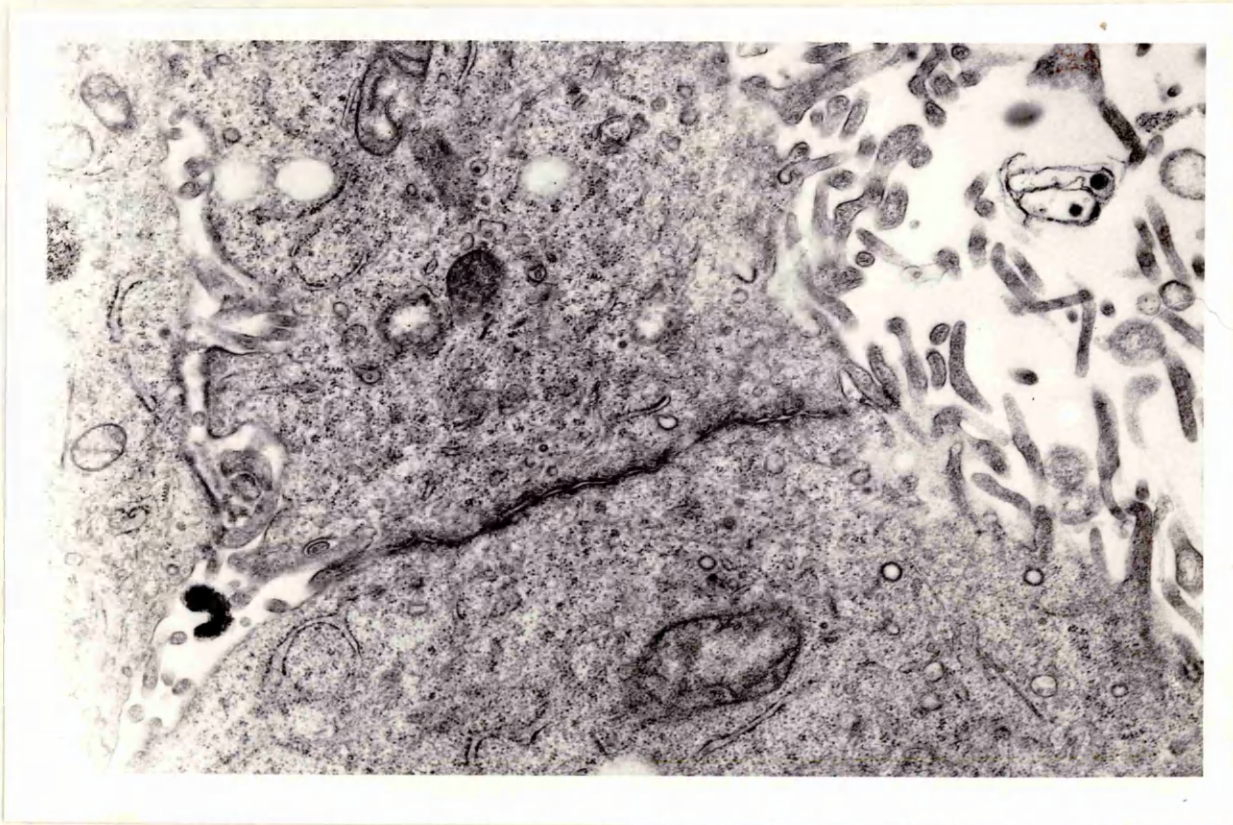


Figure 6.8 High power electron micrograph of L-DAN spheroids showing close membrane apposition and a desmosomal junction (magnification x 9800)

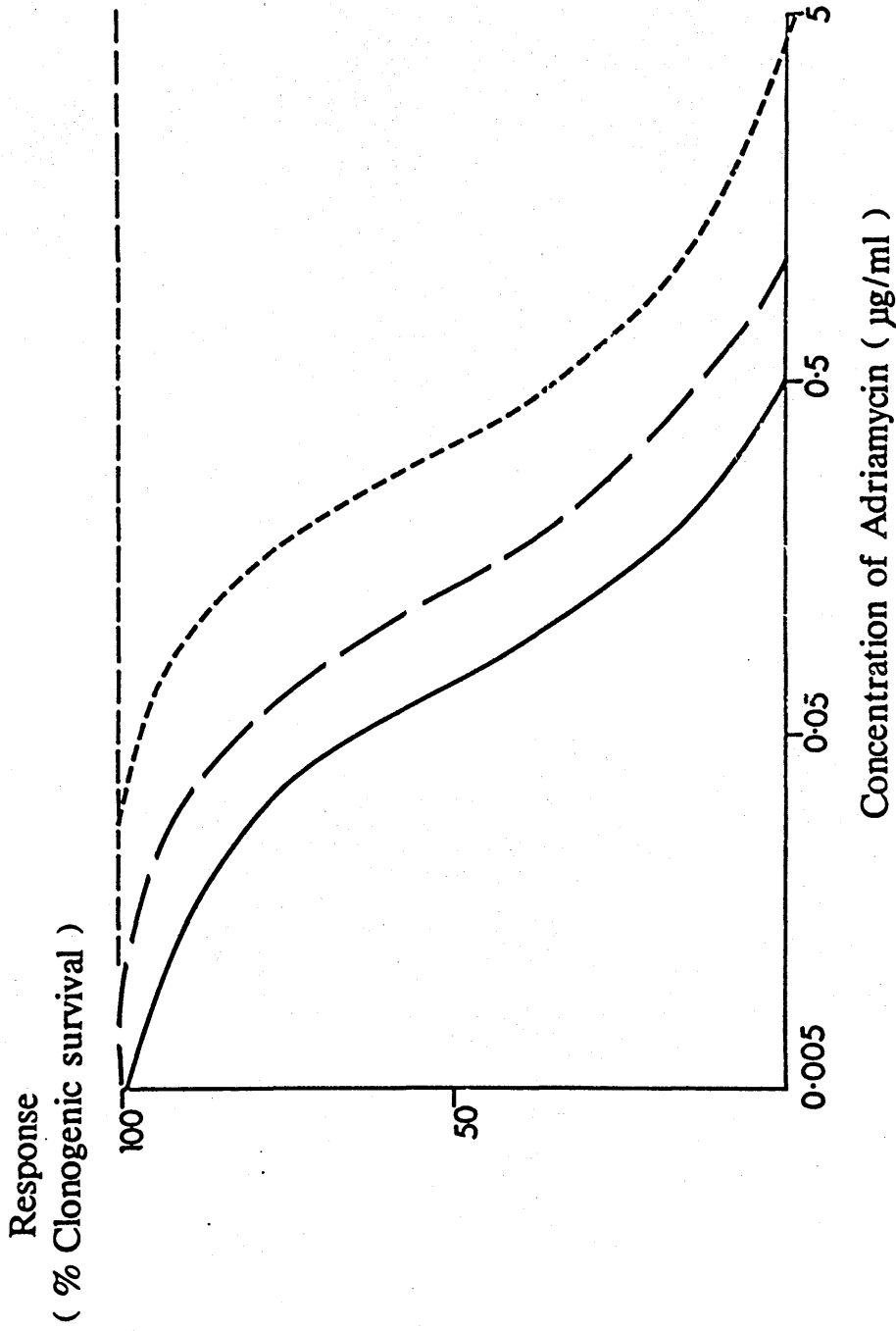


Figure 6.9 Stylised dose-response curves of clonogenic cell survival vs log adriamycin concentration
Adriamycin alone (both cell lines) - - - - -
Adriamycin + Brij 30 (granulocytes) - . - . -
Adriamycin + Brij 30 (myeloid leukaemia line) _____

The pharmacokinetics and disposition of adriamycin following its administration, in solution or encapsulated in niosomal vesicles, to tumour bearing nude mice.

Introduction

Many attempts have been made to alter the specificity and pharmacokinetics of cytotoxic agents by complexing them with macromolecular carriers (chapter 9) such as liposomes. These are microscopic particles composed of one or more phospholipid bilayer membranes which can carry lipid soluble drugs in their bilayers and water soluble drugs in their aqueous compartments. The liposomes vary in size, the number of enveloping lamellae and in lipid composition, although the common bilayer-forming lipids which are used include the phosphatidyl cholines, sphingomyelins, phosphatidyl serines and phosphatidylethanolamines. Liposomes have been shown to react with cells in several different ways such as fusion, endocytosis, stable adsorption on the cell surface and by lipid transfer. Numerous hypothetical reasons have been advanced for considering liposome use, some of which are more compelling than others: reduction of cytotoxic drug clearance and prolongation of its circulation; protection of the host against liposome contents eg reduction of adriamycin cardiotoxicity; delivery of drugs designed for endocytic uptake; circumvention of cell membrane permeability barriers by liposome - cell fusion; physical targeting by introducing the liposomes into a specific compartment of the body eg peritoneal cavity; natural targeting to cells of the reticulo-endothelial system, which tend to remove liposomes by phagocytosis. These considerations must be balanced by the problems and limitations of liposomes as carriers for cytotoxic drugs; a variable, but usually high, uptake of liposomes in the liver and

spleen; inability of liposomes to escape from the vascular compartment; vesicular disruption by serum components; liposomes are potentially antigenic and they can evoke an immunogenic response from the host.

A number of studies have demonstrated enhanced cytotoxicity of liposome encapsulated drugs in vitro (Kimelberg and Mayhew, 1978). It has been proposed that this effect is mediated via increased cellular drug uptake by a fusional or endocytic process. However, it is unlikely that these processes would occur in vivo, where systemically administered liposomes would be mainly confined to the vascular compartment or phagocytosed by cells of the reticulo-endothelial system. There is in vivo evidence, however, that administration of liposomes to tumour bearing rodents decreases adriamycin associated cardiac toxicity without loss of therapeutic effect (Forssen and Tokes, 1979 and 1983; Olson et al, 1982). A preliminary report of a phase I clinical study with liposome-associated adriamycin indicated that liposome administration is feasible and has potential advantages over free adriamycin with regard to some of its immediate toxic side effects (Gabizon et al, 1986).

In association with the French drug company Loreal, Professor A.T. Florence, Department of Pharmacy, University of Strathclyde has developed a novel drug carrier termed the niosome, which has properties similar to the liposome.

Niosomes are multilamellar vesicles made of surfactant and cholesterol and are neutral, whereas liposomes are composed of phospholipids and are therefore usually charged. In view of

previous results with the surfactant Brij 30, it was incorporated into the niosomes which were used to encapsulate adriamycin. The effect of niosomal encapsulation on the pharmacokinetics and disposition of adriamycin in tumour xenograft bearing nude mice is described.

Preparation and characterisation of niosomes

Niosomes (fig 7.1) were prepared by the hand-shaken and ether-injection techniques (i) Hand shaken technique; 150 μmol of surfactant or surfactant/cholesterol mixture was dissolved in diethylether (10 ml) in a 50 ml round-bottomed flask, and the ether evaporated on a rotary evaporator (Buchli) at 40 °C under reduced pressure. The dried film was hydrated with water or with 200 mM aqueous solutions of Carboxyfluorescein (CF) (3-5 ml) at 50 °C, for 15 min, with gentle agitation. (ii) Ether injection technique; 150 μmol of surfactant or surfactant/cholesterol mixture was dissolved in diethylether (20 ml) and injected slowly (0.25 ml min^{-1}) through a 14-gauge needle into water or aqueous solutions of CF (200 mM, 5 ml) maintained at 60 °C. After injection of solvent the system was maintained at 60 °C for 1 h to ensure complete evaporation. For in vitro experiments the hydrating solution contained 0.2 mg ml^{-1} adriamycin whereas for the in vivo studies, where the hand-shaken technique was used exclusively, the solution was usually 2-5 mg ml^{-1} adriamycin. Hand shaken niosomes were 987 ± 123 nm in diameter and had approximately 6 concentric layers (fig 7.1).

Separation of free and entrapped adriamycin

Each niosome sample was suspended in a final volume of approximately 20 ml PBS (pH 7.2) and centrifuged (7000 g, 20°C, 30 min). Supernatants were discarded and the pellets washed three times with buffer and resuspended in PBS (25ml).

Estimation of adriamycin concentration with niosomes

The niosome suspension (5ml) was adjusted to pH5 to ionise the adriamycin, shaken with chloroform (10ml, 30 sec) in a 50ml

funnel, and after 5 min the two phases were separated. The upper, cloudy, aqueous phase contained adriamycin and the lower chloroform the surfactant. The aqueous phase was clarified by gentle addition of double distilled water (5ml) then collected and adriamycin concentration analysed directly by HPLC (sec 2.2). The chloroform layer was evaporated to dryness, avoiding heat, and was reconstituted in methanol (1ml) prior to immediate analysis. It was therefore possible to derive the amount of adriamycin entrapped by the niosomes.

Murine pharmacokinetic studies

WIL, a human squamous lung tumour xenograft characterised in our department, was serially passaged in 100mg fragments into nude mice bred from our own colony. The tumour fragments were inserted into a surgically created subcutaneous pouch on the right flank of ether anaesthetised mice. The wound was closed with surgical clips, which were removed seven days later. The mice were housed in a sterile environment and received food and water ad libitum. Approximately 3 weeks after initial transplantation, the flank tumours were approximately 1 cm in diameter and easily palpable. Free adriamycin or niosome encapsulated adriamycin was administered intravenously via the tail vein in a dose of 10mg/Kg, in a volume of 0.1 - 0.2 ml. The mice were sacrificed by exsanguination under light ether anaesthesia at specified time points thereafter (30 mins, 1 hour, 2 hours, 4 hours, 12 hours, 24 hours and 48 hours). Four mice were used per time point.

Blood samples (1 - 2 ml per mouse) were collected into lithium heparin tubes, centrifuged (2,000 rpm for 5 minutes) and the plasma separated and stored until analysis at -20°C . The liver, kidneys, heart and tumour were dissected out, washed once in ice cold

phosphate buffered saline and blotted dry. Individual tissues were then frozen rapidly in liquid nitrogen and stored at -20°C until analysis.

Drug analysis - this has been previously described in detail (sec 4.2)

Mathematical Analysis - Plasma drug levels were fitted to a 2 compartment open model by the technique of least squares based on the Marquardt algorithm using an "in house" programme. It was therefore possible to calculate the drugs clearance and volume of distribution (central and peripheral compartments) from the microscopic rate constants. This model is described in further detail in chapter 11. Tissue drug levels were expressed as μg drug/gram of tissue, and the area under the concentration-time curves (AUC) was calculated by the trapezoidal rule. Statistical comparisons were made by two way analysis of variance or Student's t-test with Bonferroni correction where appropriate.

7.3 Results

Peak drug levels and tissue AUC's are outlined in table 7.1. The plasma concentration-time curve is shown in fig 7.2. The plasma decay profile of free adriamycin was best fitted by a biexponential equation; plasma concentration, $c = 165e^{-31.5t} + 0.91e^{-2.3t}$. Peak levels of free adriamycin were significantly higher than with niosomal adriamycin. Niosomal adriamycin levels were maintained at roughly constant levels for the first 4 hours following bolus injection and declined monoexponentially thereafter.

Plasma adriamycin levels were significantly higher between 4 - 12 hours with the niosomes, and this was reflected in a higher mean AUC. As it is impossible to take multiple plasma samples from single mice, it is impossible to statistically compare AUC's as this parameter is derived from single samples from multiple animals. Nevertheless, the form of the plasma concentration profiles differs. Adriamycin clearance (free = 0.51/hour; niosomes = 0.381/hour), volume of distribution (free = 5.71; niosomes = 1.11) and plasma half lives (free = 8 hours; niosomes = 2 hours) were calculated. The high volume of distribution indicates extensive tissue binding of adriamycin. The terminal half life of adriamycin in plasma is thought to represent diffusion of the drug from binding sites in the tissue compartments.

The niosomal adriamycin half life is shorter than for free drug. It is possible that the terminal phase of adriamycin disposition is occurring below the limit of our assay (1ng/ml) and that the concentration-time curve has been shifted to the left with niosomal drug administration. This situation is similar to

the pharmacokinetics of adriamycin when administered by infusion, with a decreased peak, constant levels for the duration of infusion followed by a monoexponential decline.

Hepatic tissue levels of adriamycin were similar regardless of its mode of administration (fig 7.3). The AUC's, peak hepatic levels (Table 7.1) and tissue half lives (17 hours) for adriamycin were statistically indistinguishable. The degree of hepatic metabolism of adriamycin was greater for niosome encapsulated adriamycin (figs 7.4). Peak levels of the 7-deoxyglycone of adriamycinol are significantly higher ($p < 0.05$) after niosome treatment. The degree of hepatic metabolism can be defined by the ratio.

$$\text{AUC adriamycin} / \text{AUC adriamycin} + \text{AUC metabolites} \times 100\%$$

The % metabolism ratio for niosomal adriamycin (85%) is less than for free adriamycin (95%) despite similar AUC's for parent drug, implying greater hepatic uptake and metabolism for adriamycin encapsulated in niosomes.

Peak renal levels are significantly ($p < 0.05$) higher after free adriamycin (fig 7.5). The renal AUC is also higher (table 7.1) and the tissue half life rather shorter (20.6 hours vs 36.4 hours) than for niosomal adriamycin. There was a minor degree (<5%) of metabolism of adriamycin to the deoxyglycones of parent drug and adriamycinol, which was similar for free and niosomal drug.

Cardiac adriamycin concentrations were significantly and consistently higher throughout the concentration time profile (fig 7.6) in the free adriamycin group. Peak level, AUC and the terminal

half life (36 hours vs 10.8 hours) were elevated over those values observed with the niosomes (Table 7.1). There was no significant intracardiac metabolism of adriamycin, with either preparation of the drug.

Intratumoural drug levels were similar with regard to peak levels and AUC (fig 7.7). The terminal half life is apparently prolonged in mice treated with free adriamycin, however this accounts for only a small fraction of the total AUC (<5%). It is possible that there is a terminal slower phase of drug decline in niosome treated mice, which is below the limit of assay sensitivity. No intratumoural metabolites were detected.

Encapsulation of adriamycin in niosome vesicles alters the pharmacokinetics and disposition of the drug in tumour xenograft bearing nude mice. The significant differences, relative to administration of adriamycin solution, are as follows; prolonged release of drug from the plasma compartment with lower peak drug levels; lower peak cardiac levels of adriamycin with a shorter tissue half life and decreased cardiac AUC; a greater degree of hepatic metabolism to inactive 7-deoxyaglycones.

One would expect that intratumoural drug content, probably best expressed as AUC, would bear some relationship to the cytotoxic effects of the drug. On the basis of the kinetic data, one would expect that the two forms of the drug would therefore have similar cytotoxic efficacy.

Cardiac levels of adriamycin are significantly lower with the niosomal drug preparation. Peak plasma levels of adriamycin are thought to be directly correlated with the development of cardiomyopathy and this concept underlay the use of prolonged infusions of adriamycin in chemotherapeutic regimens in order to decrease peak drug levels and hence the chance of cardiac damage (Unverferth, 1982). The niosomes decreased peak plasma and cardiac adriamycin concentrations and total cardiac drug exposure (as assessed by the lowered tissue AUC). Although the cardiac toxicity of the niosomes relative to equimolar doses of adriamycin has not been formally assessed, it is possible, on pharmacokinetic grounds, that the niosomes will be relatively cardioprotective. It may be possible, then, to give greater doses as the therapeutic ratio would be improved by formulation of adriamycin in niosomal form and thus improve their cytotoxic action.

Although the niosomes are constitutively and physicochemically distinct from liposomes, the results reported in this chapter are, on the whole, similar to previously executed studies employing liposomes as the carrier vehicle for adriamycin.

Forsen and Tokes (1979) and Olsen et al (1982) reported reduced cardiac uptake of encapsulated adriamycin in association with less electron microscopic evidence of cardiomyopathic damage than that due to free drug.

The degree of hepatic uptake and metabolism was greater with the niosome preparation. As with other carriers, a considerable percentage of intravenously administered liposomes are removed from the circulation by reticuloendothelial cells in the liver and spleen. It would appear that the Kupffer cells of the liver trap niosomes in a similar manner, and promote the intrahepatic metabolism and deactivation of adriamycin.

It can be concluded, therefore, that niosome encapsulated adriamycin has a different tissue distribution than free adriamycin, with the predominant effect being of lowered cardiac drug concentrations. It is possible, as total dose limitation in tumours is related to cardiotoxicity that even a modest reduction in cardiotoxicity could enable an increase in the total dose of adriamycin administered or a reduction in the likelihood of toxicity.

	FREE ADRIAMYCIN		NIOSOME ENCAPSULATED ADRIAMYCIN	
	Peak level	AUC (0-∞)	Peak level	AUC (0-∞)
Plasma	0.1 ± 0.01	0.4	0.075 ± 0.01*	0.53
Heart	11.7 ± 0.10	110	5 ± 0.27*	43.6
Kidney	24 ± 1.8	295	11.3 ± 1.2*	160
Liver	27.9 ± 1.9	195	14.2 ± 1.5	175
Tumour	4.5 ± 0.5	32.1	7.5 ± 0.9	48

TABLE 7.1

Comparative total tissue and plasma contents of adriamycin following administration of free or niosome encapsulated drug. Peak levels are expressed as $\mu\text{g/g}$ ($\mu\text{g/ml}$ for plasma) and the AUC as $\mu\text{g/g}$ tissue x hour ($\mu\text{g/ml}$ x hour for plasma) ± 1 standard deviation.

*Indicates significant ($p < 0.05$) differences in peak levels.

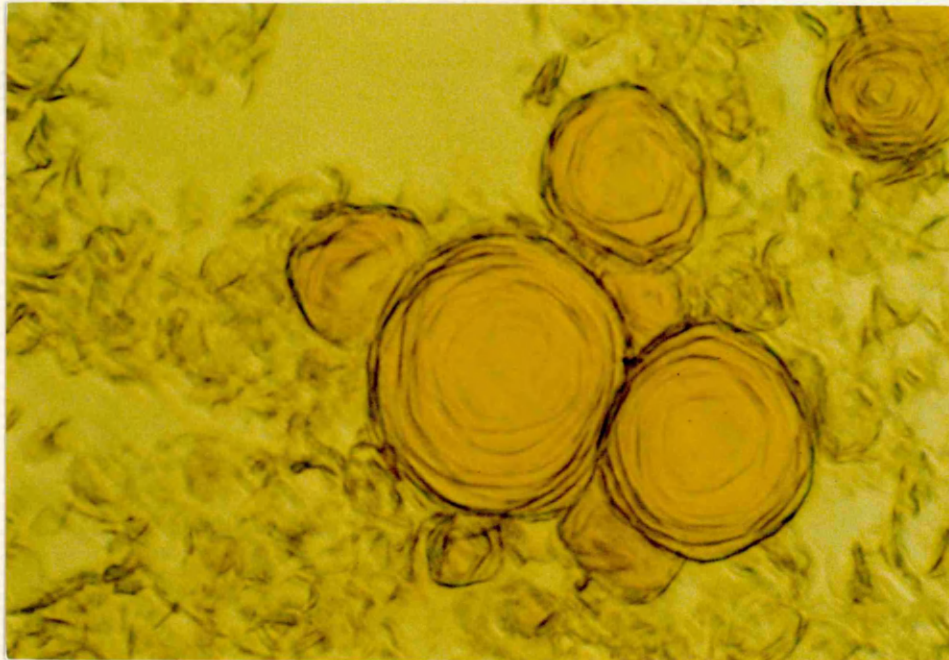


Figure 7.1 Phase contrast photomicrograph of a multilamellar niosome containing adriamycin (magnification x 100)

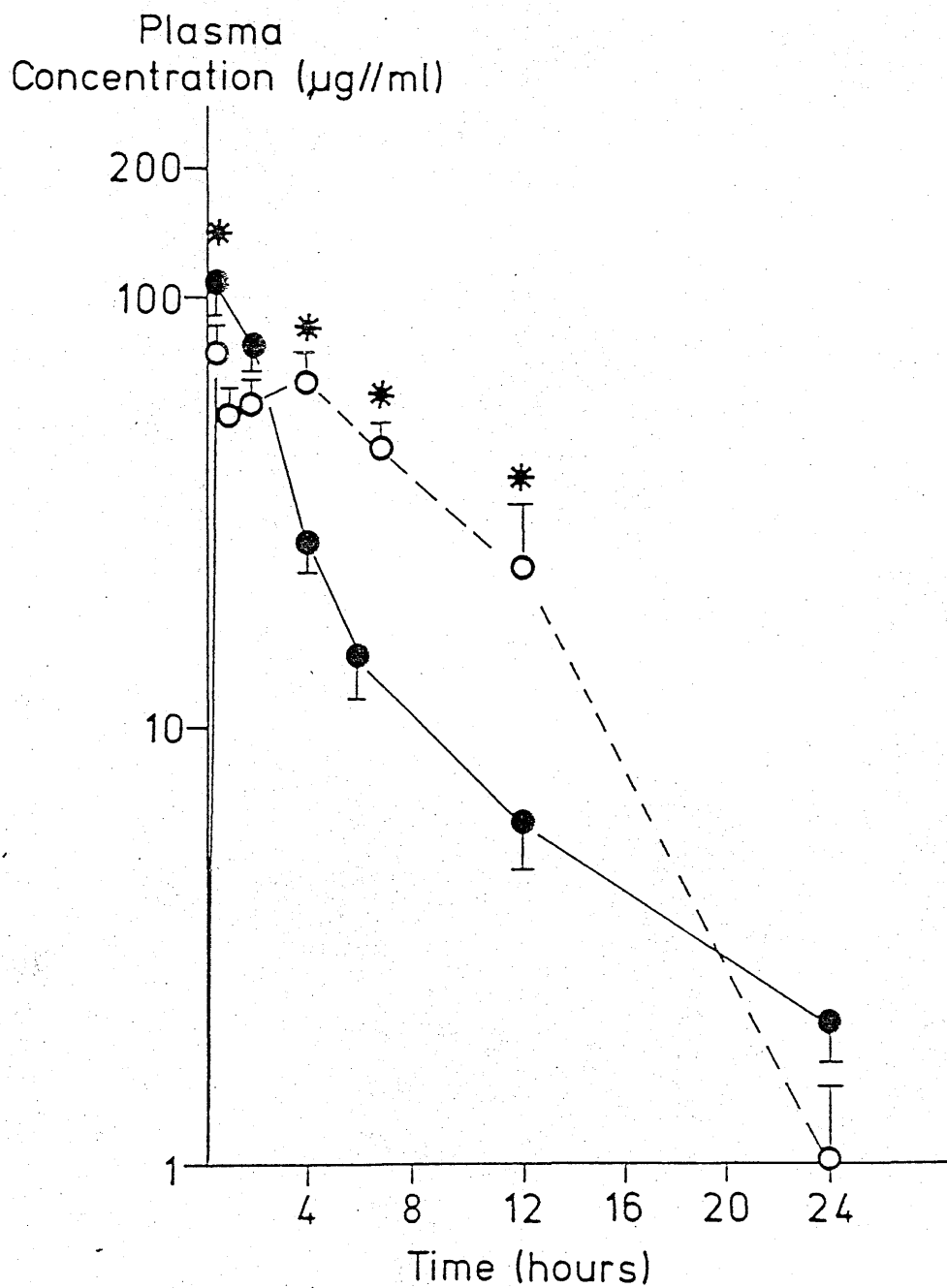


Figure 7.2 Plasma concentration-time profile following treatment with free adriamycin (●) and niosome encapsulated adriamycin (○). Each point is the mean of 4 mice and the vertical bar denotes 1 standard deviation. *implies a statistically significant difference at the $p < 0.05$ level.

Adriamycin
Concentration ($\mu\text{g/g}$)

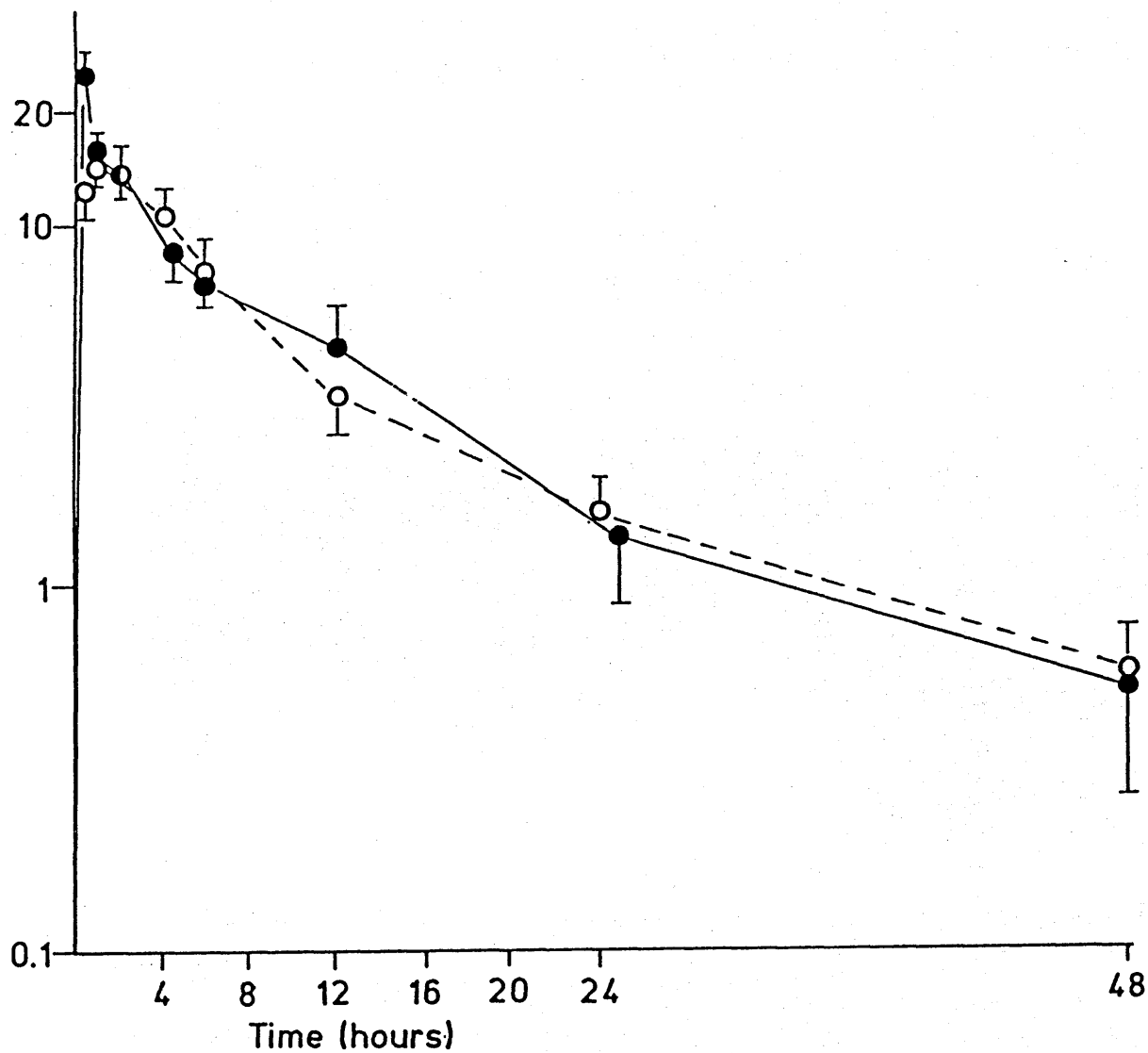


Figure 7.3 Hepatic concentration-time profile following treatment with free adriamycin (\bullet) or niosome bound adriamycin (\circ). Each point is the mean of 4 mice and the vertical bar denotes 1 standard deviation.

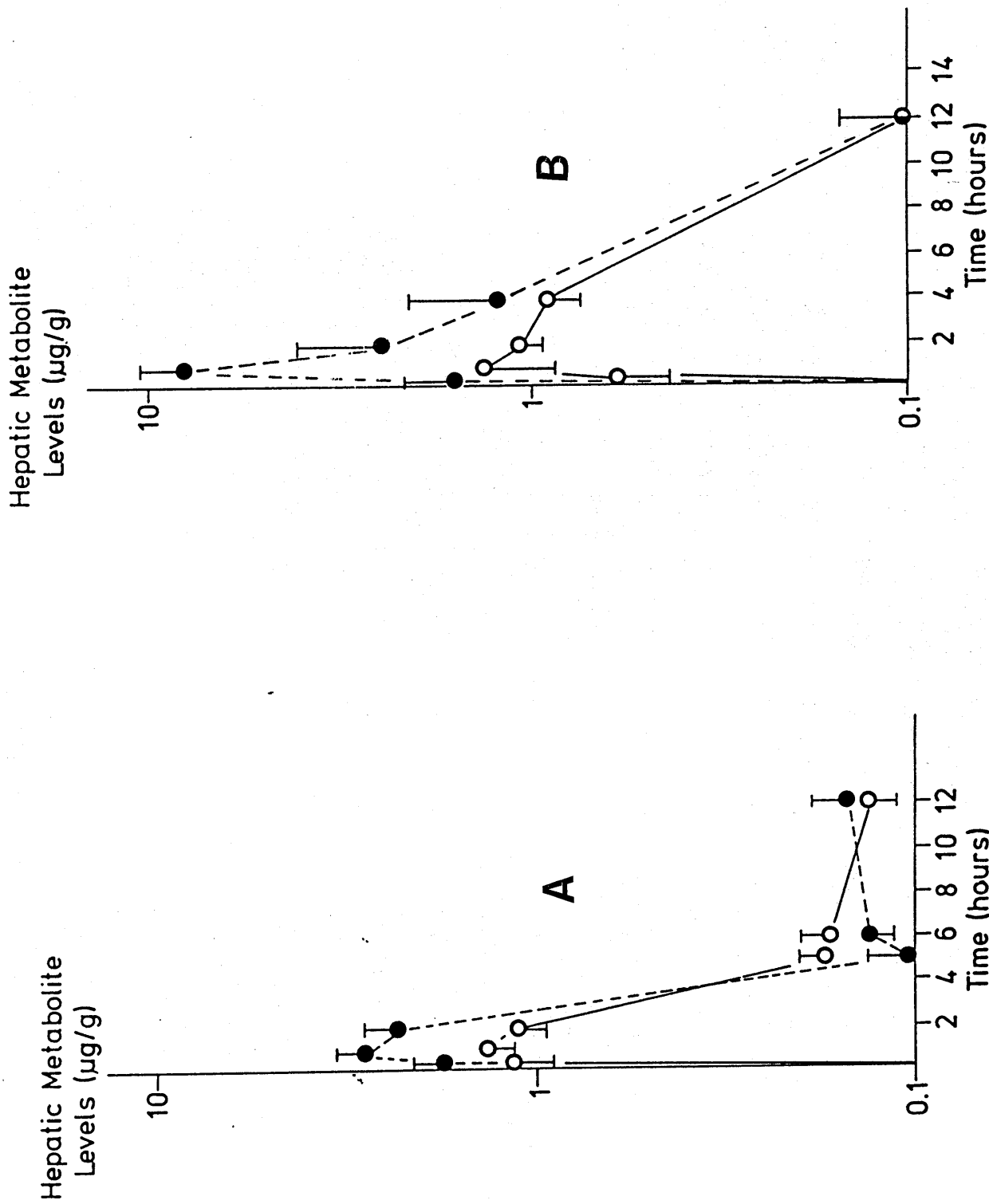


Figure 7.4 A. Hepatic metabolite levels after treatment with niosomal adriamycin.
B. Hepatic metabolite levels after treatment with free adriamycin

○ 7-deoxyglycone of adriamycin
● 7-deoxyglycone of adriamycinol

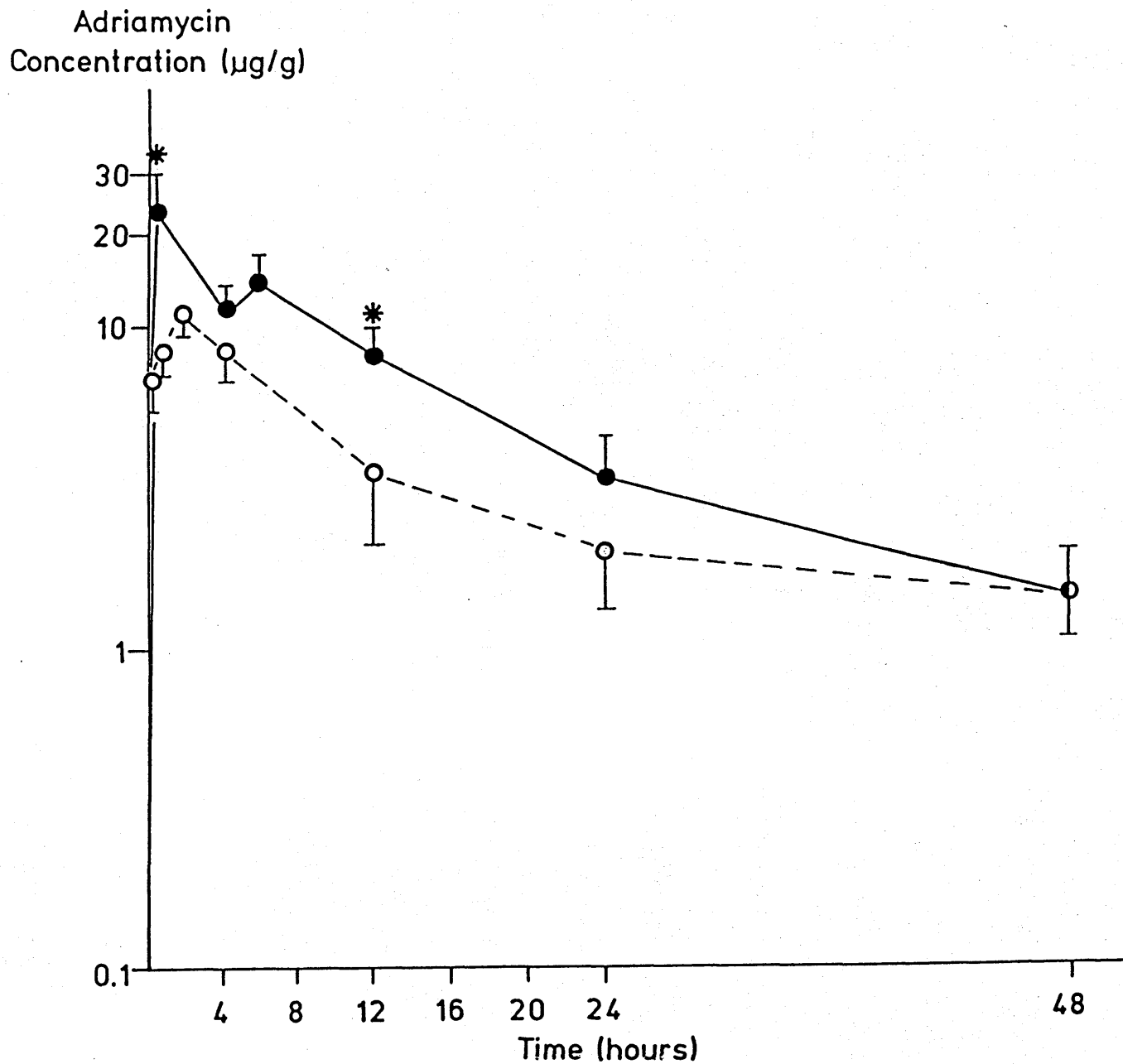


Figure 7.5 Renal concentration-time profile following treatment with free adriamycin (●) or niosome encapsulated adriamycin (○). Each point is the mean of 4 mice and the vertical bar denotes 1 standard deviation. *Statistical difference at $p < 0.05$ level.

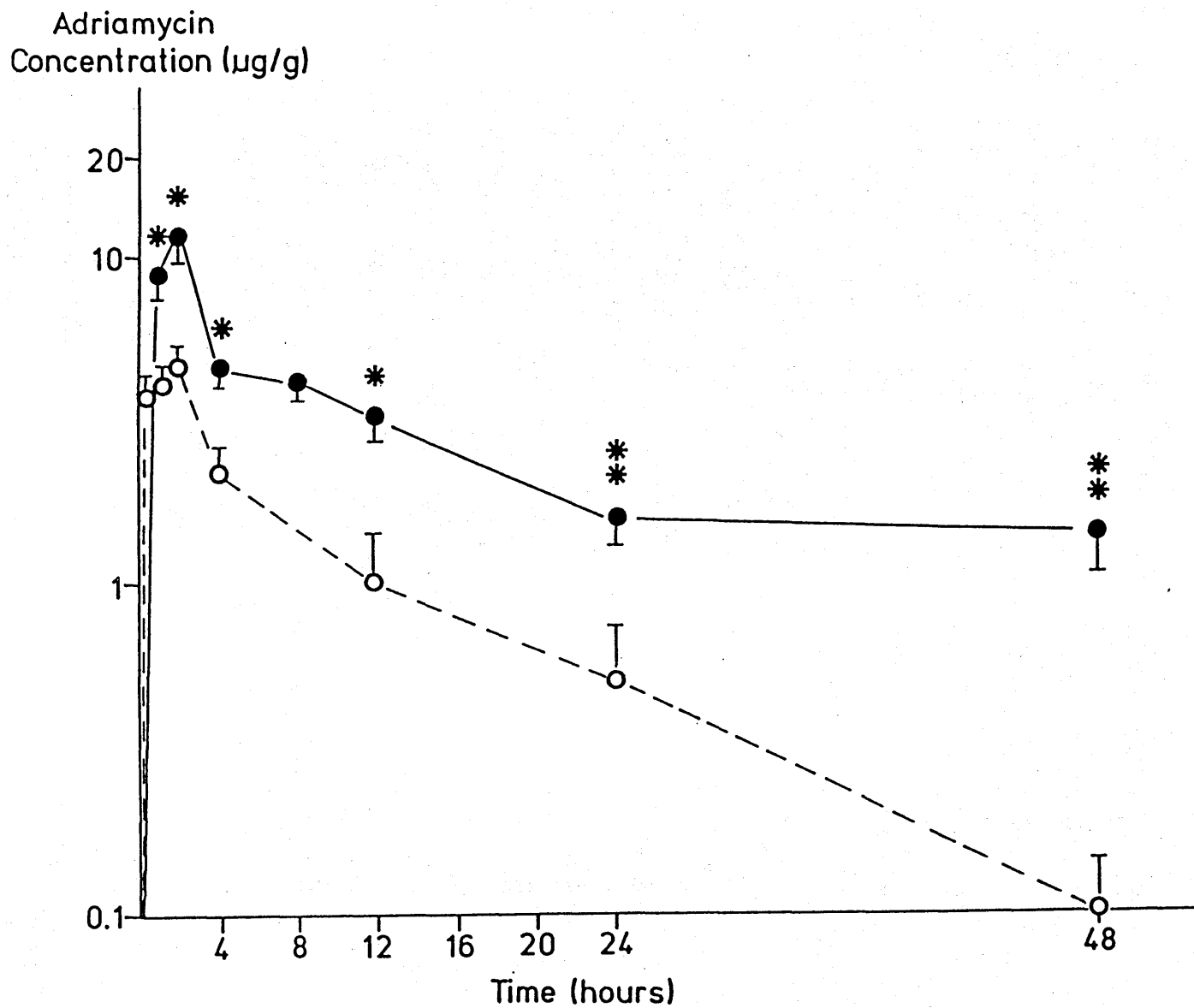


Figure 7.6 Cardiac concentration time profile following treatment with free adriamycin (●) or niosome bound adriamycin (○). Each point is the mean of 4 mice and the vertical bar denotes 1 standard deviation. *Statistical difference at p < 0.05 level
**Statistical difference at p < 0.01 level

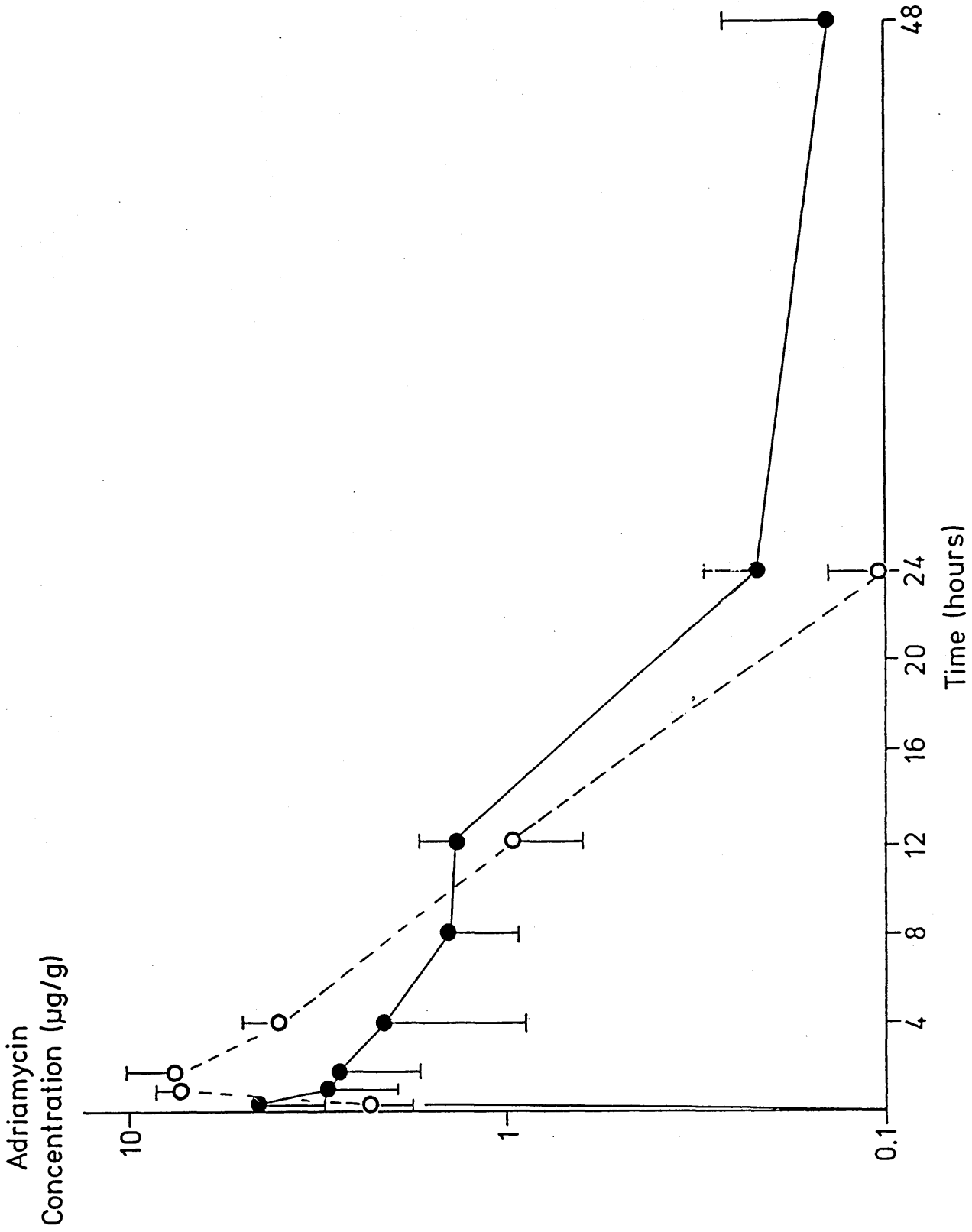


Figure 7.7 Tumour concentration-time profile following treatment with free adriamycin (●) and niosome (○) encapsulated adriamycin. Each point is the mean of 4 mice and the vertical bars denote 1 standard deviation.

Antitumour activity of niosome encapsulated adriamycin in monolayer, spheroid and xenograft.

8.1 Introduction

The pharmacokinetics and disposition of niosome encapsulated adriamycin were described in the previous chapter. Studies on the in vitro cytotoxicity of liposome encapsulated drugs have been conflicting, with evidence of decreased, increased or maintained activity (reviewed by Kimelberg and Mayhew, 1978). In this section, the cytotoxic activity of equimolar doses of adriamycin in free solution or entrapped in niosomes is examined in monolayer, spheroid and solid xenografts of human lung tumour cells.

8.2 Materials and Methods

Niosome preparation - niosome preparation was described in chapter 7.

Monolayer and spheroid culture systems L-DAN monolayers and spheroids were grown as previously described. Standard monolayer clonogenic assays were performed after exposure to free or niosome bound adriamycin for 1 hour over a wide concentration range (0.1 - 10 $\mu\text{g/ml}$). Spheroid growth delay was assessed following identical drug exposures.

Tumour growth delay in vivo - WIL, the squamous lung tumour xenograft used in the pharmacokinetic studies, was serially passaged in 100 mg fragments into nude mice bred in our own laboratory. The tumour fragments were inserted into a surgically created subcutaneous pouch on the flank of ether anaesthetised mice. The wound was closed with surgical clips which were removed 1 week later. The mice were housed in a sterile environment and received

food and water ad libitum. Approximately 3 weeks after initial tumour transplantation, the flank tumours were approximately 1 cm in diameter and easily palpable. Three groups of tumour bearing mice (10 mice in each group) were treated with; free adriamycin 7.5 mg/kg; niosome encapsulated adriamycin 7.5 mg/kg (an equimolar dose of adriamycin); normal saline as control. Thereafter the tumour volume was measured 3 times per week for 3 weeks. Volume was assessed by measuring the 2 largest diameters with specially adapted calipers and converting these measurements into volume (cm^3) using the formula $\text{Vol} = 4/3 \pi r^3$. There is a direct linear correlation between tumour volume and tumour weight ($y = 1.28 x - 0.87$; $n = 66$, $r = 0.96$) which was characterised by Dr S Merry, fig 8.1.

Monolayer clonogenic survival - the survival curves are shown in fig 8.2. There is no difference in clonogenic cell kill between niosomes and adriamycin with respective ID_{90} s of 2.1 μ g/ml and 2.2 μ g/ml.

Spheroid growth delay - the growth delay data has been tabulated (table 8.1). Growth delay is similar at each drug concentration whether free or entrapped in niosomes.

Tumour growth delay in vivo The percentage increase in tumour weight (relative to pretreatment values) has been plotted against time for each of the 3 treatment groups (fig 8.3). Tumour growth in the control group increased exponentially. The growth delay (i.e. the time taken for the tumour weight to double) was longer for adriamycin (15 days) and niosomal adriamycin (11 days) than for control (5.8 days). Tumour weights were not statistically different comparing free adriamycin vs Niosomes, but both the adriamycin treated groups tended to be significantly smaller than controls ($p < 0.05$) (Table 8.2)

The cytotoxic activity of adriamycin is maintained in vitro and in vivo despite encapsulation in niosomal vesicles. The niosomes can probably interact with cells in vitro in several different ways. Adsorption is likely to be a non specific lipid-surfactant interaction occurring at the cell surface. This could allow locally high concentrations of drug to accumulate at the cell surface by diffusion out of the niosome and thus promote cellular uptake of drug. Alternatively, adsorption may lead to endocytic incorporation of the niosomes and their contents into the cell. It is possible that the Brij 30 surfactant component of the niosome could diffuse from the vesicle and interact with the tumour cell membrane to increase its permeability to adriamycin. It is most likely, however, that endocytosis is the most important form of interaction. Following endocytic uptake, the vesicles are presumably degraded within the cell thus allowing the drug to diffuse to its site of action within the nucleus.

Spheroid growth delay for niosomal adriamycin is virtually the same as for free adriamycin. It is difficult to envisage niosomes disrupting spheroid structure or diffusing within the spheroid substance therefore presumably enough adriamycin is taken up by the external cell annulus to allow production of a sufficiently large intraspheroidal concentration gradient to match the growth delay associated with free adriamycin.

It is unlikely that any of these mechanisms of niosome-cell interaction occur in vivo. Niosomes, like liposomes, are too large to efficiently pass across endothelial and epithelial cell layers or across intact basement membranes. The distribution of the micro-encapsulated drug therefore depends on its mode of administration.

This vehicle will lend itself to a regional chemotherapeutic approach, where one objective is to confine the drug to a specific body compartment eg intraperitoneal, intrarticular, intrathecal and intrarterial chemotherapy.

It has been shown (sec 7.3) that the niosomes circulate for a prolonged period in the blood stream and maintain relatively high adriamycin levels before declining thereafter with a reduction in adriamycin clearance. This has profound effects on intracardiac drug levels, which are lower, whilst maintaining tumour drug levels. The antineoplastic efficacy of free and niosomal adriamycin in equimolar doses is similar in vivo. This would be predicted from the pharmacokinetic study as the AUC for tumour drug exposure was likewise independent of the form in which adriamycin was administered. In view of the finding of identical antitumour activity in this model with free and niosome entrapped adriamycin, and the alluded association between peak intracardiac adriamycin levels and the subsequent development of cardiomyopathy, then it would appear that niosome encapsulated adriamycin has a higher therapeutic ratio than free adriamycin.

As previously detailed, the pharmacokinetics of diffusion of active drug from slow release pharmaceutical preparations such as niosomes, can be mimicked by intravenous infusion. It would be possible to design an adriamycin infusion which would achieve a similar plasma profile to that seen with the niosomes. There are pragmatic problems with infusional chemotherapy but with the advent of new pump designs and improved methods of vascular access, this is

becoming a relatively common means of administering cytotoxic drugs. There is evidence to suggest, in man, that adriamycin infusions are less cardiotoxic than bolus injection, with maintenance of antineoplastic activity. (Unverferth et al, 1982).

It remains to be tested whether niosomal encapsulation of adriamycin offers any significant biological advantages over altering the drug schedule.

MEDIAN SPHEROID GROWTH

DELAY (days)

Drug concentration ($\mu\text{g}/\text{ml}$)	Free Adriamycin	Niosome - Adriamycin
0 (control)	8.1 (6.3 - 8.9)	7.6 (6.5 - 8.3)
1	11.5 (10 - 14.2)	12 (11.0 - 13.3)
5	13.1 (12 - 14.9)	12.9 (11.8 - 14.2)
10	17.3 (15.4 - 18.3)	17.2 (16.0 - 19.3)
20	17.4 (16.1 - 19.4)	18.1 (16.9 - 19.6)

Table 8.1

Spheroid growth delay in response to treatment with free and niosome bound adriamycin. The figures in brackets correspond to 95% confidence limits around the median value.

% Increase in tumour volume

Day	Control	Free Adriamycin	Niosome - Adriamycin
0	100	100	100
2	135 \pm 9	100 \pm 10 ^{a,d}	130 \pm 6 ^{a,d}
4	163 \pm 8	142 \pm 7 ^{a,d}	145 \pm 11 ^{a,d}
7	232 \pm 27	163 \pm 19 ^{a,b}	177 \pm 8 ^{a,d}
9	242 \pm 18	143 \pm 6 ^{a,b}	186 \pm 13 ^{a,d}
11	262 \pm 41	160 \pm 29 ^{a,b}	204 \pm 23 ^{a,d}
15	354 \pm 11	203 \pm 21 ^{a,c}	216 \pm 18 ^{a,c}
17	456 \pm 26	250 \pm 18 ^{a,c}	265 \pm 24 ^{a,c}

Table 8.2

The percentage increase in tumour volume (taking mean pretreatment volumes as 100%) with time, following treatment with free adriamycin (10 mg/Kg, intravenous), niosome encapsulated adriamycin (10 mg/Kg, intravenous), or normal saline (control) .

Student's t-test values; a, N.S. comparing free vs niosomes

b, $p < 0.05$ comparing free vs control

c, $p < 0.01$ comparing free and niosome vs control

d, N.S. comparing niosome vs control

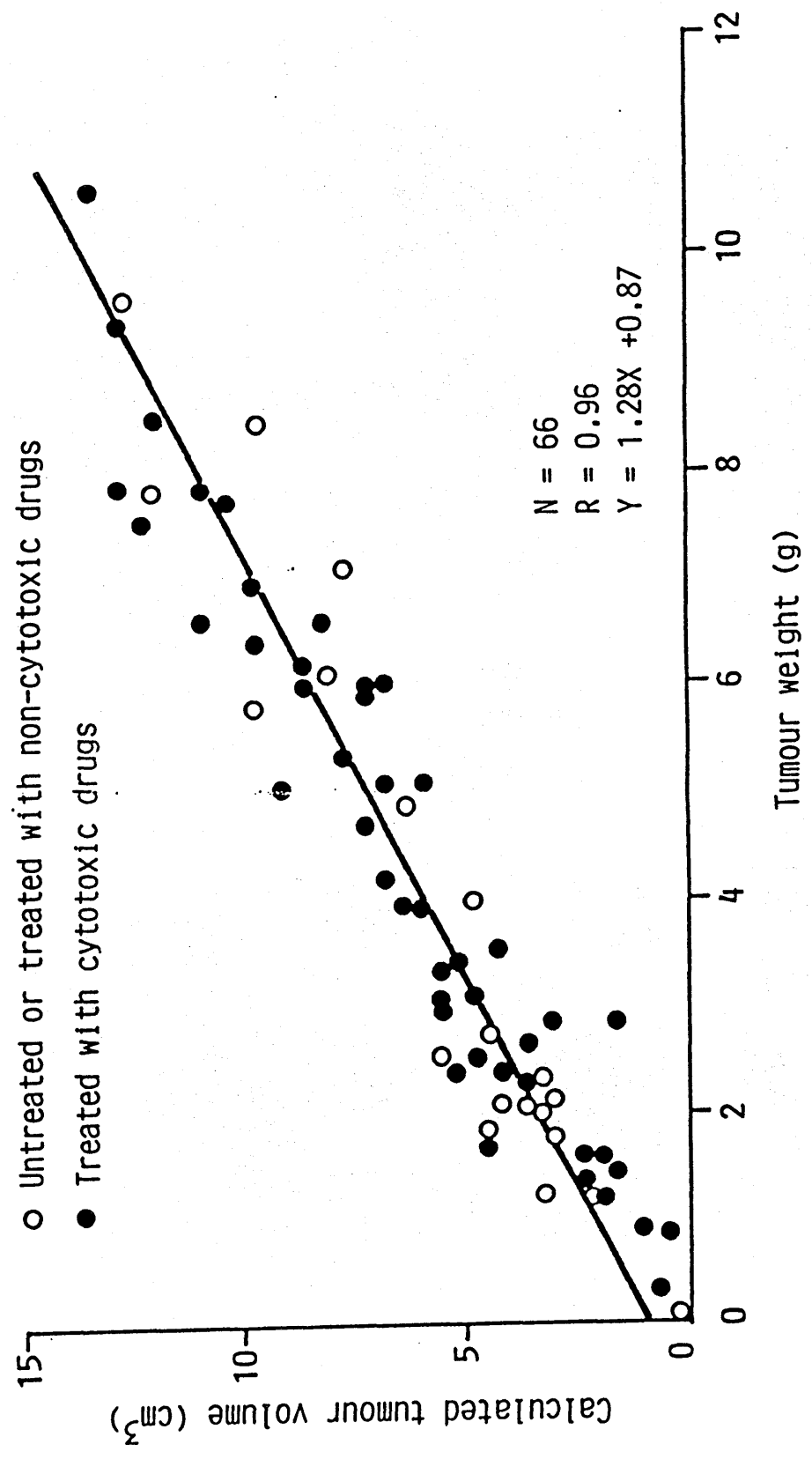


Figure 8.1 Correlation of tumour volume (caliper measurements) with weight of excised tumour for treated and untreated wil xenografts (Dr S Merry, Department of Medical Oncology).

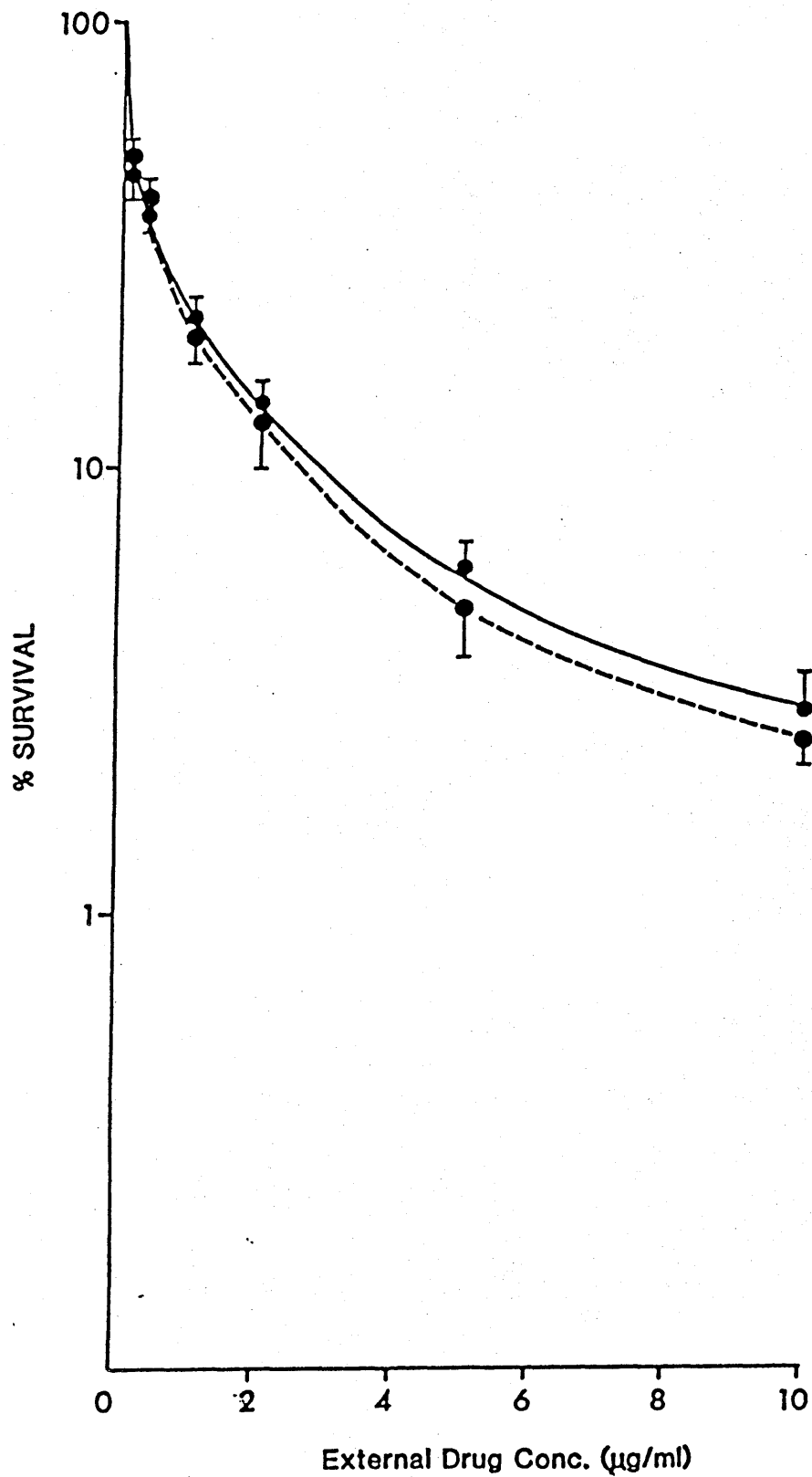


Figure 8.2 Clonogenic survival of LDAN monolayers following treatment with free adriamycin (●—●) or niosome encapsulated adriamycin (●- -●). Each point is the mean of 4 experiments and the vertical bar denotes 1 standard deviation.

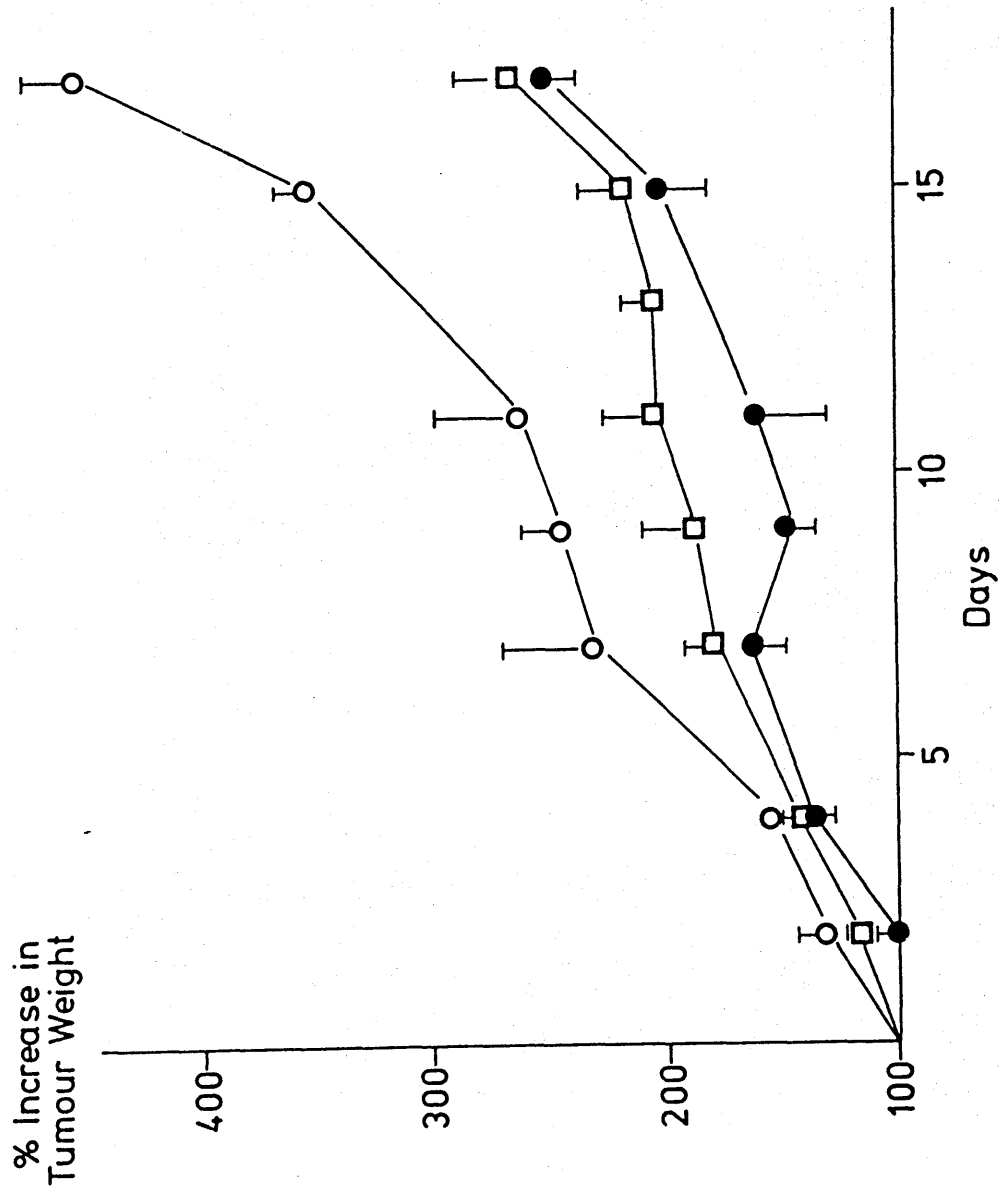


Figure 8.3 The relationship between tumour mass and time following treatment with free adriamycin (●), niosome bound adriamycin (□) or 0.9% saline as control (○). Each point is the mean of 6 tumours and the vertical bar denotes 1 standard deviation.

Cellular uptake and cytotoxicity of daunomycin and a complex of daunomycin - low density lipoprotein in monolayer and spheroid

9.1 Introduction

Numerous attempts have been made to enhance the selectivity of antineoplastic agents by linking them to a carrier moiety. Human albumin in microspherical form, macroaggregated protein (Szeberke et al, 1972) monoclonal antibodies (Seto et al, 1982), DNA-anthracycline complexes (Deprez-De Campaneere et al, 1979), drug - hormone conjugates (Varga et al, 1977; Kaneko, 1981) and encapsulation of the cytotoxic agent in liposomes (Abra et al, 1983; Gregariadis, 1976). There is no doubt that in most cases the pharmacokinetics of the anticancer drug are altered, sometimes favourably, with a resultant decrement in toxicity. However a number of problems remain to be overcome to provide a clinically useful carrier system:

- a) specificity of the carrier for tumour cells in vivo
- b) stability of the carrier complex in vivo
- c) release of the active agent at the target site
- d) non specific uptake of exogenous material by the reticulo-endothelial system (Poste, 1983).
- e) adverse immunological reactions to the exogenous carrier.

Low density lipoprotein (LDL) is the major cholesterol-carrying lipoprotein in human plasma. The LDL particles contain a lipid core of approximately 1,500 ester molecules surrounded by a polar shell of free cholesterol, phospholipids and protein (apoprotein B). It has been shown that a variety of human cell types express cell surface receptors for LDL. After binding to the receptor, an auto-regulated sequence of events occurs which culminates in lysosomal degradation of the lipoprotein and subsequent release of the

cholesterol for use in the cell. Recent reports indicate that cells which are undergoing active cell division show a greater LDL receptor activity than non-dividing cells. For example, Gal et al (1981) have demonstrated in vitro that replicating epidermoid cervical carcinoma (EC-50) cells metabolise LDL some 20 times faster than cervical fibroblasts. Similar evidence has accumulated for leukaemic cells relative to normal marrow stem cells.

Attempts have been made to utilise the LDL-receptor pathway by complexing LDL with cytotoxic drugs. LDL-aclacinomycin A is effective against human glioma cells in culture and LDL-methotrexate covalent complex is active against murine leukaemia cells in vitro. Iwanik et al (1984) have prepared an LDL-daunomycin complex in which daunomycin appears to be located in the surface region and the hydrophobic domain of the LDL particle. They demonstrated significantly higher cell associated levels of daunomycin after treatment of P388 leukaemic cell lines with the LDL-daunomycin complex, than after exposure to free daunomycin under similar conditions.

In this study, the LDL-receptor activity of the L-DAN cell line has been characterised and the cellular uptake, metabolism and cytotoxic efficacy of LDL-daunomycin complex has been examined in monolayer and spheroid.

9.2 Materials and Methods

Isolation of lipoprotein This follows the method of Patsch et al 1974. Briefly, human plasma was isolated from venous blood (100 ml) drawn from normolipidaemic adults after overnight fasting. LDL was extracted by rate zonal ultracentrifugation using a linear NaBr gradient in a Sorvall refrigerated centrifuge. The LDL was then dialysed and its purity checked by SDS-polyacrylamide gel electrophoresis. Iodination of lipoproteins were accomplished by the iodine monochloride method, modified by Bilheimer et al (1972).

LDL-daunomycin complex formation This follows the method of Iwanik et al (1984). Daunomycin in methanol was evaporated to dryness in a Buchler Vortex Evaporator and resuspended with 2-5 mg of LDL in 1 ml of LDL buffer. The mixture was stirred with a Teflon-coated stirrer for 2 hours in the dark at room temperature. The mixture was then passed down a sephadex G-120-15 column equilibrated in LDL buffer, which separated the free from complex associated daunomycin. The complex was then sterilised by passage through a 0.44 μ m Millex Millipore filter.

Cellular degradation of 125 I-LDL

Isolated L-DAN cells (approximately 2×10^6) were incubated for 24 hours with 125 I-LDL in 1 ml of F10DMEM culture medium, at 37°C in humidified air containing 5% CO₂. Blank incubations were performed under identical condition in the absence of cells. The degradation of LDL was determined from the appearance of non iodide trichloroacetic acid (TCA) soluble material in the incubation medium, as described by Goldstein et al (1974). In brief

undegraded high molecular weight ^{125}I -LDL in the medium was precipitated by TCA. After centrifugation, free iodide was separated from degradation fragments of ^{125}I -LDL in the supernatant by oxidation with H_2O_2 and extraction with chloroform. An aliquot of the aqueous phase was then assayed for radioactivity to determine the degradation of ^{125}I -LDL.

^{125}I -LDL Binding to intact cells

2×10^5 cells were grown in petri dishes, and on Day 7 after 24 hours of growth in medium containing lipoprotein-deficient serum, the medium was removed from each dish and replaced with 2 ml of Medium A, consisting of Eagle's minimum essential medium containing penicillin and streptomycin; 20mM Glycine, pH 7.4; and 5 mg of lipo-protein-deficient serum, and the indicated amounts of ^{125}I -LDL protein and native LDL protein. After incubation on a rotatory shaker (80 oscillations per min) in air at 37° , the medium was removed and all subsequent operations were carried out at 4° in a cold room. Each monolayer was washed 3 times in rapid succession with 3 ml of buffer containing 50 mM Tris-HCl, pH 7.4; 0.15 M NaCl; and 6 mg of bovine serum albumin, after which a further 3 ml of the same buffer was added and the monolayer was incubated for 2 min. This latter step was repeated once, each monolayer was washed finally with 3 ml of buffer containing 50 mM Tris-HCl, pH 7.4 and 0.15 M NaCl, and the cells were removed from the dish by dissolution in 1 ml of 0.1 N NaOH. Aliquots of 500 μl were removed from each dish for scintillation counting in a gamma counter and 50- μl aliquots were taken for measurement of protein concentration. In all figures, each point represents the value obtained from a

single dish and is expressed as the counts per min of 125 bound per mg of total cell protein. Each dish contained 350 to 500 μ g of total cell protein. Duplicate determination of 125 I-LDL binding varied by less than 10% of the mean values.

Conditions of cell growth - LDAN monolayers and spheroids were grown as previously described.

Assays of cytotoxicity - monolayer clonogenic survival and spheroid growth delay were assessed after exposure to daunomycin or LDL-daunomycin, for 1 hour over a concentration range of 0.1 - 5 μ g/ml.

Cellular localisation of daunomycin by fluorescence microscopy

Monolayers of L-DAN in the exponential phase of growth were exposed to LDL-daunomycin or free drug at a concentration of 5 μ g/ml for up to 2 hours. The monolayers were washed twice with ice cold PBS, wet mounted and examined under the Polyvar fluorescent microscope (filters set at the same for adriamycin). Spheroids were prepared for fluorescent microscopy as previously described (sec 3.2) after exposure to daunomycin or LDL-dauno, 5 μ g/ml for 1 hour.

Determination of the intracellular concentrations of daunomycin and its metabolites

Monolayers of L-DAN in the exponential phase of growth were treated with complexed or free drug at an external concentration of 10 μ g/ml for varying times (15 minutes to 2 hours). The cells were washed twice with ice cold PBS, harvested by brief trypsinisation (0.25%) counted, and then resuspended in 2 ml of distilled H₂O. Parent drug and its metabolites were then extracted and measured by HPLC with fluorescence detection, as previously described (sec 4.2). Drug levels were expressed as ng/10⁵ cells and drug accumulation curves were approximated by non-linear least squares fitting.

Cellular accumulation and metabolism of daunomycin

Cellular uptake of daunomycin and LDL-daunomycin proceeded rapidly and approached equilibrium by approximately 3 hours. It is of note that parent drug concentrations, on a cellular basis are similar and statistically indistinguishable at each experimental time point (table 9.1; figure 9.1) regardless of whether free drug or the complex was used. The degree of intracellular drug metabolism, however, differed markedly. Daunorubicinol which is synthesised by a ubiquitous cytoplasmic NADPH reductase from parent drug was the chief metabolite formed (at the highest drug concentration, small amounts of the deoxyglycone of daunorubicinol were measurable). During prolonged incubation with free drug (> 90 minutes) daunorubicinol predominated over parent drug (table 9.1). If parent drug is expressed as a per centage of total intracellular drug i.e. $\text{daunomycin}/(\text{daunomycin} + \text{daunomycinol}) \times 100\%$, then it is apparent that relatively less daunomycin is converted to the alcohol after treatment of the cells with the LDL-daunomycin complex.

The total cellular drug content (daunomycin + daunomycinol), is higher after exposure of the cells to free daunomycin. (Table 9.1)

Intracellular localisation of drug by fluorescence microscopy

The subcellular distribution of daunomycin is apparently independent of its mode of delivery to the cell. Daunomycin is present in a granular distribution within the cytoplasm, the nucleus and the nuclear membrane. This is similar to the fluorescent staining pattern previously reported by 4'-deoxy (sec 2.3). The LDL-daunomycin complex does not appear to markedly alter the intracellular disposition of the cytotoxic agent despite

the fact that the drug is presented to the cell in a markedly different physico-chemical state, and presumably enters the cells by a different pathway.

Sectional analysis of spheroids by fluorescent microscopy showed that visible drug was nuclear bound and had diffused slightly further into the spheroid after presentation bound to LDL.

Cytotoxicity to monolayer and spheroid

The monolayer clonogenic cell survival curves for daunomycin and LDL-daunomycin are shown in figure 9.2. The degree of cell kill produced by both drugs is similar (ID_{90} daunomycin, 1.0 $\mu\text{g/ml}$; ID_{90} LDL-daunomycin 0.7 $\mu\text{g/ml}$). The cell survival curves are biphasic with a point of inflection at 5 $\mu\text{g/ml}$.

Spheroid growth delay data is summarised in Table 9.2. LDL-daunomycin induces significantly longer growth delays at equal medium concentrations than free daunomycin. Despite similar monolayer clonogenic survival curves the disaggregated spheroid clonogenic survival curves reveal that LDL-dauno is significantly more active in spheroids than free daunomycin if one compares relative clonogenic cell survival at concentrations of 5 $\mu\text{g/ml}$ ($p < 0.05$).

^{125}I -LDL degradation and binding to L-DAN cells

The degradation of ^{125}I -LDL by L-DAN cells as a function of the incubation concentration of ^{125}I -LDL is shown in figure 9.3. At concentrations below 40 $\mu\text{g/ml}$ the degradation rate rose sharply with increasing concentration. Further increase in the

concentration of ^{125}I -LDL led to a considerably less steep rise in the degradation rate, which approached linearity above 70 ug/ml. In the presence of a 20-fold excess of unlabelled LDL the degradation of radiolabelled LDL was inhibited and degradation increased linearly with the incubation concentration of ^{125}I -LDL. The slope of this curve was similar to the terminal part of the degradation curve obtained in the absence of unlabelled LDL. By subtracting the values for degradation of ^{125}I -LDL in the presence of unlabelled LDL from the degradation values in its absence, a saturable curve with a maximal velocity at 70 ug/ml results, which probably correspond to high affinity degradation sites.

High affinity binding sites for ^{125}I -LDL can be demonstrated in a similar manner (fig 9.3). The high affinity binding sites start to saturate above 100 ug/ml of ^{125}I -LDL. Reciprocal Lineweaver-Burke type plots of 1/cpm per ug cell protein versus 1/LDL (ug/ml) allow calculation of V_{max} and K_{m} for degradation ($V_{\text{max}} = 385$ cpm per ug cell protein; $K_{\text{m}} = 23$ ug/ml) and binding ($V_{\text{max}} = 133$ cpm per ug cell protein; $K_{\text{m}} = 71$ ug/ml).

¹²⁵I-labelled LDL was found to associate with monolayers of cultured human lung tumour cells by two processes, one of high affinity and one of low affinity. The high affinity association appears to represent binding of LDL to specific receptor sites on the cell surface. This binding process exhibited saturation kinetics at low concentrations of the lipoprotein. The other process, designated low affinity uptake, may represent non specific endocytosis since the uptake was proportional to the lipoprotein concentration in the medium with no apparent saturation.

Daunomycin is extensively metabolised within the cells to daunomycinol by the cytosolic NADPH dependent reductase. This occurs to a greater extent after exposure of the cells to free daunomycin, such that after 2 hours incubation, intracellular levels of daunomycinol exceed those of the parent drug by approximately 2 - fold. There is less metabolism of daunomycin after treatment of the cells with LDL-daunomycin. So, despite the fact that total intracellular drug levels (daunomycin plus daunomycinol) are greater following incubation with free daunomycin, the cellular concentration of unchanged daunomycin is similar at each time point. This implies that the LDL-daunomycin complex inhibits or protects daunomycin from cytoplasmic reduction.

Daunomycin, like adriamycin, enters the cells by diffusion of the electroneutral molecule through the lipid domain of the cell membrane. It is a more lipophilic molecule than adriamycin and this is reflected in its higher degree of cellular uptake for similar concentration-time exposures. On the basis of total intracellular drug, there would appear to be greater drug uptake following treatment with free daunomycin. The LDL-daunomycin complex must

first bind to LDL receptors on the cell surface before being internalised and degraded within lysosomes with release of the cytotoxic agent. There are a number of potential rate limiting steps in this sequence which could serve to limit uptake of LDL-encapsulated daunomycin, relative to diffusion of free daunomycin through the cell membrane.

The monolayer clonogenic cell survival curves for daunomycin and LDL-daunomycin are similar. Daunomycin has considerably greater cytotoxic efficacy than daunomycinol (Bachur, 1979), and one would therefore expect that intracellular daunomycin levels would correlate with clonogenic cell kill. Despite the differing degrees of drug metabolism, daunomycin levels were virtually identical regardless of its mode of presentation to the tumour cells, and this could account for the similar clonogenic cell survival curves.

Although the mechanisms for transmembrane transport were different, the subcellular distribution of daunomycin, demonstrated by fluorescence microscopy was indistinguishable, whether free or carrier bound daunomycin was used. The drug was bound to the nucleus, the nuclear membrane and was distributed within the cytoplasm in a granular fashion. It has been demonstrated (Egorin et al, 1984) that subcellular organelles cause differential fluorescence quenching of bound daunomycin and therefore fluorescence microscopy remains a useful but rather insensitive method for determining the subcellular distribution of anthracyclines. Iwanik et al, (1984) examined the subcellular localisation of daunomycin by membrane subfractionation of P388 cells after incubation with ^{125}I -LDL-daunomycin or free daunomycin they noted that approximately 50% of free daunomycin and about 70% of LDL-daunomycin

was associated with the membrane - organelle fraction of the cell, with the remaining percentage being either loosely bound or located within the cytoplasm. The ^{125}I -labelled fragments of LDL were especially enriched in plasma-membranes, microsomal-lysosomal-mitochondrial membranes and the insoluble nuclear pellet. In contrast to daunomycin derived from LDL, free daunomycin showed a strong preference for localisation in the insoluble nuclear pellet. Various other workers (Egorin et al, 1980; Gagliardi et al, 1980; Noel et al, 1978), using different tumour monolayer systems suggest an enrichment of daunomycin in nuclei and/or lysosomal organelles. We were unable to quantitate binding in our study, yet the results of the experiments based on fluorescent localisation are in broad agreement with the authors quoted (Egorin et al, 1980) given the relative insensitivity of our method.

Despite identical monolayer cytotoxicity, LDL-daunomycin induced prolonged spheroid growth delay and greater clonogenic cell kill compared to free daunomycin. This was apparently associated with a greater degree of spheroid penetration by LDL-associated daunomycin. It has been demonstrated previously that enhanced drug spheroid penetration tends to be associated with perturbed growth kinetics of the spheroid. However, the lipophilic drugs and vehicles used previously to improve spheroid penetration were associated with altered kinetics of drug uptake in monolayer. For example, Brij 30 increased adriamycin uptake by 2 - 3 fold and 4'-deoxy was taken up to a far higher extent than adriamycin by virtue of its lipophilicity. This is not the case with LDL associated daunomycin, where intracellular parent drug levels are identical to those obtained with free adriamycin. It is speculative, but Iwanik et al, (1984) did demonstrate a

higher degree of membrane association of daunomycin following treatment with LDL-daunomycin and this could result in a more available, easily-transportable form of the drug which would diffuse more readily towards the centre of the spheroid. Daunomycin which has intercalated into DNA is bound in a stable situation with a relatively long half life of dissociation, and would therefore be less able to diffuse from cell to cell.

Further experiments are required in vivo, probably in nude mice with human lung tumour xenografts, to examine the affinity of LDL-drug complexes for tumour and normal host tissue, the comparative pharmacokinetics relative to free drug and if there is a differential tumouricidal effect. Nevertheless, these preliminary experiments imply that LDL-daunomycin complexes could be a realistic means of biological targetting of active cytotoxic drugs to tumour.

Time (minutes)	FREE DAUNOMYCIN		LDL-DAUNO	
	Intracellular drug		Intracellular drug	
	(ng/10 ⁵ cells)		(ng/10 ⁵ cells)	
	Daunomycin	Daunomycinol	Daunomycin	Daunomycinol
0	0	0	0	0
15	4.8 ± 0.41	6.6 ± 0.5	4.5 ± 0.38	6.7 ± 0.52
30	5.2 ± 0.49	13.1 ± 1.2	7.1 ± 0.62	16.2 ± 1.72
60	10.1 ± 1.2	53.6 ± 4.8	10.4 ± 1.15	41.8 ± 4.3
90	13.2 ± 1.4	82.3 ± 6.7	13.9 ± 1.4	58.5 ± 5.1

Table 9.1 Intracellular levels of daunomycin and daunomycinol following treatment of LDAN monolayers with identical concentrations (5 µg/ml of daunomycin and LDL-daunomycin).

Drug concentration (ug/ml)	Median Growth delay (days)
Daunomycin	
0 (control)	7.3 (6.8 - 7.5)
0.5	13.9 (11.2 - 14.6)
1	15 (14.0 - 16.7)
2.5	18.2 (17.6 - 19.3)
5	20.3 (19.1 - 21.5)
LDL-Dauno	
0 (control)	6.8 (5.1 - 7.4)
0.5	14.2 (14.0 - 16.7)
1	17.2 (16.2 - 18.4)
2.5	20.9 (19.1 - 22.8)
5	24.3 (22.6 - 25.9)

Table 9.2 Spheroid growth delay following treatment with daunomycin or LDL-dauno at differing concentrations for 1 hour. The growth delay was taken to be the time to reach $\times 10$ original volume. The figures in brackets denote the 95% confidence limits around the median value.

Intracellular Drug
(ng/10⁵ Cells)

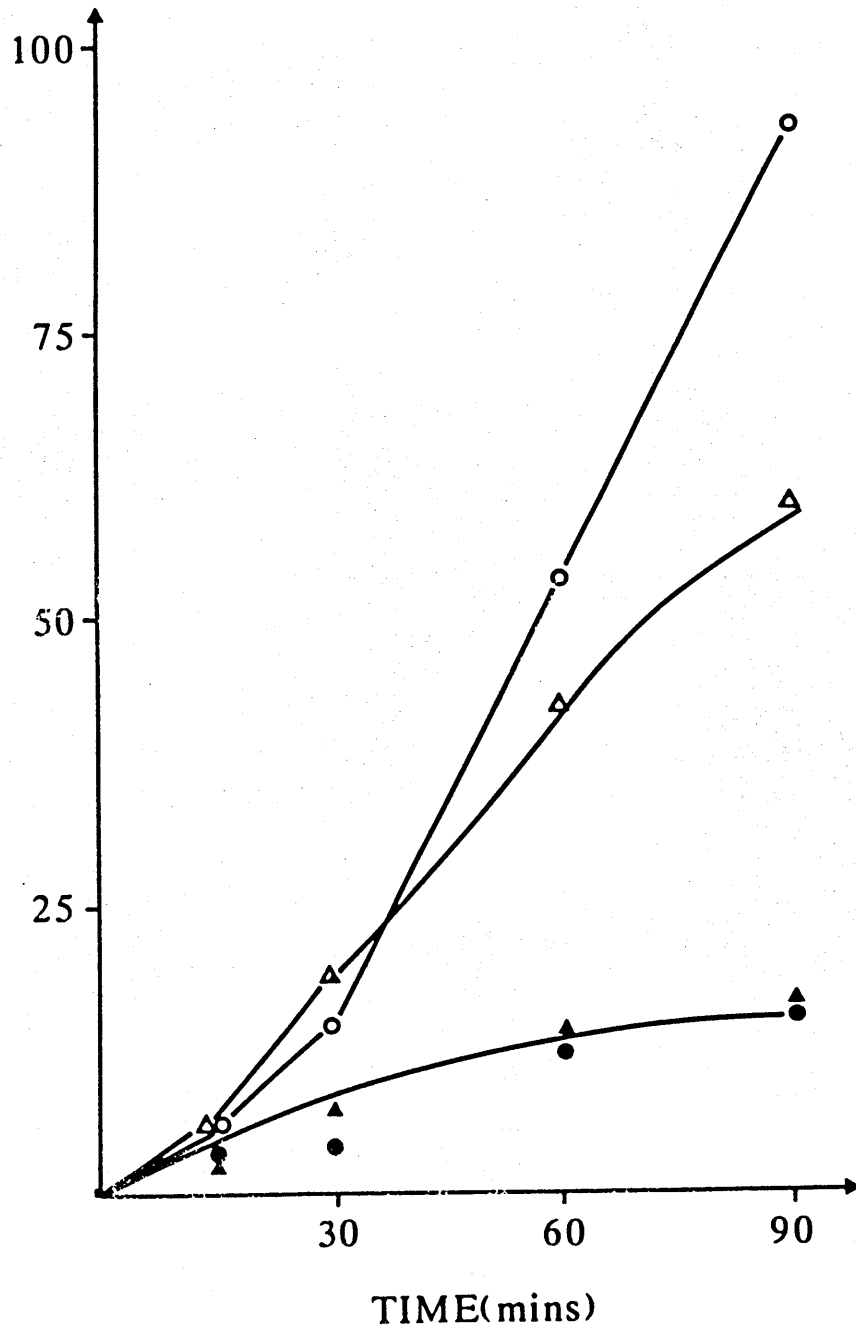


Figure 9.1 Intracellular uptake and metabolism of daunomycin after exposure to free drug (●) or LDL - associated drug (▲)

Free drug - daunomycinol (○)
 daunomycin (●)
 LDL associated drug - daunomycinol (△)
 daunomycin (▲)

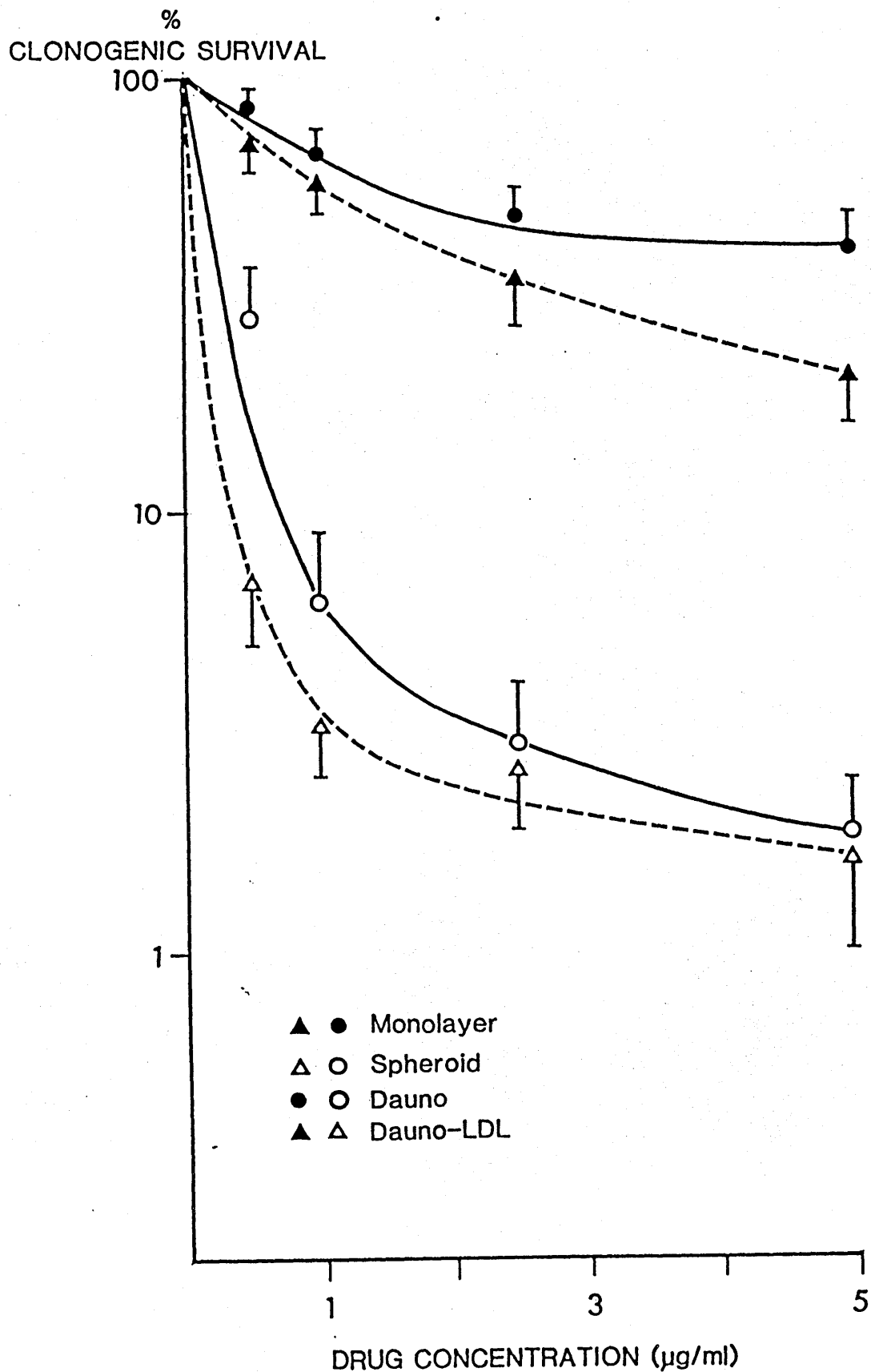


Figure 9.2 Clonogenic cell survival for monolayers and disaggregated spheroids following exposure to daunomycin or LDL-daunomycin. Each point is the mean of 4 experiments and the vertical bar denotes 1 standard deviation.

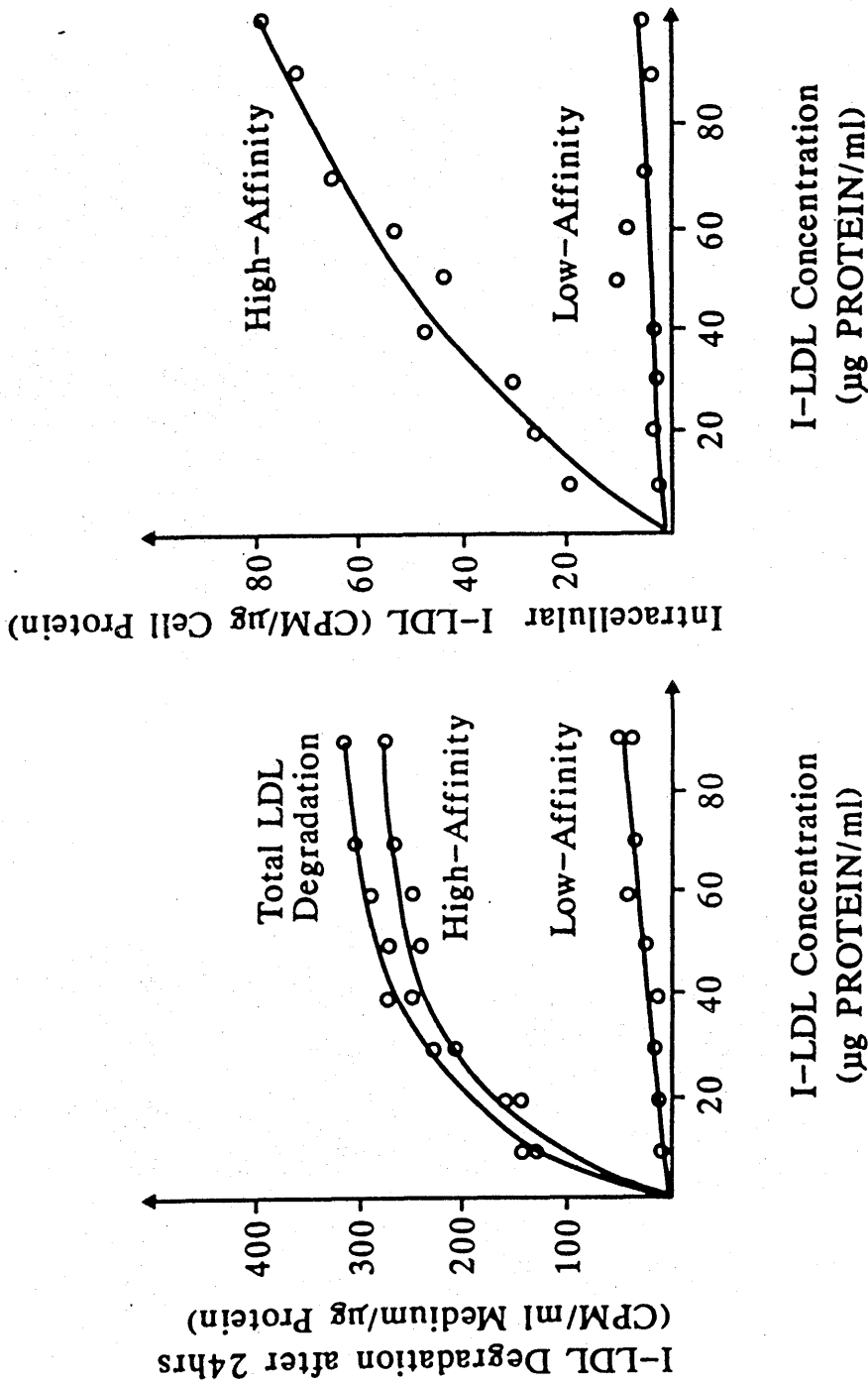


Figure 9.3 Relationship between LDL binding and degradation to external concentration in LDAN cells grown in monolayer culture. High affinity binding/degradation is derived by subtracting the non-specific or low affinity binding/degradation from the total values.

The association of gap junctional communication with cytotoxic drug resistance and intercellular drug transfer.

10.1 Introduction

Cell junctions are defined as structurally specialised domains that are formed at regions of contact between two cells, to which both cells contribute a part. These junctions are subclassified on the basis of ultrastructure and serve a variety of functions; provision of structural links between cells; conduits through adjoining cell membrane pairs; mediation of unidirectional propagation of electrochemical impulses from cell to cell; the means of sealing cells tightly together.

This chapter will examine the tumour biological significance of gap junctional communication in human lung tumour cells in vitro. During the last decade it has become apparent that gap junctions are mediators of metabolic cooperation, or coupling, between cells, Subak-Sharpe et al, 1969, demonstrated that mutant Chinese hamster fibroblasts deficient in the enzyme inosinic guanylic pyrophosphorylase could not incorporate hypoxanthine into DNA when they grew alone, but that they did so when grown in contact with wild-type cells. The enzyme block in the mutant was bypassed by nucleotidyl transfer from the wild type cells, presumably via gap junctions. The structure of gap junctions has been reviewed by Lowenstein (1981), and it is apparent that individual channels of the gap junctions allow exchange of "small" molecules (mol weight < 900 daltons) with specific charge and shape configurations (fig 10.1) Substances such as cations (Na^+ and K^+), cyclic AMP, inositol, purine nucleotides, uridine nucleotides, thymidine

nucleotides, deoxycytidine nucleotides, glucose-6-phosphate and other small molecules required for the cells intermediary metabolism are known to diffuse freely through gap junctions.

The development of direct junctional communication represents an important evolutionary step towards formation of highly differentiated multicellular organisms, and small molecular transfer during embryogenesis develops long before complex hormonal or electrical communication. Gap junctions have been demonstrated in many different types of tumour but their function or possible contribution to maintenance of the malignant phenotype remains unknown.

Dertinger and his co-workers (Dertinger and Hulser, 1981; Dertinger, Hinz and Jakobs, 1982; Dertinger, Guichard and Malaise, 1983; Dertinger, Guichard and Malaise, 1984) have studied the phenomenon of contact resistance in Chinese hamster ovary spheroids. Contact resistance is the relative radioresistance to γ -irradiation of cells grown as spheroids rather than as monolayer. These authors have speculated that contact resistance may arise from some functional differentiation occurring in gap junctionally coupled cells.

Nederman, Acker and Carlsson (1981) have showed that 5-fluorouracil penetrates human glioma and thyroid tumour spheroids efficiently within a few minutes, whereas vinblastine requires several hours to achieve a similar degree of penetration. Existing data indicate that for mammalian cells, the translocation of purine and pyrimidine nucleosides across the cell membrane is a combination of carrier-mediated transport and passive diffusion. One would

expect that 5-fluouracil would pass from cell to cell via gap junctions given its molecular size and this could represent a relatively rapid mode of intercellular transfer.

In this chapter, the relationship between gap junction formation in tissue culture systems and cytotoxic drug resistance and transport is examined.

Monolayer and spheroid culture - the conditions of LDAN culture have been previously described. The agar underlay technique was used in a similar manner to grow spheroids from two Chinese hamster ovary lines (DON and DON6). The mutant (DON6) differs from the parent line (DON) only in that it does not form gap junctions in tissue culture.

Determination of gap junction formation

Recipient cell cultures were prepared by plating 1×10^5 cells in 2 ml of F10-DMEM medium into 3.5 cm Petri dishes each containing 4 sterile glass coverslips (13 mm in diameter) and incubating at 37°C over night. Donor cell cultures were prepared by plating 2.5×10^5 cells in 5 ml of medium in 5 cm Petri dishes and incubating at 37°C in a humid environment overnight. The donor cells were then labelled by adding 50 μCi ($5\text{-}^3\text{H}$) uridine to the medium and replacing in the incubator at 37°C for 3 hours. Residual ^3H -uridine was removed by washing the donor cells 3 times with 5 ml of ice cold PBS. Donor cells were then detached by rinsing with trypsin and resuspended in 2 ml of medium. To each dish of recipient cells, 200 μl of the labelled donor cells were added and the mixture co-cultured for 1 hour and 3 hours.

Following co-culture, the medium was removed, the cells washed twice with 2 ml PBS and then fixed with 2 ml of formol saline for 30 minutes at room temperature. The coverslips were placed in racks and the acid soluble nucleotides removed by washing twice with 5% (W/V) TCA at 4°C for 2 minutes and then rinsed twice in distilled water. The coverslips were finally rinsed in ethanol and dried before being mounted, cells uppermost, with DPX on microscope slides and processed for autoradiography.

DON and DON6 spheroids, approximately 600 μm in diameter, were exposed to ^3H -(7)-5-fluorouracil 50 μCi for 30 minutes at 37°C. The spheroids were allowed to sediment, the radioactive medium removed, and they were then washed twice with ice cold PBS. The spheroids were then transferred into gelatine capsules containing OCT embedding gel and frozen in liquid N_2 . Thin sections (5 μm) were then cut in a cryotome and mounted on microscope slides before being processed for autoradiography.

Autoradiography

The slides were dipped in Ilford K₂ emulsion (1 part emulsion; 2 parts water) at 45°C, dried under a stream of cold air and placed in a light tight box at 4°C. For grain counting, the autoradiographs were exposed for up to 7 days, for photography, they were exposed for up to 1 month.

After the exposure period, the slides were developed with Kodak D19 developer at 20°C for 5 minutes washed in water for 2 minutes and then fixed for 4 minutes with Ilford Hypam Fixative. After washing for 5 minutes in running water the cells were stained with freshly diluted giemsa (5% W/V in water) for 30 seconds. After a further wash, the slides were air dried and a second coverslip mounted on top with DPX.

Chemosensitivity Assay

The in vitro sensitivity of five different human lung tumour lines was established. The cell lines were established from individual cases of human lung cancer and their characteristics are

summarised in table 10.1. The drugs used in the study were adriamycin, actinomycin D (trade name "Lyovac Cosmegen" Merk Sharp and Dohme International, Rahway, NJ, USA), VP16-213 (trade name "Vepesid", Bristol Myers Pharmaceuticals, Slough, UK), 5-fluorouracil (Roche Products Lts, Welwyn Garden City, UK), melphalan (trade name, "Alkeran", The Wellcome Foundation Ltd, London, UK) and mitomycin C (Martindale Pharmaceuticals Ltd, Essex, UK). They were diluted according to manufacturer's instructions for injections and stored at -20°C until required. They were then further diluted in culture medium to the required concentrations. In the case of melphalan, care was taken to ensure that these operations were carried out within 30 minutes because of the instability of the drug. In no case did the volume of diluent added with the drug exceed 1% of the final volume. Drug sensitivity assays were carried out using a modification of a method described previously (Morgan et al, 1983). Exponentially growing cells were trypsinised and seeded into 96 - cell Linbro microtitration plates to give 10^3 cells per well. After 3 days the medium was removed from the plate by suction and replaced by fresh drug free medium. After a further 24 hours, serial dilutions of the drugs were added to duplicate wells in the plate. Two wells of each row were left free of drugs to act as controls. The drug-containing medium was replaced with fresh drug containing medium after 24 and 48 hours during a total exposure to drugs of 72 hours. The drug containing medium was then replaced with drug-free medium and the cells were allowed a recovery period of 5 days with medium changes after 3 and

4 days. The viability of cells remaining in each well was determined by isotopic precursor incorporation into protein as described below. This technique has been previously demonstrated to produce equivalent results to cloning for the lung tumour cell lines.

In all drug experiments, cell counts (using a model ZB, Coulter Counter) were made of replicate plates of each cell line to determine population doubling time and to ensure that the control cultures remained in exponential growth throughout the period of drug-treatment and recovery. The period of drug exposure of 72 hours exceeded one population doubling time with all the cell lines used in these experiments.

At the end of the experiment, cell number was assayed by exposing the cells to medium containing 3 $\mu\text{Ci/ml}$ [^{35}S] - methionine (specific activity 638-1275 Ci mmol^{-1}) or 1 $\mu\text{Ci/ml}$ L-4, 5 [^3H] leucine (specific activity 10 mCi mol^{-1}) for periods of between 4 - 24 hours. During this period the rate of incorporation of labelled amino acid has been shown to be linear (Morgan et al, 1983). The plates were then washed and cell protein (solubilised in 1M NaOH) counted as previously described. The incorporation of labelled amino acid of each well was expressed as a percentage of the control in that row and the doses of drug that inhibited protein synthesis by 50% (the ID_{50}) was determined.

Gap junction formation

Typical autoradiographs are shown in fig 10.2. It is possible, as previously described, to quantitate the number of donor cells forming gap junctions with the recipients. The results for individual cell lines are shown in table 10.2.

Chemosensitivity of human lung tumour cells in culture

The respective ID_{50} 's for each cell line and drug are tabulated (table 10.2). There is considerable variation in the sensitivity of individual cell types to different drugs. The ID_{50} values for individual drugs and the percentage of cells forming gap junctions have been ranked from 1 - 5. The cell line forming most gap junctions is ranked 1, and the cell line with the highest ID_{50} (i.e. cell line which is most resistant to that drug) is similarly ranked 1. This data is summarised in table 10.3. Using the non parametric Spearman Rank Correlation Coefficient, there is a significant ($p < 0.05$) direct correlation between gap junction formation and ID_{50} (fig 10.2).

Spheroid autoradiographs with [3 H]-5-fluorouracil

The autoradiographs for DON and DON6 spheroids show that the silver grains are evenly distributed throughout the DON spheroids, but are limited to an external annulus in DON6 spheroids, implying limited drug penetration.

10.4 Discussion

There is preliminary evidence to suggest that the ability to form gap junctions in tissue culture is related to cytotoxic chemosensitivity. The greater the ability of the cells to form gap junctions in vitro, the greater their resistance to a variety of antineoplastic agents. The evidence for this is indirect in that there is a statistically significant correlation between the two variables. It is important to realise that the existence of a correlation between 2 variables does not signify a cause/effect relationship, as gap junction forming ability could be an indirect "marker" of some other cellular function which is the determinant of anticancer drug sensitivity. Nevertheless, in view of the finding of Dertinger and co-workers on the relationship of contact resistance and radiosensitivity it is tempting to speculate that gap junctional communication could play a role in cytotoxic drug resistance.

At the very least, gap junctions determine that small molecules will diffuse between cells according to concentration gradients which implies that interconnected cells will have "equilibrium" levels of small diffusible molecules. If a toxic stimulus impinges locally on this diffusely connected cell network, with loss or alteration in the concentration of a vital biochemical component, then there would tend to be an alteration in the "intercellular equilibrium". This this way the healthy or unaffected cells could replace vital biochemical components or remove toxic products from damaged cells in such a way as to minimise the effects of the toxic stimulus at its site of application.

The most elementary function of the gap junction is probably equilibration of concentration differences of channel permeant molecules between tissue cells which creates the bases for tissue homeostasis. Such a mechanism could account for a degree of cytotoxic drug resistance, if the permeant molecules had some role to play in genesis of their antineoplastic effect.

Autoradiographic drug penetration studies with tritiated 5-Fluorouracil imply that the drug diffuses more rapidly into spheroids which are coupled by gap junctions (DON) than those which do not form gap junctions (DON6). These Chinese hamster ovary spheroids are identical in every respect other than their ability for junctional communication. One would expect that 5-Fluorouracil has the correct size and shape characteristics to be transported through gap junctions, and therefore possibly bypass the potentially rate limiting step of transmembrane diffusion/transport within the spheroid. A "snakes and ladders" analogy would perhaps be appropriate as the drug could reach the spheroid centre rapidly by means other than the conventional one of diffusing from cell to cell. There is no relationship between chemosensitivity to 5-fluorouracil and gap junction formation in monolayer (table 10.3). Cells in monolayer exposed to drugs have approximately 50% of their cell surface area in direct contact with the drug containing solution therefore drug access, other than for the effect of membrane limited diffusion, is not a problem. In order to determine whether improved drug penetration via gap junctions altered the cytotoxic response of spheroids, the efficacy of 5-fluorouracil in DON and DON6 monolayers could be compared against a spheroid cytotoxic endpoint.

From these preliminary studies, it is apparent that gap junctional communication could be associated with cytotoxic drug resistance, although the underlying mechanism is not known, and that gap junctions could provide an intercellular conduit for cytotoxic drugs with appropriate size and shape characteristics.

CELL LINE	PATHOLOGY	SOURCE
Calu-3	Adenocarcinoma	American Type Culture Collection, U.S.A.
SK-MES-1	Squamous carcinoma	American Type Culture Collection, U.S.A.
L-DAN	Squamous carcinoma	Medical Oncology, Glasgow, UK
WIL	Adenocarcinoma	Ludwig Institute, Sutton, UK
A549	Bronchiolo-alveolar carcinoma	American Type Culture Collection, U.S.A.

Table 10.1 Non small cell lung cancer lines used in the gap
junction study.

Cell Line	DRUG ID ₅₀						
	ADR (x 10 ⁻⁹ M)	AD (x 10 ⁻¹⁰ M)	VC (x 10 ⁻⁹ M)	VP16 (x 10 ⁻⁸ M)	L-PAM (x 10 ⁻⁷ M)	MC (x 10 ⁻¹¹ M)	SFU (x 10 ⁻⁷ M)
Calu-3	2.7	20	1.6	2.3	7.8	20	7.4
SK-MES-1	48-53	60	13-22	81-120	24	100	86
L-DAN	34-70	50	17-17	92-110	84	60	42
WIL	168	55	136	70-83	100	30	69
A549	204-228	20-40	27-28	360	87	200	15

Table 10.2 The cytotoxicity (ID₅₀) data for each cell line. The abbreviations used are: adriamycin, ADR; actinomycin D, AD; vincristine, VC; melphalan, L-PAM; mitomycin C, MC; 5-fluorouracil, 5-FU.

Cell Line	Gap Junction Formation	ADR Sensitivity	AD Sens.	VC Sens.	VP-16 Sens.	L-PAM Sens.	MC Sens.	5-FU Sens.
A549	1	1	1	2	1	2	1	4
SKMES-1	2	4	2	3	2	4	2	1
L-DAN	3	3	4	4	3	3	3	3
WIL	4	2	3	1	4	1	4	2
Calu-3	5	5	5	5	5	5	5	5

Table 10.3 The order of ranking gap junction formation is from high (1) to low (5), whereas cell sensitivity data is ranked from most resistant (1) to most sensitive (5).

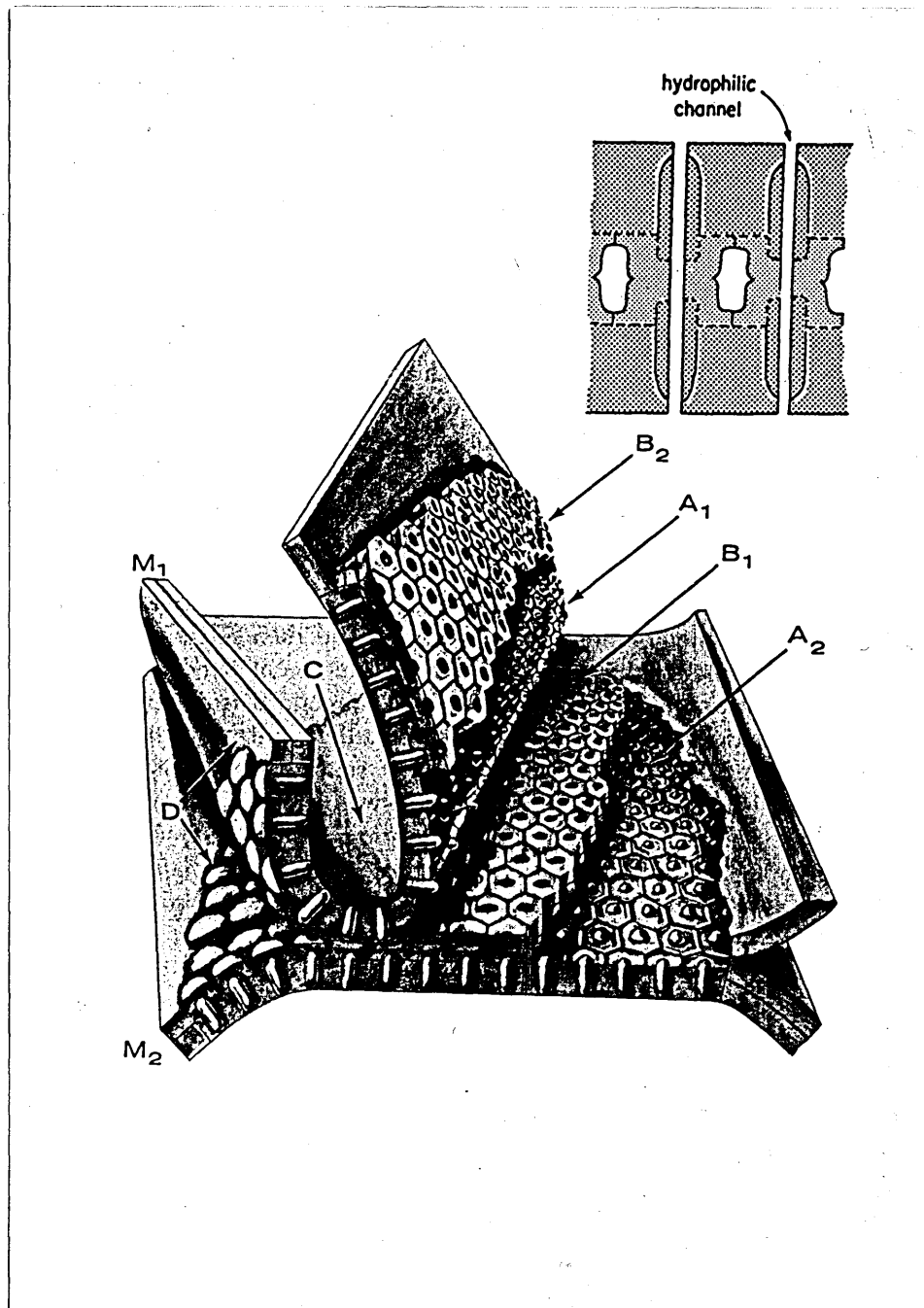


Figure 10.1 The McNutt-Weinstein Model: An interpretation of the ultrastructure of the gap junction (left). The junctional membranes (M_1 and M_2) are shown pulled down to demonstrate the appearance of foot processes that normally project from each membrane and meet in the extracellular space at the midline (right). Aspects of the gap junction are shown as they appear in freeze-fracture replicas. Intermembrane particles, which partially (? or completely) span the junctional membranes are present on the A face. The inset illustrates an interpretation of the position of hydrophilic channels within the gap junction. These channels may provide the structural basis for low-resistance electrotonic coupling of neighbouring cells. The model is not drawn to exact scale. Reprinted from McNutt and Weinstein (1970), with permission of the Rockefeller University Press.

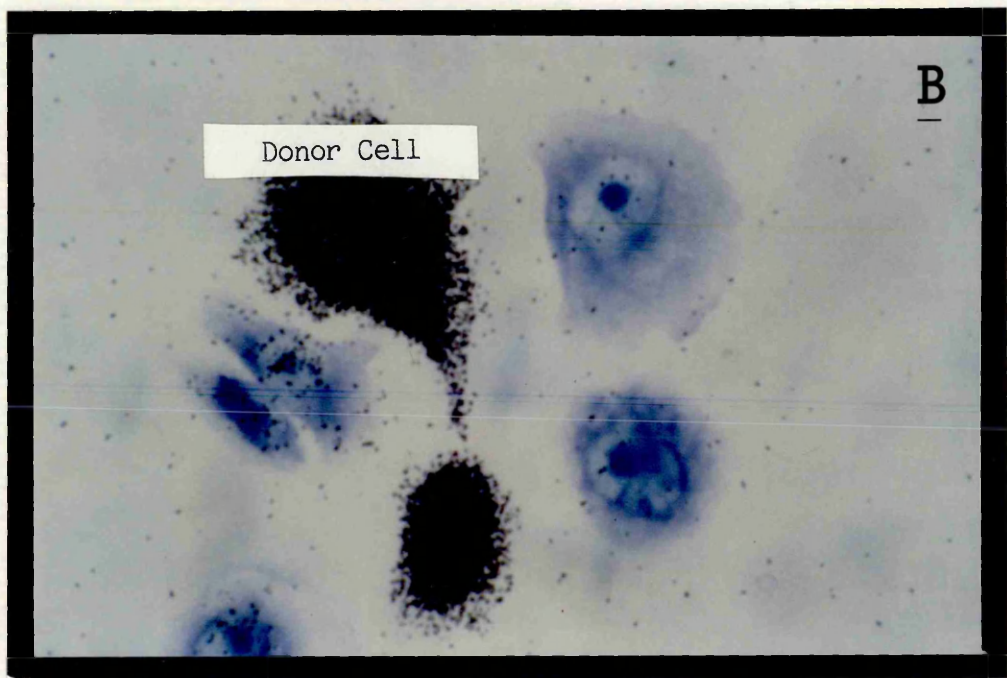
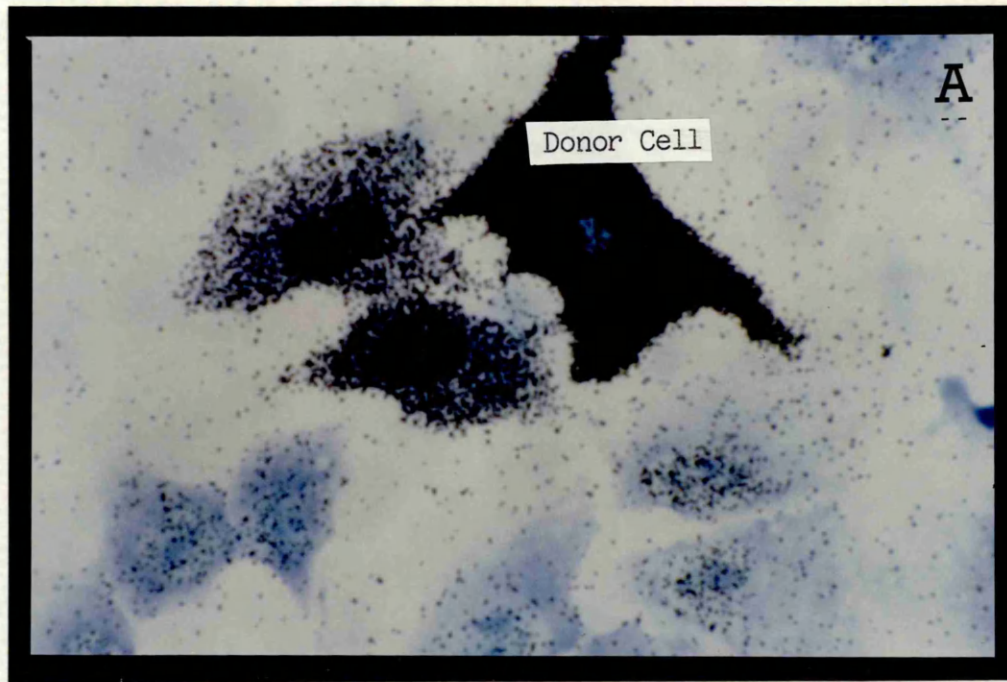


Figure 10.2 Autoradiographs showing the distribution of 3H-uridine in cells that

A. Form gap junctions
(magnification x 100)

B. Do not form gap junctions

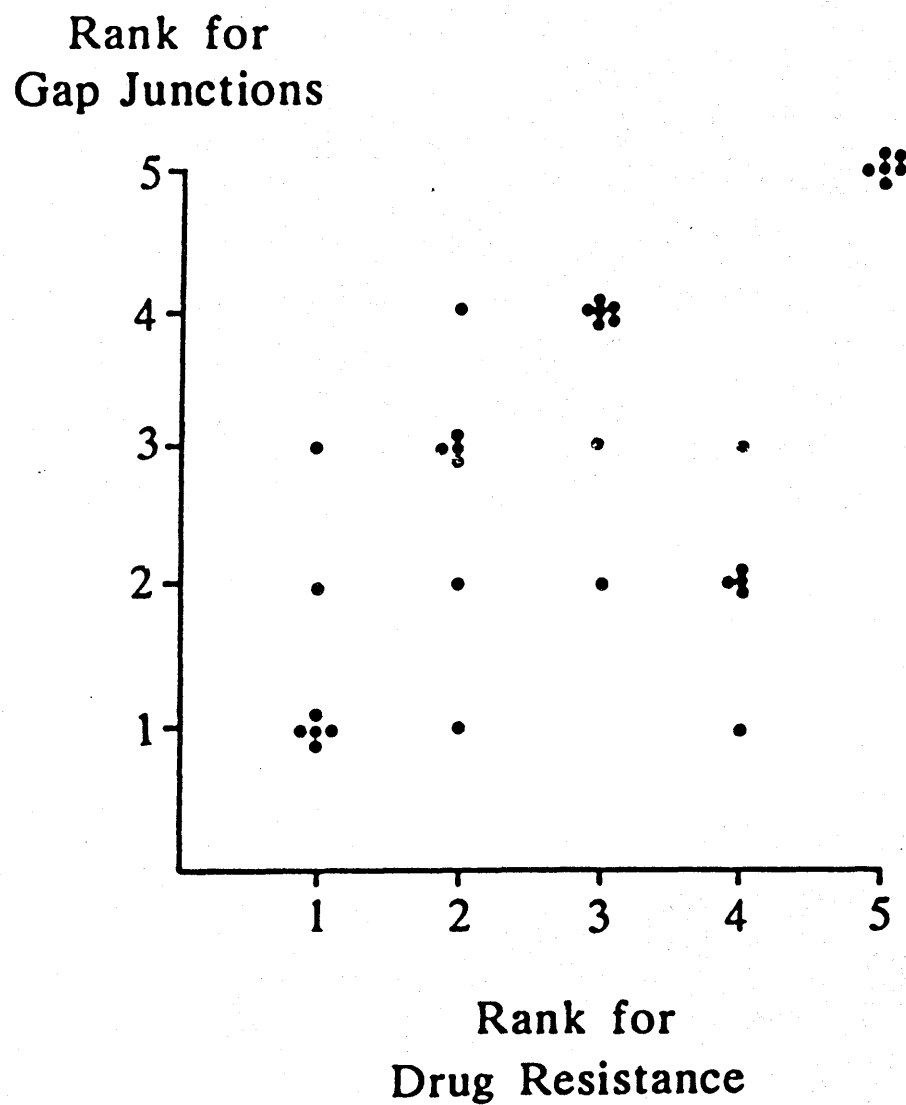


Figure 10.3 Correlation between gap junction formation and cytotoxic drug resistance ($r = 0.63$, $p < 0.05$). Dots which are grouped together represent single point repeats.

A concentration-effect model for spheroid drug diffusion

11.1 Introduction

A considerable amount of information is available on the pharmacokinetics of anticancer drugs, but much less is known of their pharmacodynamics, that is of the relationship between therapeutic or toxic response and drug concentration. The pharmacodynamic aspect of quantitative pharmacology attempts to relate drug concentration at the receptor site to biological response. Since the drug concentration at the receptor site can rarely be measured directly, it is more usual to measure the drug concentration in plasma and assume that it reflects receptor site concentrations indirectly.

Powis (1985) has recently reviewed the relationship of tumour response to a number of pharmacokinetic parameters governing anticancer drug disposition, such as peak drug concentration and the area under the plasma concentration-time curve (AUC). He noted that there are no studies relating parameters of tumour response *in vitro* to those *in vivo*. It is apparent from the preceding data presented in this thesis that the multicellular spheroid would appear to be a better predictive model *in vitro* than monolayer. In the initial part of this chapter a mathematical concentration-effect model is presented which attempts to quantitate and correlate *in vitro/in vivo* tumour clonogenic survival.

In addition, it has been possible to design a mathematical model which predicts spheroid clonogenic cell survival on the basis of drug diffusion gradients. The model is described with supportive experimental details.

11.2 Materials and Methods

Concentration-Effect Model

Clonogenic cell kill in monolayers, spheroids and xenografts of MGH-UI human bladder carcinoma cells in response to adriamycin treatment has been described by Erlichman and Vidgen (1984). This is a unique set of information in that they have adriamycin sensitivities for the same cell line grown at 3 different levels of complexity (monolayer, spheroid and xenograft) assessed by a common cytotoxic assay. The xenografts were dissociated at intervals following treatment, and clonogenic cell survival was measured, rather than using tumour growth delay as a cytotoxic end point.

The monolayer and disaggregated spheroid clonogenic cell survival curves were redrawn as % cells killed Vs log adriamycin concentration (fig 11.1) in order to convert them to recognisable standard dose-response curves.

The EMax model, developed by Langmuir and modified by Hill was adapted for use (Goodman and Gilman, 1975) as follows;



Where [D] = number of drug molecules

[R] = number of free receptors

[DR] = drug/receptor complex

n = number of drug molecules reacting with 1 receptor.

then it can be shown that

$$E = \frac{[C] E_{\max}}{[C_{50}] + [C]}$$

Where E = observed effect (% clonogenic cell kill)

E_{max} = maximum possible response

n = number of drug molecules reacting with 1 receptor

At E = 1/2 E_{max}, [C] = [C₅₀]

C = drug concentration in plasma.

The assumptions on which this model is based, include;

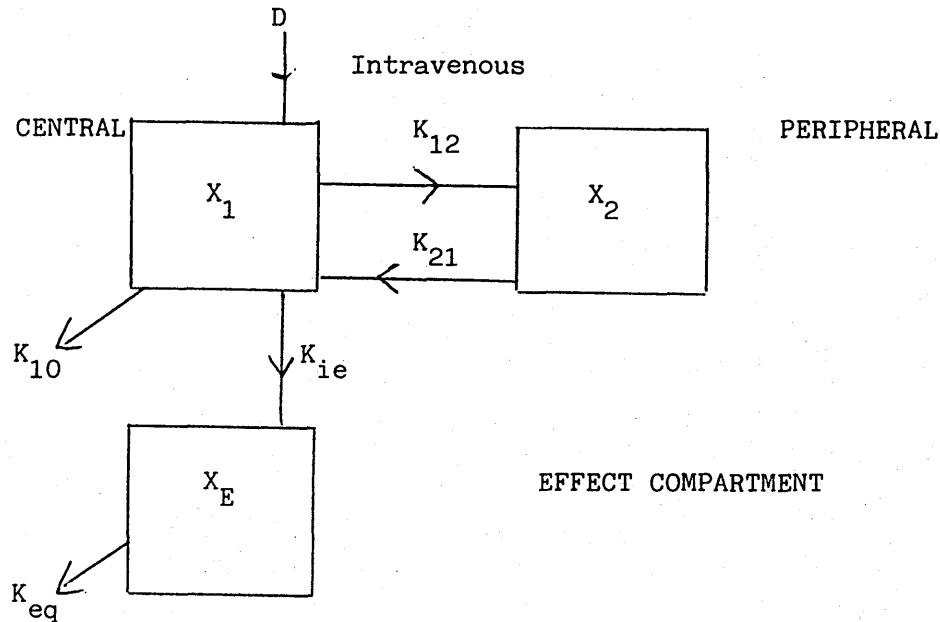
$E \propto [DR]$ and that the system is in equilibrium.

The dependence of cytotoxic response on both the concentration and duration of drug exposure has already been documented (sec 2.3). In view of these findings the cumulative AUC for total drug exposure in monolayer, spheroid or xenograft has been entered in the concentration-effect model rather than instantaneous plasma concentration as this is more likely to bear a quantitative relationship to tumour response. It must be emphasised that most concentration-effect modelling hitherto has concentrated on acute effects eg relating drug levels to instantaneous changes in blood pressure, heart rate, electrocardiographic parameters etc, rather than delayed or chronic response experiments such as tumour growth.

The pharmacokinetics of adriamycin in nude mice bearing tumour xenografts has been described (sec 7.3) Sheiner (1982) has devised a compartmental model to relate some estimate of plasma concentration to effect. The properties of the effect compartment (vide infra) are defined as follows.

1. The amount of drug in the effect compartment is governed by first order processes.
2. The amount of drug in the effect compartment is relatively small.
3. The measured effect is related to the drug concentration in the effect compartment.

The compartmental model can be described graphically as follows.



This model accounts for drug distribution into 2 compartments. D is the dose of drug administered by intravenous bolus. X_1 is the amount of drug in the central compartment; X_2 is the amount of drug in the peripheral compartment; X_E is the amount of drug in the effect compartment. The microscopic rate constants governing intercompartmental drug transfer are K_{21} and K_{12} , whereas K_{10} is the excretion rate constant K_{ie} and K_{eq} are the rate constants defining the effect compartment.

By a series of Laplace transforms (Gibaldi and Perrier, 1975) it is possible to deduce that

$$X_E = \frac{A \cdot V_1 \cdot K_{ie}}{(K_{eq} - \alpha)} (e^{-\alpha t} - e^{-keqt}) + \frac{B \cdot V_1 \cdot K_{ie}}{(K_{eq} - \beta)} (e^{-\beta t} - e^{-keqt})$$

$$\begin{aligned} \text{Where, } \alpha &= K_{21} + K_{10} \\ \alpha + \beta &= K_{10} + K_{12} + K_{21} \\ A + B &= \text{dose}/V_1 \end{aligned}$$

V_1 = volume of the central compartment

X_E = the amount of drug in the effect compartment.

By using the compartmental model to calculate the amount of drug in the effect compartment of the basis of plasma drug levels it is then possible to work out the cumulative AUC of drug in this compartment. This value can then be used in the Emax model derived from the monolayer and spheroid in vitro data.

The % cell kill v log concentration curves were fitted to asymptotic sigmoid curves by the method of least squares using an "in-house" programme based on the Marquardt algorithm (Bevington, 1978).

This approach allowed calculation of Emax and $[C_{50}]$ for adriamycin in monolayer and spheroid culture systems. The murine adriamycin plasma profiles were fitted to the compartmental effect model using non linear least squares as above. It was possible to derive X_E , the amount of drug in the effect compartment, using these programmes. The cumulative AUC's were calculated by the log trapezoidal rule. The calculated effect (clonogenic cell kill) was then compared with the actual xenograft clonogenic cell kill found by Erlichman and Vidgen.

Spheroid drug penetration model

A mathematical model of spheroid drug penetration and its relationship to cytotoxicity was developed to facilitate comparison of actual with "ideal" drug penetration. A number of variables which would be expected to have some bearing on intact spheroid cell sensitivity have been included as model parameters; the gradient of drug diffusion (variable); the degree of cell kill per unit of drug exposure (fixed); the cell cycle specificity of the drug (fixed) the cell cycle kinetics of the spheroid cells and their variation with spheroid depth (fixed).

The descriptive mathematics are simple and are based on the assumption that the spheroid is a perfect sphere made up of a series of concentric annuli (fig 11.2). The sphere consists, arbitrarily of ten annuli whose volume is described by the formula $2\pi RA$ (R = mean radius of annulus; A = the area of cross section of annulus). Annular volume is directly proportional to cell number, assuming a constant cell volume. A given drug exposure, in arbitrary units will produce a consistent degree of cell kill (8% cell kill per unit drug exposure for cycling cell; 2% cell kill per unit drug exposure for non cycling cells). It is assumed that drug exposure within a separate annulus is homogeneous.

A number of computer simulated gradients for drug diffusion and the variation of cell cycle kinetics with spheroid depth were constructed (fig 11.3). The gradient for cell cycle kinetics was fixed at that which conformed most closely to the experimental data (vide infra). The only variable which was not fixed was the drug diffusion gradient. The % cell kill associated with each of the hypothetical gradients shown in figure 11.3 was calculated. The derived formula for the degree of cell kill within a spheroid annulus was:

$$\% \text{cell kill} = D V C$$

Where D = units of drug exposure

V = annular volume

C = cytotoxic dose correction factor for the proportion of cycling cells per annulus.

Determination of intraspheroidal gradients in drug diffusion and the proportion of cycling cells

Selective disaggregation of spheroids has been described by Wibe (1981) and Kwok and Twentyman (1985). Their method has been

modified for use with L-DAN spheroids. Twenty spheroids of approximately 350 μm in diameter were placed in a race track Petri dish (external diameter, 5 cm, internal diameter 3 cm). The culture medium was removed and replaced with 3 ml of 0.125% trypsin. The spheroids were incubated at 37°C with intermittent agitation. After 20 minutes, 3 ml of ice cold medium containing 10% foetal calf serum was added to inactivate the trypsin. After gentle pipetting the spheroid cores were allowed to sediment and the medium containing disaggregated cells was removed and the cells counted in a Coulter Counter. The residual spheroid cores were reincubated with 0.125% trypsin at 37°C for a further 20 minutes before the reaction was stopped by addition of fresh ice cold medium. The spheroid cores were then disaggregated by gentle pipetting to a single cell suspension prior to counting. Using this method it was possible to strip 40-45% of spheroid cells from the external surface. Using the televisual image analysis system (sec 3.2) it was possible to follow changes in size and shape of individual spheroids in filter wells, following treatment with adriamycin. If spheroids were treated for longer than 20-25 minutes with 0.125% trypsin, then in some instances the diameter of the spheroids increased. Prior to this there was relatively uniform slight diminution in diameter which varied directly with the duration of trypsin exposure. Presumably, with prolongation of trypsinisation beyond 20-25 minutes, there is an alteration in the 3 dimensional geometry of the spheres and they adopt a disciform shape. This would explain the apparent increase in diameter despite fewer component spheroid cells. It would be impossible to determine in that situation if disaggregated cells came from peripheral annuli or the spheroid core. Trypsinisation

was therefore limited to 20 minutes and produced 2 cell populations - external (probably corresponding to the 2 outermost annuli) and internal (corresponding to the remainder of the spheroid core).

Intracellular drug levels were characterised following exposure to adriamycin, 5 $\mu\text{g}/\text{ml}$ for 1 hour. The spheroids were treated, washed, differentially trypinised and the external/internal cell populations were separated and stored at -20°C until drug analysis as previously described (sec 2.2).

The cell cycle kinetics of the two populations were assessed by flow cytometry following differential trypinisation. The cell suspension was treated enzymatically to produce a suspension of cell nuclei thus eliminating non specific cytoplasmic fluorescence. After washing in phosphate buffered saline, the nuclei were stained with 2.5×10^{-5} M ethidium bromide in tris-EDTA buffer (with a molarity of 395 mOsmoles); this high molarity further reduces the risk of non specific binding of ethidium bromide. The DNA contents of the cell nuclei were then analysed using a rapid flow cytofluorometer (Becton-Dickinson FACS II cell sorter) with a flow rate of up to 1,000 cells/minute. Excitation and emission wavelengths were 455-490 nm and 590-630 nm, respectively. The machine output was sorted with a 256 multichannel analyser. The number of cells in G_1 , S and G_2M phases was then calculated.

Concentration - Effect Model

The cell kill vs log concentration curves were fitted by least squares to yield the Hill parameters, E_{max} and C_{50} (fig 11.1).

The sigmoid curves for monolayer and spheroid are parallel, with a shift to the left for spheroids along the concentration axis. The E_{max} values are similar (spheroid = 99.99%; monolayer = 99.99%) whereas the C_{50} values reflect the axial shift (spheroid = 3.2 $\mu\text{g/ml}$; monolayer = 1 $\mu\text{g/ml}$).

The plasma concentration-time profile for adriamycin in tumour bearing nude mice (fig 7.2) has already been described. The data was fitted to the concentration-effect model and the cumulative AUC for the effect compartment was derived. Erlichman and Vidgen (1984) disaggregated the MGH-UI xenografts and measured clonogenic cell survival following treatment with adriamycin, at 2 hours and 18 hours therefore the cumulative AUC at 2 and 18 hours was calculated. The relationship between clonogenic cell survival and the cumulative AUC for monolayer, spheroids and xenografts is shown in figure 1.4.

As there is a common expression for drug exposure (cumulative AUC), this allows direct comparison of the effects of adriamycin on each model system, as assessed by a common cytotoxic end point. Spheroid clonogenic survival would appear to be a better predictor of clonogenic survival in vivo than monolayer.

By substituting the E_{max} and C_{50} values for monolayer and spheroid in the modified Hill equation with the appropriate drug concentration from the effect compartment it is possible to calculate the expected effect (clonogenic cell kill).

The actual and predicted clonogenic cell kill following intraperitoneal administration of 20 mg/kg adriamycin is shown in table 11.1.

Again, the values predicted from the spheroid model are significantly closer to the reality governed by drug distribution and penetration in vivo than the monolayer derived figures.

Spheroid penetration model

Intracellular adriamycin levels (mean \pm standard deviation) were significantly higher ($p < 0.001$) in the external spheroid cells (5 ± 2.1 ng/ 10^5 cells) compared to the internal cells (0.8 ± 0.15 ng/ 10^5 cells). There was no evidence of drug metabolism by the external cells, however approximately 5% of intracellular adriamycin was converted to the 7-deoxyaglycone of the parent drug in cells from the interior of the spheroid.

Fluorescent microscopy demonstrated that adriamycin did not diffuse into the centre of the spheroid at drug concentration and exposures used. On this basis, the computer simulated drug diffusion was fitted to the experimental data and constrained to go through zero at the spheroid centre. Of the computer simulated diffusion gradients (figure 11.3), number 5 is closest to the experimental data. The expected clonogenic cell kill for each gradient assuming constant annular cell sensitivity and cell cycle kinetics, is summarised in table 11.2. As is obvious, the best results in respect of clonogenic cell kill were achieved with the homogeneous drug distribution (gradient 1) and the worst with the gradient most representative of the experimental data (gradient 5).

Cognisance must be taken, however, of the cell cycle phase of cells in different annuli. Differential sensitivity of exponential and plateau phase cells to adriamycin has already been demonstrated (sec 3.3). The cell cycle state of cells from the two different regions was different ($p < 0.01$); external layer, G_1

phase $62 \pm 15\%$, S phase $28 \pm 14\%$ and G_2 phase $10 \pm 5\%$; internal core, G_1 phase $80 \pm 18\%$, S phase $15 \pm 6\%$ and G_2 phase $5 \pm 3\%$. It is likely that the G_1 population of cells increases towards the centre of the spheroid, and that a cellular subpopulation exists with G_1 phase DNA content yet with a low RNA content (Allison et al, 1983). These cells are G_0 cells and most resemble the relatively resistant plateau phase cells in monolayer. The experimental data (in concert with published data on the relative percentage of G_1 cells with low RNA levels in the spheroid core, Allison et al, 1983) was fitted to cell cycle kinetic gradient. The effect that inclusion of the cell cycle sensitivity factor has on spheroid clonogenic cell kill has been calculated for the homogeneous and monoexponential drug diffusion gradients (table 11.3). Despite considering this factor, homogeneously distributed drug still produced approximately twice the cell kill that the exponential gradient did.

These relatively simple models have been presented for two reasons

1. to illustrate that a concentration-effect relationship between in vitro and in vivo drug sensitivity testing can be devised.
2. to demonstrate the major differences in cytotoxicity in a spherical tumour mass between homogeneously and non-homogeneously distributed drug.

The concentration effect formulae predict that the multicellular spheroid would be a better model in vitro than monolayer for assessing a drug's activity in vivo, at least in mice.

There is little doubt that clinical oncologists would like to have available to them a reliable system of predictive chemosensitivity testing. The facility of sending to the laboratory a small piece of tumour tissue from a readily accessible site and receiving back within a few days a statement of which of a panel of cytotoxic drugs will kill a high proportion of the malignant cells present in the sample, at clinically achievable drug exposure levels, would radically alter the basis of current chemotherapeutic practice. Current methodology includes clonogenic assays, medium term assays using cell culture and short term biochemical assays. Clonogenic assays have been most widely used, however, there are theoretical and pragmatic problems with this approach which have been well reviewed by Sellby, Buick and Tannock (1983). The use of multicellular spheroids in such systems has not been adequately assessed. Jones et al (1982) examined tumour cells from 7 patients with ovarian cancer and from 22 different human tumour xenografts (representing a wide range of histological subtypes) for multicellular spheroid forming ability. Spheroid formation was

limited to cells derived from xenografts. Volume growth delay was used as an end point and differences in spheroid response broadly reflected patient and in vivo xenograft response. Their data suggests that spheroid formation from human tumour material does not occur with the same frequency and readiness as spheroid formation from established in vitro cell lines. This may represent a major drawback to the use of spheroids in routine chemosensitivity predictive assays.

The spheroid model could be used in preclinical drug development, as it could differentiate which amongst many cytotoxic analogues goes forward for testing in murine models. This would have the dual advantages of economic and simple analogue screening.

It is virtually impossible to rank in vivo cytotoxic drug efficacy on the basis of in vitro sensitivity testing. Although it is possible to derive terms such as the ID_{50} or ID_{90} for individual drug exposures in vivo. Using concentration-effect relationships such as the one described, it should be possible to marry in vitro data with the drugs known pharmacokinetics and rank drug efficacy in this way.

The geometric drug diffusion model was constructed in such a way as to allow comparison of ideally distributed drug with a theoretical curve for drug diffusion which corresponded most closely to the experimental situation. A series of fixed assumptions was made and the drug exposure gradient was varied. Homogeneously distributed drug was associated with an approximately two-fold greater degree of cell kill than poorly penetrated drug. The model presented has been spherical but this could be modified to

cylindrical conformations, more in keeping with drug diffusion from the tumour vasculature (fig 11.3). It is important to recognise, however, that the surface area/volume characteristics of a cylinder are markedly different from those of a spheroid and therefore a different relationship between drug penetration and effect would exist.

It is interesting to note that there was a small but easily detectable degree of metabolism of adriamycin to its 7-deoxyglycone. As mentioned previously (sec 4.4) this could imply anaerobic bioreduction with free radical production. Dertinger, Guichard and Malaise (1984) have demonstrated significant gradients in oxygen diffusion into spheroids such that the central core, even in relatively small spheroids is quite hypoxic (external $pO_2 = 100$ mmHg, central $pO_2 = 10$ mmHg). It is possible that the spheroid model would be appropriate for tumour drug metabolism studies in vitro, as it mimics the microenvironment of tumour in vivo, more closely than monolayer.

	Surviving Xenograft Clonogenic Fraction (time of sacrifice after treatment)		
	<u>2 hours</u>	<u>18 hours</u>	
Experimental data (Erlichman & Vidgen, 1984)	0.83	0.76	(actual)
Concentration-effect model (monolayer parameters)	0.74	0.37	(predicted)
Concentration-effect model (spheroid parameters)	0.9	0.65	(predicted)

Table 11.1 The actual and predicted xenograft clonogenic surviving fraction according to the concentration-effect model.

% CLONOGENIC CELL KILL PER ANNULUS

Annulus	A	B	C	D	E	F	G	H	I	J	% Total spheroid cell kill
Gradient 1	80	80	80	80	80	80	80	80	80	80	80%
Gradient 2	80	79.2	78.4	75.2	73.6	72	70.4	68.8	67.2	65.6	76.9%
Gradient 3	80	75.2	72	68.8	65.6	62.4	59.2	56	53.6	50.4	72.5%
Gradient 4	80	67.2	57.6	49.6	41.6	35.2	30.4	25.6	22.4	18.4	59.6%
Gradient 5	80	56	29	15	7	3.7	1.8	1	0.4	0	42%

TABLE 11.2 The fractional clonogenic cell kill per annulus for the different drug diffusion gradients shown in figure 11.2

Annulus	A	B	C	D	E	F	G	H	I	J	% Total Spheroid Cell Kill
% Total Spheroid Volume	27.1	21.7	16.9	12.7	9.1	6.1	3.7	1.9	0.7	0.1	
Drug Exposure (units per annulus)	10	10	10	10	10	10	10	10	10	10	
Homogenous Drug Sensitivity	80	80	80	80	80	80	80	80	80	80	80%
% Clonogenic cell kill	74	72.5	70.4	68	65	61.4	56.6	50	42.4	33.2	70%
Drug Exposure (units per annulus)	10	7	3.6	1.9	0.9	0.46	0.23	0.12	0.05	0	
Homogenous Drug Sensitivity	80	56	29	15	7	3.7	1.8	1	0.4	0	42%
% Clonogenic cell kill	74	51.8	26.3	13.2	6	3	1.2	0.8	0.16	0	39%

Table 11.3 The effect of varying the composition of the cell cycle compartments, and hence drug sensitivity, of concentric spheroid annuli.

% Clonogenic Cell Kill

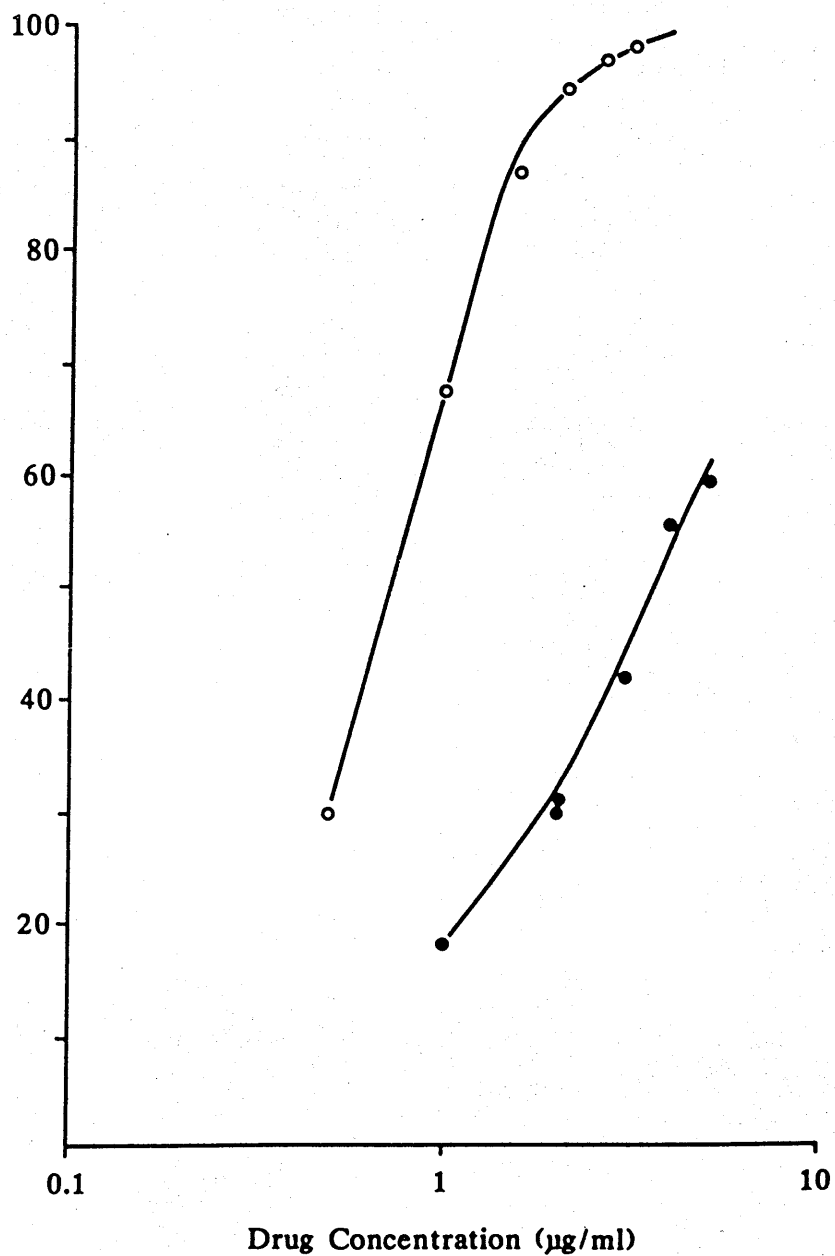


Figure 11.1 Dose-response curves for clonogenic cell kill vs log drug concentration in MGH-UI monolayers (O) and spheroids (●). This data was fitted by non linear squares to a Hill-plot function to derive E_{max} and C_{50} .

SPHEROID ANNULI

/220

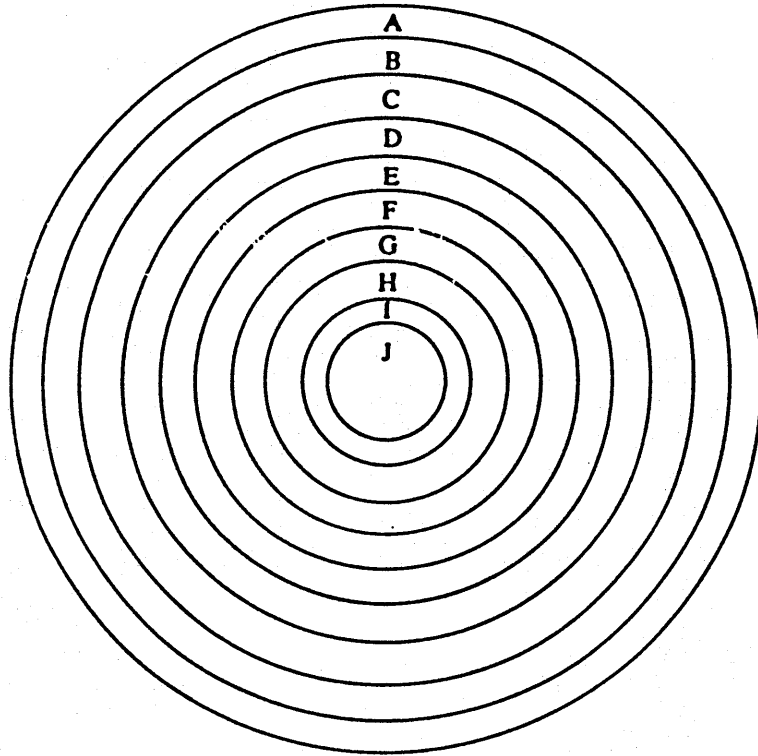


Figure 11.2 Diagrammatic representation of spheroid annuli.

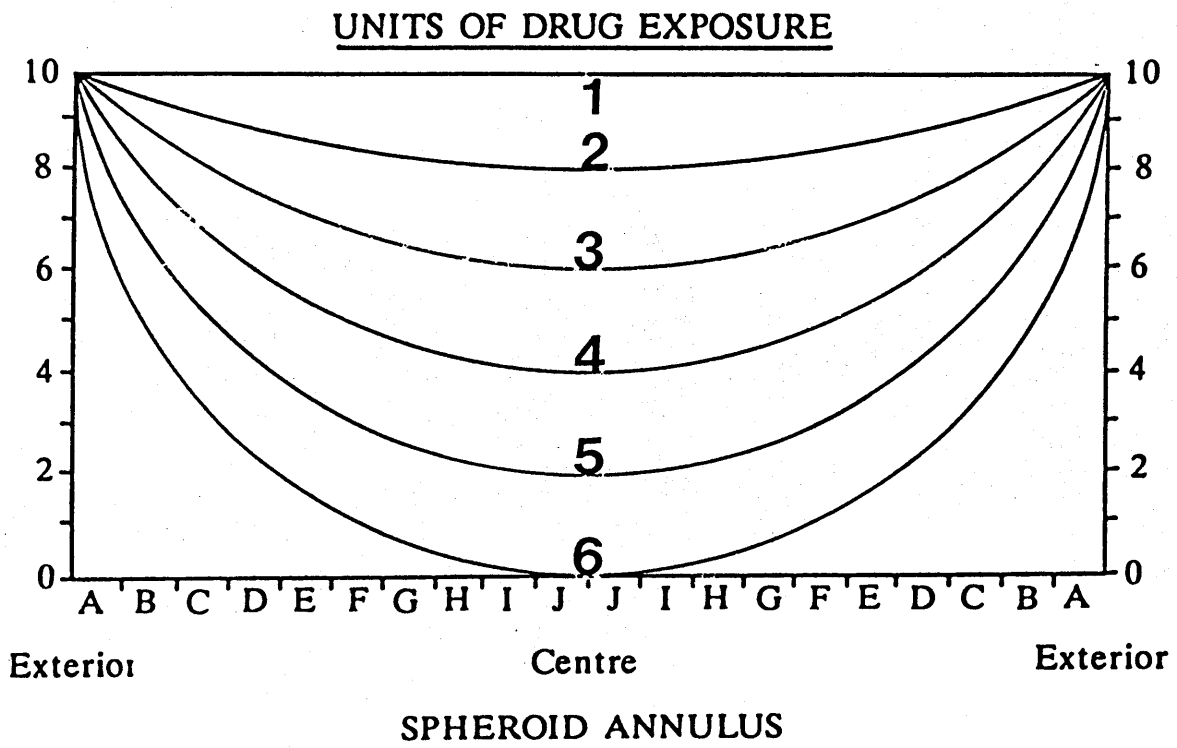


Figure 11.3 Arbitrary drug exposure (1-6) gradients from the spheroid surface to its centre.

CHAPTER 12Clinical Relevance and Future Aims

In summary, it has been possible to overcome cytotoxic drug penetration barriers in a variety of in vitro and in vivo model systems, either by altering the physicochemical properties of the class of drugs under study, or by coadministering chaotropic agents which increase membrane permeability to the antineoplastic agent. A usual sequitur of enhanced penetration was ameliorated cytotoxicity.

The spheroid model would appear to be a better means for pre-clinical predictive testing of drug activity in vitro, than monolayer, as it has been shown that drugs with identical clonogenic survival curves for monolayer conditions, can differ significantly with regard to spheroid activity. The spheroid clonogenic response to adriamycin appears to be more closely related to tumour response in vivo, as defined by the concentration-effect model. This is, perhaps an area where further investigation might prove fruitful, with spheroid drug testing as part of a decision network for extended drug studies in vivo, especially if the analogue under study is a lipophilic derivative.

There are a number of clinical situations in which enhanced penetration would prove relevant. The aim of adjuvant chemotherapy is to eradicate clinically undetectable micrometastases after radiotherapeutic sterilisation or surgical debulking of the primary tumour. If we consider the spheroid an adequate model of a micrometastasis prior to vascularisation, then apart from problems related to drug distribution in vivo, there would be significant penetration barriers in tumour spheroids only a few hundred microns in diameter. It may well be that lipophilic anthracycline derivatives, which are otherwise equipotent in advanced disease, would be more efficacious than adriamycin. Cummings and McCardle

(1986) have carried out a pilot study wherein they administered 25 mg of adriamycin intra operatively and removed the primary breast tumour some 30 minutes later. Adriamycin levels were then measured within the tumour and surrounding normal breast tissue removed at mastectomy. Epirubicin a hydrophobic epimer of adriamycin is undergoing clinical evaluation in advanced breast cancer in the departments of Radiotherapeutics and Medical Oncology in Glasgow University. A study has been initiated to measure tumoural levels of epirubicin in breast cancer patients, as described. In addition, in collaboration with Dr G W Aherne, Department of Biochemistry, University of Surrey, an immunocytochemical stain based on the immunoperoxidase technique is being developed which will allow staining for intercalated adriamycin and epirubicin in formalin fixed breast tissue. It will therefore be possible to assess comparative penetration of adriamycin and epirubicin by dual methods; quantitative measurement of the amount of drug within the tumour; immunohistochemical demonstration of the pattern of anthracycline binding relative to the tumour vasculature.

Certain tumours have a propensity for metastasising to specific compartments within the body and often the metastases rather than the primary tumour produce morbidity. Cytotoxic agents tend to have steep dose response/toxicity curves which limits their systemic use. In this setting the concept of regional chemotherapy has undergone a renaissance over the past decade for several reasons; improved understanding of the pharmacokinetic principles governing regional drug administration; improved pump technology allowing safe and reliable drug perfusion; improved radionuclide imaging which allows determination of the degree of regional perfusion.

Ozols et al (1979) have described the failure of intraperitoneal adriamycin to penetrate further than a few cell layers in solid ovarian tumour nodules in a murine model. Adriamycin has been tested clinically in patients with advanced ovarian cancer, with presumably similar problems with nodular drug penetration. Similarly, adriamycin has been extensively used by intravesical installation in patients with bladder cancer (Eksborg, 1983).

Pharmacological studies have shown that despite installation of therapeutic amounts of the drug (50 mg) that systemic absorption is minimal (Eksborg, 1983). This has been attributed to the relatively impermeant nature of the vesical wall, but one could imagine penetration problems both for tumour as well as normal vesical urothelium. Studies are planned to look at the tumour distribution (by fluorescent microscopy) of adriamycin and epirubicin following intraperitoneal (ovarian carcinoma) and intravesical (superficial bladder tumours) administration. These studies will be conducted in tandem with pharmacological studies and attempts will be made to correlate tumour penetration with systemic levels of the anthracycline. The evident drawback of using agents which might have a better penetration pattern, or co-administering adriamycin with surfactant, is that drug absorption from the corporeal cavity will be promoted and this will reduce the so-called regional advantage, codified by Dedrick et al (1978).

Nevertheless, improved drug penetration results in enhanced cytotoxicity and this would negate any regional disadvantage caused by increased systemic drug exposure.

Intrahepatic arterial administration of adriamycin loaded albumin microspheres is currently being investigated in the Departments of Medical Oncology and Surgery (Glasgow Royal Infirmary). Preliminary evidence suggests that these microspheres can be targeted to intrahepatic metastases following intra-arterial administration by co-infusing the vasoconstrictor, angiotensin II (Lewi et al, 1985; Kerr et al, 1986). It is possible that future regional infusion studies will include assessment of niosomes. Organ entrapment rates of niosomal particles and the pharmacokinetics of adriamycin release would be examined.

Further studies are planned in the field of intercellular communication of cancer cells and its contribution to drug resistance. Coculture experiments between gap junction forming cells which are either resistant or sensitive to a particular cytotoxic agent will be performed. The different cell lines display different phenotypic markers which can be demonstrated by immunocytochemical staining. Therefore although equal cell numbers are co-incubated at a drug concentration which will virtually eradicate one cell type, but not the other, the percentage of the parent cells surviving can be quantified and compared with expected values from pre-existing drug sensitivity data.

Mutant chinese hamster ovary cells which do not form gap junctions do form spheroids and have similar growth kinetics to the wild type cells. Radiobiological experiments are underway to determine whether the spheroids which form gap junctions (wild type) are relatively radioresistant.

A series of studies with cytotoxic drug-low density lipoprotein complexes are envisaged. In vivo experiments aimed at defining relative cytotoxicity and pharmacology of free and LDL-bound

daunomycin in nude mice bearing lung tumour xenografts will be carried out. Further characterisation of the use of LDL as a biological targeting carrier can be done clinically. Radiolabelled LDL will be administered to patients with differing primary and metastatic tumours and it will be possible to determine tumoural uptake relative to normal tissues by external radionuclide scanning.

One of the major drawbacks precluding clinical use of LDL-daunomycin is the relatively small amount of drug incorporated per molecule of LDL. Scaling up calculations show that approximately 1 litre of plasma would have to be harvested from each patient to allow separation of sufficient LDL for a therapeutic dose of daunomycin to be subsequently given. This problem could be overcome by attempting to load LDL with more lipophilic drugs. A series of lipophilic congeners of adriamycin and daunomycin is available from Farmitalia Carlo Erba Ltd. In this respect the cyano-morpholinyl derivatives are especially interesting as they are extremely lipophilic and extremely potent at low doses. Perhaps relatively little of these derivatives would need to be incorporated into LDL to maintain full potency.

Peterson et al, 1986, have demonstrated a significant inverse relationship between LDL receptor activity and survival in stored breast tumour specimens from patients who had undergone mastectomy. We have access to stored tumour tissue from patients who have had gastric, breast and pulmonary tumours resected and adequate clinical follow up. Using a receptor binding assay it should be possible to investigate the use of receptor activity as an independent prognostic factor for each of these tumour types.

Ozols et al (1979) have described the failure of intraperitoneal adriamycin to penetrate further than a few cell layers in solid ovarian tumour nodules in a murine model. Adriamycin has been tested clinically in patients with advanced ovarian cancer, with presumably similar problems with nodular drug penetration. Similarly, adriamycin has been extensively used by intravesical installation in patients with bladder cancer (Eksborg, 1983).

Pharmacological studies have shown that despite installation of therapeutic amounts of the drug (50 mg) that systemic absorption is minimal (Eksborg, 1983). This has been attributed to the relatively impermeant nature of the vesical wall, but one could imagine penetration problems both for tumour as well as normal vesical urothelium. Studies are planned to look at the tumour distribution (by fluorescent microscopy) of adriamycin and epirubicin following intraperitoneal (ovarian carcinoma) and intravesical (superficial bladder tumours) administration. These studies will be conducted in tandem with pharmacological studies and attempts will be made to correlate tumour penetration with systemic levels of the anthracycline. The evident drawback of using agents which might have a better penetration pattern, or coadministering adriamycin with surfactant, is that drug absorption from the coporeal cavity will be promoted and this will reduce the so-called regional advantage, codified by Dedrick et al, 1978).

Nevertheless, improved drug penetration results in enhanced cytotoxicity and this would negate any regional disadvantage caused by increased systemic drug exposure.

A number of questions have been raised by this thesis, therefore the work must be considered, in a sense preliminary, however, active investigation with a secondary series of experiments has already been initiated.

ABRA R.M., HUNT C.A., FU K.K. and PETERS J.H. Delivery of therapeutic doses of doxorubicin to the mouse lung using lung accumulating liposomes proves unsuccessful. *Cancer Chemotherapy Pharmacology*, 1983, 11, 98 - 101.

ACKER H., HOTTERMANN G and CARLSSON J. Microelectrode measurements of pH in cellular spheroids. *Pflugers Archives*, 1982, 394, 199.

ARCAMONE, F. New tumour anthracyclines. *Lloydia*, 1977, 40 (1), 45 - 66.

ALLISON D.C., YUHAS J.M., RIDOLPHO P.F., ANDERSON S.L. and JOHNSTONE T.C. Cytophotometric measurement of the cellular DNA content of (H3) thymidine-labelled spheroids. Demonstration that some non-labelled cells have S and G2 DNA concentration. *Cell and Tissue Kinetics*, 1983, 16, 237 - 247.

ARLANDINI E., FORMELLI F., DI MARCO A. and CASSAZA M.A. Interaction of new derivatives of daunorubicin and adriamycin with DNA. *Il Farmaco*, 1977, 5, 315 - 323.

ASMIN M.N., STUART J.F.B. and FLORENCE A.T. The distribution and elimination of methotrexate in mouse blood and brain after concurrent administration of polysorbate 80. *Cancer Chemotherapy and Pharmacology*, 1985, 14, 238 - 242.

BACHUR N.R. Anthracycline antibiotic pharmacology and metabolism. *Cancer Treatment Reports*, 1979, 63, 817 - 820.

BAURAIN R., ZENEBERGH A. and TROUET A. Cellular uptake and metabolism of daunorubicin as determined by high-performance liquid chromatography; application to L1210 cells. *Journal of Chromatography*, 1978, 157, 331 - 336.

BENJAMIN R.S., RIGGS C.E. and BACHUR N.R. Plasma pharmacokinetics of adriamycin and its metabolites in humans with normal hepatic and renal function. *Cancer Research*, 1977, 37, 1416 - 1420.

BERTAZOLLI C., DI MARCO A, GERANO R.I. and VILLANI, F. Quantitative experimental evaluation of adriamycin cardiotoxicity in the mouse. *Cancer Treatment Reports*, 1979, 63, 1877 - 1882.

BEVINGTON P.R. Data reduction and error analysis for the physical sources. Klein (ed) McGraw-Hill, New York 1978 pp 235 - 236.

BHUYAN B.K., MCGOVERN J.P. and CRAMPTON S.L. Intracellular uptake of 7-con-O-methylnogarol and adriamycin by cells in culture and its relationship to cell survival. *Cancer Research*, 1981, 41, 882 - 887.

BILHEIMER D.W., EISENBERG S. and LEVY R.I. The metabolism of very-low-density lipoprotein proteins. 1. Preliminary in vitro and in vivo observations. *Biochimica Biophysica Acta*, 1972, 260, 212 - 221.

BRODIE B.B. Physico-chemical factors in drug absorption. Absorption and Distribution of Drugs Ed, Binns T.B. Baltimore, Williams and Wilkers, 1964, 16 - 48.

BROWN M.S and GOLDSTEIN J.L. Receptor-mediated endocytosis. Insights from the lipoprotein receptor system. Proceeding of National academy of Science (USA), 1979, 76, 3330 - 3337.

CASSAZA A.M., PRATESI G., GUILLIANI F., FORMELLI F. and DI MARCO A. Enhancement of the antitumour activity of adriamycin by Tween 80. Tumori, 1978, 64, 115 - 119.

CASSAZA A.M. Preclinical studies for the evaluation of the new anthracycline analogs. Chemioterapia Oncologica, 1978, 4, 310 - 326.

CASSAZA A.M. Experimental evaluation of anthracycline analogues. Cancer Treatment Reports, 1979, 63(s), 835 - 844.

CASSAZA A.M. Effects of modifications in position 4 at the chromophore or in position 4' at the amino sugar, on the antitumour activity and toxicity of daunorubicin and doxorubicin. Anthracyclines; Current status and new developments, Crooke S.T. and Reich, S.D. eds Academic Press, New York, 1980 pp 403 -430.

CHAMBERS S.H., BLEEHEN N.M. and WATSON J.V. Effect of cell density on intracellular adriamycin concentration and cytotoxicity in exponential and plateau phase EMT6 cells. British Journal of Cancer, 1984, 49, 401 - 306.

CHAPLIN D.J., DURAND R.E. and OLIVE P.L. Cell selection from a murine tumour using the fluorescent probe Hoechst 33342. British Journal of Cancer, 1985, 51, 569 - 572.

COLQUHOUN D. Lectures on biostatistics. Clarendon Press: Oxford, p 103.

COUNSELL R.E. and POHLAND R.C. Lipoproteins as potential site-specific delivery systems for diagnostic and therapeutic agents. Journal of Medical Chemistry, 1982, 25, 1115 - 1120.

CROOKE, S.T. and DUVERNAY V.H. Fluorescence quenching of anthracyclines by subcellular fraction. S T Crook and S P Reich (eds) Anthracyclines: Current status and New developments, Chapter 9 pp 151 - 155. New York: Academic Press, Inc, 1980.

CUMMINGS J., STUART J.F.B. and CALMAN, K.C. Determination of adriamycin, adriamycinol and their 7-deoxyglycones in human serum by high performance liquid chromatography. Journal of Chromatography, 1984, 311, 125 - 133.

CUMMINGS J. and McARDLE C.S. Studies on the in vivo disposition of adriamycin in human tumours which exhibit different responses to the drug. British Journal of Cancer, 1986, 53, 835 - 838.

DALMARK M. Characteristics of doxorubicin transport in human red blood cells. *Scandinavian Journal of Clinical and Laboratory Investigation*, 1981, 41, 663 - 639.

DALMARK M. and STORM H.H. A Fickian diffusion transport process with features of transport catalysis. *Journal of General Physiology*, 1981, 78, 349 - 364.

DALMARK M. Adriamycin transport in nucleated and non-nucleated cells shows features of a simple diffusion transport process. *Proceedings of American Association for Cancer Research*, 1982 Abstract 14.

DANO K., FREDERIKSEN S and HELLUNG-LARSEN P. Inhibition of DNA and RNA synthesis by daunorubicin in sensitive and resistant Ehrlich ascites tumour cells in vitro. *Cancer Research*, 1972, 32, 1307 - 1314.

DEDRICK R.L., MYERS C.E., BUNGAY P.M. and DE VITA V.T. (JR). Pharmacokinetic rationale for peritoneal drug administration in the treatment of ovarian cancer. *Cancer Treatment Reports*, 1978, 652, 1 - 11.

DEPREZ-DE CAMPANEERE D., BAURAIN R., HUYBRECHTS M. and TROUET A. Comparative study in mice of the toxicity, pharmacology and therapeutic activity of daunorubicin - DNA and doxorubicin - DNA complexes. *Cancer Chemotherapy and Pharmacology*, 1979, 2, 25 - 30.

DETINGER H., GUICHARD M. and MALAISE E.P. Relationship between intercellular communication and radiosensitivity of human tumour xenografts. *European Journal of Cancer and Clinical Oncology*, 1984, 20, 561 - 566.

DETINGER H. and HULSER D. Increased radioresistance of cells in cultured multicell spheroids. Dependence on cellular interaction. *Radiation and Environmental Biophysics*, 1981, 19, 101 - 107.

DETINGER H., HINZ G. and JAKOBS K.H. Intercellular communication, three-dimensional cell contact and radiosensitivity. *Biophysics and Structural Mechanics*, 1982, 9, 89 - 93.

DETINGER H., GUICHARD M. and MALAISE E.P. Is there a relationship between hypoxia, contact resistance and intercellular communication? *Radiation and Environmental Biophysics*, 1983, 22, 209 - 214.

DI MARCO A., CASSAZA A.M., GAMBELTA R. and ZUMINO F. Changes of activity of daunorubicin, adriamycin and stereoisomers following the introduction or removal of hydroxyl groups in the amino sugar moiety. *Chemical-Biological Interactions*, 1977, 19, 291 - 302.

DORR R.T. and ALBERTS, D.S. Pharmacology of doxorubicin. *Current Concepts in the use of doxorubicin chemotherapy.* (ed) Jones S.E. pp 3 - 20.

DURAND R.E. Flow cytometry studies of intracellular adriamycin in multicell spheroids in vitro. *Cancer Research*, 1981, 41, 3495 - 3498.

DURAND R.E. The use of Hoechst 33342 for cell selection from multicell systems. *Journal of Histochemistry and Cytochemistry*, 1982, 30, 117 - 121.

EGORIN M.J., MILDEBRAND R.C., CIMINO E.F. AND BACHUR N.R. Cytofluorescence localisation of adriamycin and daunorubicin. *Cancer Research*, 1974, 34, 2243 - 2245.

EGORIN M.J., CLAWSON R.E., COHEN J.L., ROSS L.A. AND BACHUR N.R. Cytofluorescence localisation of anthracycline antibiotics. *Cancer Research*, 1980, 40, 4669 - 4676.

EKSBORG S. Intravesical installation of antineoplastic drugs : Some general aspects. *Anthracyclines and Cancer Therapy*, Eds. Hansen H.H. Excerpta Medica, 1983 pp 147 - 157.

ERLICHMAN C AND VIDGEN D. Cytotoxicity of adriamycin in MGH-UI cells grown as monolayer cultures, spheroids and xenografts in immune-deprived mice. *Cancer Research*, 1984, 44, 5369 - 5375.

FACHINETTI T., RAZ A. AND GOLDMAN R. A differential interaction of daunomycin, adriamycin and N-trifluoroacetyl adriamycin-14-valerate with mouse peritoneal macrophages. *Cancer research*, 1978, 38, 3944 - 3949.

FINGAL E AND WOODBURG D.M. The pharmacological basis of therapeutics Eds, Goodman L.S. and Gilman A. Macmillan Publishing Co., Inc., (New York) 1975, pp 1 - 47.

FLORENCE A.T. Surfactant interactions with biomembranes and drug absorption. *Pure and Applied Chemistry*, 1981, 4 53, 2057 - 2067.

FLORENCE A.T., TUCKER I.G. AND WALTERS, K.A. Interactions on anionic polyoxyethylene alkyl and aryl ethers with membranes and other biological systems. Rosen M.J. (ed) *Structure/Performance relationships in surfactants*, ACS Symposium Series No 253, 1984 pp 189 - 207.

FORSSEN E.A. AND TOKES Z.A. In vitro and in vivo studies with adriamycin liposomes. *Biochemical and Biophysical Research Communications*, 1979, 91, 1295 - 1301.

FORSSEN E.A. AND TOKES Z. Improved therapeutic benefits of doxorubicin by entrapment in anionic liposomes. *Cancer Research*, 1983, 43, 546 - 550.

FREYER J.P. AND SUTHERLAND R.M. Selective dissociation and characterisation of cells from different regions of multicell tumour spheroids. *Cancer Research*, 1980, 40, 3956 - 3965.

GABIZON A., PERTZ T., BEN-YOSEF R., CATANE R., BIRAN S. AND BARENHOLZ Y. Phase I study with liposome-associated adriamycin : preliminary report. Proceedings of American Society of Clinical Oncology, 1986, No. 169, 43.

GAL D., OHASHI M., MACDONALD P.C. BUCHSBAUM H.J. AND SIMPSON E.R. Low-density lipoprotein as a potential vehicle for chemotherapeutic agents and radionuclides in the management of gynaecologic neoplasms. American Journal of Obstetrics and Gynaecology, 1981, 139, 877 - 882.

GIBALDI M. AND PERRIER D. Pharmacokinetics. Marcel Dekker, Inc., New York and Basel (1975).

GINSBERG H., GILBERT H.S., GIBSON J.C., LE N. AND BROWN W.V. Increased low density lipoprotein catabolism in myeloproliferative disorders. Annals of Internal Medicine, 1982, 96, 311 - 317.

GOLDACRE R.J. AND SYLVEN B. On the access of blood-borne dyes to various tumour regions. British Journal of Cancer, 1962, 16, 306 - 322.

GOLDSTEIN J.L. AND BROWN M.S. Binding and degradation of low density lipoproteins by cultured human fibroblasts. Comparison of cells from a normal subject and from a patient with homozygous familial hypercholesterolaemia. Journal of Biological Chemistry, 1974, 249(16), 3153 - 3162.

GOLDSTEIN J.L. AND BROWN M.S. Atherosclerosis: the low density lipoprotein receptor hypothesis. Metabolism, 1977, 26, 1257 - 1262.

GREGORIADIS G. The carrier potential of liposomes in biology and medicine. New England Journal of Medicine, 1976, 295, 704 - 710 and 765 - 770.

HALBERT G.W., STUART J.F.B., AND FLORENCE A.T. A low density lipoprotein - methotrexate covalent complex and its activity against L1220 cells in vitro. Cancer Chemotherapy and Pharmacology, 1985, 15, 223 - 227.

HARRISON S.D., CUSIC A.M. AND MCALEE S.M. Tween 80 increases plasma adriamycin concentrations in mice by an apparent reduction of plasma volume. European Journal of Cancer, 1980, 17(4), 387 - 389.

ISRAEL M AND POTTI G. Structure-activity correlates of 9, 10-anhydro and 9-deoxyadriamycin analogues. Journal of Medical Chemistry, 1982, 25, 187 - 191.

IWANIK M.J., SHAW K.V., LEDWITH B.J., YANOVICH S. AND SHAW J.M. Preparation and interaction of a low-density lipoprotein : daunomycin complex with P388 leukemic cells. Cancer Research, 1984, 44, 1206 - 1215.

JONES A.C., STRATHFORD I.J., WILSON P.A. AND PECKHAM M.J. In vitro cytotoxic drug sensitivity testing of human tumour xenografts grown as multicellular tumour spheroids. *British Journal of Cancer*, 1982, 46, 870 - 879.

KAELIN W.G.Jr., SHRIVOSTAV S. SHAND J.G. AND JIRTLE R.L. Effect of verapamil on malignant tissue blood flow in SMT-2A tumour bearing rats. *Cancer Research*, 1982, 42, 3942 - 3944.

KANEKO Y. Thyrotropin-daunomycin conjugate shows receptor-mediated cytotoxicity in cultured thyroid cells. *Hormone and Metabolism Research*, 1981, 13, 110 - 114.

KAYE S. AND MERRY S. Tumour cell resistance to anthracyclines - a review. *Cancer Chemotherapy and Pharmacology*, 1985, 14(2), 96 - 103.

KIMELBERG H.K. AND MAYHEW E. Properties and biological effects of liposomes and their uses in pharmacology and toxicology. *Critical Reviews on Pharmacology and Toxicology*, 1978, 6, 25 - 79.

KWOK T.T. AND TWENTYMAN P.R. The response to cytotoxic drugs of EMT6 cells treated either as intact or disaggregated spheroids. *British Journal of Cancer*, 1985, 51, 211 - 216.

LEVIN V.A., PATLAK C.S AND LANDAHL H.D. Heuristic modeling of drug delivery to malignant brain tumours. *Journal of Pharmacokinetics and Biopharmaceutic*, 1980, 8, 257 - 296.

LOEWENSTEIN W.R. Junctional intercellular communication: the cell-to-cell membrane channel. *Physiology Reviews*, 1981, 61, 829 - 913.

LOVELESS H., ARENA E. FELSTEOD R.L. AND BACHUR N.R. Comparative metabolism of adriamycin and daunorubicin. *Cancer Research*, 1978, 38, 593 - 598.

MATTSON J AND PETERSON F. Influence of vasoactive drugs on tumour blood flow. *Anticancer Research*, 1981, 1, 59 - 61.

MAURER H.R. AND HENRY R. Automated scanning of bone marrow cell colonies growing in agar-containing glass capillaries. *Experimental Cell Research*, 1979, 103, 271 - 277.

METTLER F.P., YOUNG D.M. AND WARD J.M. Adriamycin-induced cardiotoxicity (cardiomyopathy and congestive heart failure) in rats. *Cancer Research*, 1977, 37, 2705 - 2713.

MORGAN D., FRESHNEY R.I., DARLING J.L., THOMAS D.G.T. AND CELIK F. Assay of anticancer drugs in tissue culture: cell cultures of biopsies from human astrocytoma. *British Journal of Cancer*, 1983, 47, 205 - 211.

NEDERMAN T., ACKER H. AND CARLSSON J. Penetration of substances into tumour tissue - a methodological study on cellular spheroids *In vitro*, 1981, 17, 290 - 298.

NEDERMAN T., CARLSSON J AND MALMQUIST M. Penetration of substances into tumour tissue - A methodological study with microelectrodes and cellular spheroids. *In vitro*, 1983, 19, 479 - 488.

NEDERMAN T. Effects of vinblastine and 5-fluorouracil on human glioma and thyroid cancer cell monolayers and spheroids. *Cancer Research*, 1984, 44, 254 - 258.

OLSON F., MAYHEW E., MASLOW D., RUSTUM Y AND SZOKA F. Characterisation, toxicity and therapeutic efficacy of adriamycin encapsulated in liposomes. *European Journal of Cancer and Clinical Oncology*, 1982, 18(2), 167 - 176.

OZOLS R.F., LOCKER G.Y., DOROSHOW J.H., GROTZINGER K.R., MYERS C.E. AND YOUNG R.C. Pharmacokinetics of adriamycin and tissue penetration in murine ovarian cancer. *Cancer Research*, 1979, 39, 3209 - 3214.

OZOLS R.F., YOUNG R.C., SPEYER J.L., SUGARBAKER P.H., GREENE R., JENKINS J. AND MYERS C.E. Phase I and pharmacology studies of adriamycin administered intraperitoneally to patients with ovarian cancer. *Cancer Research*, 1982, 42, 4265 - 4269.

PAPADIMITRIOU J.M. AND WOODS A.E. Structural and functional characteristics of the microcirculation in neoplasms. *Journal of Pathology*, 1974, 116, 65 - 79.

PATSCH J.R., SAILER S., KOSTNER G., SANDHOFER F., HOLOSAK A. AND BRAUNSTEINER. Separation of the main lipoprotein density classes from human plasma by rate-zonal ultracentrifugation. *Journal of Lipid Research*, 1974, 15, 356 - 362.

PETERSON C. AND PAUL C. Pharmacokinetics of doxorubicin and daunorubicin in the treatment of acute leukemia. *Anthracycline and cancer therapy*, Ed. Hansen H.H. *Excerpta Medica*, 1983 pp 7 - 17.

PETERSON C., VITOLS S., RUDLING M., MASQUELIER M., LINDQUIST R., SKOOG L., BJORKHOLM AND GAHRTON G. Low density lipoprotein receptors in malignancy : possible diagnostic and therapeutic implications. *Proceedings of American Society of Clinical Oncology*, 1986, Vol 5, 108.

POSTE G. Liposome targeting *in vivo* : problems and opportunities. *Cell Biology*, 1983, 47, 19 - 38.

POWIS G. Anticancer drug pharmacodynamics. *Cancer Chemotherapy and Pharmacology*, 1985, 14, 177 - 183.

PRABHAKAR Y.S., GUPTA S.P. AND RAY A. Effect of molecular size on the activity of adriamycin analogues : a quantitative structure - activity relationship study. *Journal Pharmacobio-Dynamics*, 1986, 9, 61 - 67.

RIEHM H. AND BIEDLER J.L. Potentiation of drug effect by Tween 80 in Chinese hamster cells resistant to actinomycin D and daunomycin. *Cancer Research*, 1972, 32, 1195 - 1200.

RIEHM H. AND BIEDLER J.L. Cellular resistance to daunomycin in Chinese hamster cells in vitro. *Cancer Research*, 1971, 31, 409 - 412.

ROSENCWEIG M., KENIS Y., ATOSSI G., STAQUET M. AND DUARTE-KARIM M. DNA-Adriamycin complex : preliminary results in animals and man. *Cancer Chemotherapy Reports*, 1975, 6, 131 - 136.

RUDLING M.J., COLLINS V.P. AND PETERSON C.D. Delivery of aclacinomycin A to human glioma cells in vitro by the low-density lipoprotein pathway. *Cancer Research*, 1983, 43, 4600 - 4605.

SCHWARTZ H.S. A fluorimetric assay for daunomycin and adriamycin in animal tissues. *Biochemical Medicine*, 1973, 7, 396 - 404.

SCHWARTZ H.S. Mechanisms of selective cytotoxicity of adriamycin, daunorubicin and related anthracyclines. *Topics Molecular and Structural Biology*, 1983, 3, 93 - 125.

SEEBER S., MESHKOV T. AND SCHMIDT C.G. Tween 80 restores adriamycin antitumour efficacy in adriamycin-resistant Ehrlich ascites tumour in vitro and in vivo. *Proceeding of the 10th International Congress on Chemotherapy*, Siegenthaler W and Luthyl R (eds) American Society of Microbiology, Washington D C, Vol 2, 1978, p 1249.

SELBY P., BUICK R.N. AND TANNOCK I. A critical appraisal of the "human tumour stem-cell assay". *New England Journal of Medicine*, 1983, 308, 129.

SETO M., UMEMOTO N., SAITO M., MASUKO Y., HARA T. AND TAKAHASHI T. Monoclonal antibody anti-MM46 : Ricin A chain conjugate : In vitro and in vivo antitumour activity. *Cancer Research*, 1982 42, 5209 - 5214.

SKOVSGAARD T. Carrier mediated transport of daunorubicin, adriamycin and rubidasone on Ehrlich ascites tumour cells. *Biochemical Pharmacology*, 1978, 27, 1221 - 1227.

STEEL G.G. *Growth kinetics of Tumours*. Oxford : Claredon Press, 1977, p 75.

SUBAK-SHARPE J.H., BURK R.R. AND PITTS J.D. Metabolic cooperation between biochemically marked cells in tissue culture. *Journal of Cellular Science*, 1969, 4, 353 - 364.

SUTHERLAND R.M., EDDY H.A., BAREHAM B., REICH K. AND VANANTWERP D. Resistance to adriamycin in multicell spheroids. *International Journal of Radiation Oncology and Biological Physics*, 1979, 5, 1225 - 1229.

SUTHERLAND R.M., CARLSSON J., DURAND R. AND YATES J. Spheroids in cancer research. *Cancer Research*, 1981, 41, 2980 - 2984.

SZEKERKE M., WADE R. AND WHISON M.E. The use of macromolecules as carriers of cytotoxic groups (Part II) Nitrogen Mustard-Protein Complexes. *Neoplasma*, 1972, 19, 211 - 215.

TERASAKI T., IGA T., SUGIYAMA Y., SAWADA Y. AND HANANO M. Nuclear binding as a determinant of tissue distribution of adriamycin, daunomycin, adriamycinol, daunorubicinol and antinomycin-D. *Journal of Pharmacobio-Dynamics*, 1984, 7, 269 - 277.

TWENTYMAN P.R. Response to chemotherapy of EMT6 spheroids as measured by growth delay and cell survival. *British Journal of Cancer*, 1980, 42, 297 - 304.

TWENTYMAN P.R. Growth delay in small EMT6 spheroids induced by cytotoxic drugs and its modification by misosidazole pretreatment under hypoxic conditions. *British Journal of Cancer*, 1982, 45, 565 - 569

UNVERFERTH D.V., MAGORIEN R.D., LEIER C.V. AND BALCERZAK S.P. Doxorubicin cardiotoxicity. *Cancer Treatment Reviews*, 1982, 9, 149 - 164

VARGA J.M., ASATO N., LANDE S. AND LERNER A.B. Melanotropin-daunomycin conjugate shows receptor-mediated cytotoxicity in cultured melanoma cells. *Nature*, 1977, 367, 56 - 58.

VAUPEL P.W., FRINAK S. AND BICHER H.I. Heterogeneous oxygen partial pressure and pH distribution in C3H Mouse mammary adenocarcinoma. *Cancer Research*, 1981, 41, 2008 - 2013.

VITOLS S. AND PETERSON C. Low density lipoprotein a possible drug carrier in the treatment of acute myelogenous leukemia. *Current Topics in Chemotherapy and Immunotherapy*, 1981, 2, 1566 - 1570.

VITOLS S., GAHRTON G., OST A. AND PETERSON C. Elevated low density lipoprotein receptor activity in leukemic cells with monocytic differentiation. *Blood*, 1984, 63(5), 1186 - 1193.

WALTERS K.A. DUGGARD AND FLORENCE, A.T. Non-ionic surfactants and gastric mucosal transport of paraquat. *Journal of Pharmaceutical Pharmacology*, 1982, 33, 207 - 213.

WEINSTEIN J.N. Liposomes as drug carriers in cancer therapy. *Cancer Treatment Reports*, 1984, 68(1), 127 - 134.

WEINSTEIN R.S., MERK F.B. AND ALROY J. The structure and function of intercellular junctions in cancer. Klein G, Weinhouse S (eds) Advances in cancer research, Academic Press, New York, 1979 pp 23 - 89

WELSH J., CALMAN K.C., STUART F., CLEFF J., STEWART J.M., PACKARD C.J., MORGAN H.G. AND SHEPHERD J. Low density lipoprotein uptake by tumours. Clinical Science, 1982, 63, 44.

WEST G.W., WEICHSSELLBAUM R. AND LITTLE J.B. Limited penetration of methotrexate into human osteosarcoma spheroids as a proposed model for solid tumour resistance to adjuvant chemotherapy. Cancer Research, 1980 40, 3665 - 3668.

WHELDON T.E. Can dose-survival parameters be deduced from in situ assays. British Journal of Cancer, 1980, 41, 79 - 87.

WIBE E. Resistance to vincristine of human cells grown as multicellular spheroids. British Journal of Cancer, 1981, 42, 937 - 941

WIBE E., LINDMO T. AND KAALHUS O. Cell kinetic characteristics in different parts of multicellular spheroids of human origin. Cell and Tissue Kinetics, 1981, 14, 639 - 651.

WILSON D.B. Cellular transport mechanisms. Annual Review of Biochemistry, 1978, 47, 933 - 965.

WILSON W.R., WHITMORE G.F.L. AND HILL R.P. Activity of 4'-(9-acridinylamino) methanesulfon-m-anisidide against chinese hamster cells in multicellular spheroids. Cancer Research, 1981, 41, 2817 - 2822.

YUHAS J.M., LI A.P., MARTINEZ A.O. AND LODMAN A.J. A simplified method for production and growth of multicellular tumour spheroids. Cancer Research, 1977, 37, 3639- 3643.

ABSTRACTS

Intracellular uptake of 4'-deoxydoxorubicin and adriamycin by human lung tumour cells in culture and its relationship to cell survival. Kerr D.J., Kerr A.M., Freshney R.I., Kaye S.B. BACR, Birmingham 5.5.

Fluorescent microscopic studies on the differential cellular distribution of adriamycin and 4'-deoxydoxorubicin. Plumb J.A., Willmott N., Burt A.D., More I.A.R., Kaye S.B. and Kerr D.J. BACR, 4 : 10, 1985 (Nov).

Comparative intracellular uptake of adriamycin and 4'-deoxydoxorubicin in human lung cells grown in monolayer. Kerr D.J., Kerr A.M., Freshney R.I. and Kaye S.B. EORTC, PAM group Winter meeting (Milan), 1985.

The effect of the surfactant Brij 30 on cellular uptake and cytotoxicity of adriamycin in lung tumour monolayers and spheroids. Kerr D.J., Wheldon T.E., Russell J., Florence A.T. and Kaye S.B. British Journal of Cancer 54 (1), 183, 1986.

Lipophilic anthracycline analogues can partially overcome drug penetration barriers in human lung tumour spheroids. Kerr D.J., Kaye S.B., Cook J., Hynds S and Wheldon T.E. Proc. Amer. Assoc. Can. Res., Vol 27, 1576, 1986.

Human tumour spheroids: a model for experimental cancer treatment. Wheldon T.E., Gregor A., Kerr D.J., and Russell J. Proc. Brit. Oncol. Assoc., No. 43, 1986

PAPERS

Comparative intracellular uptake of adriamycin and 4'-deoxydoxorubicin by non small cell lung tumour cells in monolayer. Kerr D.J., Kerr A.M., Freshney R.I. and Kaye S. Biochemical Pharmacology 35(16), 2817 - 2823, 1986.

The effect of adriamycin and 4'-deoxydoxorubicin on cell survival of human lung tumour cells grown in monolayers and as spheroids. Kerr D.J., Wheldon T.E., Kerr A.M., Freshney R.I., and Kaye S.B. Brit. J. Cancer. 54, 423 - 429, 1986.

The effect of verapamil on the pharmacokinetics of adriamycin. Kerr D.J., Graham J., Cummings J., Morrison J.G., Thompson G.G., Brodie M.J. and Kaye S.B. Cancer Chemotherapy Pharmacology, 18, 239 - 242, 1986

Aspects of cytotoxic drug penetration with particular reference to anthracyclines. Kerr D.J. and Kaye S.B. Cancer Chemotherapy Pharmacology, 19 : 1 - 5, 1987.

The effect of the non ionic surfactant Brij 30 on the cytotoxicity of adriamycin in monolayer and spheroid culture systems. Kerr D.J., Wheldon T.E., Russell J.G., Maurer H.R., Florence A.T., Freshney R.I. and Kaye S.B. Euro. J. Cancer Clin. Oncol (in press).

In vitro chemosensitivity testing using the multicellular tumour spheroid model. Kerr D.J., Kerr A.M., Wheldon T.E. and Kaye S.B. Cancer Drug Delivery (in press).

The activity of low density lipoprotein - daunomycin complex against lung tumour cells grown as a monolayer and multicellular tumour spheroids. Kerr D.J., Hynds S., Wheldon T.E. and Kaye S.B. Xenobiotica (in press).

Microparticulate drug delivery systems as an adjunct to cancer therapy. Kerr D.J. Cancer Drug Delivery (in press).

Comparative cardiotoxicity and antitumour activity of adriamycin and 4'-deoxydoxorubicin and the relationship to in vivo disposition and metabolism in the target tissues. Cummings J., Willmott N., More I., Kerr D.J., Morrison J.G. and Kaye S.B. Biochemical Pharmacology (in press).

Antitumour activity and pharmacokinetics of niosome encapsulated adriamycin in monolayer, spheroid and xenograft. Kerr D.J., Rogerson A., Florence A.T., Morrison G.J. and Kaye S.B. Cancer Research (submitted).

